BEHAVIOUR OF SOIL NAILED SLOPE UNDER SURCHARGE LOADING

A Thesis Submitted
In Partial Fulfilment of the Requirements
for the Degree of

DOCTOR OF PHILOSOPHY

by

PRASHANT CHUDAMAN RAMTEKE

(Enrollment No. 2K16/PHDCE/12)

Under the Supervision of

Prof. ANIL KUMAR SAHU

Delhi Technological University, Delhi

Department of Civil Engineering

DELHI TECHNOLOGICAL UNIVERSITY

(Formerly Delhi College of Engineering)

Shahbad Daulatpur, Bawana Road, Delhi- 110042. India

February, 2025

ACKNOWLEDGEMENT

I am deeply grateful to Prof. Anil Kumar Sahu, my supervisor, whose unwavering mentorship, encouragement, and insightful evaluation have been invaluable throughout this research endeavour. His guidance significantly influenced the development of this thesis.

My thesis committee members have my heartfelt appreciation for their invaluable feedback, constructive criticism, and encouragement, which have surpassed my expectations. Their diverse perspectives have enriched the quality of this endeavour.

I sincerely thank Delhi Technological University, Delhi and G. B. Pant, DSEU Okhla-III Campus (Formerly G. B. Pant Institute of Technology) New Delhi, for providing essential resources, facilities, and opportunities that have greatly contributed to the success of this research undertaking.

My gratitude also goes out to my colleagues and other fellow researchers for their collaborative spirit, engaging dialogues, unwavering support and review of this thesis. Their camaraderie and insights have been helpful in this journey.

Special recognition is owed to my family members, who have supported and encouraged me throughout this endeavour. I extend heartfelt gratitude to my mother Smt. Ramabai C. Ramteke, my brother Arvind C. Ramteke, my wife Dr. Mrunalini P. Ramteke, my sister Neetu and my loving daughters, Aaradhya, and Ananya. Their enduring encouragement, unwavering support, and profound understanding have been a constant source of strength during challenging times, inspiring and motivating me to pursue excellence in this research journey.

Lastly, I extend my sincere appreciation to all individuals who generously shared their time and expertise to participate in this research endeavour. Their contributions are deeply valued.

DELHI TECHNOLOGICAL UNIVERSITY
(Formerly Delhi College of Engineering)
Shahbad Daulatpur, Main Bawana Road, Delhi-110042

CANDIDATE'S DECLARATION

I, **Prashant Chudaman Ramteke** (enrollment no. 2K16/PHDCE/12) hereby certify that the work which is being presented in the thesis entitled **"Behaviour of Soil Nailed Slope Under Surcharge Loading"** in partial fulfilment of the requirements for the award of the degree of **Doctor of Philosophy**, submitted in the Department of Civil Engineering, Delhi Technological University is an authentic record of my own work carried out during the period from 13-07-2016 to 19/01/2024 under the supervision of **Prof. Anil Kumar Sahu**.

The matter presented in the thesis has not been submitted by me for the award of any other degree of this or any other Institute.

(Prashant Chudaman Ramteke)

This is to certify that the student has incorporated all the corrections suggested by the examiners in the thesis and the statement made by the candidate is correct to the best of our knowledge.

Signature of Supervisor **Signature of External Examiner**

DELHI TECHNOLOGICAL UNIVERSITY

(Formerly Delhi College of Engineering)

Shahbad Daulatpur, Main Bawana Road, Delhi-110042

CERTIFICATE BY THE SUPERVISOR

Certified that **Prashant Chudaman Ramteke**, (enrollment no. 2K16/PHDCE/12) has carried out their search work presented in this thesis entitled **"Behaviour of Soil Nailed Slope Under Surcharge Loading"** for the award of **Doctor of Philosophy** from Department of Civil Engineering, Delhi Technological University, Delhi, under my supervision. The thesis embodies results of original work, and studies are carried out by the student himself and the contents of the thesis do not form the basis for the award of any other degree to the candidate or to anybody else from this or any other University/Institution.

Signature

(Prof. Anil Kumar Sahu)
Professor in Civil Engineering Dept.,
Delhi Technological University, Delhi,
Shahbad Daulatpur, Bawana Road,
Delhi- 110042, INDIA.

Place: New Delhi

Date:

BEHAVIOUR OF SOIL NAILED SLOPE UNDER SURCHARGE LOADING

Prashant Chudaman Ramteke

ABSTRACT

This thesis presents a comprehensive study of soil nailing as an effective and versatile technique for slope stabilization. Soil nailing has proven to be a reliable solution in civil engineering for reinforcing slopes, retaining walls, and stabilizing natural and man-made earth/soil structures. The research establishes a strong foundation by outlining the development, significance, and objectives of soil nailing. It provides an in-depth overview of suitable ground conditions, applications, and construction methods, along with a robust methodological framework incorporating slope stability analysis methods, earth pressure theories, cohesive backfill principles, and failure mode analyses. A detailed review of relevant literature synthesizes findings from physical modelling, numerical simulations, and different investigations on soil nail behaviour.

The study investigates soil slope stability performance through experimental and numerical approaches. The experimental program includes soil testing procedures conducted using a Computerized Universal Testing Machine (UTM) for precise soil slope characterization. Materials and their physical and mechanical properties are thoroughly examined, along with laboratory testing procedures, experimental setups, and slope preparation techniques. Numerical modelling is also introduced, employing 2D FEM for slope stability analysis under surcharge loading and 3D FEM for bearing plate analysis. This integrated approach ensures a comprehensive understanding of the materials, methods, and software utilized.

A meticulous investigation evaluates the effect of nail inclinations on slope stability using numerical simulations and experimental analyses, unveiling optimal nail inclination angles for enhancing stability and mitigating slope failure risks. Further

analysis explores the stability and behaviour of soil-nailed slopes, including the effects of tensile forces on soil nails, bearing plate behaviour under stressed conditions, and the pullout function of grouted nails. Flexural failure at the slope-facing is examined, highlighting critical failure mechanisms. Experimental investigations compare the performance of soil-nailed walls with grouted and non-grouted nails, offering valuable insights into their effectiveness.

The research findings emphasize the superior effectiveness of soil nailing in slope stabilization. Validation through rigorous finite element model simulations strengthens the credibility of the conclusions. The study highlights the importance of optimal nail inclinations and grouted nails in mitigating slope instability and enhancing overall stability. The potential future scope and social impact of soil nailing in geotechnical engineering are also discussed, particularly in areas prone to landslides or hilly terrains. These insights contribute to robust and sustainable geotechnical solutions, emphasizing the need for continued research and innovation in this field.

In summary, this thesis provides significant insights into the technical importance of soil nailing, offering practical recommendations for its widespread application in Civil Engineering projects. The research enhances understanding through experimental investigations and advanced numerical analyses, underscoring soil nailing's pivotal role in modern geotechnical engineering practices.

LIST OF PUBLICATIONS

(a) Papers Published in SCI/SCIE Journals

(1) Ramteke, P.C., and Sahu, A.K. (2024). Soil-slope stability investigation using different nail inclinations: a comprehensive LSD, FEM and experimental approach. Sādhanā, 49, (62). https://doi.org/10.1007/s12046-023-02418-3.

(2) Ramteke, P. C. and Sahu, A. K. (2024). Reliability Assessment of Soil Nailed Slope Under Surcharge Loading: A Numerical and Experimental Investigation with Theoretical Aspects. Zeitschrift Der Deutschen Gesellschaft Für Geowissenschaften (J. Appl. Reg. Geol.) 175(3):417 – 440. https://doi.org/10.1127/zdgg/2024/0422.

(3) Ramteke, P. C., and Sahu, A. K. (2023). Enhancing soil slope stability by soil nailing: A comprehensive review. Zeitschrift Der Deutschen Gesellschaft Für Geowissenschaften (J. Appl. Reg. Geol.),174(4):729-744. https://doi.org/10.1127/zdgg/2023/0403.

(b) Participation in the International Conferences/Paper Published

(1) Ramteke, P. C., and Sahu, A. K. (2023). Ground improvement technique by soil nailing: A theoretical analysis. International Conference on Smart Materials and Structures, ICSMS-2022, vol. 2810, AIP Publishing 050001–12. https://doi.org/10.1063/5.0146861.

(2) Ramteke, P. C., and Sahu, A. K. (2022). Slope Stability Analysis of Soil Nailed Structure by using ASD and LRFD Methods. IARJSET: International Advanced Research Journal in Science, Engineering and Technology, https://doi.org/10.17148/iarjset.2022.9258.

TABLE OF CONTENTS

Page No.

LIST OF TABLES

Page No.

LIST OF FIGURES

Page No.

LIST OF SYMBOLS, ABBREVIATIONS AND NOMENCLATURE

(A) LIST OF SYMBOLS

A	Total cross-sectional area of soil
A_G	Areas of cement grout
A_S	Area of steel bars
a	Adhesion
B_L	Length of the horizontal failure surface
c	Cohesion of soil
C_b	Soil cohesion strength along the base
C_{ef}	Effective cohesion of soil
D	Diameter of the nail
D_C	Conical failure surface diameter on the back of the facing
D'_c	Equivalent conical failure surface diameter at the center of the facing
D_{DH}	Average or effective diameter of the drill-hole
E	Modulus of elasticity of the nail
E_{def}	Deformation modulus
E_G	Elastic modulus of cement grout
E_s	Elastic moduli of steel bar
Eg	Young's modulus of elasticity of the surrounding cement slurry and steel rebar
FS_{FF}	Factor of safety for facing flexure
FS_P	Factor of safety against pullout failure
FS_T	Factor of safety for nail bar tensile strength
FS_{SL}	Factor of safety for global Stability (sliding)
f_y	Yield strength of steel bar
H	Total height of the wall
H_1	Effective height over which the earth's pressure acts
H_{eq}	Equivalent wall height
I	Moment of inertia of the nail

k_1	Force on the slip surface resisted by soil
k_2	Force on the slip surface resisted by nails
K_a	Coefficient of active earth pressure
K_{ac}	Coefficient of active earth pressure due to cohesion
$Ka^{Coulomb}$	Coefficient of active earth pressure due to Coulomb
K'_a	Coefficient of active earth pressure due to Mazindrani
K_o	Transfer the length of the nail
K_p	Coefficient of passive earth pressure
K'_p	Coefficient of passive earth pressure due to Mazindrani
K_s	Coefficient of subgrade reaction
L	Length of the nail
L_o	Transfer length (elastic analysis)
L_F	Length of the failure plane
L_p	Pullout length or nail length behind the failure surface
Ls	Distance between points of maximum moment on either side of the shear plane
l_b	Maximum required length beyond the point of maximum bending moment
M	Bending moment in a nail
M_{max}	Maximum bending moment in a nail
M_o	Maximum bending moment in pure bending
M_p	Bending moment capacity per nail
Nc	Bearing capacity factor
N_F	Normal force on the failure surface
P_s	Shear force in the nail
P_u	Ultimate load
Q	Surcharge loads
Q_D	Permanent portion of the total surcharge load
Q_H	Uniform horizontal loading
Q_i	Generic load (or effect)
Qu	Pullout capacity per unit length
Q_v	Uniformly applied vertical load

q	Mobilized shear stress acting around the perimeter of the nail-soil interface
q_u	Ultimate bond strength
Rc	Cohesive component of Shear Force
R_F	Facing capacity
R_n	Nominal resistance of a structural component selected for a given limit state
R_p	Allowable nail pullout resistance
R_T	Nail bar tensile capacity
R_ϕ	Frictional component of shear force
S_F	Shear force on the failure surface
S_H	Nails spacing horizontal
Su	Undrained shear strength of the soil
S_V	Nails spacing vertical
s	Current shear strength in soil
T	Tensile force at a distance "x" along the bar
T_c	Shear force in a nail
T_{EQ}	Equivalent nail force
T_{max}	Maximum tensile force along the nail bar
T_{max-s}	Design nail tensile load
T_p	Axial force capacity of each nail
T_o	Nail experiencing a tensile force at facing
t_g	Friction factor
u	Pore water pressure
V_F	Punching shear force acting through the facing section
W	Weight of soil nail block
z	Depth below the ground surface/Assumed depth
Ø	Resistance factor related to R_n
γ_i	Load factor associated with Q_i,
η_i	Load-modification factor relating to ductility, redundancy, or operational classification (equal to 1.0 for soil nail walls)
σ_a	Active earth pressure
σ_{eff}	Effective stress (active)

σ_z	Vertical geostatic stress/ total stress
τ	Shear Strength of Soil
γ	Weight of soil
γ_{eff}	Submerged unit weight of soil
γ_{sat}	Saturated unit weight
γ_w	Unit weight of water
δ	Angle of friction between structure and soil
δ_h	Horizontal wall displacement at the top of the wall
δ_v	Vertical wall displacement at the top of the wall
δ	Lateral displacement of the nail
δ'_b	Maximum soil-bearing pressure
$\delta\Delta$	Maximum wall deflection at the top of the wall
ΔH	Equivalent overburden
φ	Angle of internal friction of soil,
φ_{ef}	Angle of internal friction effective
β	Slope inclination
α	Back face inclination of the structure
ψ	Reduction coefficient /dilation angle
ν	Poisson's ratio
β_{eq}	Equivalent backslope angle
ΣD	Total driving force
ΣF	Sum of all vertical forces
ΣR	Total resisting force

(B) ABBREVIATIONS AND NOMENCLATURE

ASCE	American Society of Civil Engineers
ASD	Allowable Stress Design
BM	Bending Moment
CDR	Capacity-to-demand ratio
COV	Coefficient of variation
DCP	Double corrosion protection
FDM	Finite Difference Method
FELEM	Finite Element Limit Equilibrium Method
FEA	Finite Element Analysis
FEM	Finite Element Method
FHWA	Federal Highway Administration
FOS	Factor of Safety
FS_G	Factor of safety against global failure
GC	Grout Cover
GWT	Ground Water Table
HYSD	High-Yielding Strength Deformed
LAM	Limit Analysis Method
LEA	Limit Equilibrium Analysis
LEM	Limit Equilibrium Methods
LRFD	Load And Resistance Factor Design
LSD	Limit States Design
LSM	Limit State Method
MSE	Mechanically Stabilised Earth
OPC	Ordinary Portland Cement
PI	Plasticity Index
PPC	Portaland Pozzolana Cement
RCC	Reinforced Cement Concrete
RFEM	Random Finite Element Method
ROW	Right-of-Way
SCM	Sequential Compounding Method
SF	Shear Force

SMSE	Shored Mechanically Stabilized Earth
SRM	Strength Reduction Method
SP	Poorly graded sand
SPT	Standard Penetration Test
UDL	Uniformly Distributed Load
U.S.	United States
UTM	Computerized Universal Testing Machine
WWM	Welded wire mesh
2D-FEM	Two-Dimensional Finite Element Method
3D-FEM	Three-Dimensional Finite Element Method

Chapter 1

INTRODUCTION

1.1 Background

Soil nailing is a ground improvement technique that enhances soil strength and provides stability to embankments/slopes. It gained recognition across various provinces for its application in retaining structures, offshore structures, structures rehabilitation, and stabilising slopes for both natural and man-made earth/soil slopes. The technique evolved by installing reinforcing elements, termed soil nails, strategically placed within the soil mass to enhance overall stability (Lazarte et al., 2003, Que et al., 2024). The concept of soil reinforcement has deep historical roots, which is important to nature's own mechanisms like root reinforcement (Fraccica et al., 2024). The modern understanding, pioneered by Westergaard in 1938 and further developed by Vidal in 1969, revolves around the idea of reinforcing weak soil with high strength by horizontal reinforcement. According to Vidal's concept, the interaction between soil and horizontal members relies on friction generated by gravity (Birendra, 2002). The practical realization of this concept marked a pivotal moment in 1986 when retaining walls were constructed in France, showcasing the efficacy of soil reinforcement (Byrne et al.,1998). Since then, slope reinforcement techniques have gained widespread acceptance and implementation in developed countries such as Germany, Japan, Malaysia, China, Taiwan, Korea, Indonesia etc. While theoretical advancements in reinforced soil have been extensive, a complete understanding of every aspect remains unresolved. However, the method's effectiveness has been demonstrated through practical applications. An early success in 1972 involved the stabilization of an 18-meter high cut slope in the sand near Versailles, France, during a widening of railroad projects (Rabejac and Toudic, 1974). The cost-effectiveness and expedited construction compared to traditional methods led to increased adoption not only in France but also in other European regions. In 1975, Germany further solidified soil nailing's credibility with the successful application of a soil nail wall, contributing

to its global acceptance (Byrne et al. 1998). Standing on the precipice of progress, there lies an invitation for collaboration, innovation, and the unlocking of the full potential of soil nailing. A future wherein soil reinforcement succeeds, shaping the world's landscape with resilience and sustainability, can be paved by researchers, engineers, and visionaries.

According to recommendations from the FHWA -2003 (Lazarte et al. 2003) soil nail walls were initially employed for interim excavation support in North America during the period 1960s and 1970s, with notable applications in locations such as Mexico City Washington, D.C. and Vancouver, B.C. A significant early instance in the United States took place in 1976 during the expansion of the Good Samaritan Hospital in Portland, Oregon, where soil nailing supported a 13.7-meter deep foundation excavation (Byrne et al., 1998). This method proved remarkably efficient, requiring nearly half the time and costing around 85% less than conventional support systems (Lazarte et al., 2003). Subsequent advancements included a prototype soil nail wall near Cumberland Gap, Kentucky, in 1984, funded by the FHWA, as well as other applications like an 8-meter high wall in 1989 by the Oregon Department of Transportation and a 12.2-meter high, 2-tiered wall along Interstate Highway 78 near Allentown, Pennsylvania (Lazarte et al., 2003). Early examples also include soil nail walls along Interstate 10 in San Bernardino, California; Interstate 90 near Seattle, Washington; and George Washington Parkway (Interstate 495) in Virginia (Byrne et al., 1998). In recent decades, the use of soil nails in slope and soil-nailed walls has significantly increased, demonstrating their technical feasibility and often cost-effectiveness for both temporary and permanent structures worldwide.

1.2 Scope of the Research Work

The scope of this research includes a comprehensive investigation into soil-nailed slope stability, focusing on both theoretical and practical aspects. The key areas of study include:

1. *Analysis Method*: To evaluate the applicability and effectiveness of slope stability assessments, the study explores the Limit State Design (LSD).

2. *Engineering Properties of Soil-Nailed Slopes*: An in-depth study of soil-nailed slopes and their engineering properties, focusing on soil behaviour and the role of reinforcement in enhancing slope stability.
3. *Comparison of Analysis Approaches*: A comparative evaluation of Finite Element Method (FEM) and experimental methods to determine their reliability and accuracy in analyzing soil-nailed slopes.
4. *Impact of Key Parameters*: A comprehensive analysis of the effects of important parameters on soil-nailed slope stability, including nail inclination, surcharge loading, and the performance differences between grouted and non-grouted nails.
5. *Stability Assessment*: Ascertaining the stability of soil-nailed slopes using multiple methods to ensure robustness and consistency in slope stabilization practices.
6. *Design Optimization*: Develop optimal designs for soil-nailed slopes, considering important factors such as nail dimensions, reinforcement properties, nail strength, and wall-facing design to ensure effective and safe stabilization.
7. *Software Utilization*: Employing advanced software tools, including Geo5 and Abaqus, for Finite Element Modeling (FEM) to simulate soil slope behaviour and validate the effectiveness of soil-nailed systems under varied conditions.

This research aims to provide a comprehensive understanding of soil-nailed slope stability, integrating experimental, numerical, and analytical methods to enhance slope stabilization practices and geotechnical design approaches.

1.3 Significance of the Research

The findings of this research hold significant implications for the geotechnical engineering community. By advancing our understanding of soil nail slope stability and analysis methods, this research aims to develop the design and construction of reinforced soil structures. The knowledge gained from this study will aid in formulating improved design guidelines and enhancing the safety and reliability of soil nail slopes in various geotechnical applications. Additionally, the research outcomes

will suggest valuable insights for optimizing the use of soil-nailing technology, contributing to sustainable and cost-effective infrastructural development.

1.4 Research Objectives

Slope stability of soil-nailed structures is an important aspect of geotechnical engineering, and soil-nailing has emerged as a promising technique for reinforcing slopes and retaining structures. The primary objectives of this research are outlined below:

(1) To develop physical and numerical models of the soil nailed slope.

(2) To observe the effects of surcharge loading on soil nailed slope.

(3) To study the failure behaviour of soil nails.

(4) To study of lateral movement of the soil-nailed slope.

(5) To investigate the impact of different parameters on the stability of soil-nailed slope.

1.5 Thesis Organization

In the realm of geotechnical engineering, slope stability remains a paramount concern due to its implications for infrastructure integrity, environmental preservation, and public safety. Over the years, various techniques have been developed to address slope instability, with soil nailing emerging as a prominent solution offering both effectiveness and versatility. This thesis embarks on a comprehensive exploration of soil nailing techniques and their application in slope stabilization, encompassing a multi-disciplinary approach that integrates experimental, numerical, and analytical methods. This thesis is organized into different chapters as outlined below:

Chapter 1: INTRODUCTION

In this chapter, the significance of slope stability in infrastructure development, environmental sustainability etc. is underscored. The historical development of soil-

nailing is briefly reviewed, also the scope, objectives, and significance of the research are outlined.

Chapter 2: LITERATURE REVIEW

Building upon previous studies and methodologies, this chapter conducts a comprehensive literature review on soil nailing. The fundamental principles, methodologies, and applications of soil nailing are explored in this chapter. Ground conditions favourable and non-favourable for soil nailing are delineated along with the elements of soil nail walls. Also, this chapter comprehensively discusses the methods utilized for slope stability analysis, earth pressure calculations, and identification of failure modes. By providing a foundational understanding of slope stability principles and their influencing factors, this chapter delves into intricate aspects such as soil-nail friction mechanisms, nail-bearing failure, and behaviour under various loading conditions. It examines physical modelling, numerical simulations, and miscellaneous studies to identify key advancements and gaps in current knowledge, providing recommendations for future research. This chapter also describes the essential preliminary design/steps requisite for the subsequent analysis and implementation of soil-nailing projects.

Chapter 3: MATERIALS AND METHODS

This chapter outlines the materials and methodologies used to investigate soil slope stability. The experimental program is thoroughly discussed, including the use of a Computerized Universal Testing Machine (UTM) for precise material characterization. Detailed descriptions of the materials utilized, along with their physical and mechanical properties, are provided. The chapter also briefly stated the study of numerical modelling, employing both 2D-Finite Element Method (FEM) analyses. The 2D FEM analysis explores slope stability under different nail inclinations. Additionally, the chapter highlights soil testing procedures performed in the laboratory and explains the experimental setup and soil slope setup preparation techniques. This comprehensive approach ensures a robust understanding of the

materials, methods, and tools utilized, setting the groundwork for the detailed analysis and discussions presented in subsequent chapters.

Chapter 4: NAIL INCLINATIONS EFFECT ON SLOPE STABILITY

This chapter delves into the influence of varying nail inclinations within the soil slope, emphasizing their impact on improving structural integrity and resisting slope failure. A detailed analysis of the relationship between nail inclinations and the Factor of Safety (FOS) is presented, highlighting how specific angles contribute to overall stability. Mathematical modelling is also included to predict nail displacement within the soil mass, providing a theoretical framework for understanding nail-soil interaction. Furthermore, the identification of settlement and embankment behaviour within the soil slope is explored through 2D FEM simulations. Additionally, experimental investigations are conducted to evaluate the effects of various nail inclinations on slope stability, bridging the gap between theoretical modelling and practical applications. This chapter provides a comprehensive understanding of the significance of nail inclinations in slope stabilization and their optimization for enhanced geotechnical performance.

Chapter 5: SOIL-NAILED SLOPES STABILITY AND PERFORMANCE

This chapter explores soil slope behaviour under surcharge loading. It examines the effects of tensile forces on soil nails, the behaviour of bearing plates under stressed conditions, and the pullout function of grouted nails. Furthermore, flexural failure mechanisms at the slope-facing are analyzed, highlighting critical failure modes. The chapter also assesses the overall slope stability performance of soil-nailed slopes, incorporating experimental investigations of soil-nailed walls in the presence of both grouted and non-grouted nails.

Chapter 6: RESULTS AND DISCUSSION

Synthesizing findings from experimental, numerical, and analytical investigations, this chapter provides a comprehensive analysis of soil nailing performance in slope

stabilization. It discusses key observations, highlights significant trends, draws conclusions etc.

Chapter 7: CONCLUSION, FUTURE SCOPE AND SOCIAL IMPACT

In this chapter, conclusions are drawn from the collective insights gained throughout the study, and actionable recommendations are presented to guide future endeavours in slope stabilization, soil nailing techniques, and accompanying social impact.

Overall, this introductory chapter provides an overview of soil nailing, outlines the scope of the research, highlights the significance of the study, and specifies the objectives of the thesis. Following this first chapter, the next chapter, “Literature Review,” will explore the specific ground conditions that are favourable and unfavourable for soil nailing, discuss the applications of soil nailing techniques, and examine various methods for analyzing and studying active and passive earth pressures. It also, introduced the components of soil-nailed walls, the construction sequences involved, and the important factors that affect slope stability.

Chapter 2

LITERATURE REVIEW

2.1 Introduction

The soil possesses certain inherent strengths within itself. Friction between soil particles also exists as frictional resistance (Sangdeh et al. 2023, Burland 2023). A change in the soil stress state occurs when it is subjected to external loads (Liu et al. 2017). Soil nailing offers a cost-effective and quick construction solution to improve slope stability within the soil mass (Basta et al. 2024, Sabermahani et al. 2025). Soil nailing is a ground improvement technique that increases soil strength and provides global stability to embankments/slopes (Ahmed et al. 2024, Pinuji et al. 2024). The process involves inserting steel nails into the soil mass and connecting them to a steel mesh in a soil nail wall (Berg et al. 2015, Byrne et al. 1998, FHWA Manual 1998, Lazarte et al. 2003). These nails are typically made of steel. First, a rotary drilling machine is used to insert the nails into the soil, which are then grouted with cement. The grout secures the nails and ensures tight compaction of the surrounding soil. Once the grout has dried and the soil has been compacted, the steel mesh is connected to the nails and completes the soil nail wall (Berg et al. 2015, Byrne et al. 1998). This wall serves as a support system, effectively preventing soil movement and collapse.

This chapter provides a comprehensive review of soil nailing as a technique for strengthening slopes and soil-nailed walls. It deliberates various methods and materials associated with soil nailing. The review incorporates previous studies to demonstrate the extensive practical application of soil nailing. To study the influence of soil nail stiffness, both physical modelling and numerical techniques, such as FEM and FDM, are studied. The study confirms that soil nailing is a reliable and very effective method for improving soil strength and minimizing settlement. Similarly, the review highlights the significance of considering the bending stiffness of soil nails to optimize the effectiveness of this technique in ground improvement projects. As a result, this review serves as a valuable resource for engineers seeking guidance in soil nailing techniques.

The primary objective of this chapter is to explore fundamental concepts and state-of-the-art approaches in soil slope stability, with a particular focus on soil-nailed slopes and walls.

2.2 Purpose of Review Study

This literature review aims to establish a global standard for the design, construction, monitoring, and maintenance of soil-nailed systems. Through a comprehensive analysis of relevant literature, this study offers valuable insights into the key parameters associated with soil-nailed systems. The findings from this review are especially beneficial for researchers and practising engineers focused on geotechnical engineering principles and practices, particularly concerning transportation infrastructure projects such as highways, railroads, tunnelling, and tunnel portals. By disseminating knowledge about the important considerations and best practices for constructing reinforced ground structures, this study enhances understanding within the field. Ultimately, this literature review serves as a significant resource to improve the effectiveness and efficiency of implementing soil-nailed systems across various geotechnical engineering projects.

2.3 Role of Soil Nailing

Soil nailing is commonly used in constructing roads, railroads, dams, and related civil engineering structures involving embankments. While stable ground with favourable geotechnical properties allows for safe construction, many projects are built on unstable, soft soil due to limited options. This can pose challenges for geotechnical engineers, as soft soils often have low bearing capacity, excessive settlement, and insufficient shear strength, resulting in potential embankment failures. To address these issues, it is crucial to improve and stabilize soft ground before construction. The main role of soil nailing is stated below:

1. Enhancing soil shear strength.
2. Stabilizing slopes and retaining walls.
3. Reducing settlement and deformation.
4. Improving liquefaction resistance.

5. Preventing sudden structural collapse.
6. Providing support during excavation.
7. Adaptability to various soil conditions particularly cohesive soils and weak rock formations.
8. Integration with other techniques, like works in conjunction with mechanically stabilized earth (MSE) walls and hybrid systems for enhanced performance.
9. Nail orientation and inclination can be adjusted to resist site-specific forces such as gravity and lateral pressure etc.
10. Reduction of lateral pressure i.e. decreases lateral forces acting on retaining structures, benefiting wall stability.
11. Durable and long-lasting structure solutions for stabilizing slopes and walls.
12. Facilitates quicker consolidation of soil by reinforcing its layers.
13. Reinforces and stabilizes soil by filling voided areas effectively.

This comprehensive approach underscores the reliability and versatility of soil nailing as a robust ground improvement technique in geotechnical engineering and enhancing stability across various applications.

2.4 Ground Conditions for Soil Nailing

Soil-nailed slopes and walls are highly versatile and adaptable, making them suitable for a variety of soil types and conditions. This section outlines the specific soil conditions where soil nailing is either appropriate or not.

2.4.1 Favorable Soil Conditions for Soil Nailing

Soil nail slopes have been successfully constructed in various soil types. Generally, the avoidance of construction challenges and long-term issues is achievable when specific favourable soil conditions are present. The following types of ground are typically considered suitable for soil nailing applications as per FHWA, 2003 recommendations :

1. Stiff to hard fine-grained soils
2. Dense to very dense granular soils

3. Weathered rock with no weakness planes
4. Glacial soils

2.4.2 Non-Favorable Soil Conditions for Soil Nailing

For soil nailing, difficult or non-favourable soil conditions refer to scenarios where the soil characteristics pose challenges to the effective installation and soil nail wall performance. Some of these challenging soil conditions include as per FHWA, 2003 code recommendations are:

1. Dry, poorly graded cohesionless soils
2. Soils with high groundwater levels
3. Soils with a large proportion of cobbles and boulders
4. Soft to very soft fine-grained soils
5. Organic soils
6. Highly corrosive soil
7. Weathered rock with prevalent unfavourable weakness planes
8. Loess soil conditions

2.4.3 Intermediate Soil Conditions for Soil Nailing

Certain soil conditions fall in between the highly favourable and unfavourable categories as described above. While their engineering properties may not be as ideal soil nail slope/walls have been installed successfully and cost-effectively in these intermediate soil conditions. Examples of such intermediate conditions include as per FHWA, 2003 code recommendations are:

1. Engineered Fill
2. Residual Soils

2.5 Application of Soil Nailing

Soil nailing, an important technique in geotechnical engineering, improves soil slope stability in various scenarios. From roadway expansions under existing bridges to tunnel portal reinforcement, its application ensures stability and seamless integration into existing structures. Soil nailing plays an important role in stabilizing Mechanically

Stabilized Earth (MSE) slopes and hybrid soil nail wall systems, offering tailored solutions for different terrains. The advent of Shored Mechanically Stabilized Earth (SMSE) walls represents an example, providing enhanced structural support in challenging geological conditions. Its presence in railway and roadway development underscores its efficacy as a cornerstone of modern infrastructure projects. With its adaptability and reliability showcased across multiple applications, soil nailing continues to exemplify scientific skills in geotechnical engineering, ensuring the resilience and longevity of important infrastructures. The following paragraph discusses various applications of soil nailing in civil engineering projects.

2.5.1 Roadway or Highway Cut Excavations

The soil nailing application in roadway cuts is particularly appealing due to several factors, including limited excavation and proper right-of-way (ROW) considerations. These factors not only contribute to the overall reduction of environmental impacts along the transportation corridor but also offer practical advantages during the construction phase. One of the key benefits of utilizing soil nailing in roadway cuts is the reduction in the extent of excavation required. Traditional methods for stabilizing slopes or retaining walls often necessitate extensive excavation to create a stable foundation for the structure. However, with soil nailing, the need for deep excavation is minimized. Instead, steel soil nails are inserted directly into the slope or embankment, providing efficient reinforcement and stability without the need for extensive groundwork. Additionally, proper right-of-way (ROW) planning plays an important role in the soil-nailing application of roadway cuts. ROW refers to the designated land area along the transportation corridor that is acquired for the construction and maintenance of the roadway. During the construction phase, soil nailing offers the advantage of minimizing traffic disruptions. The soil nail installation typically involves the use of small equipment and machinery, which can be easily manoeuvred in confined spaces. As a result, traffic flow can be maintained with minimal interruptions, making the construction process more efficient and reducing the inconvenience to commuters and travellers. Figure 2.1 illustrates the tangible benefits of employing soil-nailing techniques. The application of soil nailing in

roadway cuts presents an attractive solution due to limited excavation requirements, proper ROW utilization, and reduced traffic disruptions during construction. By harnessing the advantages of soil nailing, it can achieve stable and sustainable roadway designs while minimizing the environmental impact and enhancing the overall efficiency of transportation projects.

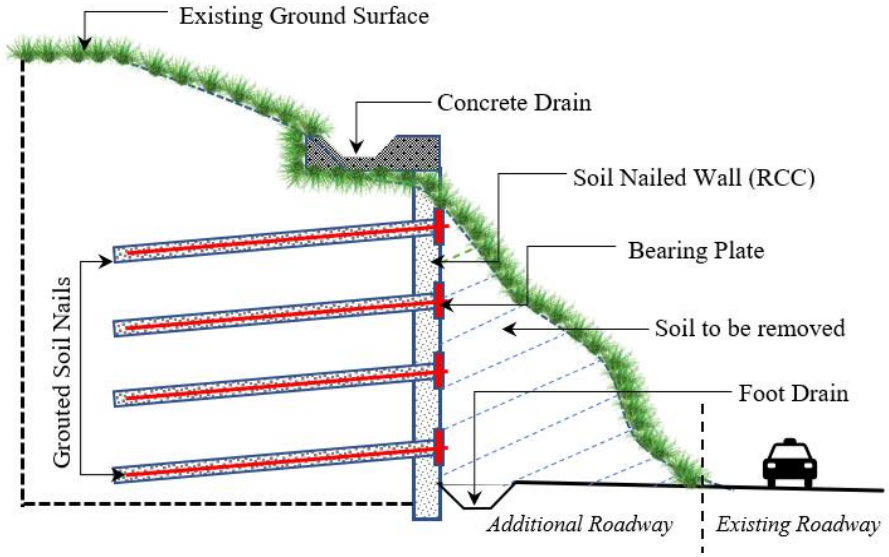

Figure 2.1: Roadway cut supported (modified after Porterfield et al.,1994)

2.5.2 Road Widening (Under Existing Bridge)

As compared to other methods, soil nails are particularly advantageous for underpass-widening projects. One of the primary benefits is the cost-effectiveness of installing soil nails under a bridge abutment. The installation cost of soil nails is more favourable compared to alternative techniques. The equipment required for soil nail installation is relatively small, which allows for easy positioning and reduces the need to disrupt traffic flow during the underpass widening process (Lazarte et al., 2003). This significantly minimizes inconveniences to commuters and ensures smooth traffic movement during construction. Furthermore, soil nail walls enable the underpass to be made functional within a limited time frame. The careful planning and well-designed implementation of soil nailing, considering factors such as length, inclination, and location, ensure a practical and efficient approach to reinforcing the underpass. In certain cases, a combination of vertical micro-piles and soil nails may be used for

added support and reinforcement. Micro-piles are employed to support the modified abutments and prevent settlements, complementing the soil nails' stabilization efforts (refer to Figure 2.2).

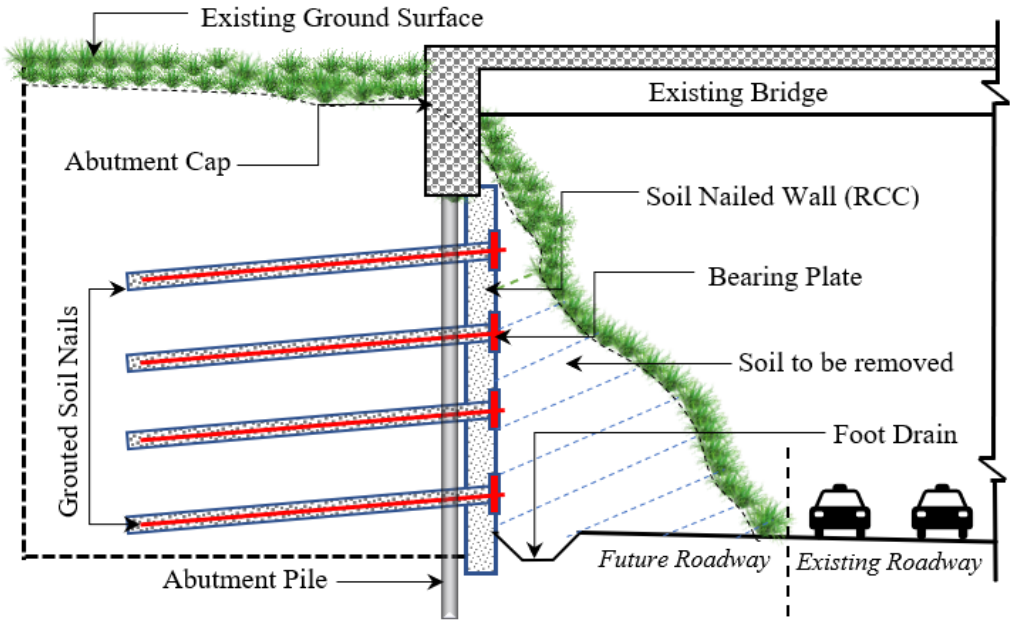

Figure 2.2: Road widening under the existing bridge (modified after Porterfield et al.,1994).

This combined use of micro-piles and soil nails proves to be a highly attractive and effective solution in underpass widening applications. One of the main advantages of using soil nailing in underpass widening projects is the ability to expedite construction. By choosing this method, the underpass widening process can be completed more efficiently, allowing the bridge to remain open for traffic movement during the construction phase. This not only reduces traffic disruptions but also enhances overall project efficiency. The soil nailing offers a multitude of advantages in underpass widening projects. Their cost-effectiveness, minimal traffic disruptions, and ability to accelerate construction make them an optimal choice for reinforcing underpasses and ensuring the smooth flow of traffic during roadway improvements. The soil nail walls combination with other reinforcing elements, such as micro-piles shown in Figure 2.2 enhance their effectiveness in stabilizing the underpass and achieving successful construction outcomes.

2.5.3 Tunnel Portals

The use of soil nails for stabilizing tunnel portals is an effective technique, similar to their application in road cuts, with some specific considerations for the unique tunnel environment (as depicted in Figure 2.3). The principles that govern soil nail construction in road cuts can be applied to tunnel portals, but careful attention is needed during the design and execution phases to ensure optimal performance. In tunnel portals, the main objective is to provide stability and support to the surrounding soil while considering the proximity to the tunnel entrance. The soil nail arrangement in tunnel portals may differ from their conventional use in roadway applications. The nails should be fixed at suitable lateral slopes and vertical angles to avoid any interference with tunnel support constituents. The goal is to provide optimal stability and reinforcement to the surrounding soil while maintaining compatibility with the tunnel's existing structure. The soil nails offer an effective solution for stabilizing tunnel portals. By applying the principles used in road cuts and addressing the specific considerations related to tunnel portals, it can create a robust and well-designed soil nail system that provides the necessary stability and support while ensuring the integrity of the tunnel structure. Thorough analysis, careful design, and precise execution are important in successfully implementing soil nails for tunnel portal stabilization.

Figure 2.3: Tunnel portal stabilization

2.5.4 Mechanically Stabilized Earth (MSE) Slope

Mechanically Stabilized Earth (MSE) slope/walls, which can sometimes experience excessive distortion due to weak construction practices sub-optimal design, or a combination of both. To address the stability concerns of MSE walls, soil nails are strategically placed in front of the wall when it is stable and can resist loads. As continues to deform the MSE wall, it transfers load onto the nails and the backfill of the wall. In these situations, extra care must be taken to guarantee that the load is successfully transferred to the stable soil behind the soil segment reinforced with MSE. It is important to take precautions so as not to endanger the stability of the current MSE wall when drilling and grouting for the installation of soil nails. The drilling and grouting activities should not damage the steady facing of the wall, and proper engineering measures should be implemented to safeguard its structural integrity. In the context of soil nailing for supporting and stabilizing MSE and masonry walls, the selection of a suitable bearing plate is of paramount importance. The bearing plate serves as a critical component in the soil nailing system as it bears and sustains the load (Viswanadham and Rotte, 2015). It is essential to choose a bearing plate that can effectively distribute the load without causing damage to the stable facing of the MSE walls. In the design process, the load considered on the bearing plate is a crucial governing factor. Carefully analyzing load distribution and considering various factors ensures that the bearing plate can effectively handle applied loads and maintain stability. The strategic service of soil nails with appropriate bearing plates reinforces and stabilizes MSE walls and masonry structures, preventing excessive distortion and ensuring the long-term stability of the soil structure.

In general, soil nailing provides an effective solution for reinforcing soil structures like MSE walls, addressing stability concerns, and preventing deformation. The proper selection and soil nail installation, along with careful consideration of the bearing plates, are crucial to maintaining the structural stability of the MSE wall while ensuring effective load transfer and distribution. Through meticulous design and engineering, soil nailing serves as a reliable method for enhancing the stability and performance of various soil structures. The representative cross-section of soil soil-nailed wall is illustrated in Figure 2.4.

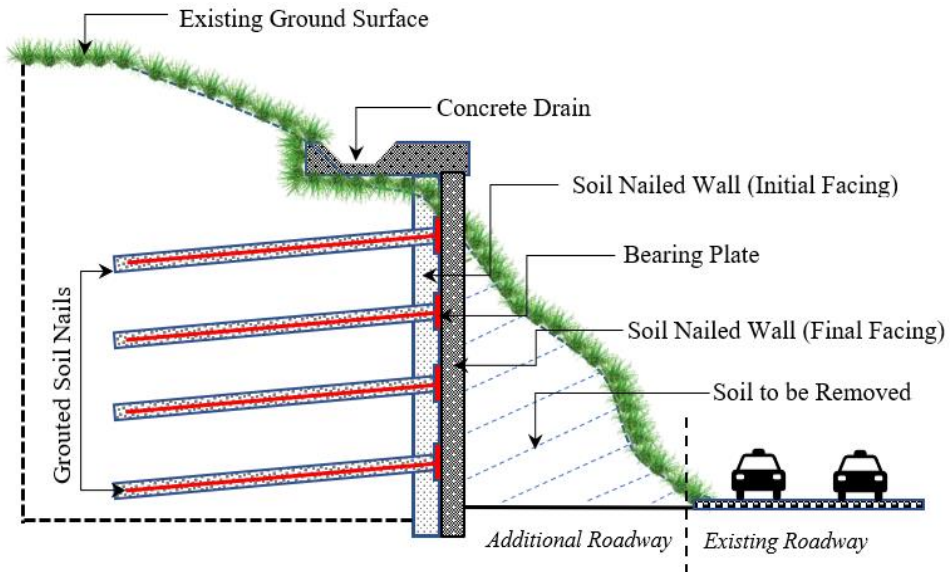

Figure 2.4: Distinctive cross-section of a soil nail wall (modified after Porterfield et al.,1994)

2.5.5 Hybrid Soil Nail Wall Systems

Soil nail walls are commonly used in conjunction with alternative techniques like MSE walls and anchor walls to leverage the benefits of both systems. This combination proves advantageous in scenarios where the area units of various earth-retaining systems are too high or when intricate wall layouts are required. Integrating soil nail walls with MSE walls results in a more economical design compared to using MSE walls alone for the entire elevation. Figure 2.5 depicts an illustration of a hybrid MSE and soil nail wall. In such cases, the wall face is often designed to function as a cantilever, and one or two rows of soil anchors are incorporated for lateral restriction on the cantilever. The lower rows of nails provide additional support and stability. While soil nail slope/walls offer admirable stability in most scenarios, they may not be suitable for effectively addressing instability on deep-seated slip surfaces (FHWA, 2015). To counter this, ground anchors are introduced alongside soil nails in proposed roadway cuts with potential instability in the deep roots. This combined use enhances the global stability and earth-retaining structure performance. Soil nail slopes can also serve as support for the topmost gradient of layer walls, providing global stability to the entire system. This integration ensures a robust and cohesive structure, optimizing

the overall performance and protection of the retaining wall. In conclusion, the combination of soil nail walls with alternative techniques like MSE walls and ground anchor walls offers various advantages in specific engineering scenarios. By carefully integrating these systems and leveraging their strengths, it can achieve more economical designs, enhance stability on deep-seated slip surfaces, and optimize the performance of earth-retaining structures. The hybrid approach enhances the efficiency and effectiveness of the retaining system, making it an important thing in the geotechnical engineering domain.

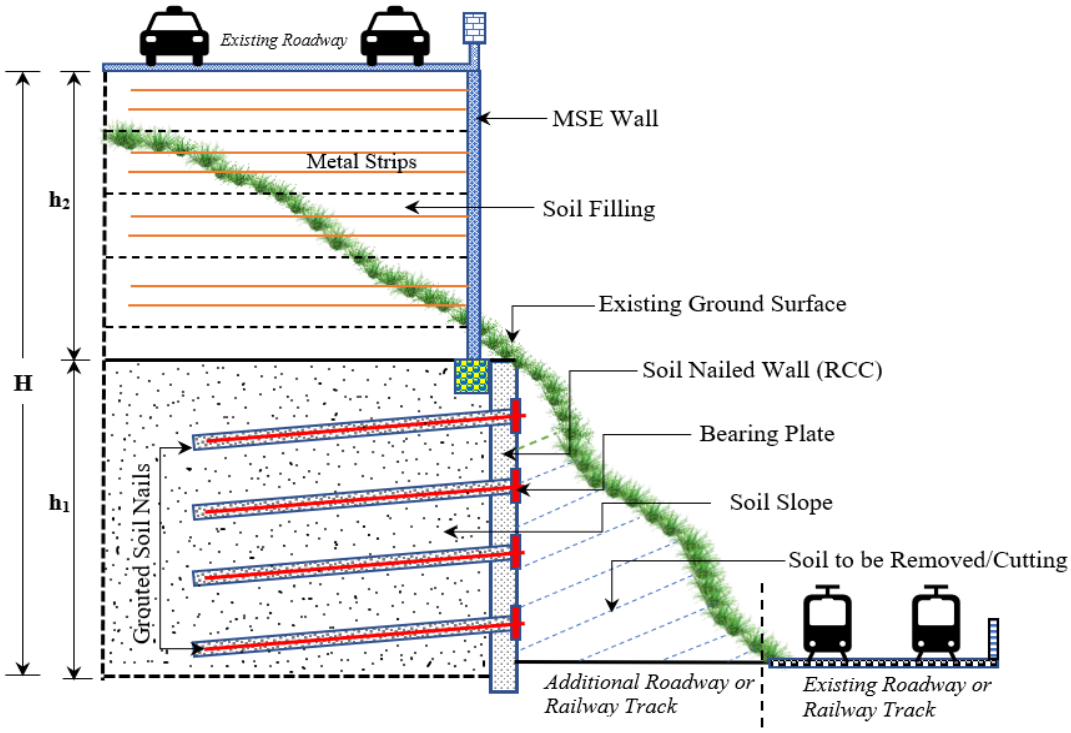

Figure 2.5: Hybrid soil nail/MSE wall (modified after Wood et al., 2009).

2.5.6 SMSE (Shored Mechanically Stabilized Earth) Walls

In the effort to widen low-traffic volume roads in steep terrains, soil nail walls have emerged as a progressive solution, often in coalition with Mechanically Stabilized Earth (MSE) walls (Figure 2.6). Traditionally, executing the construction of an MSE wall on flat ground involves reinforcing the soil by excavating and creating a flat bench. However, in cases where the slope is very steep or where maintaining transportation throughout the widening is essential, excavation becomes impractical.

However, in front of the soil nail wall, traditional MSE wall construction may not be sufficient to handle the lateral pressure effectively, this is where soil nails play a crucial role. By introducing soil nails, the prolonged lateral pressure on the MSE wall can be significantly mitigated, leading to enhanced stability and long-term performance (FHWA, 2003, 2015).

In this context, the soil nail wall is designed to be a permanent structure, forming which is known as an SMSE (Soil Nail Mechanically Stabilized Earth) wall. This innovative arrangement has been modernized and extensively covered in the FHWA (Federal Highway Administration) report under the Load and Resistance Factor Design (LRFD) platform (refer to FHWA, 2003). Overall, the combined use of soil nail walls and MSE walls presents an efficient and robust solution for widening low-traffic volume roads in steep terrains. Integrating soil nails strategically, can stabilize the initial slope, reduce lateral pressures on the MSE wall, and create a permanent and stable SMSE wall. This innovative approach enhances the complete stability performance of an earth-retaining system, making it a significant tool in the field of geotechnical engineering.

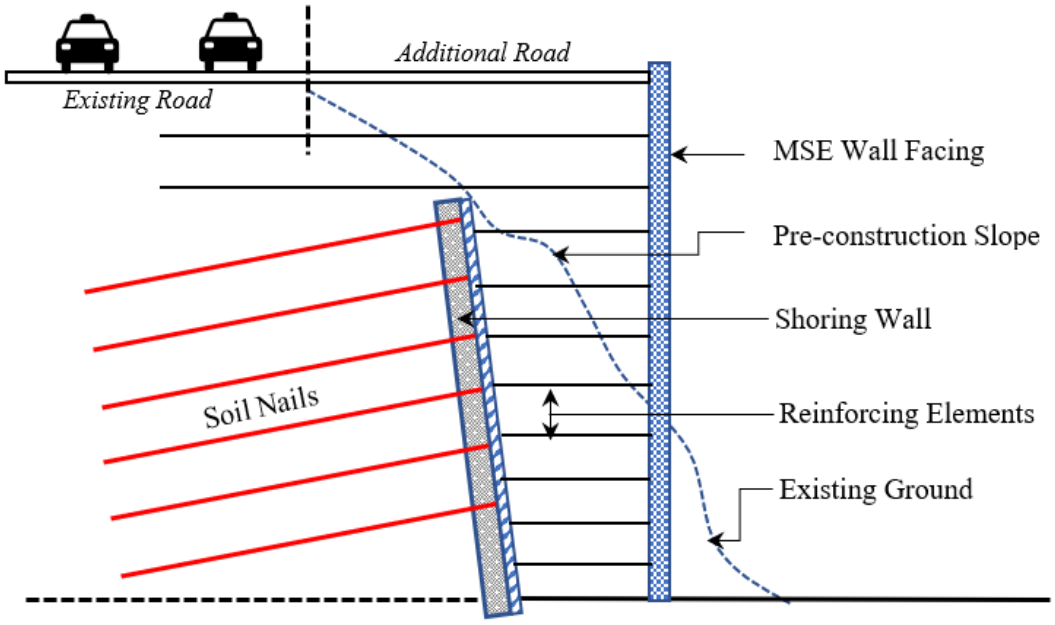

Figure 2.6: SMSE wall for steep terrain (modified after Morrison et al., 2006).

2.6 Elements of Soil Nailing Systems

The soil nail slope/wall elements refer to the various components and features that make up this geotechnical engineering structure (refer to Figure 2.7). Soil nail slopes are constructed using a combination of wall, soil nails, facing material, and shotcrete, creating a stable and reinforced system to support and stabilize excavated or unstable slopes. Let's delve into the key elements of a soil nail wall or slope:

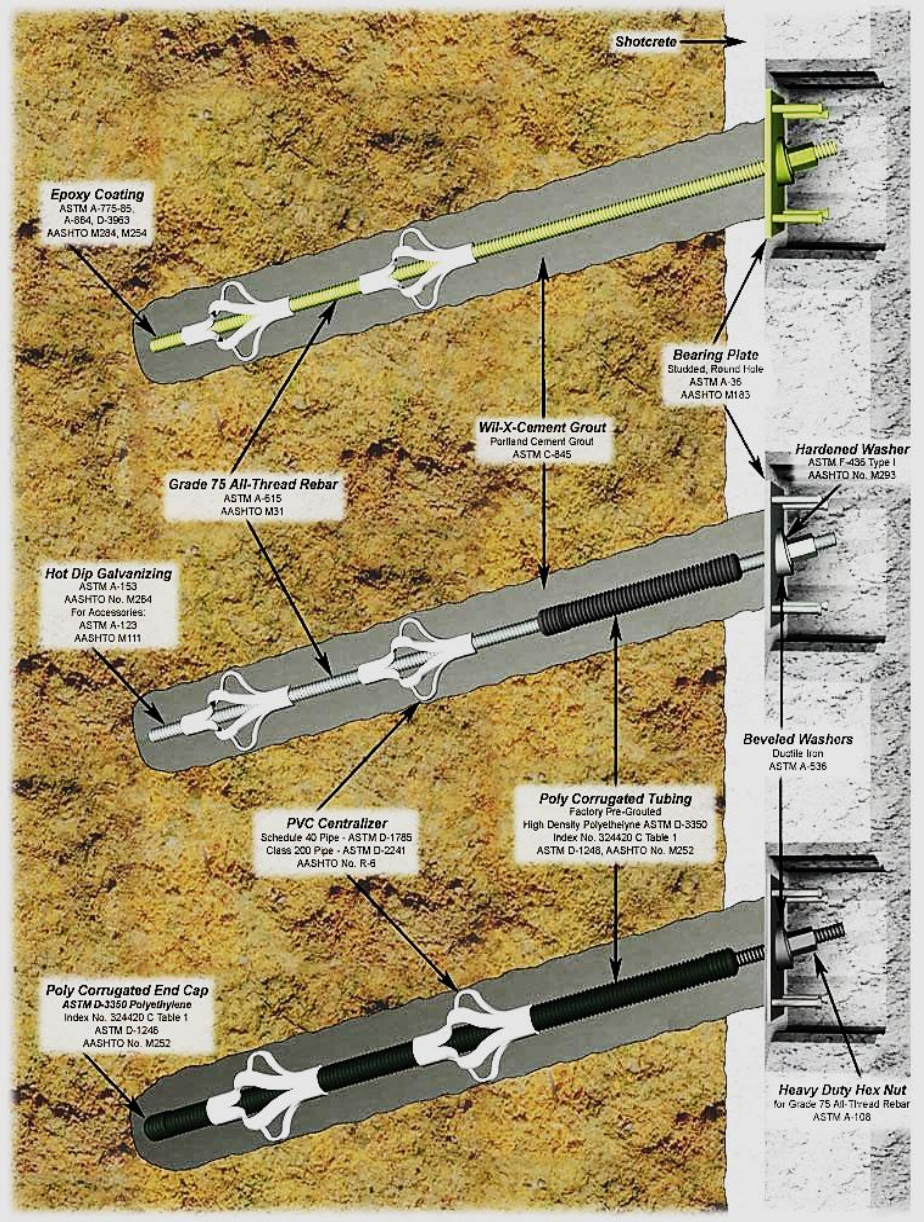

Figure 2.7: Elements of soil nailed wall (Source:https://www.regnumstroy.ru/en/soilnail.php)

2.6.1 Soil Nails

Soil nails are the primary structural elements of the slope. These are typically made of steel and are inserted into the ground at specific angles and depths. Soil nails serve as tension members, reinforcing the soil mass. The nails are installed in closely spaced rows and grouted into the surrounding soil to enhance their bonding and frictional resistance with the ground.

2.6.1.1 Different Soil Nail (Tendons) With Corrosion Protection Options

In soil-nailing steel nails (tendons) are installed into the ground to improve the stability and strength of the soil mass. To enhance the durability and longevity of soil nails, corrosion protection options are employed. Let's explore the different soil nail (tendons) and their corrosion protection options in detail:

(A) Drill Hollow Bar : (refer to Figure 2.8)

(a) *Bare*: In the bare configuration, the drill hollow bar is made of plain steel without any additional protective coating. This option is the most basic and economical, but it provides limited corrosion protection. It is suitable for non-corrosive environments or short-term applications where long-term durability is not a significant concern.

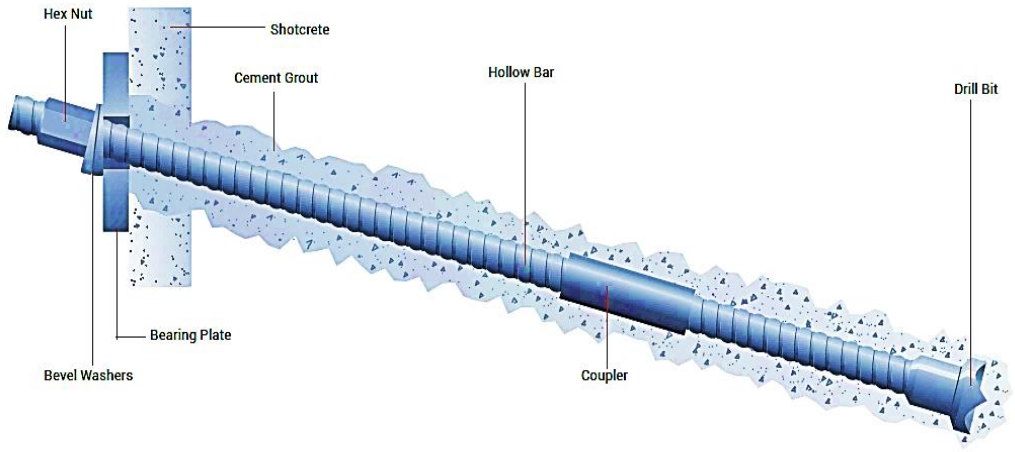

Figure 2.8: Drill hallow bar: Bare, Epoxy Coated, Galvanized (DYWIDAG,2022)

(b) *Epoxy Coated*: In this option, the drill hollow bar is coated with an epoxy layer. The epoxy coating acts as a barrier between the soil surrounding and the steel bar, protecting it from corrosion caused by moisture and/or chemicals. Epoxy-coated soil nails offer improved corrosion resistance compared to bare steel, making them suitable for moderate to mildly corrosive environments.

(c) *Galvanized*: Galvanized drill hollow bars are coated with a layer of zinc to provide enhanced corrosion protection. Galvanization is effective in preventing rust and corrosion, making the soil nails more suitable for highly corrosive environments or long-term applications where durability is crucial.

(B) Thread Bar: (refer to Figure 2.9)

(a) *Bare*: Similar to the drill hollow bar, a bare thread bar is made of plain steel without any protective coating. As with the drill hollow bar, this option is the most economical but offers limited corrosion protection, making it suitable for non-corrosive or short-term applications.

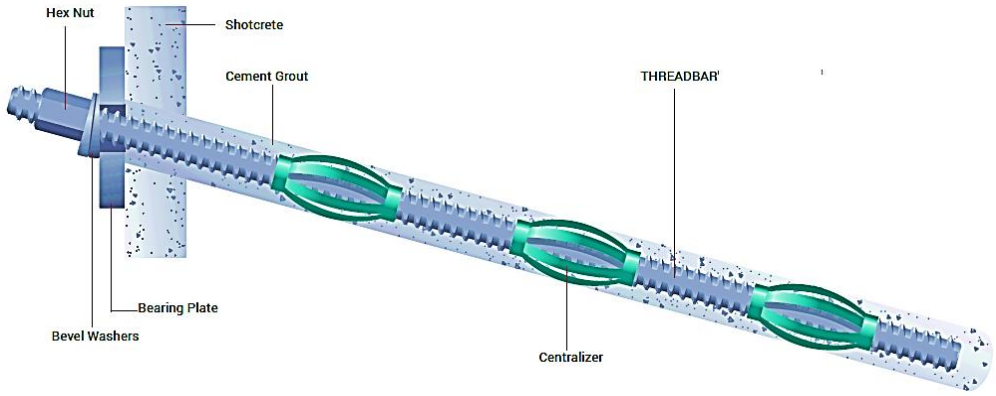

Figure 2.9: Thread bar: Bare, Epoxy Coated, Galvanized (DYWIDAG, 2022)

(b) *Epoxy Coated*: Thread bars with epoxy coatings provide improved corrosion resistance compared to bare steel. The epoxy layer acts as a barrier against moisture and chemicals, making them suitable for moderate to mildly corrosive environments.

(c) *Galvanized*: In this type galvanized thread bars are coated with zinc, offering a high level of corrosion protection. These soil nails are ideal for highly corrosive environments or long-term applications where durability is a concern.

(C) Thread Bar with Epoxy Coating Plus Partial (Double Corrosion Protection):

In this option, the thread bar is first coated with epoxy, as mentioned earlier, to provide a primary level of corrosion protection (Figure 2.10). Additionally, a Partial DCP (Double Corrosion Protection) system is employed. The Partial DCP involves placing a layer of sacrificial zinc-based material or smooth sheathing around the thread bar's exposed section before the final installation. This sacrificial material provides an extra layer of protection and acts as a sacrificial anode. In corrosive environments, the steel bar is protected from corrosion, thereby safeguarding the integrity of the thread bar. This epoxy coating or smooth sheathing combined with Partial DCP provides superior corrosion resistance, rendering it well-suited for demanding and highly corrosive conditions.

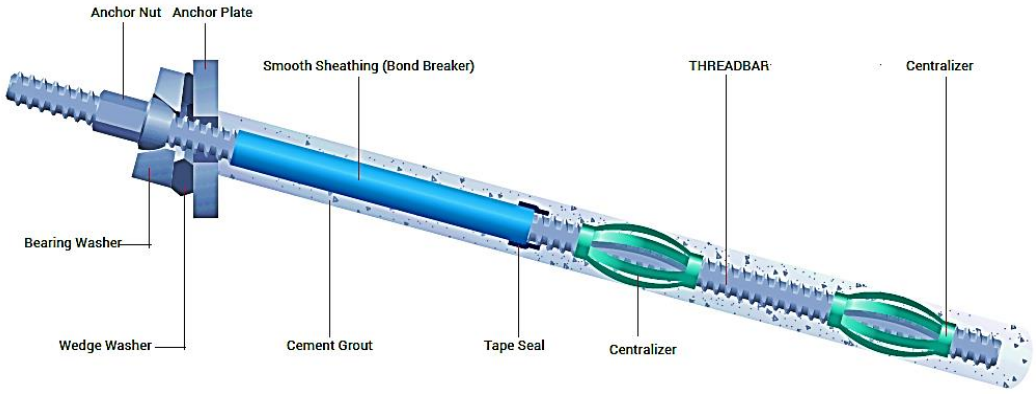

Figure 2.10: Thread bar: Epoxy Coated Plus Partial DCP (DYWIDAG, 2022)

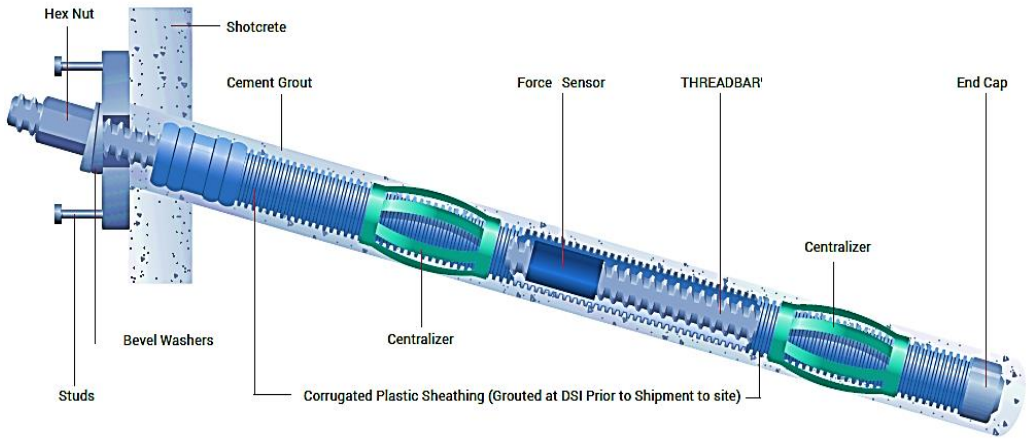

Figure 2.11: Thread bar with full-length DCP (DYWIDAG, 2022)

(D) Thread Bar with Full-Length DCP :

Similar to the previous option, this configuration includes the use of an epoxy-coated thread bar. However, instead of applying Partial DCP, the entire length of the thread bar is surrounded by the sacrificial zinc-based material or corrugated plastic sheathing (Figure 2.11). This Full-Length DCP system provides the highest level of corrosion protection, making it suitable for extremely harsh and aggressive environments with high corrosion potential.

(E) Self-Drilled Soil Nails:

Self-drilled soil nails (Figure 2.12) are a type of nail that already incorporates a drilling mechanism. These nails are typically made of high-strength steel and often come with an integral corrosion protection system. The corrosion protection options available for self-drilled soil nails are similar to those mentioned above, such as epoxy coating, smooth or corrugated plastic sheathing, galvanization, or DCP systems etc. The specific corrosion protection used in self-drilled soil nails may vary based on the manufacturer and project requirements.

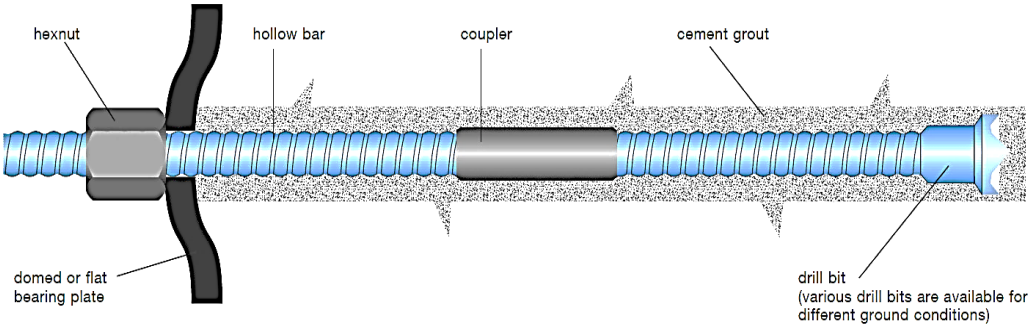

Figure 2.12: Self-drilled soil nails

(Source: https://structurae.net/en/media/109417-dywisupsup-drill-hollow-bar-anchors)

The choice of soil nail tendon and corrosion protection options depends on the specific project conditions, the level of environmental corrosion, and the desired service life. Factors such as groundwater conditions, type of soil, and the presence of corrosive substances in the soil all play a role in determining the most suitable corrosion protection for soil nails.

2.6.2 Hole Centralizers

In soil nailing, a hole centralizer is a device used during the installation of nails to safeguard the proper alignment and positioning of the nail within the borehole (Figure 2.13). Its primary aim is to maintain the soil nail's position in the center of the hole during the grouting process. The centralizer typically consists of a cylindrical or semi-cylindrical frame that fits around the soil nail. It has arms or fins extending outward, which make contact with the borehole walls. The arms help guide and center the soil nail within the hole, preventing it from deviating or tilting off-center. By using a hole centralizer, the soil nail is held securely in place, ensuring that the grout material flows evenly around the nail and bonds effectively with the surrounding soil. This proper bonding is crucial to achieve the desired stabilizing effect and increase the soil mass's overall strength and stability.

Figure 2.13: Hole centralizer (source- https://www.regnumstroy.ru/en/soilnail.php)

2.6.3 Facing Material

The facing material is the outer layer or surface of the soil nail wall or slope. It is the visible part of the structure that helps retain and protect the soil mass behind it. The facing material can vary, and common choices include shotcrete (sprayed concrete), concrete panels, or geogrid-reinforced materials. The facing material provides support and stability to the excavated slope or the retained soil.

2.6.4 Shotcrete

Shotcrete is a key element in soil nail walls and slopes, used as both the facing material and as a means to encapsulate and protect the soil nails. It is a high-strength concrete mixture that is pneumatically sprayed onto the exposed face of the slope or wall. Shotcrete reinforces the facing and soil nails, enhancing the overall stability of the structure.

2.6.5 Grout

In the installation process, in-situ steel bars are centrally positioned within drilled holes using centralizers (Figure 2.13) and then filled completely with a cement paste known as cement grout (Lazarte et al. 2003). Grout is a cement-based or epoxy material injected into the boreholes around the soil nails. It fills any voids and builds up the bond between the surrounding soil and nails. The grout also helps in distributing the load from the nails to the surrounding soils, ensuring a more uniform distribution of forces. Theoretical considerations in soil nailing encompass two primary interfaces: (a) the steel bar and cement grout interface and (b) the soil and grouted nails interface, as illustrated in Figure 2.14.

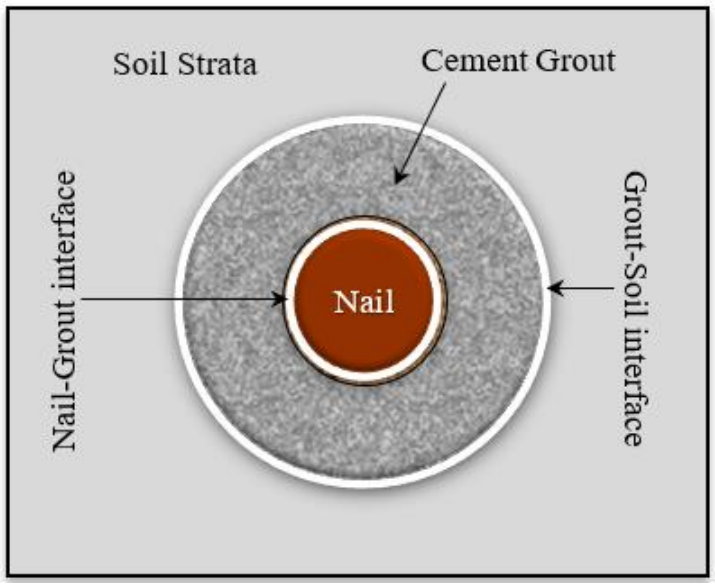

Figure 2.14: Soil-nailed and grout interface

2.6.6 Drainage System

Proper drainage is essential in soil nail walls and slopes to manage water flow and prevent water accumulation behind the structure as shown in Figure 2.15. A well-designed drainage system helps prevent hydrostatic pressures that could potentially destabilize the wall or slope.

2.6.7 Reinforcement Mesh

In some cases, a reinforcement mesh or geogrid may be used in conjunction with shotcrete to provide additional reinforcement and structural integrity to the facing material (Refer to Figure 2.15)

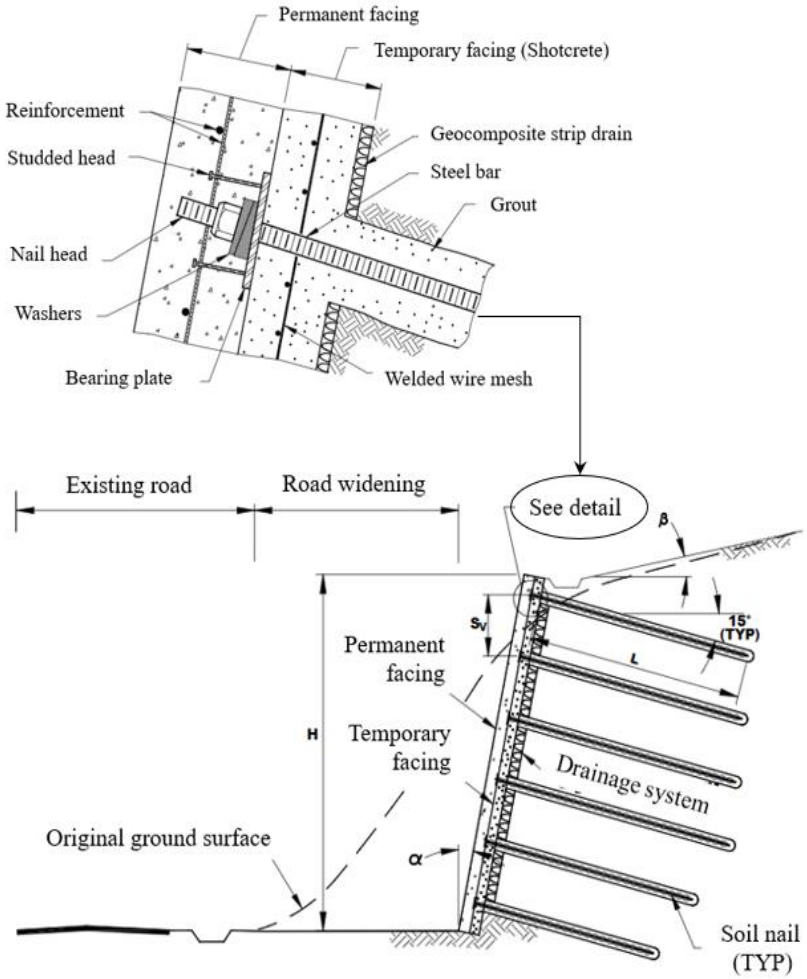

Figure 2.15: Typical cross-section of soil nailed wall (Lazarte et al. 2003)

2.7 Construction Sequence

Soil nailing is employed in various construction projects such as highways, railways, dams etc., particularly for embankment construction. The construction sequence for a soil-nailed slope involves several steps to ensure a stable and well-supported structure. The construction sequence is illustrated in the flowchart provided in Figure 2.16, while a pictorial representation can be found in Figure 2.17. Below is a detailed explanation of each stage:

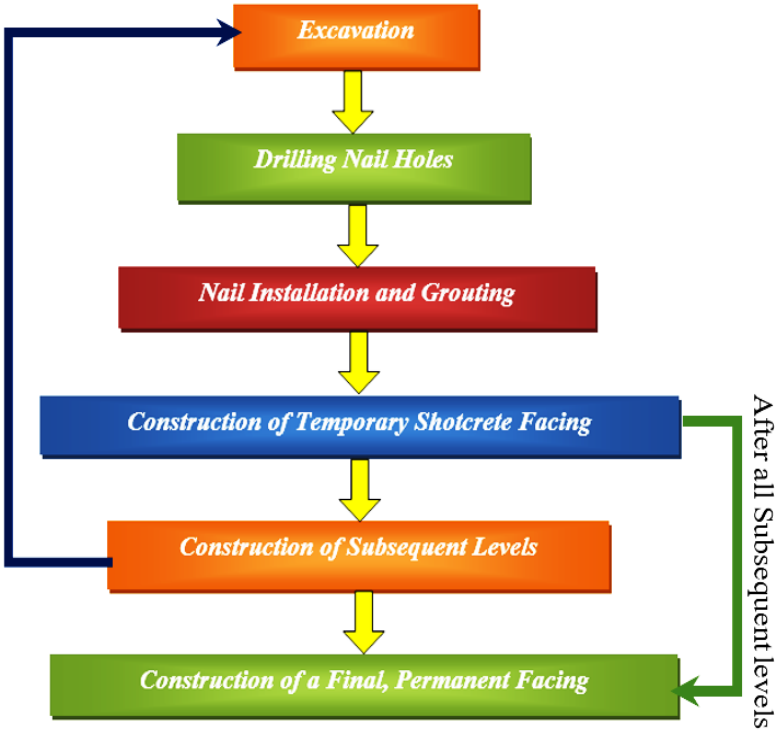

Figure 2.16: Construction sequence of soil nail slope/wall flow chart

(1) *Excavation*: The construction begins with excavation, which includes removing soil or rock to make the desired slope profile. The excavation process is carefully planned and executed to confirm the safety and stability of the site throughout construction.

(2) *Drilling Nail Holes*: After the excavation is completed, the next step is to drill holes into the exposed slope face. These holes will accommodate the soil nails that provide reinforcement and stability to the slope. The spacing and orientation

of the nail holes are determined based on engineering design considerations, taking into account factors such as soil properties and slope geometry.

(3) *Nail Installation and Grouting*: Soil nails are inserted into the drilled holes. These nails act as tension members and are typically coated with corrosion protection to ensure long-term durability. After the nails are placed in the holes, a grout material, usually cement-based or epoxy material, is injected into the holes to fill voids and bond the nails to the surrounding soil. The grouting process enhances the connection between the soil nails and the slope.

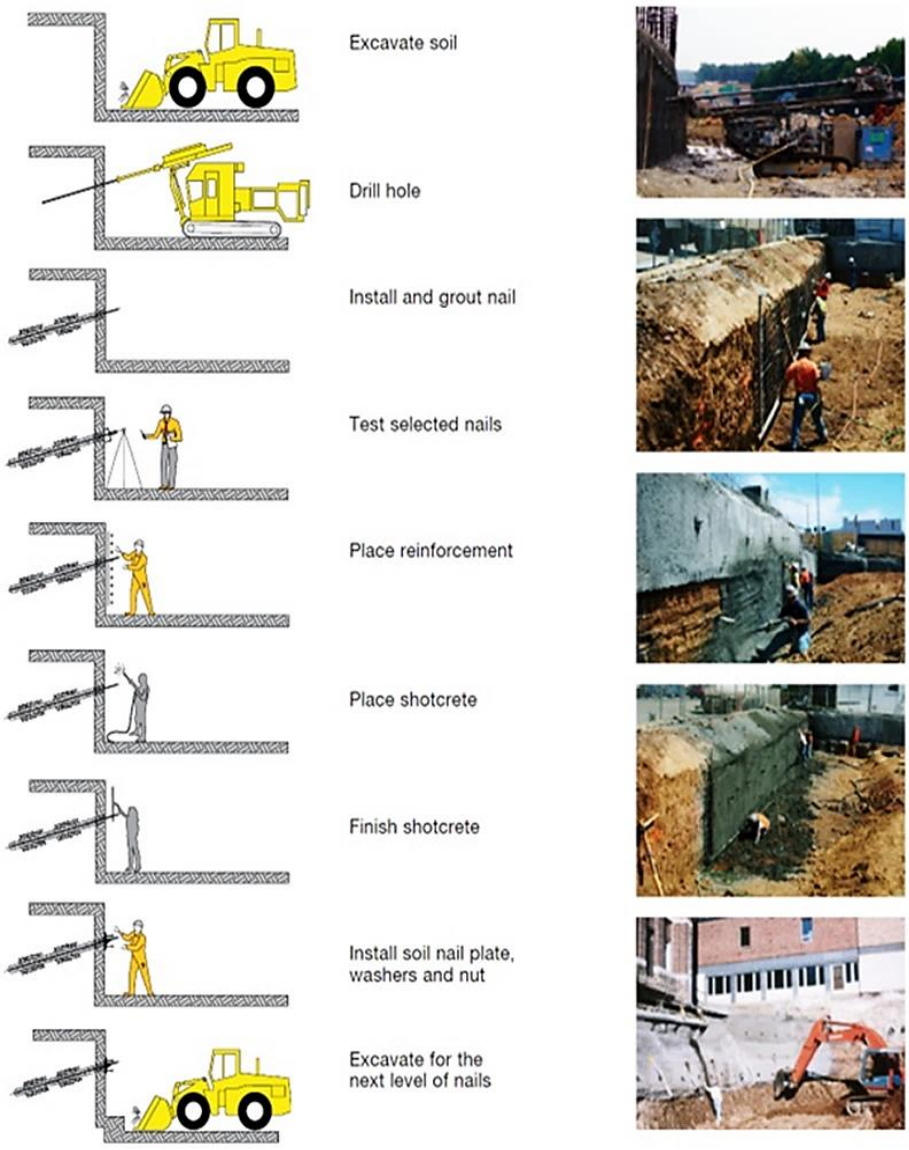

Figure 2.17: Soil nail wall construction sequence (Liu Jinyuan, HIIFP-120, 2014)

(4) *Construction of Temporary Shotcrete Facing*: To provide immediate support and stability to the slope during further construction, a temporary shotcrete facing is applied over the soil nails. Shotcrete is a high-strength concrete mixture that is pneumatically sprayed onto the slope face. It adheres to the soil nails and the exposed soil, creating a robust temporary facing that helps prevent erosion and protect the underlying slope during subsequent construction stages.

(5) *Construction of Subsequent Levels*: For slopes with multiple levels or tiers, the construction process is repeated for each level. Excavation, drilling, nail installation, grouting, and temporary shotcrete facing are carried out iteratively to stabilize each level before proceeding to the next.

(6) *Construction of a Final, Permanent Facing*: After all necessary levels are completed and the soil nails have provided the required stabilization, a final, permanent facing is constructed. This permanent facing can vary based on design specifications and project requirements. Common choices include reinforced shotcrete, concrete panels, or geogrid-reinforced materials. The permanent facing not only provides a finished appearance to the slope but also ensures long-term stability and protection against weathering and erosion.

Throughout the construction sequence, maintaining proper quality control and monitoring is essential to ensure that each step is executed correctly and that the final soil-nailed slope meets the required safety and stability standards. By adhering to this detailed construction sequence, reliable and durable soil-nailed slopes can be created, providing effective support and protection in various engineering projects.

2.8 Modes of Failure of Soil Nail Slope/Wall

Considerations of modes of failure in soil-nailed slopes or walls are crucial in geotechnical engineering, especially when designing and analyzing soil nail reinforcement systems. These failure modes represent potential mechanisms by which the stability of the slope or wall can be compromised. Understanding and addressing these failure modes are important for confirming long-term stability and structure safety. Proper reinforcement and design measures are employed to mitigate the risk of

these failure modes and create safe and reliable slope or wall systems. Regular monitoring and maintenance are also essential to address any potential issues and maintain long-term stability. The primary modes of failure for soil nail slopes or walls include: (a) “External Failure Modes” (b) “Internal Failure Modes” and (c) “Facing Failure Modes” (FHWA, 2003).

2.8.1 External Failure Modes

External failure modes pertain to potential failure surfaces that pass through or are located behind soil nails, irrespective of their interaction with them. In evaluating these modes, soil nail walls are treated as interconnected systems, with stability calculations incorporating soil forces along the potential failure surface to maintain equilibrium. When a failure surface intersects soil nails, these nails provide stabilizing forces that are considered alongside soil resisting forces. Assessing external stability is important in soil nail wall design due to the thoughtful implications of failure. The Byrne et al. (1998), study ensures that the wall can withstand destabilizing forces from excavation, service loads, and extreme events like seismic activity across various failure modes. Key factors influencing external stability include wall height, soil composition behind and beneath the wall, nail length, and the strengths of the soil, nails, and interfaces etc. This failure mode focuses on three main external failure modes: global, sliding (shear at the base), and bearing (basal heave), as shown in Figure 2.18, each examined for vulnerability to seismic effects.

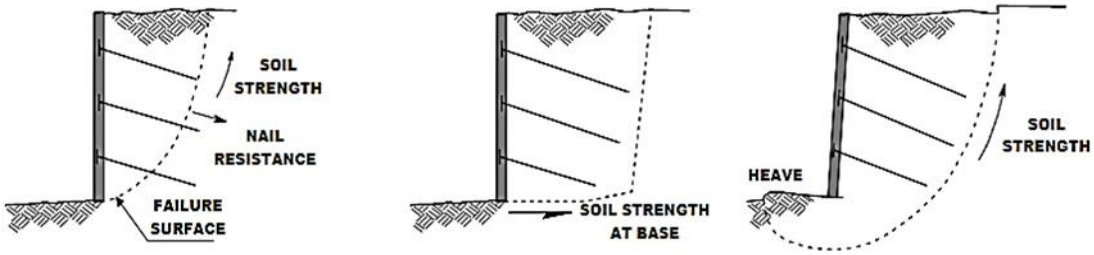

(a) Global Stability Failure (b) Sliding Stability Failure (c) Bearing Failure

Figure 2.18: External modes failure modes (Lazarte et al. 2003)

2.8.1.1 Global Stability

Global stability pertains to the overall stability of the reinforced soil nail wall system, encompassing both the retained soil mass and the nail-reinforced zone. In this failure mode, the resisting forces provided by the soil along the slip surface, as well as stabilizing forces from intersected nails, are insufficient to counteract the destabilizing forces. As excavation progresses, lateral deformation increases, activating additional shear stresses along the soil-nail/soil interface and generating axial forces in previously installed nails. This leads to the slip surface extending beyond and beneath the soil nail wall system, as illustrated in Figure 2.18a. With deeper excavation, the retained soil mass grows larger, increasing the potential for failure. To maintain global stability, soil nails must be installed such that their lengths extend well beyond the anticipated failure surface, as depicted in Figure 2.19.

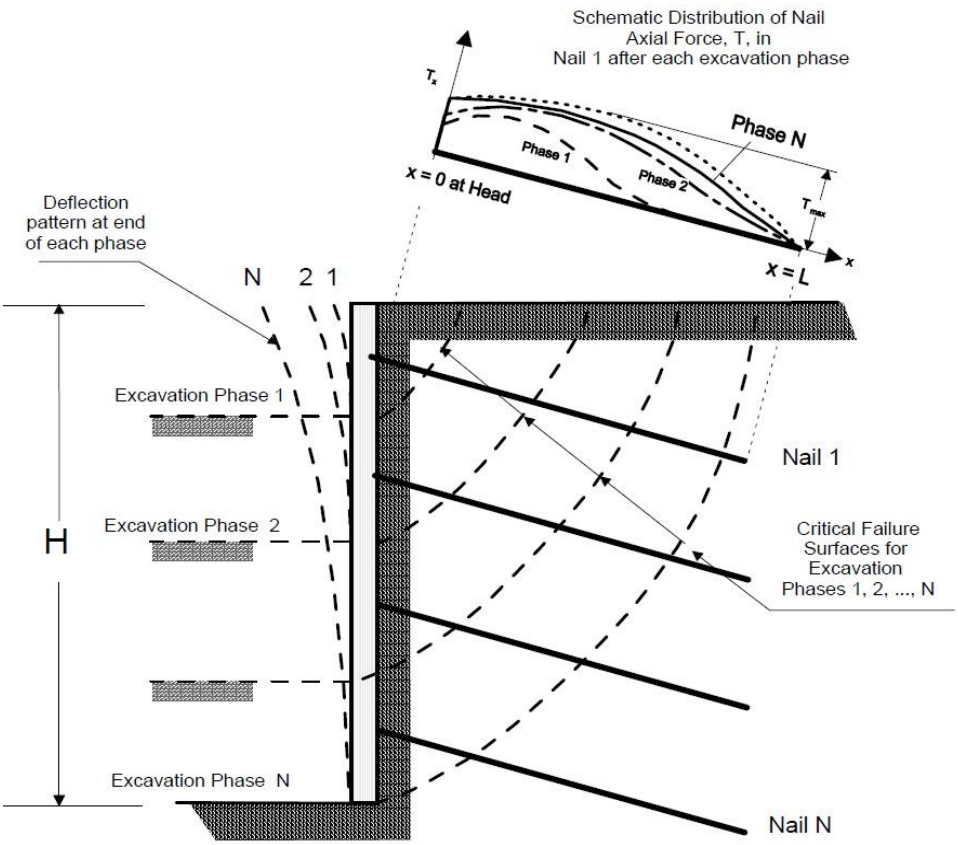

Figure 2.19: Tensile forces of soil nails and possible failure surfaces (Lazarte et al. 2003)

Assessing the global stability of soil nail walls is commonly based on two-dimensional limit-equilibrium principles, similar to traditional slope stability analyses. In this approach, the potentially sliding mass is modelled as a rigid block, and a factor of safety (FOS) is calculated by balancing stabilizing and destabilizing forces. Various methods, each with unique assumptions and computational procedures, are used to evaluate global stability. These methods consider different failure surface geometries behind the soil nail wall, such as planar, bi-linear (two-wedge slipping mass), parabolic, log spiral, and circular shapes etc.

However, the main limitation of limit-equilibrium methods is their inability to predict deformations or account for the mobilisation of resisting forces within the soil and soil nails. Numerical techniques, such as the Finite Element Method (FEM) and Finite Difference Method (FDM), address these limitations by estimating deformations, making them valuable tools in soil nail wall design. Despite this, designers often rely on semi-empirical methods, derived from prior experiences, to estimate deformations within acceptable serviceability limits. Subsequent sections of this chapter provide detailed guidance on permissible deformation thresholds for soil nail walls to ensure their performance and safety.

(A) Global Stability Analysis

The destabilizing forces include the weight (W) and surcharge loads (Q), while stabilizing forces along the failure surface are the shear force (SF) and the collective tensile force (TF) of all nails at depth H, referred to as T_{EQ}. The factor of safety against global failure (FS_G) compares resisting forces, acting tangentially to the potential failure plane, to driving forces. Figure 2.20 illustrates a simple, single-wedge failure mechanism to illustrate the elements involved in analyzing the global stability of soil nail walls.

$$FS_G = \frac{\sum \text{Resisting Force}}{\sum \text{Driving Force}} \tag{2.1}$$

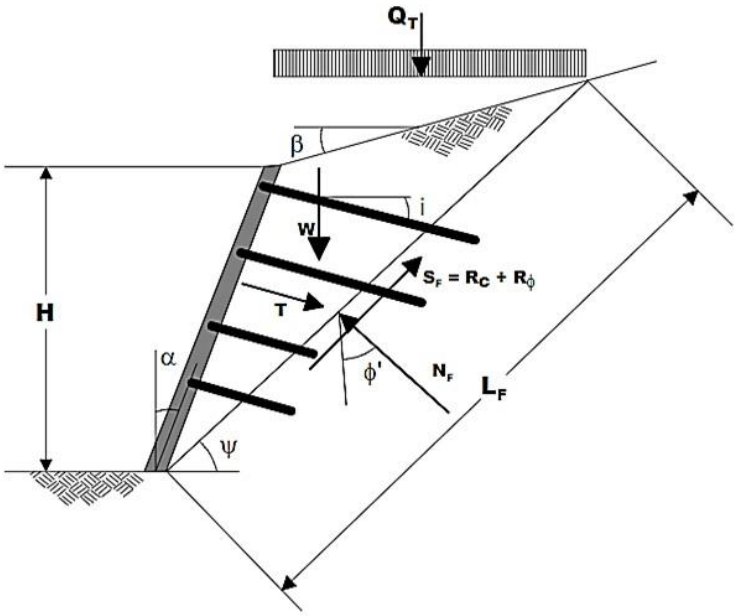

Figure 2.20: Failure mechanism of soil nailed wall in single-wedge failure (Lazarte et al. 2003)

Where, "α is wall face batter angle (from vertical); β is slope angle; ϕ' is soil effective angle of internal friction; c' is soil effective cohesion; ψ is the inclination of failure plane; i is nail inclination; LF is the length of failure plane; W is weight of sliding mass; Q_T is surcharge load; T_{EQ} is equivalent nail force; N_F is the normal force on failure surface; S_F is shear force on failure surface; Rc is cohesive component of SF; and R_ϕ is frictional component of SF".

On the failure plane, the normal and tangent forces are (FHWA, 2003):

$$\sum \text{Normal Forces} = (W + Q_T)\cos\psi + T_{EQ}\cos(\psi - i) - N_F = 0 \qquad (2.2)$$

$$\sum \text{Tangent Forces} = (W + Q_T)\sin\psi - T_{EQ}\sin(\psi - i) - S_F = 0 \qquad (2.3)$$

Where; $S_F = R_c + R_F = c_m L_s + N_F$; $\text{Tan}\,\phi_m = \frac{\text{Tan}\phi'}{FS_G}$; $c_m = \frac{c'}{FS_G}$

The paragraph explains the methods used to ensure the stability of soil nail systems. Typically, a single safety factor is applied to account for both the soil's cohesion and friction, though separate factors could be used. Most analyses focus on balancing forces, but in some cases, rotational stability also needs to be considered. While advanced calculations for different failure shapes, like wedges, are possible, they are

rarely used in practical design. Instead, designers rely on computer programs to create soil nail system designs. To confirm the accuracy of these designs, a simple model shown in Figure 2.20, along with basic equations, can be used for validation.

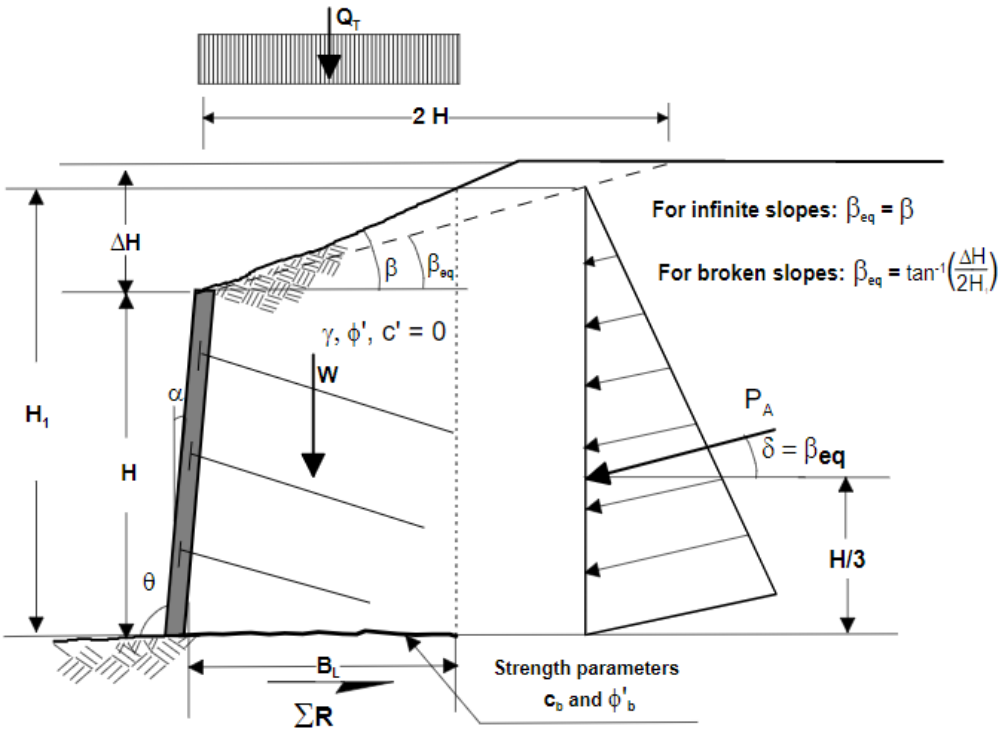

Figure 2.21: Soil nail wall sliding stability (Lazarte et al. 2003)

Where, "H is wall height; ΔH is slope rise up to bench (if present); βeq is equivalent backslope angle [for broken slopes βeq = $\tan^{-1}$(ΔH/H), for infinite slopes βeq = β]; α is faced batter angle; θ is the inclination of wall face from horizontal (i.e., θ = α + 90°); δ is wall-soil interface friction angle [for a broken slope, δ = βeq, for infinite slope, δ = β]; γ is the total unit weight of soil mass; H_1 is effective height over which the earth pressure acts [H_1 = H + (B_L + tan α) tan βeq]; K_A is active earth pressure coefficient for soil behind the soil nail wall system; c_b is soil cohesion strength along the base; B_L is the length of the horizontal failure surface where c_b is effectively acting; W is the weight of soil nail block; Q_D is the permanent portion of total surcharge load Q_T; P_A is the active lateral earth pressure; β is backslope angle; ϕ'$_b$ is the effective angle of internal friction of the base (remoulded or residual value maybe needed if the significant movement takes place); ϕ' is effective friction angle of soil behind soil nail block."

Global Stability Analysis Steps:

1. This analysis helps calculate the minimum safety level needed for the soil to not slide, based on the lengths of the nails.
2. It also determines the force required in each nail to prevent global failure.

(B) Sliding Stability Failure

The analysis of sliding stability evaluates the ability of a soil nail wall to resist lateral earth pressures from the retained soil and prevent movement along its base. Sliding failure happens when the lateral pressures from excavation exceed the resistance at the base, as shown in Figure 2.21. To assess sliding stability, methods similar to those used for gravity-retaining structures, such as Coulomb or Rankine earth pressure theories, are applied. In this approach, the soil nail wall system is treated as a solid block subjected to lateral earth forces from the retained soil. This block has a nearly flat base at the bottom of the wall (or slightly below, if a weak horizontal soil layer exists) and extends behind the nails, sloping steeply upward toward the surface behind the reinforced area (see Figure 2.21). The movement along the base is significant enough to mobilize the assumed lateral pressures. According to FHWA (2003), the factor of safety against sliding (FS_{SL}) is calculated by dividing the resisting forces (ΣR) by the applied driving forces (ΣD).

$$FS_{SL} = \frac{\sum \text{Resisting Force } (\Sigma R)}{\sum \text{Driving Force } (\Sigma D)} \tag{2.4}$$

$$\sum R = c_b + B_L\,(W + Q_D + P_A \sin\beta)\tan\phi'_b \tag{2.5}$$

Where, "c_b is soil cohesion strength along the base, B_L is length of the horizontal failure surface where c_b is effectively acting, W is the weight of soil nail block, Q_D is permanent portion of total surcharge load Q_T, P_A is the active lateral earth pressure, β is backslope angle, ϕ'_b is effective angle of internal friction of the base (remoulded or residual value may be needed if significant movement takes place), ϕ' is effective friction angle of soil behind soil nail block."

$$\sum D = (P_A \cos\beta) \tag{2.6}$$

The active lateral earth force (P_A) is defined as (FHWA 2003):

$$P_A = \frac{\gamma H1^2}{2} K_a \quad (2.7)$$

Where, "γ is the total unit weight of soil mass, H_1 is the effective height over which the earth pressure acts, β is the backslope angle, K_a is the coefficient active earth pressure."

$$[H_1 = H + (B_L + \tan \alpha) \tan \beta_{eq}] \quad (2.8)$$

Where, "H_1 is effective height over which the earth pressure acts, H is wall height, B_L is the length of the horizontal failure surface where c_b is effectively acting, α is wall face batter angle (from vertical), β_{eq} is an equivalent backslope angle."

The active earth pressure coefficient (K_a) can be calculated using a formula derived from either the standard Coulomb or Rankine theory for cohesionless soil. This implies that the soil behind the soil nail wall behaves as though it lacks cohesion (c' = 0) during prolonged loading situations.

As per the Coulomb theory K_a is (Lazarte et al. 2003),

$$K_a = \frac{\sin^2(\theta + \emptyset')}{\sin^2\theta \sin(\theta - \delta)\left[1 + \sqrt{\frac{\sin(\emptyset + \delta)\sin(\emptyset' - \beta)}{\sin(\theta - \delta)\sin(\theta + \beta)}}\right]^2} \quad (2.9)$$

The Rankine theory offers the coefficient of active earth pressure (K_a) for walls with face batter angles (α) less than 8 degrees and dry, sloping ground behind the wall as follows (Lazarte et al. 2003):

$$K_a = \cos\beta \left[\frac{\cos\beta - \sqrt{\cos^2\beta - \cos^2\emptyset'}}{\cos\beta + \sqrt{\cos^2\beta - \cos^2\emptyset'}}\right] \quad (2.10)$$

In the particular scenario of a vertical wall (where $\alpha = 0^0$ or $\theta = 90^0$), with dry, flat ground behind the wall ($\beta = 0$), and no shear stresses acting on the wall-soil interface ($\delta = 0$), the Rankine theory simplifies the coefficient of active earth pressure to the commonly recognized expression (Lazarte et al. 2003):

$$K_a = \tan^2\left(45 + \frac{\emptyset'}{2}\right) \quad (2.11)$$

In contrast, Equation 2.9 derived from the Coulomb theory and Equation 2.10 from the Rankine theory. Despite this, both theories produce nearly identical outcomes. Nevertheless, it's crucial to recognize that Equation 2.11 is a highly simplified expression and should be reserved for preliminary estimations only. For more comprehensive analyses, it's advisable to employ the complete formulations of either the Rankine or Coulomb theories.

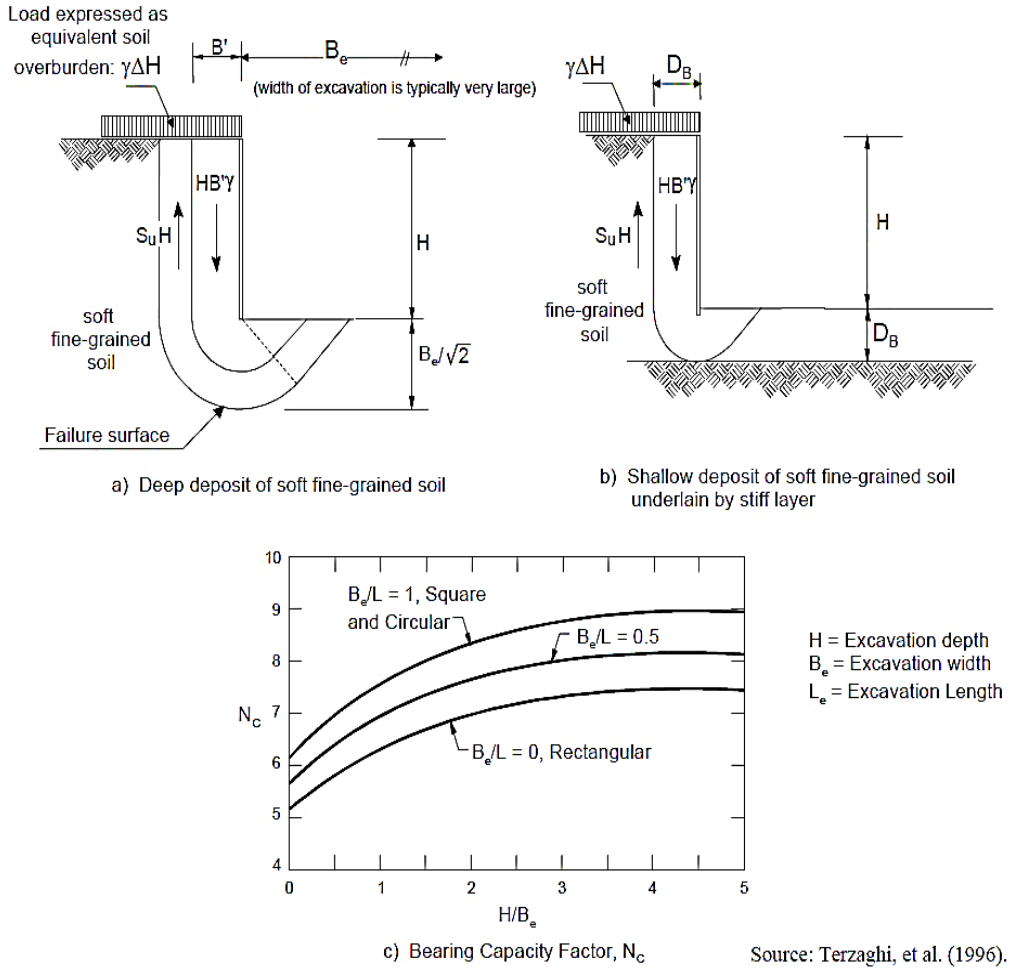

Figure 2.22: Bearing capacity (heave) analysis (Lazarte et al. 2003)

(C) Bearing Failure (Basal Heave)

Sometimes, the bearing capacity can pose a challenge when digging a soil nail wall in soft, fine-grained soils. Unlike soldier piles in cantilever or ground anchor walls, the

facing of soil nail walls doesn't extend below the excavation bottom. This can result in an uneven load during excavation, causing the bottom of the excavation to rise and possibly triggering a bearing capacity failure of the foundation, as depicted in Figure 2.22a (Lazarte et al. 2003).

To assess this type of failure, equations are available to evaluate the potential for rising at the bottom of excavations. The factor of safety against rising (FS_H), as provided by Terzaghi et al. (1996), can be utilized:

$$FS_H = \frac{S_u \, N_c}{H_{eq} \left[\gamma - \frac{S_u}{B'}\right]} \tag{2.12}$$

Where, "S_u is the undrained shear strength of the soil; N_c is bearing capacity factor (Figure 2.22); γ is the unit weight of the soil behind the wall; H is the height of the wall; H_{eq} is equivalent wall height i.e. (H+ΔH), with ΔH is an equivalent overburden; B' is the width of influence i.e. $B' = \frac{B_e}{\sqrt{2}}$, where B_e is the width of excavation."

The bearing capacity factor relies on geometric conditions. For wide excavations, where soil nail walls are common, H/B_e can be assumed as 0 for conservative estimation. For exceptionally long walls, it's prudent to set $B_e / L_e = 0$ and $N_c = 5.14$. If there's a strong layer beneath the soft one, at a depth $D_B < 0.71B_e$ below the excavation bottom (as depicted in Figure 2.22b), B' in Equation 2.12 should be replaced with D_B. Also, when the excavation width is significant or the shearing resistance contribution (S_u H) outside the failure block of width B' is ignored, Equation 2.12 becomes a conservative $FS_H = N_c / \gamma H_{eq}$. These equations are conservative as they overlook the shear contribution of nails intersected by the failure surfaces shown in Figures 2.22a and 2.22b (Lazarte et al. 2003). Alternatively, slope stability analysis programs can be utilized to conduct equivalent bearing capacity analyses, considering deep-seated failure surfaces through the foundation. However, in most cases, bearing capacity analyses aren't necessary for soil nail walls unless soft soils (e.g., $S_u \leq 25$ kPa) are present at the excavation bottom. An exception to this is when significant loads are applied behind the proposed soil nail wall, in which case a bearing capacity analysis is advisable regardless of soil conditions. For FOS against heave in soil nail walls, typical values of 2.5 and 3 are suitable for temporary and permanent walls,

respectively. Since the majority of soil nail walls are not constructed in soft fine-grained soils, this failure mode isn't important for most soil nail projects (Lazarte et al. 2003).

2.8.2 Internal Failure Modes

Internal failure modes relate to failures occurring within the load transfer mechanisms connecting the soil, nails, and grout. The process involves mobilizing the bond strength between the grout and the surrounding soil, and this occurs as the soil nail wall system undergoes deformation during excavation. Throughout this deformation, the bond strength is progressively activated along the entire soil nail. The activation is influenced by various factors that come into play during this process. Consequently, the activation of bond strength leads to the development of tensile forces within the nail. These forces depend on multiple factors, such as the soil nail's tensile strength, its length, and the bond strength itself. It is important to consider these factors as they directly affect the distribution of bond stress along the nail. Due to the variability in bond stress distribution, different internal failure modes can be realized. The occurrence of these internal failure modes is crucial to understand as they provide insights into the behaviour of the soil nail system under various conditions. To illustrate these internal failure modes related to the soil nail, Figure 3.23 offers visual representations that help in comprehending the phenomena better. By examining these figures, one can gain a clearer understanding of how the system responds to different conditions and failure scenarios.

(a) Nail-Soil Pullout

The primary mode of internal failure in a soil nail slope/wall is termed as pullout failure. This type of failure occurs when either the pullout capacity per unit length is insufficient or when the length of the nail itself is not adequate to withstand the applied forces behind the slip surface. The measure commonly used to describe this phenomenon is the mobilized pullout per unit length, which is also referred to as the load transfer rate (Q). This parameter indicates how effectively the soil nails are transferring the load to the surrounding soil. When the pullout capacity or the nail

length is insufficient, the load transfer rate may not be able to adequately support the applied loads, leading to the occurrence of pullout failure (Q) within the soil nail wall (FHWA 2003).

$$Q = \pi \, q \, D_{DH} \tag{2.13}$$

Where, " q is mobilized shear stress acting around the perimeter of the nail-soil interface; D_{DH} is the average or effective diameter of the drill hole."

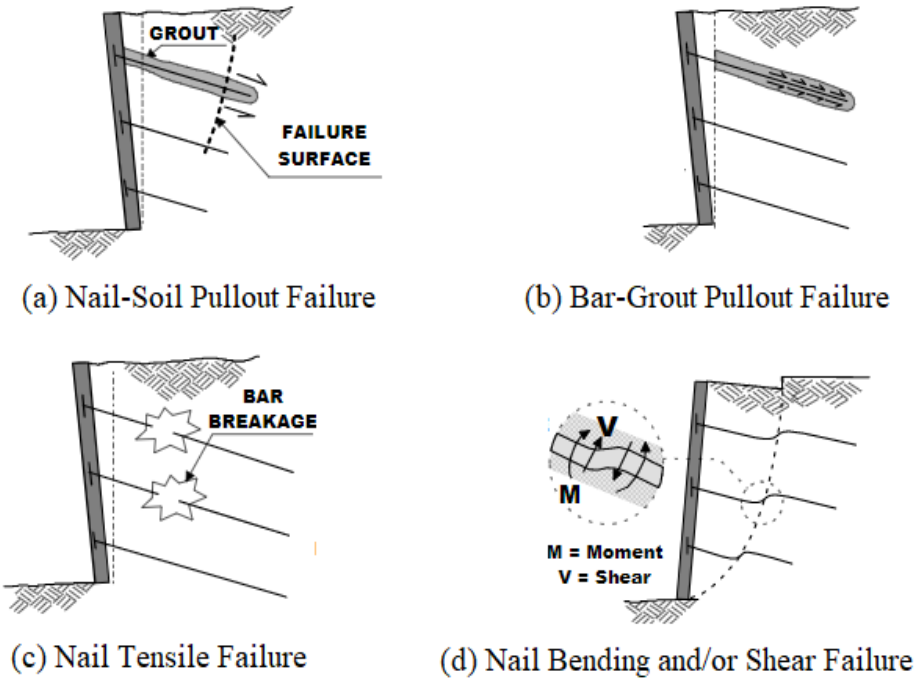

Figure 2.23: Internal failure modes (Lazarte et al. 2003)

Taking into account a solitary segment of a nail experiencing a tensile force (T_o) applied at one end, and employing the concept of force equilibrium along the incremental length of the nail depicted in Figure 2.24. The tensile force can be correlated with the interface shear stress in the following manner (FHWA 2003):

$$dT = \pi \, q \, D_{DH} \, dx \quad = Q \, dx \tag{2.14}$$

The mechanism for shifting stresses from the interface between the nail and soil to the tensile forces inside the nail bar is shown by the provided equation. Typically, the

following expression can be used to represent the tensile force (T) at a distance "x" along the bar (FHWA 2003):

$$T(x) = \int_0^x \pi\, q\, D_{DH}\, dx \quad = \int_0^x Q\, dx \tag{2.15}$$

The distribution of mobilized bond shear stress is non-uniform, as shown in Figure 2.24, and depends on multiple factors like nail length, applied tensile force magnitude, grout properties, and soil conditions. To simplify the analysis, it's frequently assumed that the mobilized bond strength stays constant along the length of the nail. This assumption leads to a uniform load transfer rate (Q) (FHWA 2003).

$$T_o = T\,(L_P) = Q\,(L_P) \tag{2.16}$$

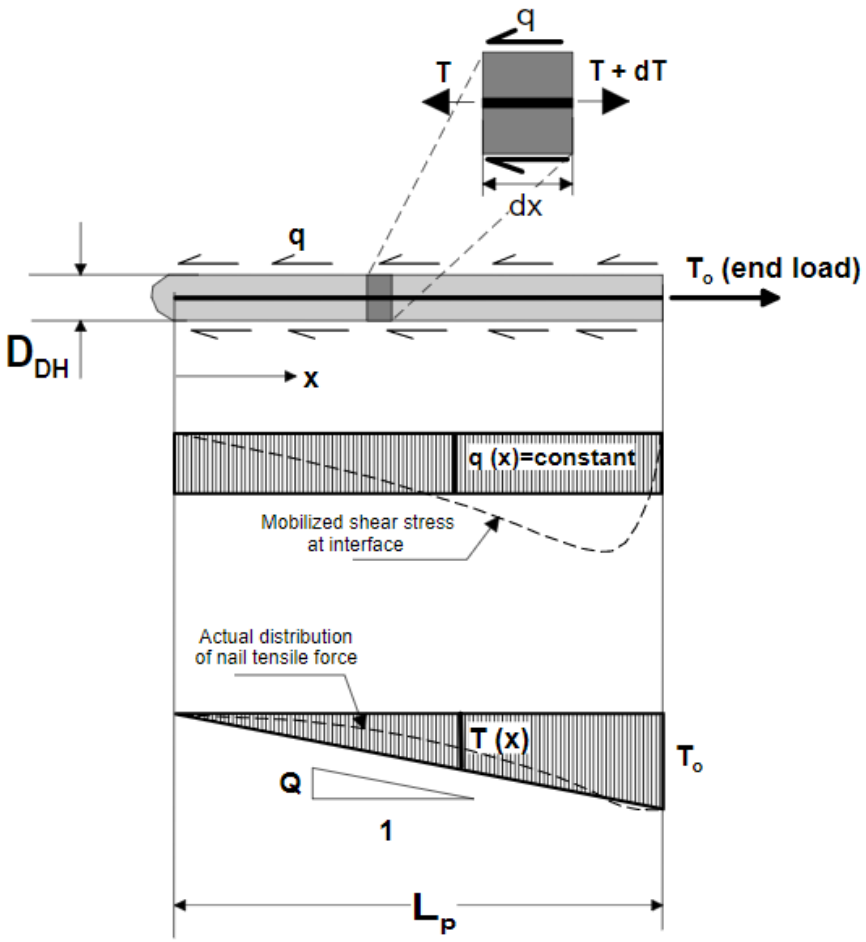

Figure 2.24: Single nail stress-transfer mode (Lazarte et al. 2003).

The pullout capacity, R_p, represents the maximum force a soil nail can endure before experiencing pullout failure, achieved when the ultimate bond strength between the soil and the nail is reached. This strength depends on soil and nail properties, and its calculation varies based on design considerations. R_p is vital for ensuring the stability and integrity of soil nail walls and is expressed in the FHWA, 2003 code as:

$$R_P = T_{max} = Q_u \, L_p \tag{2.17}$$

As per FHWA, 2003 recommendations the pullout capacity per unit length is

$$Q_u = \pi \; q_u \, D_{DH} \tag{2.18}$$

Where, "q_u is ultimate bond strength and $\pi \, D_{DH}$ is the circumference of drill hole diameter."

In the existing literature, mentions of "q_u" or "Q_u" are the bond strength relies on several factors, including soil type, soil conditions, and the method of nail installation. Table 2.1 displays typical values of ultimate bond strength for various soils and drilling techniques. An alternative approach involves using previously mentioned equations to compute consistent ultimate bond strengths and pullout capacity per unit length via nail pullout tests. This alternative method offers valuable insights into the behaviour of the nail-soil system under specific conditions, contributing to a comprehensive grasp of load transfer mechanisms. To manage uncertainties concerning bond strength and soil-grout interaction, design considerations integrate the following permissible values for bond strength or pullout capacity per unit length (FHWA, 2003):

$$q_{All} = \frac{Q_u}{FS_p} \tag{2.19}$$

$$R_{p\,All} = \frac{R_p}{FS_p} \tag{2.20}$$

Where, "$R_{p\,All}$ is allowable nail pullout resistance, R_p is nail pullout resistance, FS_P is the factor of safety against pullout failure. In general, against pullout failure a minimum factor of safety 2 is recommended ."

Table 2.1: Estimated bond strength of soil nails in soil and rock. (Source: Elias and Juran, 1991). (Lazarte et al. 2003)

Material	Construction Method	Soil/Rock Type	Ultimate Bond Strength, q_u (kPa)
Rock	Rotary Drilled	Marl/limestone	300 - 400
		Phyllite	100 - 300
		Chalk	500 - 600
		Soft dolomite	400 - 600
		Fissured dolomite	600 - 1000
		Weathered sandstone	200 - 300
		Weathered shale	100 - 150
		Weathered schist	100 - 175
		Basalt	500 - 600
		Slate/Hard shale	300 - 400
Cohesionless Soils	Rotary Drilled	Sand/gravel	100 - 180
		Silty sand	100 - 150
		Silt	60 - 75
		Piedmont residual	40 - 120
		Fine colluvium	75 - 150
	Driven Casing	Sand/gravel	
		low overburden	190 - 240
		high overburden	280 - 430
		Dense Moraine	380 - 480
		Colluvium	100 - 180
	Augered	Silty sand fill	20 - 40
		Silty fine sand	55 - 90
		Silty clayey sand	60 - 140
	Jet Grouted	Sand	380
		Sand/gravel	700
Fine-Grained Soils	Rotary Drilled	Silty clay	35 - 50
	Driven Casing	Clayey silt	90 - 140
	Augered	Loess	25 - 75
		Soft clay	20 - 30
		Stiff clay	40 - 60
		Stiff clayey silt	40 - 100
		Calcareous sandy clay	90 - 140

(b) Bar-Grout Pullout

Bar-Grout Pullout failure is a type of failure mechanism that can occur in soil-nailed slopes. In the context of grout pullout failure, the failure can occur due to the loss of bond between the soil nail (bar) and the grout surrounding it. The bond between the grout and nails is essential for load transfer and providing stability to the slope. However, several factors such as soil properties, grout material, grout quality, construction practices, and external loads can contribute to the degradation of this bond

over time. As the bond weakens or deteriorates, the load transfer efficiency between the surrounding soil and the nail decreases. This can lead to reduced resistance against sliding or shearing forces acting on the slope, making it vulnerable to failure. To prevent bar-grout pullout failure, it is crucial to ensure proper installation practices, including adequate grouting to achieve a strong bond between the surrounding soil and nails. Additionally, regular inspections and maintenance are necessary to identify any signs of bond degradation or deterioration, allowing for timely remedial measures to be implemented. Proper design and consideration of factors affecting bond strength are also essential to enhance the enduring stability of soil-nailed slopes and mitigate the risk of bar-grout pullout failure.

(c) Nail Tensile Failure

Nail Tensile Failure is failure mechanism that can occur in soil-nailed slopes. In the soil nailing technique, steel nails or bars are entrenched into the slope and grouted to enhance the slope's stability. The nails act as reinforcement elements that transfer tensile forces from the slope to the grouted mass and the surrounding soil. Nail tensile failure happens when the tensile force in the nail exceeds its strength, leading to the nail's rupture or pulling out from the grouted mass or soil slope. This can occur due to various reasons, such as excessive external loads, inadequate nail dimensions, poor-quality materials, or inadequate installation etc. When the soil-nailed slope is subjected to tensile forces, the nails are stressed, attempting to pull them out of the grouted mass or soil slope. If the applied tensile forces exceed the nails' tensile strength, they may fail, reducing their ability to reinforce the slope. To prevent nail tensile failure, it is crucial to carefully design the soil nailing system, considering the magnitude of the expected tensile forces and selecting appropriate nail dimensions and materials. The nails must be capable of withstanding the anticipated tensile loads to ensure their long-term effectiveness in stabilizing the slope. Regular inspections and monitoring of the slope's condition are also essential to detect any signs of nail deterioration or overstressing, allowing for timely maintenance and repair. Implementing proper design, construction, and maintenance practices, can reduce the risk of nail tensile failure and confirm the overall stability and safety of soil-nailed slopes. The interaction

between the nails positioned behind the wall and the soil involves complex dynamics. As mentioned earlier refer to Figure 2.19, the wall's outward movement during soil excavation ahead of the wall imposes loads on the soil nails. Within the nail, the section known as the anchoring zone, situated behind the failure surface, experiences a pulling force away from the soil slope. These tensile forces (T), vary along the length of the soil nail. They start from zero at the nail's end, reach a peak value (T_{max}) at the midpoint, and then decrease to a final value (T_o) at the facing, as illustrated in Figure 2.25.

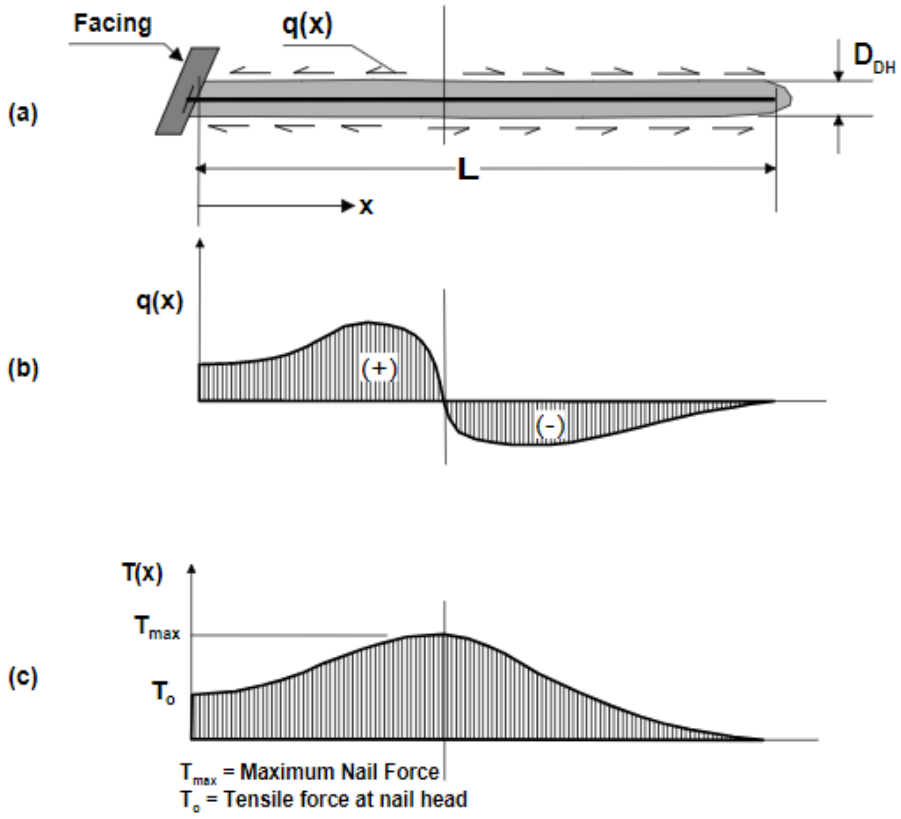

Figure 2.25: Transfer mechanism - soil nail stress (Lazarte et al. 2003).

Later explanations will reveal that the peak tensile force within the nail bar may not consistently align with the spot where the nail intersects the failure surface. Along the interface between grout and soil, the activated shear stress, denoted as q, displays a varied pattern transitioning from "positive" to "negative," as demonstrated in Figures 2.25a and 2.25b. Figure 2.25c provides a schematic representation of how the tensile force (T) distributes along the soil nail.

(1) *Simplified Distribution of Nail Tensile Forces*:

For design, the distribution of tensile force along the nail, illustrated in Figure 2.25, can be further detailed as simplified in Figure 2.26. Within this schematic, the tensile force within the nail undergoes a gradual increase at a consistent slope denoted as Q_u, which equates to the pullout capacity per unit length. It rises gradually until it reaches its peak value, T_{max}, and subsequently declines at a rate Q_u towards the value T_o at the nailhead. Regarding Figure 2.26, three conditions regarding the maximum tensile force deserve attention. T_{max} is constrained by three limiting factors: the pullout capacity (R_P), the tensile capacity (R_T), and the facing capacity (R_F). Should R_P be inferior to both R_T and R_F, the value of T_{max} is governed by pullout failure. Conversely, if R_T falls short of R_P and R_F, tensile failure dictates T_{max}. Finally, if R_F proves lesser than both R_T and R_P, the facing's failure may control T_{max}, depending on the ratio of T_o to T_{max}. To achieve a well-balanced design, all resisting components in the system should possess comparable margins of safety; no component must be significantly over or undersized. When considering nail tensile forces, an effective design should strike a balance among the capacities of all resisting elements. Therefore, the values of R_P, R_T, and R_F need to be appropriately aligned to ensure a stable and reliable design (Lazarte et al. 2003). Additionally, Figure 2.27 illustrates the limitations related to tensile forces in nails, including pullout and tensile resistance control.

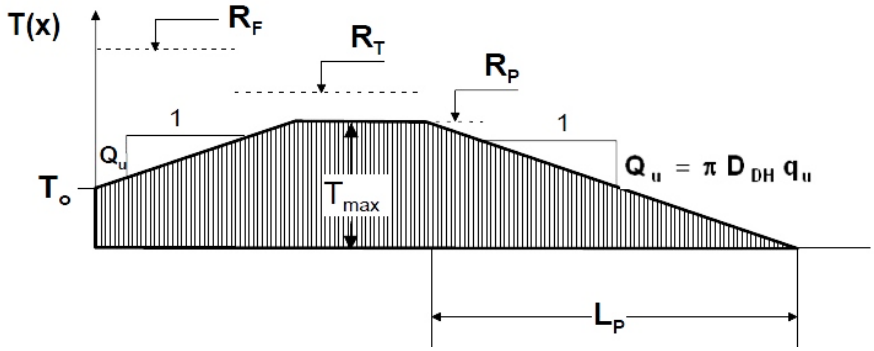

Figure 2.26: Nail tensile force distribution (FHWA, 2003)

Where, "R_T is Nail Tensile Capacity, R_F is Facing Capacity, R_P is Pullout Capacity, Q_u is Ultimate load transfer rate and q_u is bond strength, $T_o \sim 0.6\text{-}1.0\ T_{max}$; $R_P < R_T < R_F$ (pullout controls); $R_T < R_P < R_F$ (tensile failure controls); $R_F < R_P$ or R_T (facing failure may control depending on T_o/T_{max})."

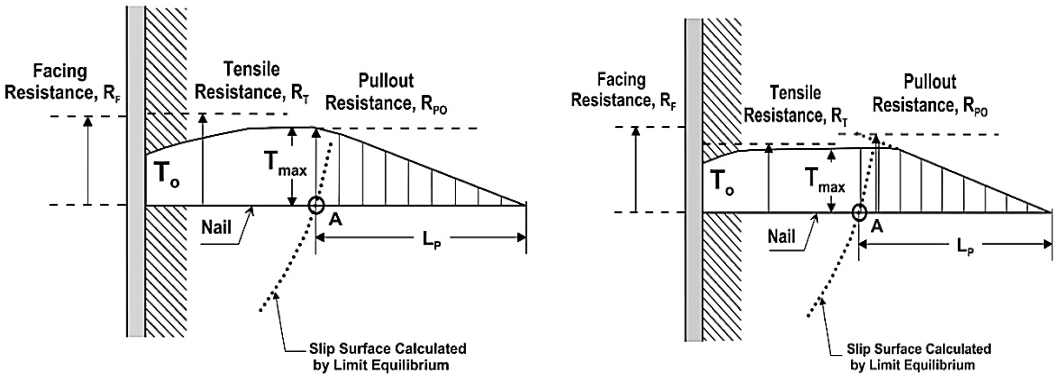

(a) Pullout Resistance Controls **(b)** Tensile Resistance Controls.

Figure 2.27: Limitations to tensile forces in nails (Source: FHWA- 2015)

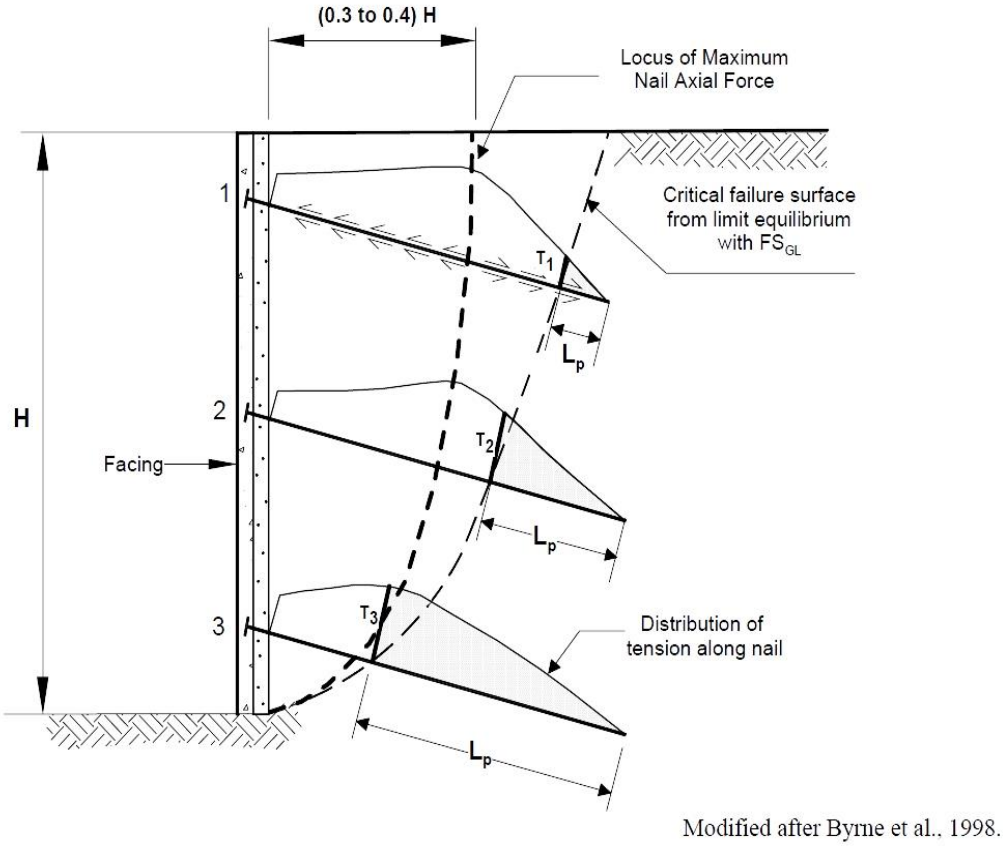

Figure 2.28: Maximum tensile forces within soil nails location (Lazarte et al. 2003)

(2) *Maximum Tensile Forces Distribution*:

The amount of tension in a nail depends on where it intersects the failure surface. Figure 2.28 shows how tensile forces vary across the wall system's cross-section.

Because of the complexities involved in distributing loads within individual nails, the location of peak tensile forces is typically close to, but not exactly, the critical failure surface identified during global stability analysis. The position of this failure surface is determined using global limit equilibrium. Measurements from instrumented soil nail walls have shown that the highest tensile force in the upper part of the wall usually occurs between 0.3H and 0.4H behind the wall facing, while in the lower portion, it is between 0.15H and 0.2H behind the facing (Lazarte et al. 2003). The degree to which tensile forces contribute to global stability varies by nail, depending on where the failure surface intersects the nail. This intersection defines the length of the nail behind the failure surface (referred as L_p). For example, in Figure 2.28, the upper soil nail, T_1, may not contribute significantly to wall stability upon completion because its length behind the critical failure surface/curve is insufficient to fully utilise the nail's potential pullout capacity (refer to Figure 2.28). However, the contributions of the lower soil nails, T_2 and T_3, are relatively significant because their pullout lengths are longer than those in the upper part of the wall. The tensile forces in the nail gradually increase as excavation progresses from top to bottom in front of the wall. Typically, the maximum nail tensile forces in a given row occur when the two following excavation lifts are exposed. Tensile forces may increase slightly after construction (i.e., by 15%) due to post-construction soil creep and stress relaxation. While this additional load is not directly calculated, it is considered in the design of soil nail walls through the use of safety factors (Lazarte et al. 2003).

(d) *Nail Bending and/or Shear Failure*

Nail bending failure happens when the soil nail, which is usually a slender and elongated element, is subjected to excessive bending moments. These bending moments can arise due to external loads or deformations in the surrounding soil. When the bending moments exceed the nail's flexural capacity, it can lead to deformation or rupturing of the nail, compromising its ability to provide reinforcement and support to the slope. Nail bending failure is more likely to occur in situations where the soil nails are relatively long, or the soil conditions cause substantial lateral movements. Nail shear failure occurs when the soil nail experiences excessive shear forces along its

cross-section. These shear forces can result from the interaction between the nail and soil, especially when the soil's strength is insufficient to resist the applied loads. Nail shear failure can lead to the failure of the soil nail's connection with the surrounding soil or the grout material, resulting in the loss of load transfer capacity. To prevent Nail Bending and Shear Failures, appropriate design and construction practices are crucial. The design should consider factors such as the soil properties, the magnitude and distribution of applied loads, the length and diameter of the nails, and the properties of the grout material. Adequate reinforcement and material selection can be used to enhance the nail's flexural and shear strength. Additionally, regular inspections and monitoring of the soil-nailed slope are crucial to detect any signs of bending or shear failure early on, allowing for timely maintenance and remedial measures. By considering these factors and implementing appropriate design and construction techniques, the risk of nail bending and shear failures can be minimized, ensuring the stability and safety of the soil-nailed slope.

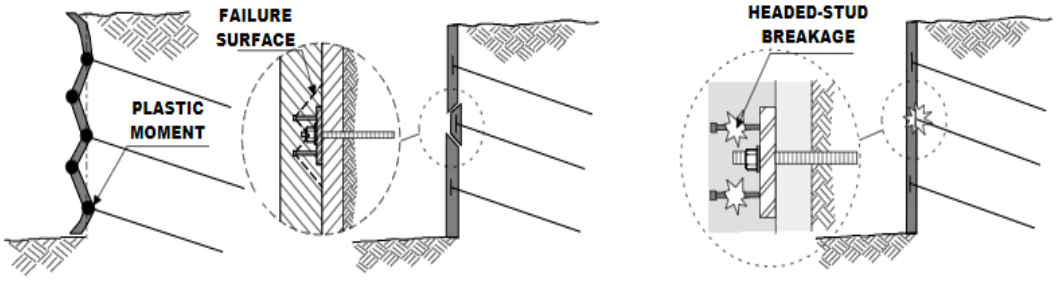

(a) Flexural failure at facing **(b)** Punching shear failure at facing **(c)** Headed stud at failure

Figure 2.29: Modes of failure at facing (Lazarte et al. 2003)

2.8.3 Facing Failure Modes

The paragraph discusses potential failure modes specifically at the connection between the facing and the nail head. These failure modes are outlined in Figure 2.29 and elaborated in Figure 2.30:

(a) *Flexure Failure*: This type of failure arises when there is excessive bending outside the flexural capacity of the facing. It's crucial to analyze this failure mode separately for both permanent and temporary facings to ensure adequate structural integrity.

(b) Punching Shear Failure: This failure mode occurs within the facing around the nails, typically due to concentrated loads. It's important to assess this mode for both temporary and permanent facings to prevent structural failure.

(c) *Headed-Stud Tensile Failure*: This failure mode involves the tension failure of the headed studs used in permanent facings. It's a concern only for permanent facings since temporary facings typically don't utilize headed studs.

These modes of failure should be carefully analyzed and considered throughout the design and construction of the facing-nail head connection to confirm the stability and safety of the soil-nailed structure. Appropriate reinforcement, material selection, and construction practices should be employed to mitigate the risks associated with these potential failure modes.

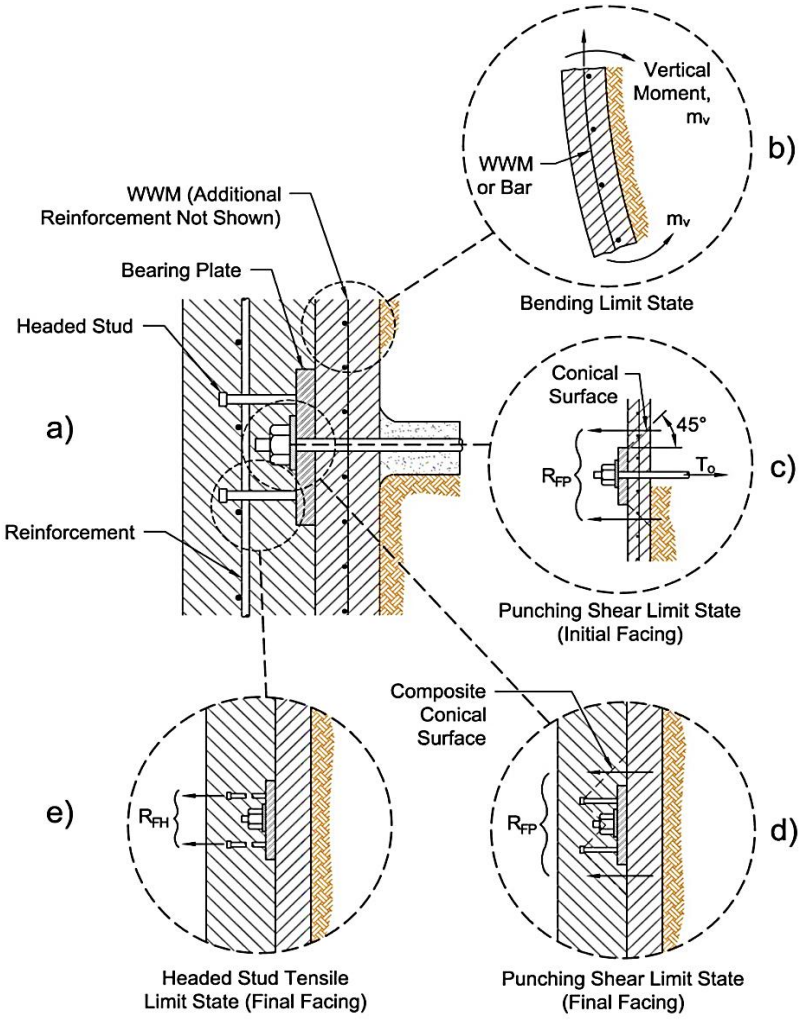

Modified after Lazarte (2011)

Figure 2.30: Facing connection failure modes. (Source: FHWA, 2015)

2.8.4 Flexural Failure in Wall Facing

The soil nail wall facing embodies a structural concept similar to that of a continuous reinforced concrete slab. In this analogy, the lateral earth pressure acting upon the facing material serves as the primary load, while the essential support is derived from the tensile forces exerted by the soil nails, as visually depicted in Figures 2.31 (a and b). The interplay between these forces engenders the development of flexural moments within the facing section. This flexural behaviour is characterized by the generation of positive moments, denoting tension on the exterior side of the section, particularly at the midspan between the soil nails. Conversely, negative moments arise, signifying tension on the interior side of the section, notably around the vicinity of the nails themselves, as elucidated in Figure 2.31b. Prominently, if these flexural moments surpass certain thresholds, there exists the potential for a flexural failure of the shotcrete, the material commonly employed in such constructions. Like other structures made of reinforced concrete or shotcrete, the process of flexural failure in soil nail wall facings transpires gradually and progressively. This phenomenon unfolds in distinct stages, and its progression is characterized by a sequence of events that can be comprehensively elucidated. The initial stage is marked by the primary yield of the facing section, as depicted in Figure 2.31c. During this stage, the material begins to experience plastic deformation, with the formation of yielding zones in the facing section. As the lateral earth pressure acting on the facing increases, a subsequent phase emerges wherein progressive cracking emerges on both sides of the facing. These cracks typically develop in response to the intensifying stresses and strains induced by the lateral earth pressure. This is a crucial indication of the structure's evolving behaviour under load. As the lateral pressure continues to escalate, these cracks propagate and extend further, leading to increased deflections (represented as δ) and augmented tensile forces in the soil nails. The fractures that manifest in the facing are indicative of localized areas where the flexural capacity of the material is being reached.

Each fracture signifies a critical point in the structure's load-carrying capability. Continuing with the increase in lateral pressure, the fractures accumulate and expand, ultimately culminating in a significant juncture. This juncture represents

an ultimate state for the structure, characterized by the interconnection of all fractures, which then act as pivot points or hinges. This coherent arrangement of fractures and hinges forms a distinctive pattern known as the critical yield line pattern. This pattern serves as a critical mechanism that redistributes forces and allows the structure to adapt to changing loads and deformations (Figure 2.31 c). The formation of yield line patterns is a complex process influenced by an array of factors. These factors encompass the lateral pressures exerted by the surrounding soil, the vertical and horizontal spacing of the soil nails, the dimensions of the bearing plate, the facing material thickness, the arrangement of reinforcement elements, and the inherent concrete strength etc. Each of these parameters plays a role in determining the precise configuration and behaviour of the yield line patterns that emerge as the structure undergoes progressive loading.

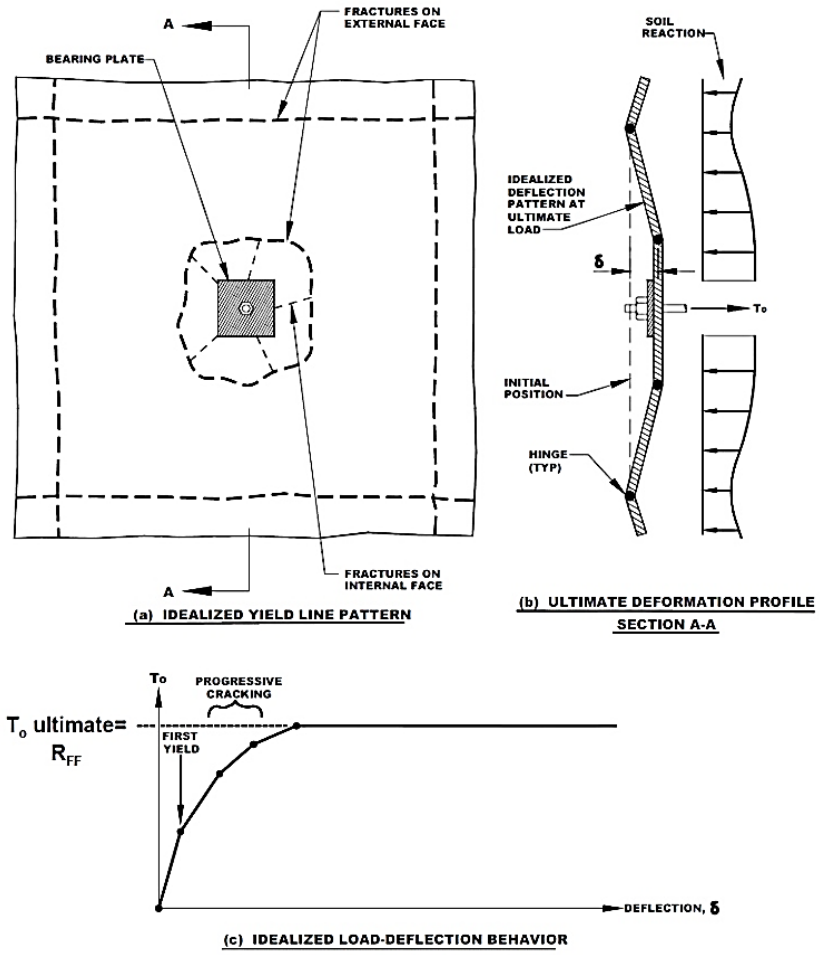

Figure 2.31: Flexural failure (wall facings). (Lazarte et al. 2003)

2.8.5 Soil Pressure Distribution Behind Facing

The distribution of soil pressure applied to the back of a soil nail wall is inherently variable and influenced by a wide range of factors. The non-uniform distribution is primarily caused by the soil's characteristics, combined with the stiffness of the facing material. This intricate interplay of soil properties and facing stiffness has a significant impact on the wall's overall displacement behaviour. The displacement of the facing material manifests itself outward in the central region between the soil nails, also known as the midspan (Lazarte et al., 2003). This outward movement is accompanied by a lower lateral earth pressure exerted on the facing. This phenomenon can be attributed to a reduced restraining force in this area as a result of the soil nails' spatial arrangement. Consequently, soil pressure on the facing at this midspan juncture is typically lower than in other regions. In contrast, soil pressure has a significantly greater influence near the heads of the soil nails. The localised soil pressure around the nail heads is significantly greater than the pressure at the midspan. This significant variation in pressure distribution is illustrated in Figure 2.32, which shows a schematic representation of soil pressure distribution patterns near a soil nail (Lazarte et al., 2003).

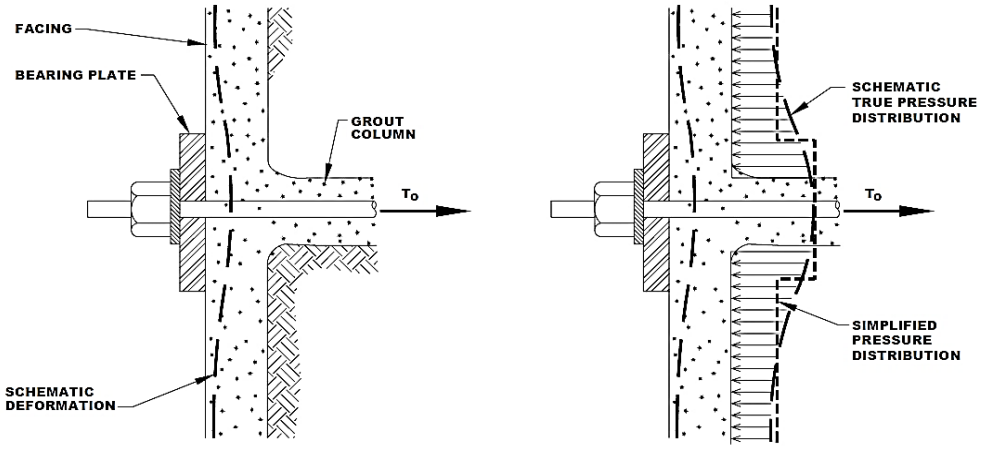

Modified after Byrne et al. (1998).

Figure 2.32: Soil pressure distribution behind facing (Lazarte et al., 2003)

The stiffness of the facing material is an important factor in determining the details of soil pressure distribution within it. When the facing material is relatively thin, as is often the case with temporary facings, its stiffness is naturally reduced. As a result,

lateral earth pressure causes significant deformation in the facing material, particularly in the midspan sections. This deformation-induced behaviour causes a decrease in the soil pressure exerted against the facing within these midspan segments. In contrast, when the facing material is relatively thicker, its stiffness significantly increases. As a result of the increased stiffness, the facing experiences fewer deformations than a thinner facing (Lazarte et al., 2003). This increased structural integrity and stiffness causes a more uniform distribution of soil pressure throughout the facing material.

2.9 Deformation Behaviour of Soil Nailed Slope/Wall

During both the construction phase and after its completion, a soil nail wall and the surrounding soil tend to deform outward. This movement occurs due to increased rotational shifts around the toe or base of the wall, much like the cantilever retaining wall behaviour. The majority of this movement is observed throughout or shortly after soil excavation in front of the wall, its a critical step in the construction process. After construction, post-construction deformation occurs as a result of stress relaxation and creep movements (Lazarte et al., 2003). These movements stem from moderate increases in tensile forces within the soil nails that emerge after construction is finalized. Notably, the most significant lateral displacements manifest at the uppermost part of the wall and gradually diminish as one moves towards the wall's base (refer to Figure 2.33). Vertical displacements, or settlements, at the facing, are usually minor and similar order of magnitude as the lateral displacements observed at the top of the wall.

The magnitude of these deformations is influenced by various factors, including:

1. Wall Height (H): Deformation increases with the wall's height increase.
2. Wall Geometry: A vertical wall experiences greater deformation compared to an angled or battered wall.
3. Soil Type: Softer soil allows for more significant deformation.
4. Nail Spacing and Excavation Lift Heights: the maximum nail spacing and increases in excavation lead to more noticeable deformation.

5. Global Factor of Safety (FS_G): Least FS_G values are linked to more deformations.
6. The ratio of Nail Length to Wall Height: A smaller ratio results in more substantial horizontal deformation.
7. Nail Inclination: Steeper soil nails tend to induce more significant horizontal deformation due to less efficient mobilization of tensile loads.
8. Magnitude of Surcharge: Permanent surcharge loads imposed on the wall contribute to increased deformation.

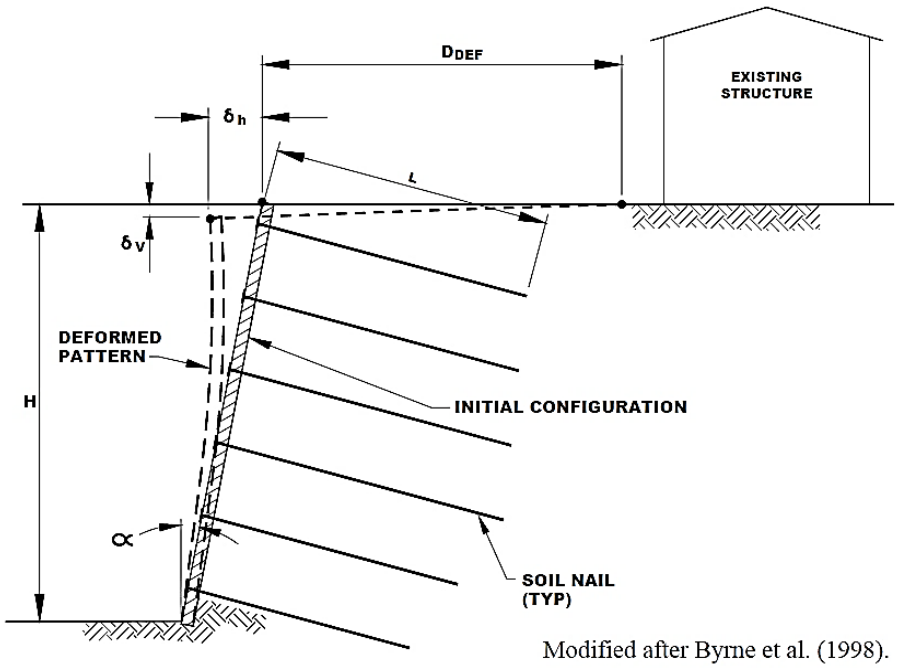

Figure 2.33: Deformation of soil nail walls (Lazarte et al., 2003)

As a FHWA 2003 preliminary guideline, horizontal deflections exceeding 0.005 times the wall height (0.005 H) during construction should be a cause for concern, as they generally represent an upper limit of acceptable performance. When excessive deformations are expected with a specific wall configuration, potential adjustments to the original design can be explored. Methods to mitigate soil nail wall deformations include using a battered wall, employing longer nails in the upper part of the wall, increasing the safety factor, or combining ground anchors with soil nails (Lazarte et al., 2003).

2.10 Slope Stability Analysis Methods

Before constructing a structure in the field, it is essential to design the soil-nailed slope to ensure stability. This process involves utilizing various analytical methods, each characterized by distinct approaches and assumptions, to thoroughly evaluate the factors influencing slope stability and potential failure mechanisms. A comprehensive study of these methods is crucial for accurate slope stability assessment. An illustration of the different methods used in slope stability analysis is stated in Figure 2.34.

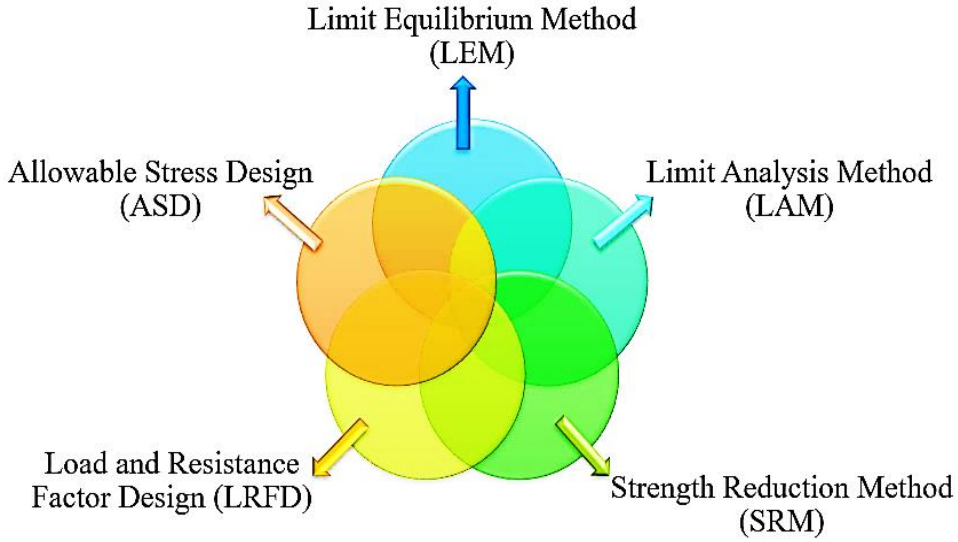

Figure 2.34: Methods of slope stability analysis

2.10.1 Limit States Design (LSD)

Strength Limit States and Service Limit States are two conditions that must be considered when designing and analysing soil nail slopes/walls.

2.10.1.1 Strength Limit States

Strength Limit States occur when stresses imposed on the system exceed either the overall strength of the system or the strengths of its components, leading to potential failure or collapse due to instability. These states arise when any potential modes of failure become realized. When designing the soil nail slopes, it's crucial to account for all potential failure scenarios classified as such:

(a) External failure mode,
(b) Internal failure mode, and
(c) Facing failure mode.

2.10.1.2 Service Limit States

'Service Limit States' refer to conditions where a structure's performance or safety is compromised, even if it doesn't collapse. For soil nail walls, excessive wall deformation is a key concern under service limit states. This discussion focuses on acceptable deformation levels in soil nail wall systems but does not address other issues like uneven or total settlement, cracking of concrete facing, or fatigue from repeated loading (FHWA 2003).

2.10.2 Limit Equilibrium Method (LEM)

Using the LEM method, the soil's shear strength and current shear stress are compared to determine the FOS. Several researchers like Duncan and Wright (2005), Cheng and Lau (2008) etc. have simply expressed this idea.

$$\text{Factor of Safety (FOS)} = \frac{\text{Soils Shear Strength } (\tau)}{\text{Current Shear Strength in Soil } (s)} \tag{2.21}$$

As per the formula (2.21) mentioned above, a slope is considered stable when the current shear stress in the soil exceeds the shear strength of the slope at any location. This factor, which indicates how much the soil's shear strength needs to decrease to reach a specific value just before the slope collapses, is universally referred to as the FOS in all LEM methods (Duncan and Wright 2005).

2.10.3 Limit Analysis Method (LAM)

The Limit Analysis Method (LAM) has emerged as a crucial method for assessing collapse loads in geotechnical problems, particularly in the domain of slope stability analysis. This method relies on two key theoretical frameworks:

- Lower Bound Theory and

- Upper Bound Theory.

The Lower Bound Theory deals with determining the minimum possible collapse load by considering a mechanism that just begins to yield or fail. On the other hand, the Upper Bound Theory focuses on finding the maximum possible collapse load by identifying the most critical mechanism of failure (Lazarte et al. 2003). Both of these theories have been extensively applied in analyzing slope stability, spanning both two-dimensional and three-dimensional scenarios. By utilizing LAM, engineers and researchers can gain insights into the potential failure mechanisms of slopes under various conditions. It's important to recognize that while the Limit Equilibrium Method (LEM) is commonly employed for slope stability analysis, it may not always fully satisfy stress equilibrium equations (Lazarte et al. 2003). Therefore, the adoption of the more comprehensive Limit Analysis Method provides a robust framework for accurately assessing collapse loads and understanding the stability of geotechnical systems.

2.10.4 Strength Reduction Method (SRM)

The Strength Reduction Method (SRM) has been used for slope stability analysis since the mid-19th century (Lazarte et al. 2003). It offers significant advantages over traditional techniques like the Limit Equilibrium Method (LEM). One notable advantage of SRM is that it provides detailed information such as displacement and stress values throughout the failure development process. This information is crucial for understanding slope behaviour. Additionally, SRM identifies where yield initiates, which helps to comprehend failure mechanisms (Naylor 1982). Moreover, with the widespread use of computers in geotechnical engineering, SRM's integration into FEM programs enhances its accessibility and efficiency. This integration enables comprehensive slope stability analyses to be conducted with ease and precision.

2.10.5 Load and Resistance Factor Design (LRFD)

In the context of slope stability analysis, it's essential to cross-check the results obtained using Allowable Stress Design (ASD) methods with those derived from Load and Resistance Factor Design (LRFD) procedures. LRFD incorporates both load

factors and resistance factors for each structural component to accommodate uncertainties. The LRFD condition is typically expressed as the resistance factor multiplied by the nominal resistance of a structural element, which should be greater than or equal to the sum of the factored loads or effects. These loads include various factors such as the yield strength of soil nails, pullout resistance of soil nails, shear strength of soils, and resistance of the facing etc.

It's important to note that in ASD platforms, the term "strength" is analogous to the LRFD term "nominal resistance." The LRFD methodology aims to ensure that the factored resistance exceeds the factored load, with the capacity-to-demand ratio (CDR) serving as a quantification of this ratio (Lazarte et al. 2003). The CDR is calculated by dividing the product of the resistance factor and the nominal resistance by the sum of the factored loads or effects, providing a measure of safety against failure for a given limit state. As per FHWA(2003), the LRFD condition is generally expressed as:

$$\emptyset\, R_n \geq \sum_{i=1}^{N} \gamma_i\, \eta_i\, Q_i \tag{2.22}$$

The CDR, which can be used to quantify the ratio of the factored resistance to the factored load, is defined as follows: (FHWA- 2003)

$$\mathrm{CDR} = \frac{\emptyset\, R_n}{\sum_{i=1}^{N} \gamma_i Q_i} \tag{2.23}$$

Where "R_n is the nominal resistance of a structural component selected for a given limit state, $\emptyset$ is the resistance factor related to R_n , Q_i is generic load (or effect), γ_i is the load factor associated with Q_i, η_i is a load-modification factor relating to ductility, redundancy, or operational classification (equal to 1.0 for soil nail walls), i is 1…N and refers to the various loads/effects in that limit state".

2.10.6 Allowable Stress Design (ASD)

Allowable Stress Design (ASD) is a methodology employed for assessing the stability of soil nail walls and similar structures, although recognized as an interim measure

until fully compatible LRFD methods become available. Currently, ASD-based computer programs are employed for overall stability assessments, with resistance factors derived from safety factors. However, a limitation of this approach lies in the inability to apply different load factors to different load components within these programs. Despite this constraint, ongoing efforts aim to develop satisfactory computational methodologies and comprehensive databases to seamlessly integrate LRFD principles into current limit-equilibrium analysis computations (Lazarte et al. 2003).

2.11 Methods for Active and Passive Earth Pressure Calculation

Methods for the calculation of active and passive earth pressure play a crucial role in geotechnical engineering and soil mechanics. These calculations are essential for analyzing the stability of soil slopes, retaining walls, sheet piles, and other earth-retaining structures. By understanding the forces exerted by soil on such structures, can design safe and efficient foundations and retaining walls that can withstand the lateral pressures induced by the surrounding soil. The field of geotechnical engineering offers several well-established methods to determine active and passive earth pressure, each with its unique assumptions and applications, enabling one to make informed decisions based on specific project requirements and soil conditions. The analysis of active and passive earth pressure commonly employs several methods including:

(1) The Coulomb Theory,
(2) The Müller-Breslau Theory,
(3) The Caquot Theory,
(4) The Mazindrani Theory (Rankine), and
(5) The Absi Theory etc.

2.12 Effective/Total Stress in a Soil

Effective stress is a basic concept in geotechnical engineering that presents the portion of total stress responsible for influencing soil behaviour. It specifically refers to the stress transmitted between soil particles, while excluding the effects of pore water pressure. In contrast to total stress, which accounts for the weight of both soil and

water, effective stress directly impacts essential soil properties such as shear strength, compressibility, and stability. This concept is crucial for conducting geotechnical analyses, including slope stability assessments and settlement predictions. In saturated soils, effective stress can diminish to zero when pore water pressure completely offsets the stress on the soil particles. Conversely, in unsaturated soils, effective stress remains nonzero, as both soil and water contribute to the material's mechanical behaviour (Geo 5, 2018). The vertical normal stress σ_z is:

$$\sigma_z = \gamma_{eff} .z + \gamma_w .z \tag{2.24}$$

Where, "σ_z is vertical normal total stress, γ_{eff} is submerged unit weight of soil, z is depth below the ground surface, γ_w is the unit weight of water."

In its broadest interpretation, this phrase summarizes the concept known as effective stress. Totata stress (overall) is

$$\sigma_z = \sigma_{eff} + u \tag{2.25}$$

Where, "σ_z is total stress (overall), σ_{eff} is effective stress (active) and u is neutral stress (pore water pressure)."

The discussion emphases on the fundamental principles of geotechnical engineering, specifically stress analysis in soils. There are two primary stress states to consider: total stress (σ_z) and effective stress (σ_{eff}). Total stress (σ_z) refers to the entire stress field within the soil mass, including normal and shear stresses caused by gravity and external loads. It is determined using theoretical mechanics, which takes into account factors like self-weight and external loading conditions. Effective stress (σ_{eff}) is the stress that affects the mechanical behaviour of the soil. Normal stress is directly proportional to effective stress, whereas shear stress (which is not transmitted by water) is considered effective. To calculate effective stress, subtract the pore pressure (or neutral pressure) from the total stress. Pore pressure is caused by the presence of water within soil pores and is usually determined using laboratory testing, in-situ measurements, or computational methods. The determination of pore pressure is essential, especially in saturated and partially saturated soils. In flowing pore water conditions, pore pressure corresponds to

hydrodynamic pressure; in static conditions, it corresponds to hydrostatic pressure. In partially saturated soils, water and air pressures must be considered. The choice between total stress and effective stress is determined by the specific engineering problem, taking into account factors such as loading conditions, soil properties, and pore water. Each stress state provides unique insights into soil behaviour and is appropriately applied in geotechnical analysis and design (Geo 5, 2018).

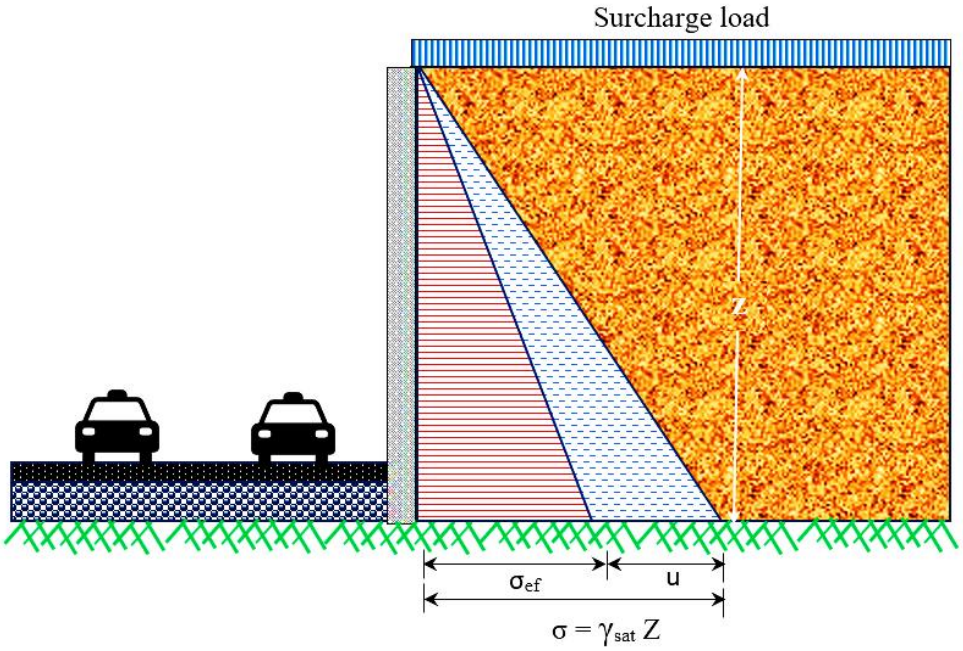

Figure 2.35: Total, effective and neutral stress in the soil.

2.13 Theory of Cohesive Backfill

Terzaghi (1943) introduced a visual method to address lateral earth pressure in cohesive backfill with inclined surfaces. However, this approach was time-consuming as it required plotting multiple Mohr circles to determine lateral earth pressure distribution. To simplify this, Mazindrani and Ganjali (1997) developed an analytical solution, including tables for active (K_a) and passive (K_p) earth pressure coefficients based on factors like wall inclination (β), soil cohesion (c), and internal friction angle (ϕ). They also provided a practical example demonstrating the application of their method, making it a valuable tool for calculating lateral earth pressure on retaining walls or slopes with cohesive inclined backfill. Mazindrani and Ganjali (1997)

presented an analytical solution to this inclined backfill problem. Their work is included in Tables 2.2 (a to g):

1. *Understanding Table* 2.2: Table 2.2, as outlined by Mazindrani and Ganjali (1997), offers a systematic layout containing values of K_a and K_p for various combinations of parameters, including soil cohesion (c/γz), internal friction angle (ϕ), and wall inclination (β).
2. *Determining K_a and K_p*: To calculate the active and passive earth pressure coefficients (K_a and K_p), one needs to identify the relevant values of c/γz, ϕ, and β from Table 2.2.
3. *Impact of* c/γz *on K_a and K_p*: Mazindrani and Ganjali's (1997) theory suggests that for a given set of values for ϕ and β, the active earth pressure coefficient (k_a) tends to decrease, while the passive earth pressure coefficient (k_p) increases with increasing values of c/γz (refer to Table 2.2). This implies that as the ratio of soil cohesion to unit weight increases, the soil's resistance to movement against the retaining wall increases, resulting in higher passive pressure and lower active pressure.
4. *Impact of β on K_a and K_p*: Additionally, the theory indicates that for constant values of c and ϕ, the active earth pressure coefficient (K_a) increases while the passive earth pressure coefficient (K_p) decreases with increasing values of β (refer to Table 2.2). This means that as the angle of wall inclination increases, the pressure exerted by the soil against the wall becomes more active, leading to a higher resistance to movement in the retained soil mass. Conversely, the passive pressure exerted by the soil decreases as the wall inclination angle increases (see Table 2.2).

Mazindrani and Ganjali's (1997) theoretical framework, illustrated by Table 2.2 (a to g), offers a systematic approach for calculating K_a and K_p values based on the parameters of soil cohesion (c), internal friction angle (ϕ), and wall inclination (β). Understanding the relationship between these parameters allows us to predict and account for lateral earth pressure in the design and analysis of retaining walls with inclined cohesive backfill.

Table 2.2: Values of k_a and k_p (from Mazindrani and Ganjali equation) for Various Values of ϕ, β and $c/\gamma z$ (Mazindrani and Ganjali; 1997)

Parameter (1)	Earth Pressure coefficient (2)	$c/\gamma z$ 0.0 (3)	0.025 (4)	0.05 (5)	0.1 (6)	0.5 (7)	1.0 (8)
(a) For $\phi = 15^0$							
$\beta = 0^0$	K_a	0.5888	0.5504	0.5121	0.4353	– 0.1785	– 0.9459
$\beta = 0^0$	K_p	1.6984	1.7637	1.8287	1.9590	3.0016	4.3048
$\beta = 5^0$	K_a	0.6069	0.5658	0.5252	0.4449	– 0.1804	– 0.9518
$\beta = 5^0$	K_p	1.6477	1.7156	1.7830	1.9169	2.9709	4.2782
$\beta = 10^0$	K_a	0.6738	0.6206	0.5707	0.4769	– 0.1861	– 0.9696
$\beta = 10^0$	K_p	1.4841	1.5641	1.6408	1.7882	2.8799	4.1993
$\beta = 15^0$	K_a	1.0000	0.7762	0.6834	0.5464	– 0.1962	– 1.0000
$\beta = 15^0$	K_p	1.0000	1.2506	1.3702	1.5608	2.7321	4.0718
(b) For $\phi = 20^0$							
$\beta = 0^0$	K_a	0.4903	0.4553	0.4203	0.3502	– 0.2099	– 0.9101
$\beta = 0^0$	K_p	2.0369	2.1110	2.1824	2.3252	3.4678	4.8959
$\beta = 5^0$	K_a	0.5015	0.4650	0.4287	0.3565	– 0.2119	– 0.9155
$\beta = 5^0$	K_p	1.9940	2.0669	2.1396	2.2846	3.4353	4.8669
$\beta = 10^0$	K_a	0.5394	0.4974	0.4564	0.3767	– 0.2180	– 0.9320
$\beta = 10^0$	K_p	1.8539	1.9323	2.0097	2.1622	3.3392	4.7812
$\beta = 15^0$	K_a	0.6241	0.5666	0.5137	0.4165	– 0.2287	– 0.9599
$\beta = 15^0$	K_p	1.6024	1.6962	1.7856	1.9556	3.1831	4.6422
(c) For $\phi = 25^0$							
$\beta = 0^0$	K_a	0.4059	0.3740	0.3422	0.2784	– 0.2312	– 0.8683
$\beta = 0^0$	K_p	2.4639	2.5424	2.6209	2.7779	4.0336	5.6033
$\beta = 5^0$	K_a	0.4133	0.3805	0.3478	0.2826	– 0.2332	– 0.8733
$\beta = 5^0$	K_p	2.4195	2.4989	2.5782	2.7367	3.9986	5.5713
$\beta = 10^0$	K_a	0.4376	0.4015	0.3660	0.2960	– 0.2394	– 0.8884
$\beta = 10^0$	K_p	2.2854	2.3680	2.4502	2.6135	3.8950	5.4765
$\beta = 15^0$	K_a	0.4860	0.4428	0.41011	0.3211	– 0.2503	– 0.9140
$\beta = 15^0$	K_p	2.0575	2.1474	2.2357	2.2357	3.7264	5.3228
(d) For $\phi = 30^0$							
$\beta = 0^0$	K_a	0.3333	0.3045	0.2756	0.2179	– 0.2440	– 0.8214
$\beta = 0^0$	K_p	3.0000	3.0866	3.1732	3.3464	4.7321	6.4641
$\beta = 5^0$	K_a	0.3385	0.3090	0.2795	0.2207	– 0.2460	– 0.8260
$\beta = 5^0$	K_p	2.9543	3.0416	3.1288	3.3030	4.6935	6.4282
$\beta = 10^0$	K_a	0.3549	0.3233	0.2919	0.2297	– 0.2522	– 0.8399
$\beta = 10^0$	K_p	2.8176	2.9070	2.9961	3.1737	4.5794	6.3218
$\beta = 15^0$	K_a	0.3861	0.3502	0.3150	0.2462	– 0.2628	– 0.8635
$\beta = 15^0$	K_p	2.5900	2.6836	2.7766	2.9608	4.3936	6.1489
(e) For $\phi = 35^0$							
$\beta = 0^0$	K_a	0.2710	0.2450	0.2189	0.1669	– 0.2496	– 0.7701
$\beta = 0^0$	K_p	3.6902	3.7862	3.8823	4.0744	5.6112	7.5321
$\beta = 5^0$	K_a	0.2746	0.2481	0.2217	0.1688	– 0.2515	– 0.7744
$\beta = 5^0$	K_p	3.6413	3.7378	3.8342	4.0271	5.5678	7.4911
$\beta = 10^0$	K_a	0.2861	0.2581	0.2303	0.1749	– 0.2575	– 0.7872
$\beta = 10^0$	K_p	3.4953	3.5933	3.6912	3.8866	5.4393	7.3694
$\beta = 15^0$	K_a	0.3073	0.2764	0.2459	0.1860	– 0.2678	– 0.8089
$\beta = 15^0$	K_p	3.2546	3.3555	3.4559	3.6569	5.2300	7.1715

Continue…..

(f) For $\phi = 40^0$							
$\beta = 0^0$	K_a	0.2174	0.1941	0.1708	0.1242	– 0.2489	– 0.7152
$\beta = 0^0$	K_p	4.5989	4.7061	4.8134	5.0278	6.7434	8.8879
$\beta = 5^0$	K_a	0.2200	0.1964	0.1727	0.1255	– 0.2507	– 0.7190
$\beta = 5^0$	K_p	4.5445	4.6521	4.7597	4.9747	6.6935	8.8400
$\beta = 10^0$	K_a	0.2285	0.2034	0.1787	0.1296	– 0.2564	– 0.7308
$\beta = 10^0$	K_p	4.3826	4.4913	4.5999	4.8168	6.5454	8.6980
$\beta = 15^0$	K_a	0.2429	0.2161	0.1895	0.1370	– 0.2662	– 0.7507
$\beta = 15^0$	K_p	4.1168	4.2275	4.3380	4.5584	6.3041	8.4669
(g) For $\phi = 45^0$							
$\beta = 0^0$	K_a	0.1716	0.1509	0.1302	0.0887	– 0.2426	– 0.6569
$\beta = 0^0$	K_p	5.8284	5.9491	6.0698	6.3113	8.2426	10.6569
$\beta = 5^0$	K_a	0.1734	0.1525	0.1315	0.0896	– 0.2444	– 0.6604
$\beta = 5^0$	K_p	5.7658	5.8868	6.0077	6.2496	8.1836	10.5996
$\beta = 10^0$	K_a	0.1792	0.1574	0.1357	0.0923	– 0.2497	– 0.6711
$\beta = 10^0$	K_p	5.5795	5.7014	5.8231	6.0665	8.0085	10.4299
$\beta = 15^0$	K_a	0.1896	0.1663	0.1431	0.0971	– 0.2590	– 0.6894
$\beta = 15^0$	K_p	2.2745	5.3978	5.5210	5.7670	7.7231	10.1535

2.14 Horizontal Deformation of the Excavation Face

The construction sequence of the nailed excavation was meticulously simulated and demonstrated by Shiu and Chang (2006) in their analysis and results are presented as depicted in Figure 2.36. The construction process was executed in a step-by-step manner, following a top-down approach, and involved the repetition of two distinct construction steps. These steps were designed to ensure the systematic and controlled progression of the excavation process while integrating the soil nail reinforcement. The construction sequence is explained as follows:

STEP 1 - Soil Excavation: The initial step entailed the excavation of soil to a depth of 0.5 meters below the level of the soil nail. This preparation phase established the groundwork for subsequent stages by creating a suitable environment for the installation of soil nails.

STEP 2 - Soil Nail and Concrete Facing Installation: The second step involved the installation of both the soil nail and the concrete facing. Soil nails were inserted into the excavated area, contributing to the reinforcement and stability of the structure. The concrete facing further fortified the system, providing additional support and structural integrity.

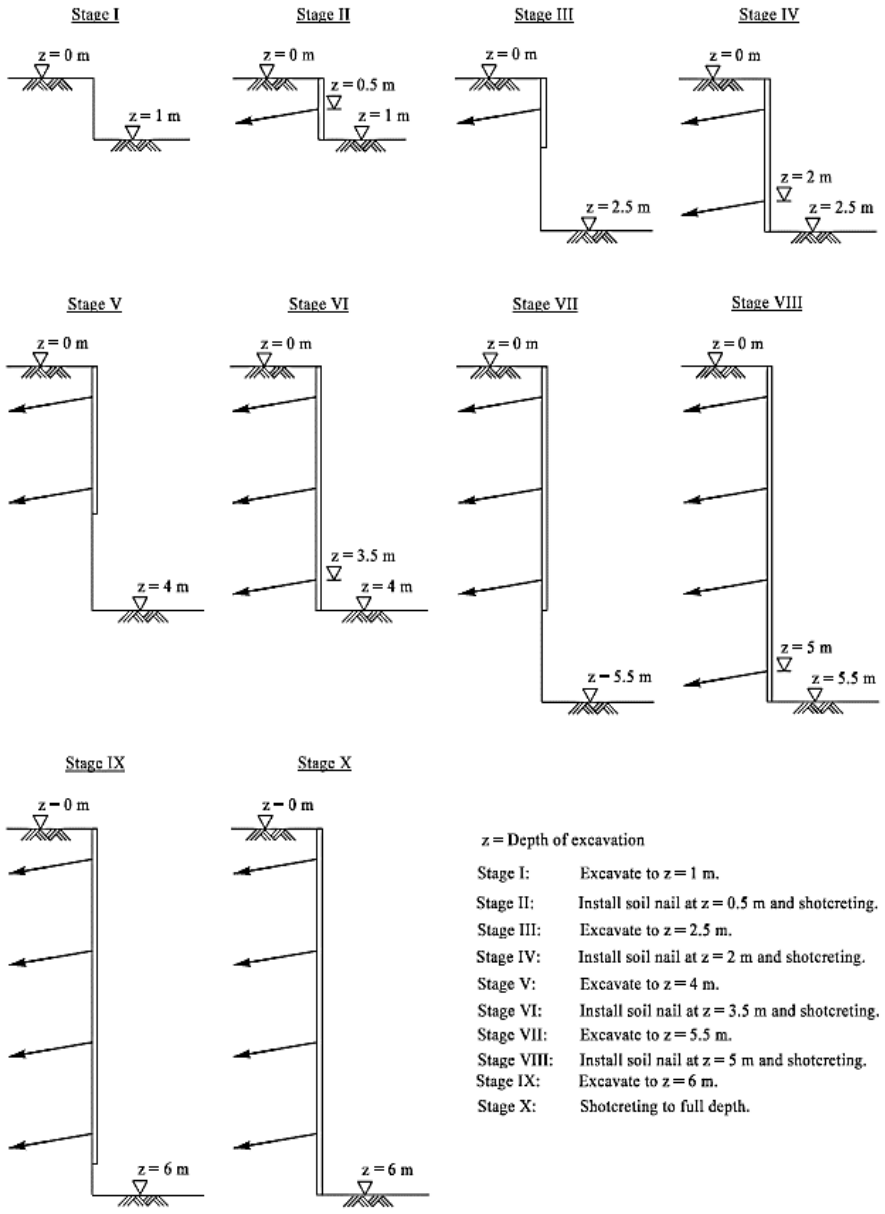

Figure 2.36: Excavation sequence (Shiu and Chang, 2006)

These two steps, namely soil excavation (STEP 1) and soil nail plus concrete facing installation (STEP 2), were repeated iteratively to progressively advance the construction process. This incremental approach ensured the gradual development of the excavation while continuously reinforcing the structure with soil nails and concrete-facing. The construction sequence was executed until the full excavation depth of 6 meters was achieved. Throughout this simulated process, various aspects were examined to measure the performance of the nailed excavation. The study

focused on the effects of nail inclinations on the stability of the construction. Nail inclinations, ranging from 0^0 to 35^0, were systematically altered to observe their influence on the behaviour of the excavation. Notably, the analysis carried out by Shiu and Chang (2006), yielded specific findings for different nail inclination angles:

(A) *Nail Inclination of 35^0*: At an inclination angle of 35^0, the excavation encountered instability issues. The collapse occurred when the excavation depth of 5.5 meters reached, even earlier the installation of the lowest nail. This outcome emphasizes the critical importance of nail inclination in maintaining the stability of the excavation.

(B) *Nail Inclinations Less Than 35^0*: Conversely, for nail inclinations less than 35^0, the excavations remained steady throughout the entire construction process. This result underscores the significance of appropriate nail inclinations in confirming the overall stability and safety of the soil-nailed structures.

The detailed construction sequence involved controlled steps of soil excavation and soil nail plus concrete facing installation, progressively forming the nailed excavation (Figure 2.36). The study's analysis of different nail inclinations highlighted their profound impact on stability, demonstrating the crucial role of nail inclination in governing the behaviour of the constructed system.

Horizontal deformation of the excavation face plays a significant role in understanding the behaviour of soil-nailed structures, particularly in the context of slope stabilization and excavation support. This phenomenon is intricately connected to the nail forces development and the overall stability of the system. The deformation of the excavation face is a direct consequence of the movement between the surrounding soil mass and nails. As the excavation progresses and external loads are applied, the soil nails distribute these forces to resist potential collapses or failures. The nail forces development is influenced by the displacements that occur within the soil mass itself. In the context of the study mentioned, the distribution and magnitude of axial forces within the soil nails are intricately tied to the inclinations of the nails and, consequently, the resulting deformations. Nail inclinations refer to the angles at which the nails are inserted into the soil. Figure 2.37 illustrates the relationship

between the horizontal deformation of the excavation face and nail inclinations at the final stage of excavation.

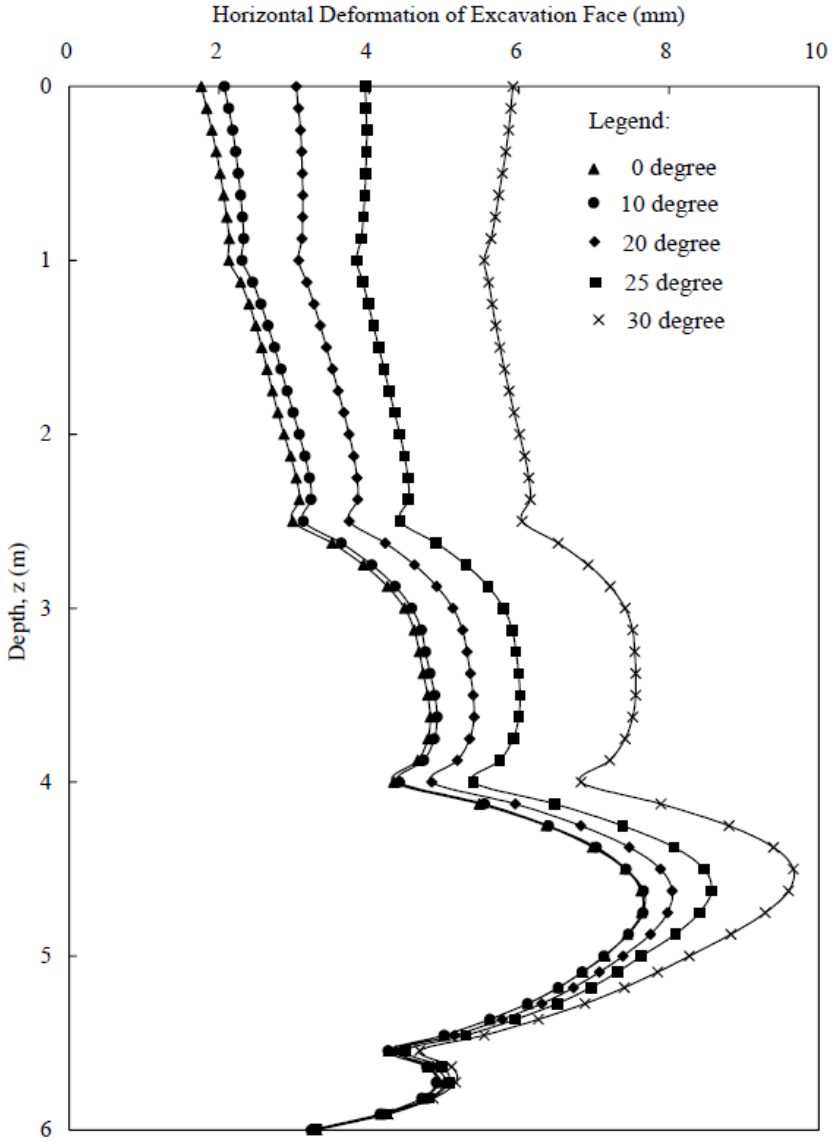

Figure 2.37: Profiles of horizontal deformations of excavation face (Shiu and Chang, 2006)

2.15 The Observations From The Study Reveal Several Important Insights

The observations gleaned from the study offer a prosperity of important insights that focus on various facets of the subject under investigation. Through meticulous analysis and interpretation, these insights provide valuable knowledge that enhances our

understanding and serves as a foundation for further investigation. Below, we'll go into the key findings unearthed by the study, which shows their implications and significance in greater detail.

(a) *Effect of Nail Inclination*: The results indicate that the inclination of the soil nails significantly influences the lateral excavation face deformation. In particular, as the angle of nail inclination increases, the horizontal deformation of the excavation face also increases. This suggests that the orientation of the soil nails plays an important role in observing the extent of deformation experienced by the excavation face.

(b) *Sharp Increase in Deformations*: The study identifies a critical threshold remarkably. There is a notable and sharp increase in horizontal deformations when the nail inclination angle increases from 25^0 to 30^0. This threshold suggests that beyond a certain nail inclination, the deformation of the excavation face becomes more pronounced and potentially less stable.

(c) *Analytical Insights*: The study's analytical results further emphasize the influence of nail inclination on the magnitude of lateral displacement. This underscores the complex interplay between nail orientation, soil behaviour, and overall stability.

In essence, the lateral deformation of the excavation face serves as a valuable indicator of the system's response to varying nail inclinations. It provides valuable information about how the soil mass interacts with the reinforcement provided by the soil nails. The findings highlight the need for careful consideration of nail orientation during the design and construction phases to optimize stability and minimize excessive deformations. Engineers and geotechnical experts can use this understanding to make informed decisions about nail inclinations, ensuring that the soil-nailed structures effectively withstand external forces and maintain the desired levels of stability throughout their lifespan.

2.16 Development of Axial, Shear and Bending Resistances Concerning Failure Criteria

Shiu and Chang (2006) analyzed soil-nailed structures by focusing on three key factors:

(1) Soil Bearing Failure: They assessed the soil's ability to support loads without failure, ensuring the soil around the nails could handle the stresses without compromising the system's stability.
(2) Plastic Hinge Formation: The study examined areas where plastic deformation might occur, particularly in soil nails or facing materials, to understand load responses and maintain overall structural stability.
(3) Nail Material Strength: Concerning the nail's tensile strength and ability to resist deformation under surcharge load, they evaluated the strength and deformation resistance of the nail materials, ensuring the nails could handle applied forces effectively and support the system's stability.

Pullout failure was not considered in the analysis due to the following reasons:

(1) Long Soil Nails: The study used 20-meter-long soil nails, which provide strong resistance to pullout forces, reducing the likelihood of pullout failure.
(2) Stable Modeling Results: The modelling showed no signs of pullout failure, indicating that the chosen nail length and design ensured system stability.

To assess soil bearing failure, the soil bearing capacity, σ'_b, was determined using equation 2.26 formulated by Jewell and Pedley (1992).

$$\sigma'_b = \frac{\sigma'_v(1 + K_a)}{2} \tan\left[\frac{\pi}{4} + \frac{\phi'}{2}\right] \exp\left\{\left(\phi' + \frac{\pi}{2}\right)\tan\phi'\right\} \qquad (2.26)$$

Where, "K_a is the active earth pressure coefficient and σ'_v is effective vertical stress in the soil."

To effectively evaluate the potential for plastic hinge failure in the soil nail (steel bar), it's imperative to employ Pedley's equation, formulated back in 1990. This equation serves as a crucial assessment, offering insights into the structural integrity and susceptibility to plastic deformation of the soil nail. By utilizing Pedley's equation 2.27, understanding the underlying mechanics and risks associated with the soil nail informs the decision-making process and ensures the implementation of appropriate measures to mitigate any potential failure.

$$\frac{P_s}{T_p} = \frac{8}{3\pi\left(\frac{L_s}{D}\right)}\left\{1 - \left[\frac{T}{T_p}\right]^2\right\} \qquad (2.27)$$

Where, " P_s is the shear force in the nail, T_p is the axial force capacity of each nail, L_s is the distance between points of maximum moment on either side of the shear plane (see Figure 2.38) and D is the diameter of the bar, and T is axial force per nail."

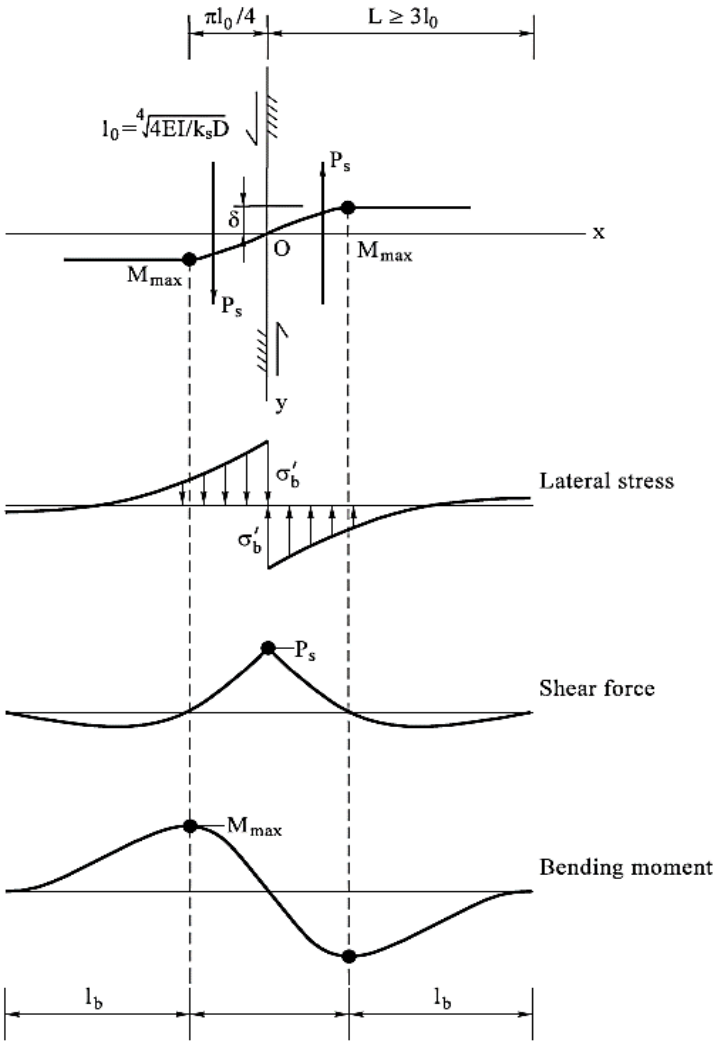

(after Schlosser, 1982)

Figure 2.38: Nails subjected to shear force and bending moment (Source: Shiu and Chang, 2006).

Where, " K_s is coefficient of subgrade reaction, K_o is the transfer length of the nail, δ is the lateral displacement of the nail, E is the Modulus of Elasticity of the nail, I is the

moment of inertia of the nail, D is the diameter of the nail, M_{max} is the maximum bending moment in a nail, P_s is the shear force in the nail, I_b is the maximum required length beyond the point of maximum bending moment, L_s is the distance between points of maximum moment on either side of the shear plane and δ'_b maximum soil bearing pressure."

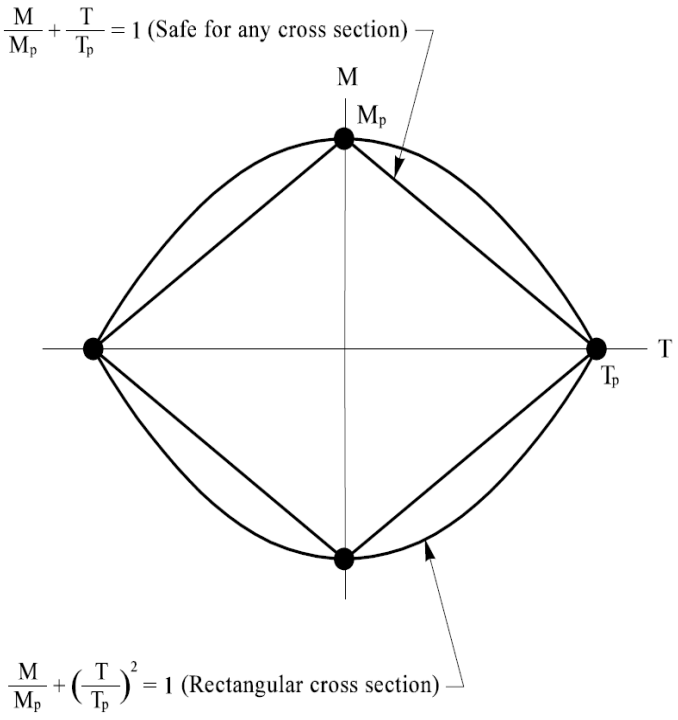

(after Calladine, 2000)

Figure 2.39: Relationship between M_p and T_p (source: Shiu and Chang, 2006).

Figure 2.39 depicts the relationship between axial force (T) and bending moment (M) concerning soil reinforcement. This critical correlation is encapsulated by the restrictive plastic envelope, particularly tailored for a rectangular cross-section bar. Equation 2.28 delineating this envelope, established by Calladine (2000), serves as a keystone in understanding the structural behaviour and limitations inherent to soil reinforcement.

$$\frac{M}{M_p} = \left(\frac{T}{T_p}\right)^2 = 1 \qquad (2.28)$$

Where, " M is the bending moment, M_p is bending moment capacity per nail, T is axial force per nail, T_p is the axial force capacity per nail."

Calladine's formulation helps simplify the interaction between axial force and bending moments (B.M.), improving soil reinforcement design. Equation 2.28 provides slightly conservative results for circular bars. Since no direct correlation exists for circular bars, Jewell and Pedley (1990) adopted this equation in their analysis.

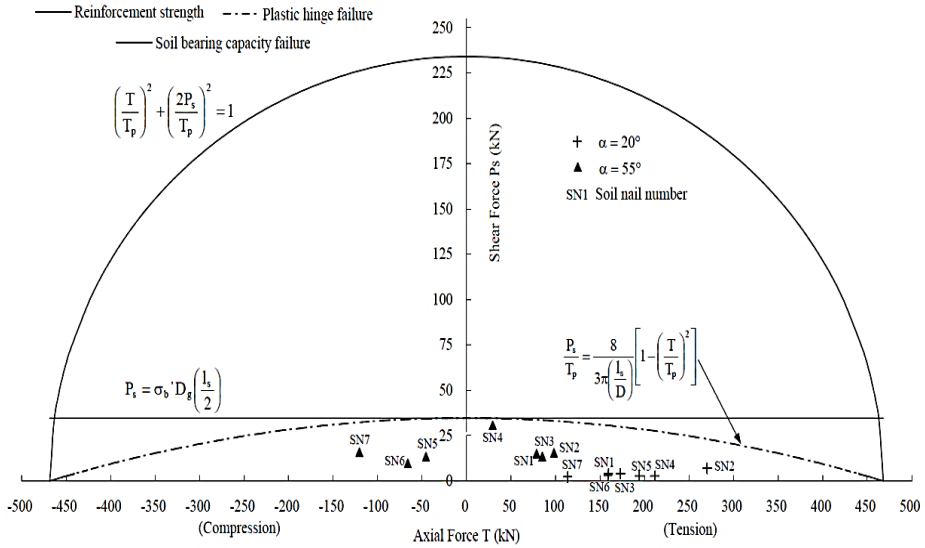

Figure 2.40: Combined loading and failure envelopes in reinforcement bar (Shiu and Chang, 2006)

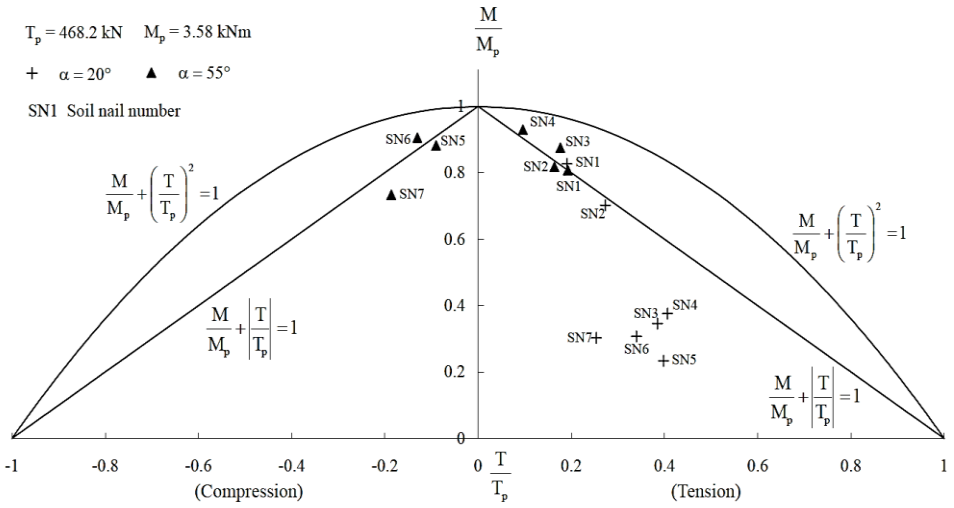

Figure 2.41: Differentiate between normalized axial force and moment (Shiu and Chang, 2006)

Figure 2.40 describes the limiting envelopes representing three distinct failure criteria, with particular emphasis on plastic hinge failure, deemed the most critical. For

comparative analysis, the shear and axial tension forces developed in individual nails at inclinations of both $\alpha = 20°$ and $\alpha = 55°$ are graphed, referencing the intersection point of the soil shear plane with the nails. The graphical depiction underscores that all shear and axial forces fall within the bounds of the limiting envelope tailored specifically for plastic hinge failure, irrespective of the inclination angle. Although nails inclined at $\alpha = 55°$ experience slightly higher shear forces compared to those at $\alpha = 20°$, the differences are minimal. Conversely, nails inclined at $\alpha = 20°$ exhibit significantly greater mobilized tensile forces compared to their $\alpha = 55°$ counterparts. Observing to Figure 2.41, it presents the stress conditions encountered by the nails in scenarios involving $\alpha = 20°$ and $\alpha = 55°$. Here, the bending moment (M) and axial force (T) generated within the nails are standardized by the plastic moment capacity (M_p) and complete plastic axial capacity (T_p), respectively. M and T values denote the utmost moment and axial force at locations proximal to the intersection between the shear plane and the nail. A comprehensive examination reveals that bending resistances activated in nails with $\alpha = 55°$ approach the threshold of complete plastic moment capacity ($M/M_p=1$). Interestingly, as moment capacity nears full mobilization, shear resistances induced in these nails remain relatively modest, as indicated by Figure 2.41. Conversely, for nails inclined at $\alpha = 20°$, the manifested bending resistances are notably passive.

2.16.1 Schlosser and Unterreiner (1991) Multi-Criterion Study of Nails Failure

Schlosser and Unterreiner (1991) carried out a multi-criterion study on nail failures. In their study, they confirmed that nails play a multifaceted role in the structure and the various types of internal failure occur. To ensure a comprehensive analysis, it is essential to consider all potential modes of failure and address them systematically. Limit Equilibrium Methods (LEM) assume that the soil mass reaches equilibrium at the limit state. In these equilibrium equations, only the normal forces (tensions and compressions, as T_n) and the shear forces (T_c) acting on the nails at the interface with the potential failure surface are considered. T_n and T_c must be calculated for each nail, typically based on the crack pattern associated with the specific surface being analyzed. To account for all potential nail failure conditions, Schlosser and Unterreiner

(1991) identified four distinct failure aspects. Each criterion in terms of its dependence on T_n and T_c is discussed below:

2.16.1.1 First criterion

It is related to an internal failure caused by pull-out and is determined by the interface frictional resistance q_s.

$$T_n \leq \pi D L_o q_s \tag{2.29}$$

Where, "T_n is axial force, πD is the circumference of the nail, L_o is length of nail behind the failure surface, and q_s is interface frictional resistance."

2.16.1.2 Second criterion

The second criterion pertains to soil nail failure. The bearing capacity pressure (P) limits the pressure exerted by a nail on the soil beneath it. When P, is reached at one point, the soil below the nail fails to yield the following criterion:

$$T_c \leq L_o P_u \left(\frac{D}{2}\right) \tag{2.30}$$

Where, "L_o is the transfer length (elastic analysis), P_u is the ultimate load and D is the diameter of the bar."

2.16.1.3 Third criterion

The third criterion pertains to nail failure due to breakage. Schlosser and Unterreiner (1991) cited in their study where Anthoine (1987) proposed the following simple criterion to represent the combination of T_n, and T_c that develops in a nail at failure, which is slightly more conservative than other proposed criteria. In the third criterion, the plane T_c and, T_n is represented by an ellipse as shown in Figure 2.42.

$$\left(\frac{T_n}{R_n}\right)^2 + \left(\frac{T_c}{R_c}\right)^2 + \left|\frac{M}{M_o}\right| \leq 1 \tag{2.31}$$

Where, "R_n is the maximum tensile force, T_c is the shear force in a nail, R_c is the maximum shear force, M is the bending moment in a nail and, M_o is the maximum bending moment in pure bending."

2.16.1.4 Fourth criterion

The nail can fail at two other points despite the points of maximum moment. Around the shear plane, the width of the shear band developed can be assumed for a distance L_s. With the progressive soil plastification, the two plastic hinges move beneath the nail after formation. In the absence of more solid details about L_s, it is constant and equal to $\pi L_0/2$. The maximum moment points are fixed assuming the two plastic hinges, the following fourth criterion equation is defined by Schlosser and Unterreiner (1991).

$$T_c \leq \left\{ c\, D\, L_o\, (P_u - P_o) + b \left(\frac{M_o}{L_o}\right) \left[1 - \left(\frac{T_n}{R_n}\right)^2\right] \right\} \qquad (2.32)$$

Where, "R_n is the maximum axial force (in simple tension), b and c are the constants, P_o is the pullout capacity."

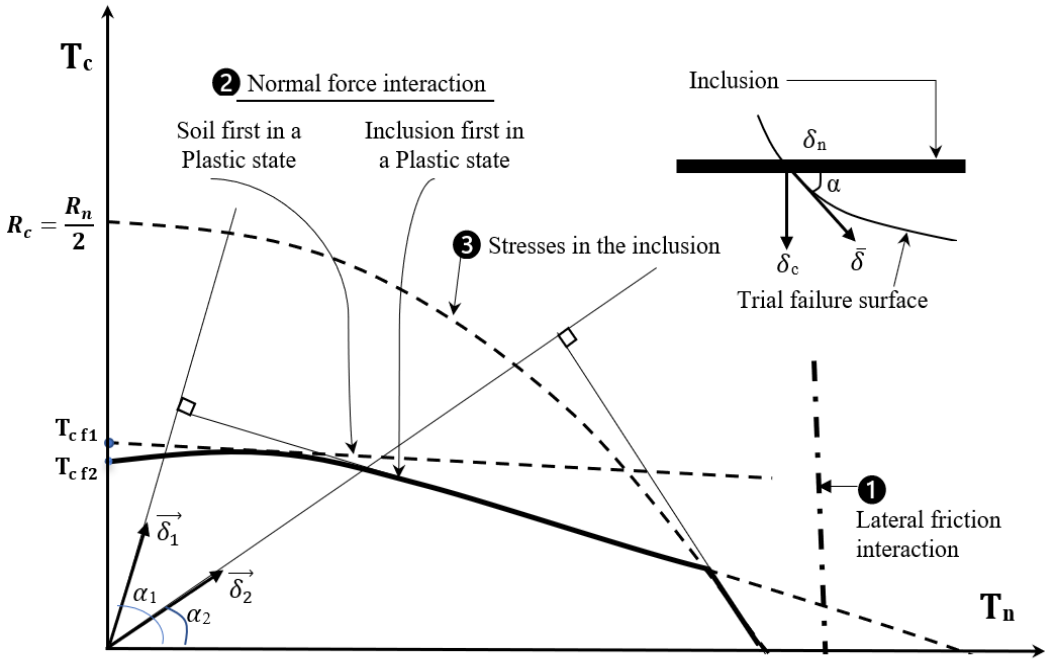

Figure 2.42: Interaction mechanisms between the plane's normal force (T_n) and shear force (T_c) (after Schlosser and Unterreiner 1991)

Schlosser and Unterreiner (1991), defined four important criteria described in the T_c and T_n plane are shown in Figure 2.42. In their study, they have defined a convex domain of stability in which the points T_c and T_n can be placed anywhere. Figure 2.42 represents a stability domain which is a combination of all four failure criteria. It is

important to note that, depending on the stiffness of the nails and types of soil, the first criterion has no bearing and the second criterion is less than the first criterion in this case. The points T_c and T_n are on the stability domain's border at failure, but their position is unknown a priori. The position of the points T_c and T_n on the border is chosen to maximize the nail's work in the potential failure mechanism under consideration. T_o maximize the dissipated work, T_c and T_n can be determined once with the failure surface where the nail point displacement is known at the intersection.

2.17 Enumerate The Tensile Forces at The Wall Facing

The FHWA 2003 Manual provides design methods to calculate tensile forces on the wall face. It shows that the maximum nail tensile force at the wall face is equal to or greater than a certain value (T_o). The nail head force, also called the facing force, follows a distribution similar to the maximum nail tensile force. The ratio of nail head force to maximum nail force ranges from 0.6 to 1.0. In the wall's upper half, the average normalized nail head force is 0.4 to 0.5, while in the lower half, it decreases and approaches zero at the bottom (Lazarte et al., 2003).

As per the FHWA-2003 recommendation, the nail head tensile force typically varies from 0.60 to 0.70.

$$T_o = 0.60\ Ka\ \gamma\ H \quad \text{to} \quad 0.70\ Ka\ \gamma\ H \tag{2.33}$$

The equivalent earth pressure on the facing is between 60% and 70% of the Coulomb's active earth pressure.

Normalized Nail Head Load (P) is,

$$P = \left[\frac{T_o}{\gamma\ H\ K_a\ S_h\ S_v}\right] \tag{2.34}$$

Where, "T_o is a tensile force at the nail head, K_a is the coefficient of active earth pressure, γ is the total unit weight of soil behind the wall; H is the height of the wall, and S_h and S_v are the nail horizontal and vertical spacing, respectively."

As per Lazarte et al. (2003) FHWA theory, the normalized allowable pullout resistance is defined as

$$P_{OR} = q_u \left\{ \left[\frac{D_{DH}}{\gamma S_h S_v} \right] \frac{1}{(FOS)_P} \right\} \quad (2.35)$$

Where, "q_u is ultimate bond strength, D_{DH} is drill hole diameter, $(FOS)_P$ is Factor of Safety against pullout (i.e. 2.0)."

The maximum normalized design tensile force in the bar is:

$$t_{max-s} = \left[\frac{T_{max}}{\gamma H S_H S_V} \right] \quad (2.36)$$

Where, "T_{max} is the maximum design nail tension, H is the height of the wall, S_H is the horizontal spacing and S_V is the vertical nail spacing."

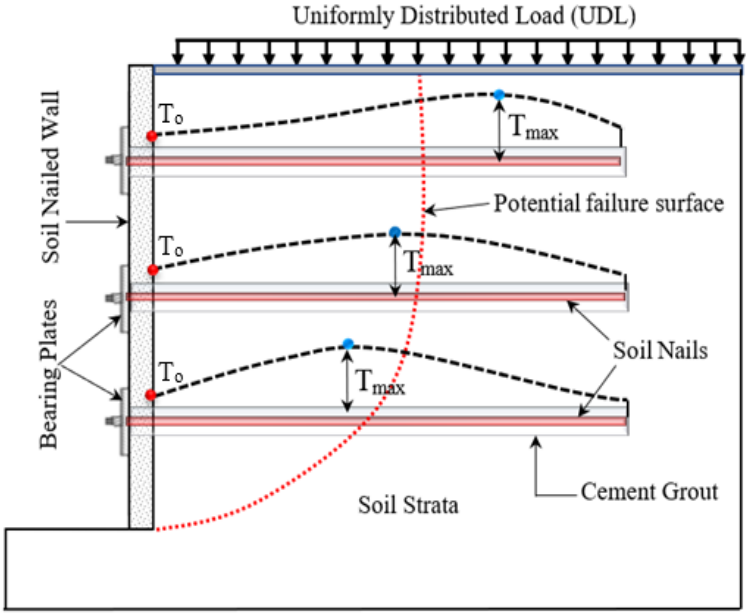

Figure 2.43: Location of maximum tensile force in soil nail wall structure (Lazarte et al., 2003).

2.18 Literature Review Based on Previous Studies on Soil Nailing

As highlighted earlier in this chapter, theoretical discussions have addressed various applications, components, and methodologies associated with soil nailing. This section

presents a comprehensive literature review on slope stability through soil nailing, drawing insights from scholarly articles, national and international technical journals, and other relevant sources.

Soil nailing is a widely used technique for stabilizing steep slopes, offering environmental and economic benefits. According to the FHWA Manual (1993a) and Ortigao (2004), soil nails are typically made of steel bars coated with cement grout, which prevents corrosion and improves durability. Nail-head plates are often added to the slope face to enhance stability, as noted by Wei and Cheng (2010). Research by Gassler and Gudehus (1981) highlights soil nailing as an effective and practical alternative to other methods due to its cost-efficiency and ease of implementation/construction. Several studies, including those from FHWA Manuals and ASCE journals, have contributed to soil nailing guidelines and methods. Notable theoretical and experimental work by researchers like Schlosser (1982, 1983), Bridle and Davies (1997), Davies and Le Masurier (1997), Tan et al. (2000), Ilan Juran (1987), Jewell and Pedley (1990, 1992), Marchal (1986), Smith and Su (1997), Jewell and Pedley (1992), and Pedley (1990) has examined the effects of shear and bending forces on soil nails, finding that bending reinforcement stiffness significantly improves performance. For soil nail design, the Limit Equilibrium Method (LEM) is commonly used due to its simplicity. Examples of LEM methods include those by Shen et al. (1981), Schlosser and Plumelle (1991), and Stocker et al. (1979). These approaches provide valuable guidance for designing stable soil-nailed structures.

The following paragraphs discuss studies conducted using various methods based on physical models and numerical studies.

2.18.1 Literature Review Based Physical Modelling

Physical modelling plays a crucial role in understanding and designing soil nailing structures by providing insights into soil and nail behaviour and their interaction. Numerous physical models have been developed to study the behaviour of soil nailing systems. Initially, physical modelling focused on investigating the impact of design parameters like nail length, spacing, and embedment depth on structure performance.

These studies provided valuable insights into the effects of nail spacing and embedment on the structure's capacity.

Nowadays, researchers mostly use physical modelling to examine soil nailing structures under static and dynamic loading conditions, focusing on the effects of soil type, nail length, spacing, and embedment depth on system performance. Physical modelling has also been utilized to investigate the behaviour of soil nail reinforcement systems during seismic loading. In addition to understanding and designing soil nailing systems, physical models have been employed to study the effects of different installation techniques, such as hollow bars or grout columns, on system performance. Furthermore, physical modelling has explored the response of soil-nailing systems to lateral loading and the influence of temperature and moisture on soil slope structure performance. By providing valuable insights, physical modelling serves as an important tool in understanding and designing soil nail slopes under various loading conditions, installation techniques, and environmental factors etc. Studies by Hayashi et al. (1988), Jewell and Wroth (1987), Jewell (1980), Marchal (1986), Shiu and Chang (2005), and Palmeira and Milligan (1989) have investigated soil reinforcement effect through laboratory experiments.

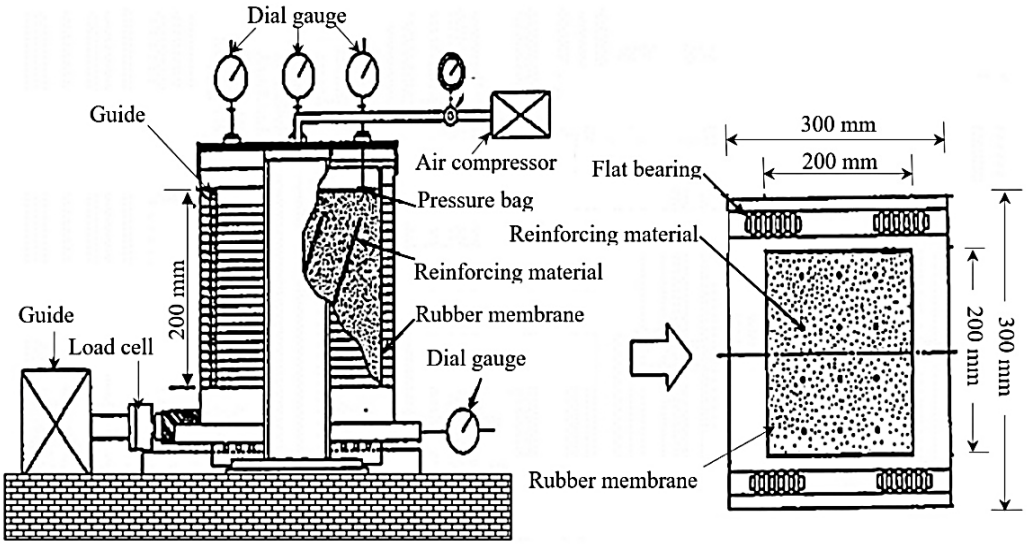

(a) Cross section of test apparatus (b) Plan of test apparatus

Figure 2.44: Versatile shear test apparatus (Hayashi et al. 1988).

Hayashi et al. (1988) conducted a shear test on sand samples using polymer grids and bronze bars as reinforcement, utilizing a newly developed versatile shear test apparatus

illustrated in Figure 2.44. The results demonstrated that specific reinforcement orientations enhanced soil shear strength, consistent with other studies. The test conducted by Hayashi et al. (1988) produced valuable insights into the effect of reinforcement orientation on soil shear strength, with strain gauges proving to be an effective means of measuring stress level changes.

This section provides a comprehensive overview of the shear test conducted by Hayashi et al. (1988), emphasizing its significance in relation to other studies. However, the description could be improved by including more details about the shear testing apparatus. Specifically, it should mention the use of flat bearings to minimize friction and describe how the specimens were restrained during the test. Additionally, further information on the installation and measurement range of the strain gauges would be helpful. A notable research gap identified in the findings of Hayashi et al. (1988) is that the effects of reinforcement orientations beyond the range of -20^0 to 20^0 were not explored. It would be useful to explore other orientations to determine if they affect soil shear strength. The effects of different types and thicknesses of latex rubber membranes could also be studied to see if they impact the results. The shear resistance of reinforced and unreinforced soil ratio (for Bronze Bar) at different orientations is shown in Figure 2.45.

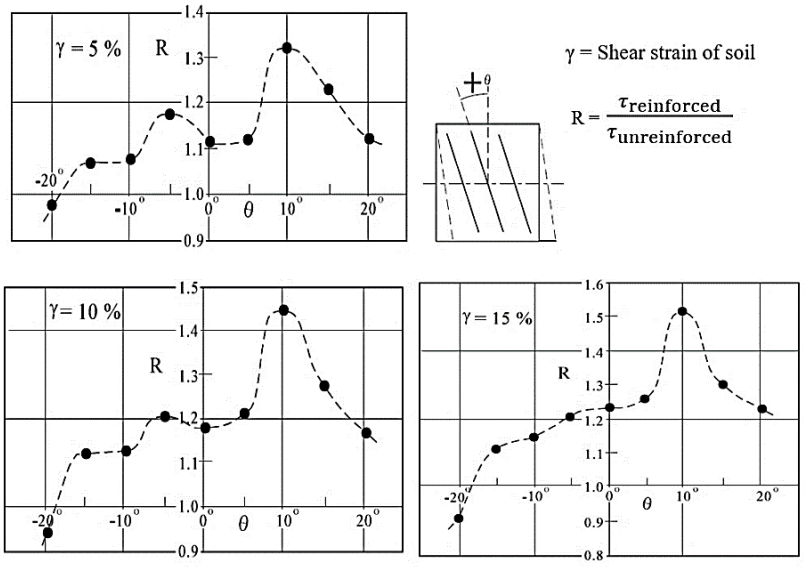

Figure 2.45: The relationship between the reinforcement ratio (R) and the direction of the reinforcing material (θ) in reinforced soil using bronze bars at various orientations (Hayashi et al. 1988).

The research conducted by Jewell and Wroth (1987) provides valuable insights regarding the application of tensile force to increase soil shear strength. Their research focuses on the behaviour of reinforced soils, the effects of grid reinforcement and direct shear box tests. Figure 2.46 Illustrated, Jewell and Wroth's (1987) research, which offers a comprehensive insight into the application of tensile force to enhance soil shear strength. Moreover, Jewell's research illustrates the stress patterns shown in Figure 2.47. In contrast to the behaviour of unreinforced soil after the peak, as shown in Figures 2.47 (a) and 2.47 (b), the presence of reinforcement in the soil increases soil stress and principal strains. Jewell and Wroth's (1987) research contributes significantly to our understanding of the application of tensile force to increase soil shear strength. Through direct shear box testing and stress pattern analysis, they focused on the reinforced soil behaviour, emphasizing the significance of appropriate reinforcement orientation for optimal results.

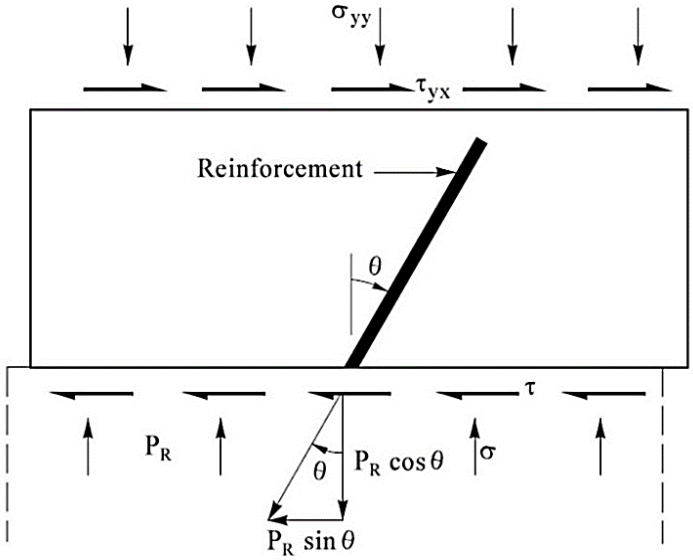

Figure 2.46: Soil increases shearing strength due to the tensile force of reinforcement (Jewell and Wroth, 1987)

Jewell and Wroth's (1987) research offers valuable insights into enhancing soil shear strength through the application of tensile force. Their study contributes to the understanding of grid reinforcement and direct shear box tests, providing useful information for geotechnical engineers. The findings emphasize the importance of aligning the tensile force with the main reinforcement direction to achieve optimal

strength improvement while deviating from this orientation diminishes the strength enhancement. This research proves to be a helpful asset for those seeking to improve soil shear strength. Future research endeavours could delve into alternative methods for enhancing soil shear strength and examine the impact of various reinforcement materials on this aspect. Therefore, further investigations should prioritize exploring how different reinforcement materials affect soil shear strength, along with exploring alternative techniques for its enhancement. Significantly, Figure 2.48 underscores the decrease in strength improvement when the reinforcement deviates from its optimal orientation.

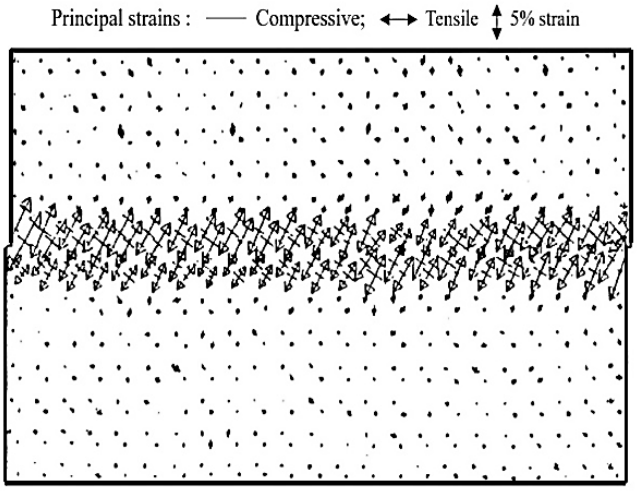

(a) Unreinforced sand

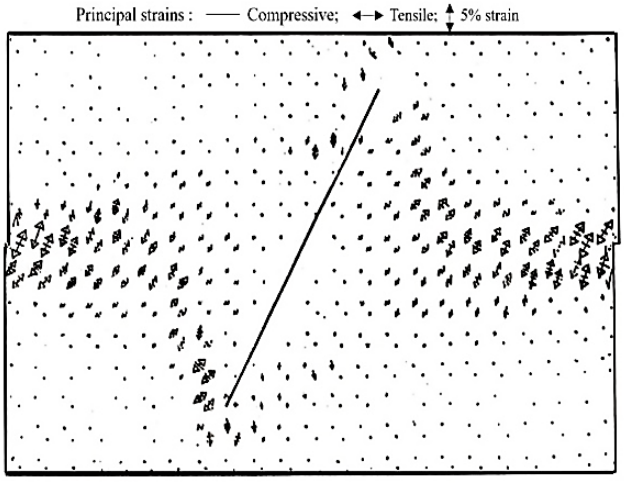

(b) Reinforced sand

Figure 2.47: Incremental strains in **(a)** Unreinforced sand and **(b)** Reinforced sand at peak shearing resistance (Jewell and Wroth, 1987)

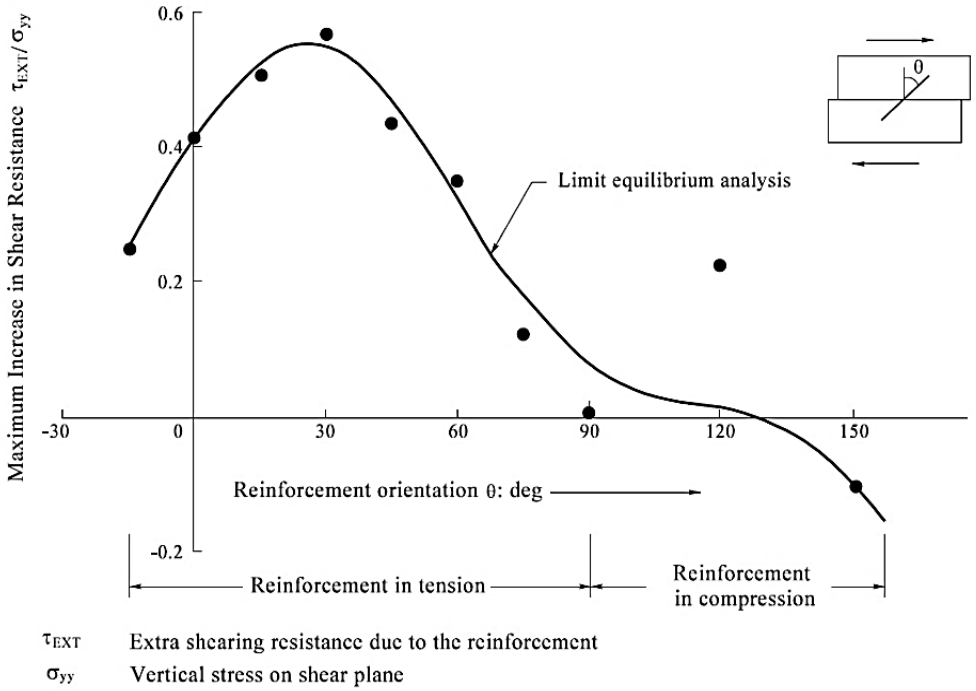

Figure 2.48: Reinforcement is placed at various orientations (measured maximum increase in shear resistance) (Jewell and Wroth, 1987).

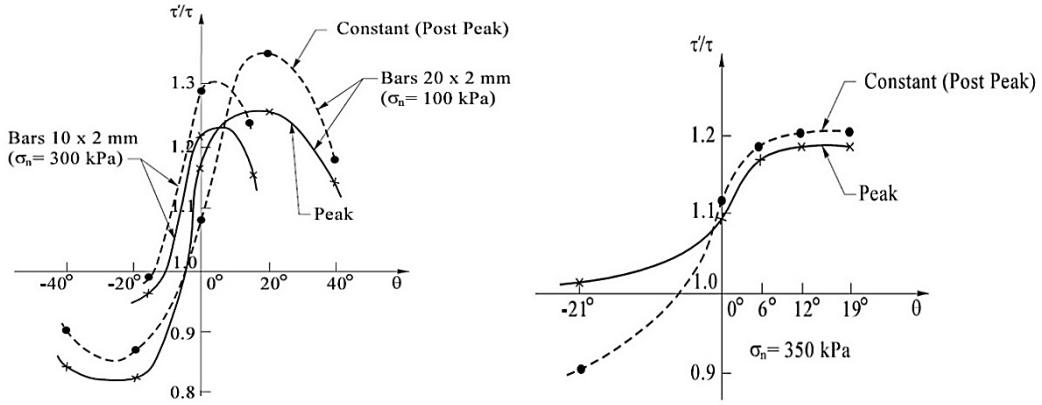

(a) Flexible reinforcement **(b)** Rigid reinforcement

Figure 2.49: The function of the orientation of nails (Marchal, 1986)

The study conducted by Marchal (1986) provides valuable insight into the behaviour of reinforced soil with nails. The research was conducted through a laboratory study with a shear box of 500 mm in height and 600 mm in diameter. The reinforcement used included steel bars with a 50 mm width and 8.8 mm thickness and a thickness of 2 mm flat bars with flexible aluminium alloy and width varying from 10 to 20 mm.

The study found that the shear resistance ratio of reinforced soils (τ') to unreinforced soils (τ) indicated the presence of a peak, for larger shear strains which was a decrease in the constant value. Compressive force or tensile force was primarily mobilised after reinforcements were progressively subordinated to shear forces, similar to both flexible and rigid reinforcements. The research also suggested the presence of an optimal reinforcement orientation in the context of soil strengthening which was confirmed by Jewell and Jewell et al. (1980, 1987, 1990, 1992). The findings of these studies are valuable in understanding the behaviour of reinforced soil with nails and can be useful in the design of reinforced soil structures. The function of the orientation of nails for (a) Flexible reinforcement and (b) Rigid reinforcement is shown in Figure 2.49. The axial force and the shear force (T/P_S) relationship developed in the reinforcement. Shear displacement (Δl) and nail inclination (α) of the soil variation are shown in Figure 2.50 (Marchal, 1986).

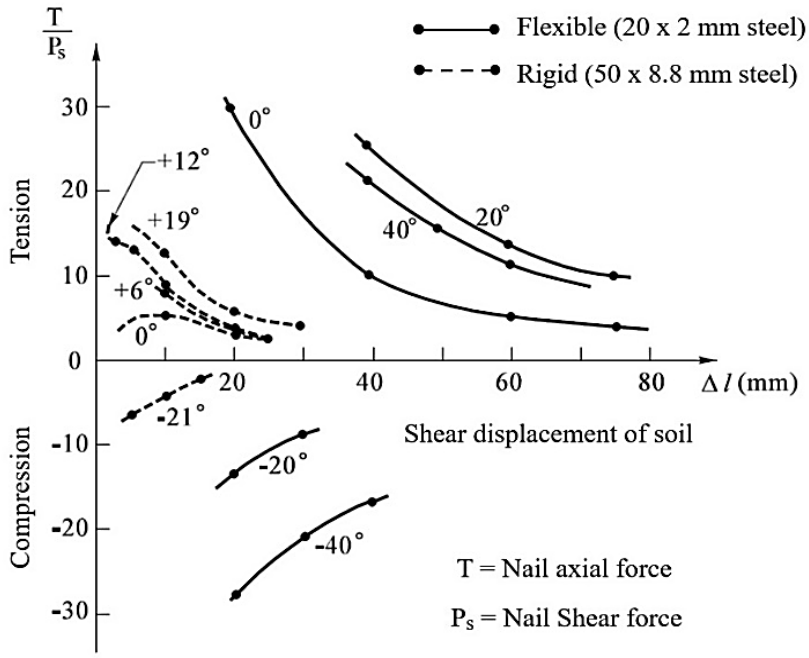

Figure 2.50: The function of nail orientation (θ) and shear displacement (Δ*l*) (in respect to relationship T/P_s) (Marchal, 1986).

Marchal's (1986) research on reinforced soil with nails highlights its significance in understanding the behaviour of such structures and aiding in their design. However, it would be advantageous to provide more specific details regarding the study's results,

including the observed range of shear resistance ratios, mobilized compressive and tensile forces, and the identification of optimal reinforcement orientations. These additional details would enhance the illustration of the research findings. Although Marchal's (1986) findings offer valuable insights into the behaviour of reinforced soil with nails, there is a gap in their investigation regarding the influence of soil moisture on the shear strength of the soil. Future research endeavours could concentrate on exploring the impact of soil moisture on the shear strength of reinforced soil with nails, further advancing our understanding of this type of structure.

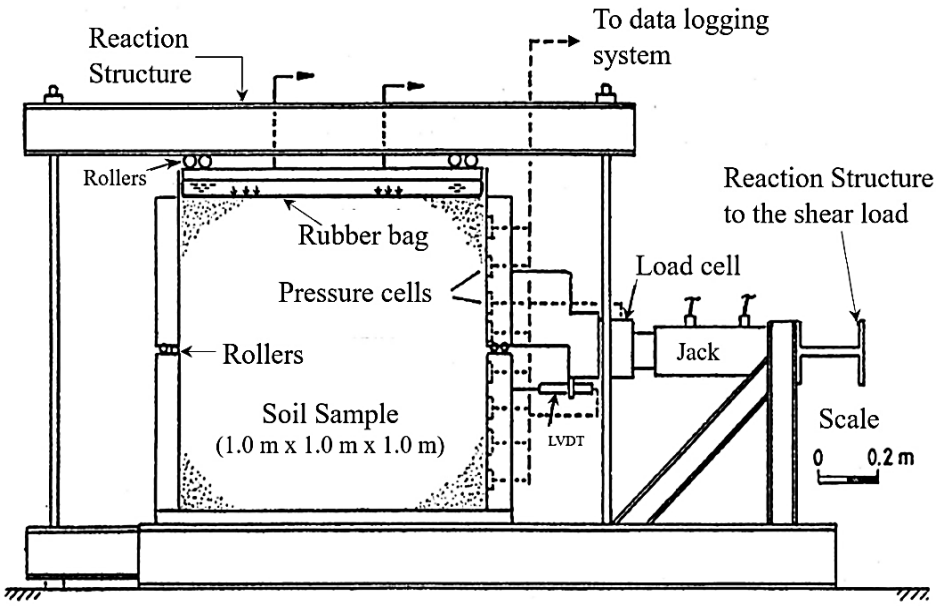

Figure 2.51: Schematic view of the large shear box (Palmeira and Milligan, 1989)

Palmeira and Milligan (1989), stated the results of experiments conducted on sand samples by direct shear tests. Sheet reinforcements and a variety of grids were used for reinforcing sand samples. For the experiments, a 1.0 x 1.0 x 1.0-meter size direct shear device was used (Figure 2.51). In the reinforced and unreinforced samples, the major strains occur at peak stress ratio. In unreinforced sand samples, the principal tensile stress is inclined at 30^0 with the vertical direction as shown in Figure 2.52 (a). A larger proportion of the soil was stretched, which then remained unchanged due to the presence of inclined reinforcements as shown in Figure 2.52 (b). Dominant tensile stress orientation was away from the reinforcement and in the central area, stagnant parallel to the reinforcement surface. In the path of principal tensile strains, a layer of

reinforcement was aligned. In shear strength, strains result in the expansion of a reinforced specimen. The reinforcement is positioned in the areas experiencing the highest tensile stresses. The horizontal component of the tensile stress in the reinforcement counters the development of shear stress. When a reinforced sample is aligned with the principal tensile strain, it demonstrates increased shear strength compared to an unreinforced soil sample (Millign and Kouji, 1998). The presence of the reinforcement layer reduces shear strain in the central region of the sample. Conversely, placing the reinforcement layer in the direction of minor principal tensile strain leads to greater shear strain due to the horizontal components of reinforcement force (Millign and Kouji, 1998).

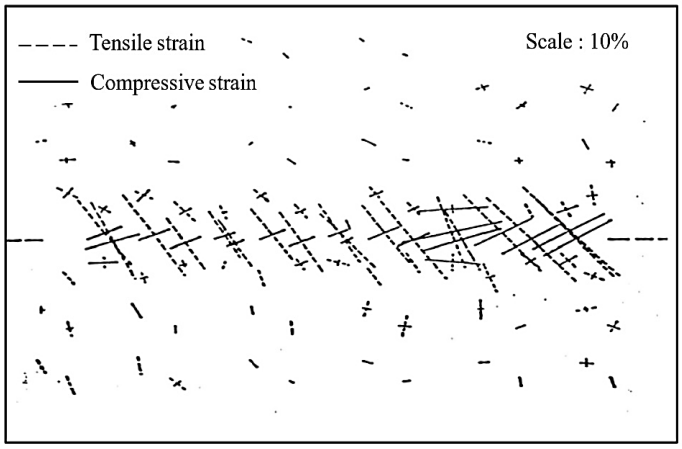

(a) Unreinforced

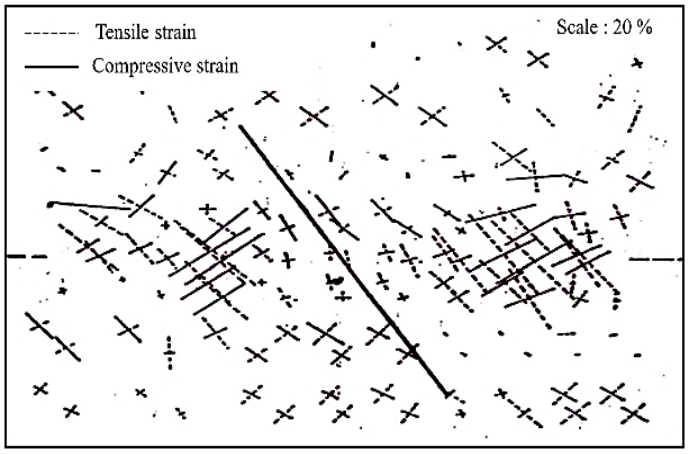

(b) Reinforced with grid 4

Figure 2.52: Principal strain orientation at peak stress ratio (Palmeira and Milligan, 1989)

The experiments carried out by Palmeira and Milligan (1989) illustrate the potential benefits of employing sheet reinforcements and grids to reinforce sand samples, leading to enhanced shear strength. Their findings indicate that incorporating reinforcement layers aligned with the principal tensile strain can elevate shear strength, while placing the reinforcement layer centrally in the sample may reduce shear strain. Moreover, the horizontal component of the reinforced tensile stress intercepts the development of shear stress. Consequently, the utilization of sheet reinforcements and grids is recommended for augmenting the shear strength of sand samples. Palmeira and Milligan (1989) suggest that employing sheet reinforcements and grids can effectively enhance the shear strength of sand samples.

Charles et al. (2022) researched to explore the triggering and failure mechanisms of loose fill slopes under conditions of increasing groundwater or precipitation. To replicate the behaviour of such slopes, two centrifuge model experiments were conducted on loose sand renowned for its susceptibility to liquefaction and tendency to contract. In terms of the experimental setup, the researchers constructed model slopes within a rectangular container. The dimensions of the container (Model) were 1245 × 851 × 350 mm, primarily made of aluminium. However, a notable feature was the inclusion of an 80 mm thick transparent side wall on the front side of the container. This transparent wall allowed for convenient observations during the tests, enabling researchers to monitor and analyze the behaviour of the model slopes in real-time. The geometry and instrumentation of the model slope are shown in Figure 2.53.

During the tests, the rainfall test only resulted in extreme settlements, while a rapid and brittle fluidized flow slide occurred on the slope subjected to rapidly increasing groundwater. The initiation of this event was caused by a localized drained surface failure, represented by a drainage ditch at the top of the slope, resulting in a significant decrease in effective stress and a decline in shear strength due to static liquefaction. To address such occurrences, a thorough three-dimensional back-analysis and parametric examination were carried out to explore the effectiveness of soil nails in averting the onset of static liquefaction in loose fill slopes. Simulation studies demonstrated that soil nailing could effectively prevent fluidized flow slides by restraining the mobilization of the soil's maximum shear strength and limiting excessive strains required for static liquefaction initiation. Consequently, catastrophic

failures can be prevented. The study emphasizes the importance of comprehending potential failure mechanisms in loose fill slopes and highlights the necessity of implementing effective mitigation techniques like soil nailing to avert disastrous outcomes.

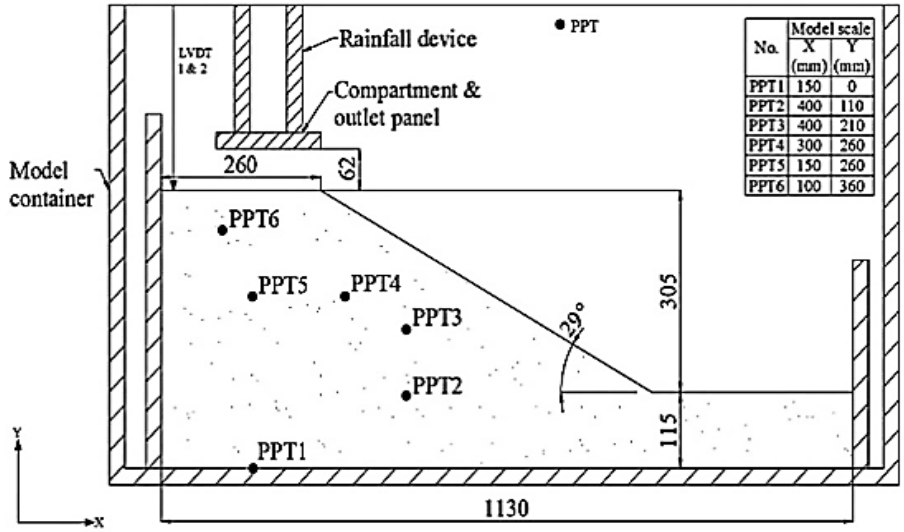

(a) Slope Model -I

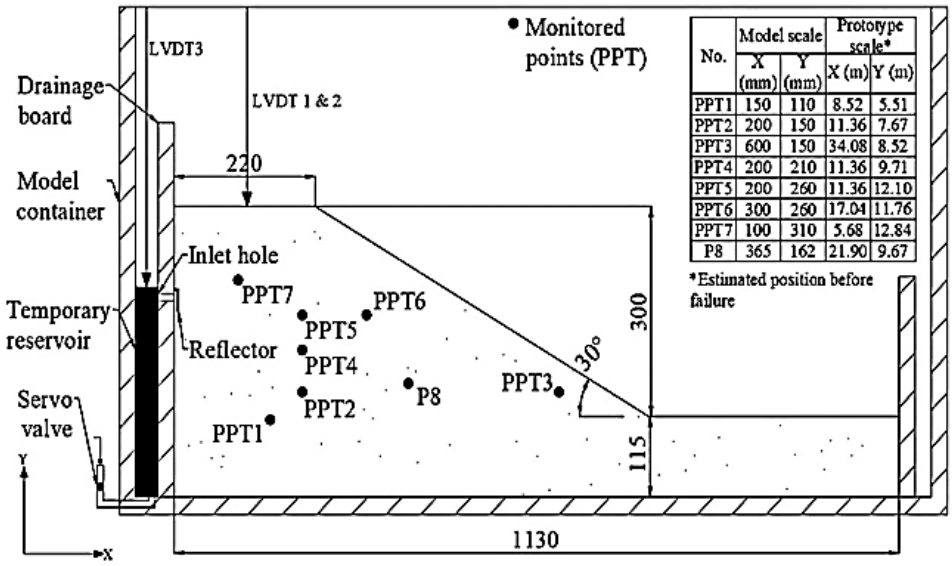

(b) Slope Model -II

Figure 2.53: Initial geometry and instrumentation of model slope for Tests (a) and (b) (Charles et al. 2022)

2.18.2 Literature Review Based on Numerical Methods

The finite element method (FEM) and the finite difference method (FDM) stand as the primary numerical approaches for analyzing soil nailing systems. FEM subdivides a region into finite elements to solve boundary value problems, while FDM breaks it down into points and computes the solution at each one. Both methodologies prove effective in examining the behaviour of soil nailing systems under various loading conditions. Researchers have utilized FEM and FDM to explore various facets of soil nailing systems, encompassing the response of soil nail walls to static, seismic, and dynamic loads. Additionally, they have scrutinized the influence of soil and nail properties on wall performance and refined their design. For instance, FEM has delved into how design parameters like nail size and spacing impact wall performance, while FDM has discerned optimal designs for varying ground conditions. These numerical methods find widespread application in analyzing soil nailing structures/slopes and enhancing wall design. Typically, the design of soil-nailing systems relies on commercial software packages or modified software solutions. Current practices in designing soil-nailed retaining structures often lean deeply on FEM analysis techniques. The ensuing discussion provides a succinct overview of the research endeavours undertaken by various scholars in this domain. FEM is a numerical technique used to solve boundary value problems arising in engineering and science. The FDM emerges as a valuable tool for simulating soil-nailed wall behaviour, as demonstrated by several investigations.

This review pursues to present a comprehensive overview of the fundamentals, applications, and advancements of the Finite Element Method (FEM) and Finite Difference Method (FDM). Numerous studies leveraging FEM have been documented and are summarised in Table 2.3 below.

Table 2.3: Summary of literature review based on FEM and FDM

Sr. No.	Author(s)	Analysis Method	Key Focus	Findings	Future Research Suggestions
A. *Finite Element Method (FEM)*					
1	Nguyen et al. (2023)	2D-FEM	Influence of spatial variability and anisotropy in silty/clayey soils on slope stability.	Higher COV increases failure probability; anisotropic soils are more prone to failure than isotropic ones.	Investigate additional factors like soil-nailing impacts and 3D-FEM applicability.
2	Rajhans et al. (2022)	LEM & FEM	Stability analysis of overburden dump in an opencast mine.	Combined use of LEM and FEM provided insights into dump stability; FEM offered detailed stress distribution analysis.	Extend to varied mining conditions and loading scenarios.
3	Azzam and Sobhey (2019)	2D-FEM	Soil nailing for sandy slopes under seismic conditions.	Soil nailing significantly improves slope stability under seismic conditions; Shear strength plays a vital role in soil reinforcement.	Study the influence of varying nail configurations and seismic intensities.
4	Potgieter et al. (2019)	2D-PLAXIS & LEM	Comparison of FOS results from FEM and LEM.	FEM yielded higher and more precise FOS; emphasized FEM's reliability for lateral support design.	Study the influence of structural parameters and boundary conditions.
5	Sharma et al. (2019)	2D-PLAXIS	Comparative FOS analysis for conventional vs. helical soil nails.	Helical nails exhibited higher FOS than conventional nails; Helical nails had better bearing capacity.	Examine the effects of soil type and loading conditions on nail performance.
6	Rawat and Gupta (2016b)	PLAXIS-2D & SLOPE/W	Comparison of FE and LEM for reinforced slope analysis.	Satisfactory agreement between software predictions and experimental results; both methods are effective.	Explore the combined use of FE and LEM for improved accuracy.
7	Olia and Liu (2011)	2D & 3D-FEM	Soil nail wall performance during construction stages.	Nail length increases displacement and force; adding more nails reduces these. Provided guidance on stability and design.	Study soil characteristics, construction techniques, and wall configuration effects.
8	Singh and Babu (2010)	2D -FEM	Performance of soil nail walls under varying soil conditions.	Soil-structure interaction significantly influences wall performance; anisotropy affects stability.	Further exploration of soil anisotropy effects and wall design optimization.
9	Fan and Luo (2008)	2D-FEM	Optimal layout of soil nails for slope stability.	Optimal nail orientation depends on soil parameters; lower third of slope is critical for stability; irregular nail patterns improve stability by up to 23.4% for vertical slopes.	Investigate the effects of wall shape, external loads, and geological contexts.

Continue …….

10	Ann T et al. (2004)	2D-FEM	Evaluation of Mohr-Coulomb failure criteria in soil-nailed slopes.	The FE analysis showed a good correlation with field data and successfully predicted stresses, displacements, and shear strength.	Applying the approach to diverse geological contexts and design scenarios.
11	Ng and Lee (2002)	3D-FEM	Stabilization of tunnel faces using soil nails.	Soil nails effectively stabilize tunnel faces; performance is influenced by soil properties, nail characteristics, and tunnel geometry.	Develop guidelines for tunnel stabilization under varying conditions.
12	Zhang et al. (1999)	3D-FEM	Ground movements induced by soil nailing construction.	FEM precisely simulated ground movements and captured the effects of soil heterogeneity and soil-nail interaction.	Examining more geological contexts and soil-nail interaction effects.
13	Sawicki et al. (1988)	FEM	Stress and bearing capacity analysis of full-scale reinforced slope.	FEM accurately predicted stresses in nails and walls but was less effective for bearing capacity.	Investigating various loading scenarios and refining bearing capacity predictions.
14	Smith and Su (1997)	3D-FEM	Influence of curved wall geometry on load-bearing capacity and stress distribution.	Curved walls showed a significant impact on stress distribution and load capacity, aligning closely with theoretical projections.	Explore external loads and different wall geometries.
B. *Finite Difference Method (FDM)*					
15	Wei and Cheng (2010)	SRM and LEM	Performance of nailed slopes under varying soil conditions and nail layouts	Similar safety factors and slip surfaces were observed using both SRM and LEM. Recommendations focus on optimizing nail layouts and aligning the line of maximum tension with the critical slip surface for improved stability.	Explore advanced computational models to analyze complex interactions between nails and soil under dynamic conditions.
16	Cheuk, Ng, and Sun (2005)	FDM using FLAC	The behaviour of soil nails in loose fill slopes subjected to rainfall infiltration	Soil nails significantly enhance slope stability by reinforcing slopes and mitigating the effects of rainfall infiltration. Emphasized the role of water content in slope stability.	Further investigation into the combined effects of rainfall intensity and slope geometry on soil nail performance.

Similarly, many researchers have broadly investigated soil slope stability using numerical simulation techniques, as demonstrated in studies conducted by Ersoy et al. (2020), He Yi et al. (2019), He Yunyong et al. (2023), Lazorenko et al. (2020), Nasvi et al. (2019), Qin et al. (2023), Sari, (2022), Sazzad et al. (2016), and Wang et al. (2021), etc. These investigations employed various numerical methods, such as the FEM (FLAC-2D and PLAXIS-2D), finite element limit analysis, and FDM. In addition, studies conducted by Ahmad et al. (2023), Ahmadi and Borghei (2018), Li and Xiao (2023), Ng et al. (2022), Pinyol et al. (2022), Sumartini et al. (2021), Zhou et al. (2023), Yi and Kang (2025) etc. focused on simulating slope behaviour under different loading scenarios, encompassing static and dynamic conditions. The primary objective of these researchers was to gain a deeper understanding of the failure mechanisms exhibited by soil slopes, including slope deformation and failure modes such as shallow and deep-seated landslides. To accurately capture the complex behaviour of slopes, they developed advanced numerical models incorporating the nonlinear behaviour of soils. These studies also examined the impact of external factors on slope stability, including seismic loads, rainfall-induced pore pressure, and changes in soil properties due to ageing or environmental factors.

2.18.3 Literature Review Based on Soil Nails Bending Stiffness Effect

This section explores the soil nails' bending stiffness effect in the design and construction of soil-nailing structures, which significantly impacts their strength and stability. Soil nails, composed of steel bars inserted and grouted in the soil, are widely used in slope stability and retaining wall construction. The bending stiffness depends on factors such as nail length, diameter and soil type. Numerous studies have examined these factors and revealed their influence on bending stiffness. Soil type has a significant impact, and increasing nail diameter can enhance stiffness up to a certain limit. The choice of grouting material also affects stiffness, with epoxy grouts exhibiting better results than cement grouts. Considering these factors is crucial for optimal soil nail structure performance. The summary of the literature review based on soil nail bending stiffness effect is stated below in Table 2.4.

Table 2.4: Summary of literature review based on soil nails bending stiffness effect

Sr. No.	Author(s)	Analysis Method	Key Focus	Findings	Future Research Suggestions
1	Rawat and Gupta (2016)	PLAXIS 2D and SLOPE/W analysis	Investigated bending stiffness in reinforced slopes with varying nail inclinations	LEM showed higher FOS values but different failure surfaces compared to FEM. Nail forces increased with steep slopes and inclinations.	Integrate bending stiffness considerations into FEM and LEM models for more precise stability predictions.
2	Tan et al. (2000)	Stratified failure mode analysis	Defined failure modes (nail yield, soil yield, simultaneous failure) based on soil-nail interaction	Failure modes are influenced by soil strength, nail stiffness, and horizontal movement. Axial and shear forces were generated in nails due to deformations.	Further research into deformation mechanisms and their implications on soil-nail interaction.
3	Davies and Masourier (1997)	Large-scale shear box tests	Studied shear load and tensile forces in nails	Tensile forces in nails peaked at 30 mm displacement; shear force increased continuously after 20 mm displacement due to the plastic moment at the nail. Nail pullout was controlled by tensile force.	Explore the effect of varying nail dimensions and grouting materials on tensile and shear capacities.
4	Smith and Su (1997)	3D finite element analysis	Examined soil-nailed walls under construction and service loads	Nails developed shear resistance and minimal bending under service loads; under surplus load, shear stress and bending moments were mobilized.	Study soil-nail interaction under dynamic or extreme loading conditions for improved designs.
5	Plumelle and Schlosser (1990)	Instrumented soil-nailed wall tests	Studied bending stiffness and tensile force mobilization in saturated conditions	Failure occurred due to large deformations and bending stiffness mobilization; tensile force was gradually mobilized during excavation.	Explore enhanced instrumentation techniques for measuring bending stiffness in soil nails.
6	Marchal (1986)	Direct shear tests	Examined shear forces induced in soil nail reinforcements	Flexible reinforcements mobilized compressive/ tensile forces at 60-70 mm displacements; rigid reinforcements mobilized forces at 20 mm. Significant deviations were observed between axial tension and shear force.	Investigate the relationship between shear displacement and reinforcement performance in various soil conditions.

2.18.4 Literature Review Based on Miscellaneous Study on Soil Nailing

Soil nailing is an effective technique that enhances the pullout resistance and strength of in-situ soil masses (Su et al. 2010). However, during top-down excavation on construction sites, face failure can occur due to reduced confining pressure (Seo et al. 2014). The friction between soil and nails generates both tension and compression forces, while shear forces (SF) and bending moments (BM) in the nails can lead to nail-bearing failure. These combined forces, along with the soil's capacity, influence the overall performance of the nails (Shiu and Chang, 2005).

Based on previous studies, soil nailing has been identified as one of the most versatile, economical, and efficient stabilization techniques (Azzam and Basha 2017; FHWA 2015; Gurpersaud et al. 2011; Lin et al. 2016, 2020; Liu et al. 2017; Pei et al. 2013; Sanvitale et al. 2013; Schlosser and Unterreiner 1991; Sivakumar et al. 2010; Tokhi et al. 2016). Its growing popularity is attributed to its suitability for stabilizing vertical or near-vertical cut slopes, excavation designs, and tunnel portal stabilization. Given its rapid construction and cost-effective advantages, soil nailing has become increasingly favourable in modern construction (Shivkumar Babu and Singh 2011; Bhuiyan et al. 2022; Derghoum and Meksaouine 2021; Guang-Hui et al. 2022; Muthukumar et al. 2022; Rajhans et al. 2022; Seo et al. 2014; Sharma et al. 2020; Tavakoli and Aminfar 2021, 2022; Zahedi et al. 2021).

To highlight the benefits and functions of soil nailing, a comprehensive literature review based on previous research is presented in Table 2.5:

Table 2.5: Summary of literature on soil nailing and stability enhancement

Sr. No.	Author(s)	Focus	Key Findings	Remarks
1	Bhuiyan et al. (2022)	Investigation of pressure-grouted soil nail systems using a newly developed test apparatus.	Higher grout injection rates lead to increased grout volumes and enhanced pullout resistance of soil nails.	Highlights the effectiveness of pressure grouting in improving soil-nail bond strength and the utility of the custom-designed apparatus for controlled laboratory testing.
2	Derghoum and Meksaouine (2021)	Development of FISH language-based programming in FLAC3D for nailed slope stability analysis.	The 3D finite difference method provides more accurate stability predictions, showing that 2D methods significantly underestimate the Factor of Safety (FOS) and critical slip surfaces.	Emphasizes the significance of using 3D analysis for slope stability evaluations, despite its higher computational demands, while providing practical insights for real-world applications.
3	Johari et al. (2020)	Stability interdependence and pullout resistance	The greatest interdependence exists between global and lateral displacement stabilities. Pullout resistance showed the lowest reliability coefficient among elements.	Used SCM and RFEM to analyze reliability in soil nailing systems.
4	Yuan et al. (2019)	Evaluation of Chinese technical specifications for soil nailing	Default methods overestimate maximum nail loads by 40% with prediction spreads of 70%–100%.	Highlights variability in default design predictions.
5	Azzam and Basha (2017)	Vertical inclusion effects on cohesive soil parameters	Strength and stiffness increase significantly, and settlement decreases as vertical inclusions increase in number.	Demonstrates enhanced geotechnical parameters through reinforcement.
6	Liu et al. (2017)	Facing tensile forces	A database of 56 measured facing tensile forces was developed. Modified models show improved accuracy compared to default conservative models.	Created a recalibrated FHWA model for short-term tensile force prediction.
7	Liu et al. (2016)	Failure modes of soil-nailing structures	Excavation displacement and shear stress are controlled within limits using random system variables and strength reduction methods.	Provides a systematic approach to assess stability using random variables.

Continue ……

8	Tokhi et al. (2016)	Pullout behaviour in conventional and screw nails	Pullout tests showed Mohr-Coulomb failure behaviour. Screw nail pullout capacity depends on overburden pressure and failure planes.	Differentiates pullout capacity mechanisms for screw and conventional nails.
9	Liu et al. (2014)	Failure process mechanism in reinforced slopes	Nailing reduces slope tension cracks and enhances stability. Failures include bending and pullout mechanisms, influenced by slope deformation and nail deflection.	Discussed the importance of load application in nail failure behaviour.
10	Seo et al. (2014)	Face failure and optimization in excavation	Confining pressure can cause face failure during top-down excavation. Optimization includes pullout failure and shear failure for enhanced design effectiveness.	Incorporates prestress, bonded length, and the total number of nails in optimization.
11	Miyata and Bathurst (2012)	Design charts for earth pressure coefficients	Developed charts for tensile reinforcement loads based on soil friction angles and measured loads from 7 instrumented structures.	Adjusted for cohesive-frictional soils with high fine content and lower friction angles.
12	Sivakumar Babu and Singh (2011)	Application of LRFD to soil-nail walls	Illustrates the calculation of reliability-based load and resistance factors for strength limit states.	Proposes LRFD as a modern alternative to traditional equilibrium-based design.
13	Su et al. (2010)	Pullout resistance and shear strength enhancement	Soil nailing improves the pullout resistance and shear strength of in-situ soil mass, preventing face failures during excavation.	Emphasizes tension and compression development due to soil-nail friction.
14	Shiu and Chang (2005)	Development of SF and BM in nails	Shear forces and bending moments in nails lead to nail-bearing failure. These forces interact with soil capacity and nail reactions.	Highlights the importance of understanding combined forces for better design.
15	Ilan et al. (1990)	Kinematical limit analysis for soil-nail wall design	Assessed the impact of design factors on maximum nail force positions. Proposed a rational procedure to anticipate progressive pullout failure.	Advocates for individual safety factor evaluations for each nail to prevent failure.

2.19 Soil-Nailed Slope Preliminary Design

The preliminary design phase of a soil-nailed slope is critical for ensuring stability and durability. This phase involves applying geotechnical principles to address slope stability challenges effectively. It includes a thorough evaluation of site-specific

conditions, geotechnical analyses, and conceptual design considerations to develop a well-informed strategy for preventing slope failures.

Geotechnical engineers, structural experts, and construction professionals collaborate to create a solid plan that balances technical precision with practical implementation. By analyzing soil properties, slope geometry, and load dynamics, the preliminary design lays the groundwork for detailed design and construction. This phase focuses on harnessing the natural forces within the soil and reinforcing slopes to withstand environmental pressures. It represents a meticulous and innovative approach to creating resilient, long-lasting structures that blend seamlessly with the natural landscape.

2.19.1 Key Steps to Confirm the Safety and Stability of the Slope

A preliminary design of a soil-nailed slope involves several key steps to ensure the safety and stability of the slope. Soil nailing is a technique used to reinforce soil slopes, retaining walls, and other structures by inserting closely spaced reinforcing elements (nails) into the soil. The nails provide additional tensile strength to the soil, preventing potential failures such as sliding or collapsing. Here's a detailed outline of the preliminary design process for a soil-nailed slope discussed below:

(A) *Site Investigation and Geotechnical Analysis*

1. Conduct a comprehensive site examination to recognize the soil conditions, groundwater levels, slope geometry, and any existing structures nearby.
2. To identify the soil properties (angle of internal friction, permeability, cohesion, shear strength etc.) soil samples were collected from various depths.
3. Analyze the data to assess potential slope stability issues, considering factors like natural slope angle, soil type, and potential triggering events (rainfall, seismic activity etc.)

(B) *Design Parameters*

1. Determine the design parameters, including the required factor of safety, slope angle, and anticipated loads (static and dynamic) on the slope.
2. Define the desired service life of the slope.

(C) *Conceptual Design*

1. Develop a preliminary layout of the soil-nailed slope, considering factors like nail spacing, slope height and angle etc.
2. Determine the length and type of nails based on the soil properties and the desired design parameters.
3. Choose the type of facing material (shotcrete, geosynthetic materials, etc.) that will be used on the slope face to avoid erosion and weathering.

(D) *Stability Analysis*

1. Perform a slope stability analysis using appropriate procedures such as LEA (e.g., Bishop's method, Spencer's method) or numerical modelling (FEM, FDM).
2. Assess the slope stability with and without nails to evaluate their effectiveness in preventing failure.

(E) *Nail Layout and Spacing*

1. Determine the best nail layout and appropriate spacing along the slope face based on stability analysis results and considering various factors like soil properties, anticipated loads, and slope geometry.
2. Account for any variations in spacing and nail length based on potential zones of higher stress or weaker soil layers.

(F) *Nails Design*

1. Calculate the required tensile and bond strength of the soil nails holdout against sliding and pullout forces.
2. Select appropriate nail materials (e.g., steel or fibreglass) based on factors such as corrosion resistance and structural properties.
3. Specify nail diameter and length based on calculated loads and soil conditions.

(H) *Facing Reinforcement*

1. Specify the facing material and its connection to the soil nails.
2. Design any additional support elements such as mesh reinforcement or geogrids to enhance the facing's structural integrity.

(I) *Construction Considerations*

1. Develop construction specifications and guidelines for the soil nailing process, including drilling, grouting, and facing installation.
2. Provide quality control measures to ensure proper installation and load transfer of the soil nails.

(J) *Monitoring and Maintenance*

1. Establish a monitoring plan to assess the performance of the soil-nailed slope over time.
2. Define maintenance requirements and intervals for inspections, repairs, or additional reinforcement if needed.

(K) *Documentation and Reporting*

1. Prepare detailed design drawings, calculations, and reports outlining the preliminary design of the soil-nailed slope.
2. Ensure that all design parameters, assumptions, and analyses are documented for review and approval by relevant experts.

It's significant to note that the preliminary design is a crucial stage that lays the foundation for the detailed design and construction phases. Collaboration between construction experts, and structural and geotechnical engineers is required to ensure the effective implementation of the soil-nailed slope while considering safety, stability, and environmental factors.

2.19.2 Preliminary Design Procedure

For preliminary design, an efficient procedure, similar to a carefully constructed flow chart (refer to Figure 3.46), serves as a visual representation of the systematic path engineers and designers follow to bring their ideas to realization/execution. This structured approach is vital extent, ensuring that every phase is thoughtfully addressed before progressing to the next, creating a seamless interaction between creativity and technical insight. This flow chart reflects the dynamic interplay between meticulous planning and creative innovation, encapsulating the essence of the preliminary design process. With each box and arrow, it encapsulates the essence of translating ideas into

tangible structures, bringing order to complexity, and imbuing each project with the potential for success. The following section outlines the preliminary design utilizing the simplified charts from FHWA 2003.

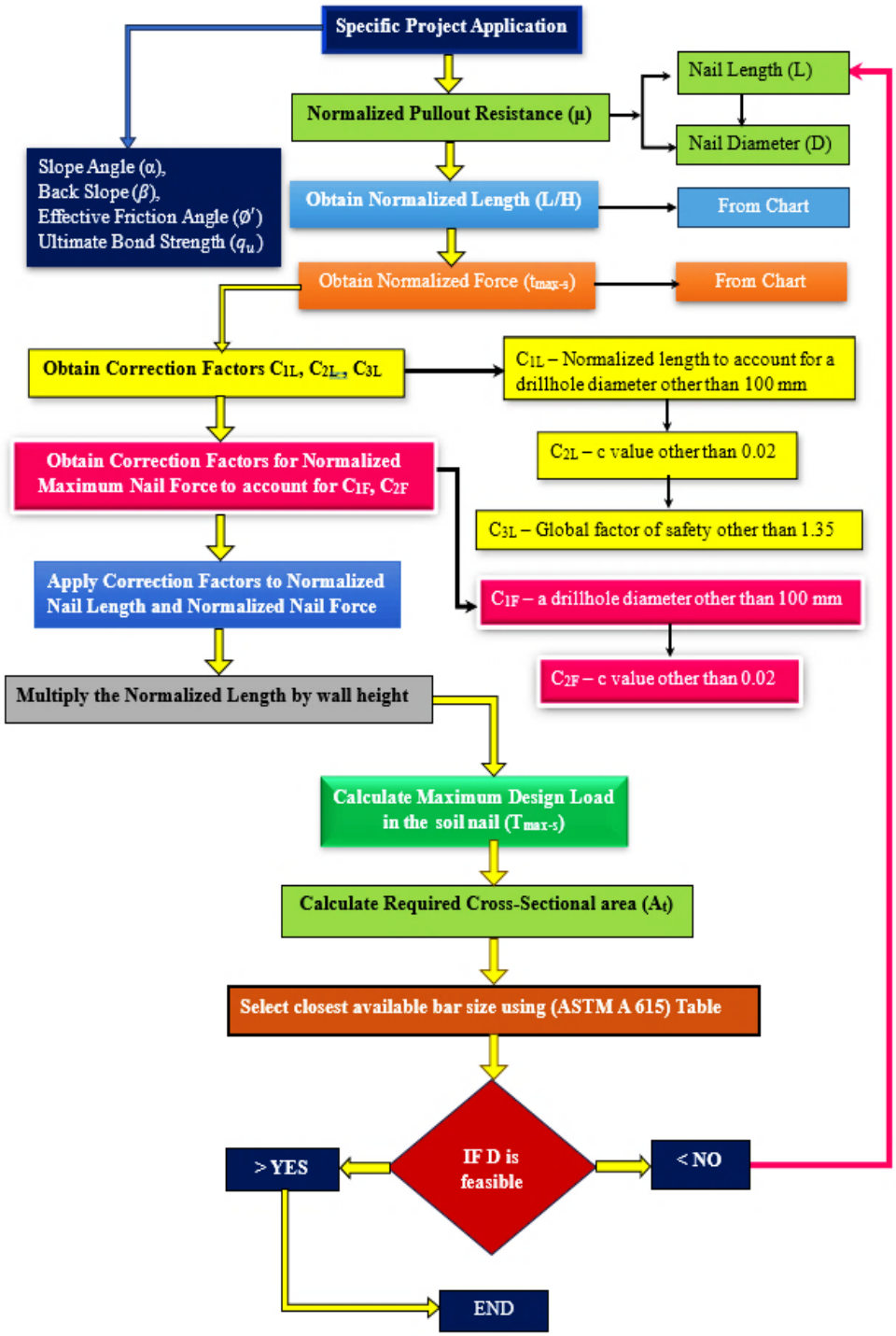

Figure 2.54: Preliminary design flow chart

Table 2.6: Soil slopes properties for preliminary design

Parameter	Symbol	Units	Values
Face Inclination	α	Degree (^{o})	0, 10
Back Slope	β	Degree (^{o})	0, 10, 30
Effective Friction Angle	ϕ	Degree (^{o})	27, 31, 35, 39
Ultimate Bond Strength	q_u	kPa	70, 120, 150, 200
Nails Inclinations	i	Degree (^{o})	15
Soil nail horizontal spacing	S_H	m	1.5
Soil nail vertical spacing	S_V	m	1.5
Drill hole diameter	D_{DH}	mm	100, 150, 200
Height of the Wall (H)	H	m	6.00
Unit weight of soil mass	γ	kN/m^3	19.5
Cohesion (Fixed value used for design chart)	c	kPa	5
Fe 500	F_y	N/mm^2	500
Factor of safety	FS_P	----	2

2.19.3 Different Cases Regarding Face Inclination (α) and Back Slope (β)

When designing structures like walls, embankments, or even buildings, designers or experts consider various factors such as stability, drainage, aesthetics, and environmental impact. One important aspect is the inclination of the structure's face and the slope of its back. In some cases, both the face and back of the structure are kept flat, without any inclination or slope. This creates a level surface, which might be preferred for architectural reasons or for specific functionalities like a smooth wall finish. However, there are situations where having a slope becomes essential. For instance, adding a slight slope to the back of a structure helps with drainage, preventing water from accumulating and causing damage. This is particularly important in areas prone to heavy rainfall or where water management is crucial. On the other hand, inclining the face of the structure can serve various purposes. It might improve visibility, enhance the architectural look, or even contribute to structural stability by

redistributing forces more effectively. Combining different inclinations and slopes offers even more possibilities. For example, a structure with a flat face and a steeply sloped back might be chosen for its erosion control capabilities, particularly in hilly or coastal areas. Ultimately, the choice of face inclination and back slope depends on the specific requirements of the project, including factors like terrain, climate, intended use, and desired appearance etc. By carefully considering these factors, designers or experts can create structures that are not only functional and stable but also harmonious with their surroundings. According to the FHWA -2003 code recommendations, Figures in ***Appendix A (A1 to A6)*** depict the different scenarios and their corresponding considerations, encompassing various factors.

Case (I): Face inclination (α) is 0^0 and Back slope (β) is 0^0
Case (II) : Face inclination (α) is 0^0 and Back slope (β) is 10^0
Case (III): Face inclination (α) is 10^0 and Back slope (β) is 0^0
Case (IV): Face inclination (α) is 10^0 and Back slope (β) is 10^0
Case (V): Face inclination (α) is 0^0 and Back slope (β) is 30^0
Case (VI): Face inclination (α) is 10^0 and Back slope (β) is 30^0

1. Normalized bond strength (μ) :

$$\mu = \frac{q_u \, D_{DH}}{FS_p \, \gamma \, S_H \, S_V} \tag{2.37}$$

Where, "q_u is ultimate bond strength (refer to table 3.7), D_{DH} is drill hole diameter, FS_P is Factor of safety against pullout failure (refer to Table 2.1), γ is unit weight of soil mass, S_H is Soil nail horizontal spacing, S_V is Soil nail vertical spacing."

2. Design Nail Tensile Load

The following is the definition of the bar's maximum normalised design tensile force:

$$t_{max-s} = \frac{T_{max-s}}{H \, \gamma \, S_H \, S_V}$$

$$T_{max-s} = t_{max-s} \, H \, \gamma \, S_H \, S_V \, C_{1F} \tag{2.38}$$

C_{1F} is the Correction for drill-hole diameter from *Appendix A, Figure A7.*

3. The essential steel cross-sectional area

$$A_t = \frac{T_{max-s}\, FS_T}{f_y} \tag{2.39}$$

Where, "T_{max-s} is design nail tensile load, FS_T is Factor of safety against soil nail tensile failure, F_y is Soil nail yield strength."

Using equations 2.37 to 2.39 (FHWA 2003), the normalized bond strength (μ), the design nail tensile load and the required cross-sectional area of the steel have been calculated and Preliminary design charts have been developed based on the geometric properties outlined in Table 2.6. The preliminary design charts found in *Appendix B (B1 and B2)* offer valuable insights into designing soil nail systems for slope stabilization stated below:

(1) *Effect of Face Inclination* (α) *and Back Slope* (β): By examining different combinations of face inclination (α) and back slope (β), we can observe how these factors influence the design parameters of soil nails. Variations in slope geometry can lead to different requirements for soil nail diameter, length, and spacing.

(2) *Friction Angle* (ϕ) *Influence*: The friction angle of the soil has a significant impact on the design parameters of soil nails. Higher friction angles generally allow for more efficient load transfer and may require smaller diameter nails or less reinforcement (refer to the tables in *Appendix B (B1 and B2)* for information from *sub-tables A to C*).

(3) *Nails Diameter* (D): This parameter represents the diameter of the soil nails used for slope stabilization. The nail diameter varies across different cases shown in Tables *Appendix B (B1 and B2)*. Larger diameters are typically needed for more challenging slope conditions, depending on the specific requirements and soil characteristics.

(4) *Drill Hole Diameter* (D_{DH}): The size of the drill hole diameter (D_{DH}) affects the design of soil nails. As the D_{DH} varies, the required nail diameter, length, and spacing may change accordingly to ensure adequate stability and load-bearing capacity. As the drill hole diameter (D_{DH}) increases, there might be a tendency for

the required soil nail diameter (D) to increase as well (refer to Table *Appendix B1, A to C*), especially if the larger D_{DH} requires larger diameter nails for effective stabilisation. However, this relationship may not be linear. In some cases, increasing D_{DH} might not significantly affect the required nail diameter if other factors like soil properties or slope geometry dominate the design requirements.

(5) *Soil nail length to the depth of the excavation (L/H)*: A higher L/H ratio generally indicates deeper soil nails, which may be necessary for stabilizing steeper slopes or deeper soil layers. L/H ratio may vary with changes in D_{DH} and q_u (refer to Tables *Appendix B1* and Tables *Appendix B2*). Larger D_{DH} might allow for deeper drilling, potentially leading to higher L/H ratios. Deeper soil nails might be necessary to anchor securely into the underlying stable soil or rock strata, especially for larger D_{DH}.

(6) *Maximum allowable tensile force in the soil nails* (T_{max-s}): This parameter reflects the load-bearing capacity of the soil nail system. Higher T_{max-s} values indicate higher load-bearing capacity, which is essential for ensuring stability against external forces. Changes in D_{DH} could influence the magnitude of T_{max-s} required for slope stability. For example, larger D_{DH} might result in increased lateral pressures on the soil nails, necessitating higher T_{max-s} values to withstand these pressures without failure (refer to Table *Appendix B2, A to C*).

These observations highlight key design parameters for soil nail systems under various slope conditions, including nail diameter, length-to-depth ratio, maximum allowable tensile stress, cross-sectional area, and bond strength with the surrounding soil etc. These parameters must meet safety requirements and ensure a sufficient FOS against slope failure. Evaluating factors like maximum tensile stress (T_{max-s}) and ultimate bond strength (q_u) is crucial for the system's stability and durability. A larger drill hole diameter (D_{DH}) may provide more surface area for soil-nail interaction, potentially leading to stronger bonding and higher C_1F values (*Appendix A*, *Figure A7*), though this depends on factors such as soil type and compaction.

2.20 Significant Recommendations Based on the Review Study

The design of soil nails requires careful consideration of several critical parameters to ensure stability and effectiveness in geotechnical applications. Based on the literature review, the following parameters are essential:

1. *Shear Strength of Soil*: Soil's inherent shear strength directly influences the overall stability of the soil-nailed system.
2. *Diameter of Nails*: Appropriate nail diameter is crucial to provide sufficient strength and resistance against applied loads.
3. *Nail Inclinations*: The inclination angle significantly affects the ability of nails to counteract forces such as gravity and lateral soil pressure.
4. *Pullout Resistance*: The resistance of nails against being pulled out of the soil is vital for ensuring long-term stability.
5. *Roughness of Nails*: The surface roughness of nails enhances the bond between the soil and nails, improving pullout resistance.
6. *Soil Moisture Content*: Moisture content affects the soil's strength and cohesion, impacting the interaction between soil and nails.
7. *Surcharge Load Effect*: The additional loads applied on the slope or retaining wall influence the design and performance of soil nails.
8. *Grouting Effect*: Proper grouting ensures enhanced bond strength and load transfer between nails and soil.
9. *Displacement of Soil-Nailed Wall*: Monitoring wall displacement is crucial to assess the system's performance and stability under operational conditions.
10. *Bearing Plate Effect*: The bearing plate's role in distributing loads and preventing nail movement is critical for structural integrity.

Considering the significance of these factors the detailed study outlined in this research.

2.21 Research Gap

Over the years, various techniques have been developed to address slope instability, with soil nailing emerging as a prominent solution offering both effectiveness and

versatility. However, despite advancements in soil nailing technology, significant gaps persist in understanding, implementation, and standardization. Based on the literature survey, it is evident that soil-nailed slopes offer substantial potential; nevertheless, a few critical gaps in the existing literature have been identified and outlines are:

(1) Inadequate synthesis and analysis of existing literature on soil nailing, resulting in gaps in understanding soil nailing effectiveness in different geological and environmental contexts.
(2) Limited exploration of slope stability principles and influencing factors, particularly regarding soil-nail friction mechanisms and nail behaviour under various loading conditions.
(3) Insufficient methodology and findings for assessing soil nailing effectiveness, including a lack of empirical data on soil properties and loading conditions.
(4) Inadequate use of probabilistic analysis to explore the reliability of soil nailed slopes and quantify uncertainties in soil nailing designs.

Overall, there is a need for comprehensive insights and actionable recommendations to address identified research gaps and advance knowledge in the field of slope stabilization and soil nailing techniques.

Overall, this chapter has provided a comprehensive review of the existing literature on soil nailing, highlighting its significance, key findings from past studies, and the research gaps that have emerged in the field. The review underscores the importance of factors such as soil conditions, nail geometry, and stability analysis methods, along with advancements and recommendations from earlier studies. However, significant gaps still exist, particularly concerning nail behaviour, the influence of varying soil types, and the optimization of design parameters for different slope conditions. Building on this chapter's insights, the next chapter will focus on the "Materials and Methods." It will be focused on the design considerations for soil nail systems, emphasizing the significance of factors like slope geometry, soil properties, and safety requirements in slope stabilization projects. This analysis aims to facilitate informed decisions regarding the selection of design parameters based on specific project requirements and site conditions.

Chapter 3

MATERIALS AND METHODS

3.1 Introduction

This chapter describes the materials and methodology employed to achieve the objectives of the current Ph.D. thesis. It begins with the identification of residual soil parameters, for the design of soil nailed slopes and walls. A concise description of the soil model used in the parametric studies is provided, along with an overview of the geotechnical software utilized in this research. Figure 3.1 illustrates the workflow for completing the study, with this chapter emphasizing step 2, the methodology. Prior to initiating the research, various materials and their properties were thoroughly tested in the laboratory are presented in this chapter.

3.2 Experimental Program

The experimental program was designed to investigate the behaviour and stability of soil-nailed slopes using advanced equipment and materials. A Computerized Universal Testing Machine (UTM) was employed to assess the output results. The study involved residual soil, nails, bearing plates, and cement for grouting etc. A soil-nailed slope model was used in a model box filled with backfill material to replicate slope conditions. The preparation of slopes followed a systematic procedure, ensuring consistency across tests and enabling a detailed analysis of the soil-nailing technique. The detailed experimentation process is also stated in this chapter.

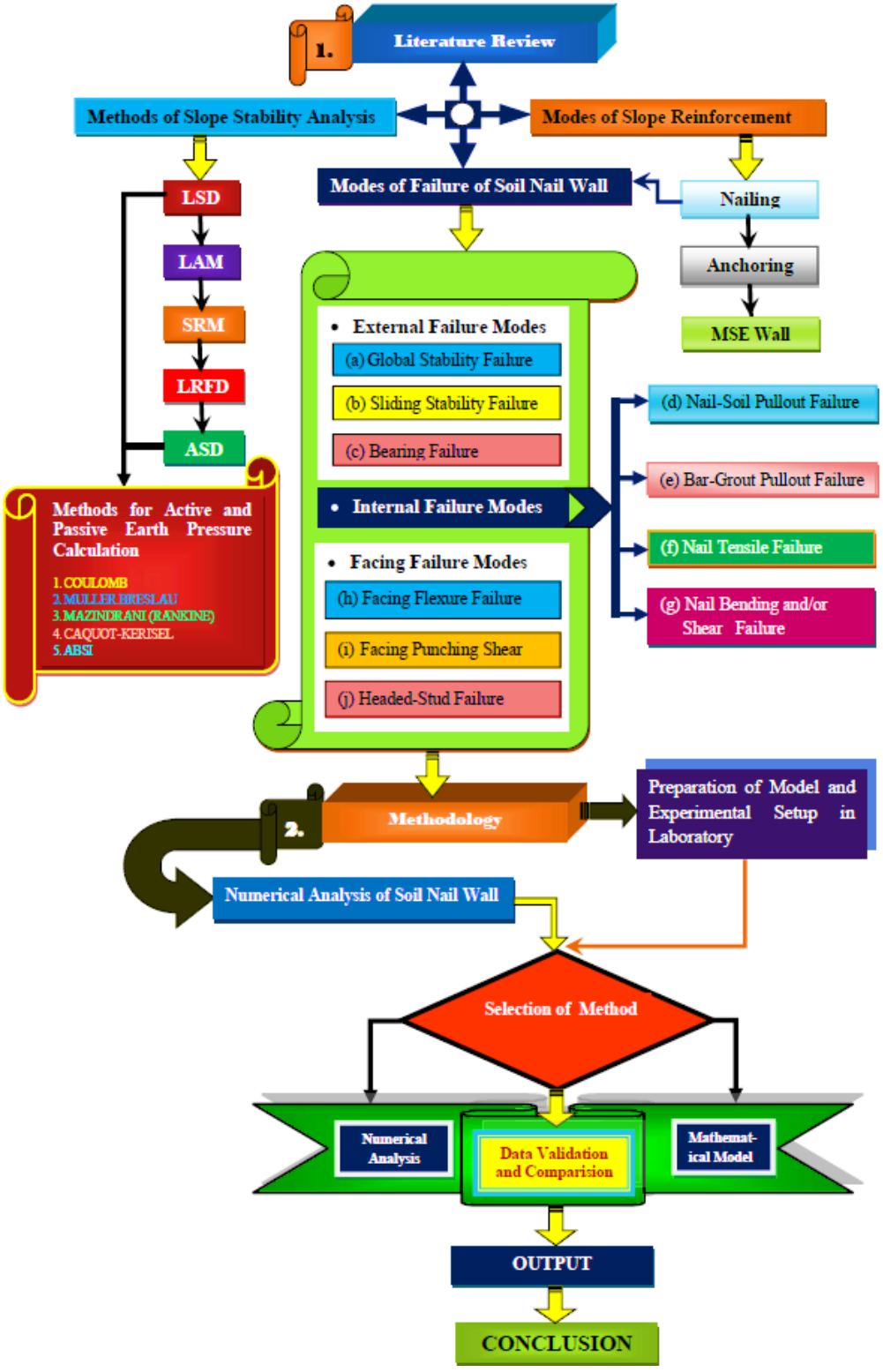

Figure 3.1: Research workflow chart

3.2.1 Computerized Universal Testing Machine (UTM)

A Computerized UTM, with a capacity of 1000 kN, shown in Figure 3.2 is used for testing. Machine calibrated in compliance with IS:1828 Grade I or BS:1610 Grade 'A,' the machine ensures an accuracy of ±1% across the load range. The loading unit consists of a central crosshead and a lower table, with the central crosshead adjustable for clearance using a geared motor. Compression tests are conducted between the central crosshead and the lower table, while tension tests occur between the central and upper crossheads. The load is measured using a strain gauge-based transducer, and the movement of the lower table (ram stroke) is tracked by a linear transducer. The machine includes essential safety features such as over-travel limits for the crosshead and ram, and overload protection, ensuring reliable and secure operation. In this Computerized UTM, the testing output/results are shown in the display unit i.e. monitor.

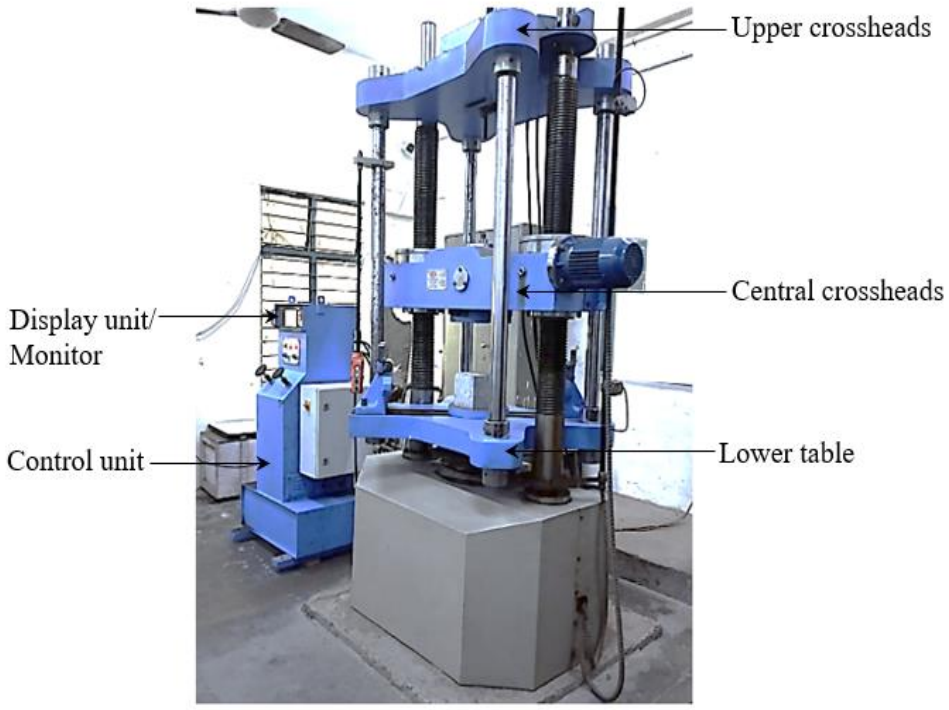

Figure 3.2: Computerized Universal Testing Machine (UTM)

3.3 Soil Testings in Laboratory

The soil used in this study was collected from the South Delhi region Okhla Phase-III (near the Govindpuri Metro Station). First, the collected soil clods were broken down with a mallet, and the processed soil was prepared for experimental purposes. A digital weighing balance with a 50 kg capacity and a sensitivity of 10 g was used for accurate weight measurements. The geotechnical properties of the soil were assessed according to IS:2720 standards to ensure its suitability for constructing the soil slope model in the laboratory. The results from these tests were subsequently utilized to design and develop the soil-nailed slope, with the findings presented in the following sections.

3.3.1 Sieve Analysis

The soil sample classification was determined through sieve analysis conducted in the laboratory. The process involved drying the soil sample to remove moisture, followed by passing it through a series of standard sieves arranged in descending order of size to separate particles by size range. The weight of soil retained on each sieve was noted to calculate the percentage passing and retained, forming the particle size distribution curve (refer to Figure 4.13). The results indicated a uniform particle size distribution with minimal variation in gradation, leading to its classification as poorly graded sand (SP) based on IS:1498-1970.

3.3.2 Specific Gravity

The specific gravity of the residual soil sample was determined following IS:2720 (Part III)-1980 standards. Oven-dried 50 g of soil passing through a 4.75 mm sieve was used for the test. The soil was placed in a pycnometer, and distilled water was added to cover the sample. The pycnometer was gently agitated, and vacuum desaturation was applied to eliminate air bubbles. The weights of the pycnometer with soil and water, and with water only, were recorded and the specific gravity was calculated. Multiple i.e. 3 tests were conducted to ensure accuracy and the average specific gravity, measured at room temperature (27°C), was found to be 2.69 for the given soil sample (SP).

3.3.3 Water Content Test in Residual Soil

The water content of the given soil sample was determined using the oven-drying method as per IS:2720 (Part II)-1973. A clean, dry container weighing 32.50 g was filled with wet soil, and the combined weight was recorded. The sample was then dried in an oven at 110°C for 24 hours. After cooling in a desiccator, the weight of the container with dry soil was measured. The weight of moisture was calculated by subtracting the dry weight from the wet weight, and the dry soil weight was determined by subtracting the container weight from the weight of dry soil plus the container. In this observation, the test was repeated for three trials, and the average water content of in-situ soil was tested as 14.17%.

3.3.4 Relative density

The relative density of the soil sample was determined using the unit weight method in accordance with IS:2720 (Part XIV)-1983, which outlines a standard procedure for evaluating the compactness of granular soils. The process began by establishing the maximum dry unit weight of the soil, which was measured at 17.52 kN/m³. This was achieved by compacting the soil in a mould with a vibrating table to reach its densest state. Next, the minimum dry unit weight of the soil was determined by loosely filling the mould without compaction, resulting in a value of 14.2 kN/m³. The field dry unit weight, representing the in-situ condition, was measured at 16.15 kN/m³ using standard field testing methods i.e. the core cutter method. With these values, the relative density of the soil was calculated to be 62.75%. According to Table 3.1 (Lambe and Whitman, 1969), this indicates that the soil description is medium dense.

Table 3.1: Relative Density (Dr) definitions (Lambe and Whitman, 1969)

Consistency	Relative Density Dr (%)
Very Loose	0 - 15
Loose	15 - 35
Medium Dense	35 - 65
Dense	65 - 85
Very Dense	85 - 100

3.3.5 Saturated Unit Weight

The saturated unit weight of the given soil sample was determined following the procedure outlined in IS:2720 (Part VIII)-1983. The soil sample was placed in a cylindrical mould of known dimensions of 100 mm diameter and/or 1000 cm^3 volume and gradually saturated by adding water until no air voids remained, ensuring full saturation. This was achieved by submerging the soil in water under controlled conditions or applying a vacuum. The weight of the saturated soil, including water, was recorded along with the volume of the mould. The saturated unit weight is calculated by dividing the ratio of the total weight of the saturated soil and the volume of the mould. Experimentally three tests were performed to ensure accuracy, and the final average value 19.5 kN/m^3 was recorded.

3.3.6 Angle of Internal Friction (ϕ)

A soil sample was prepared for a direct shear test using a digital data acquisition system. The sample was compacted in the shear box at its optimal moisture content.

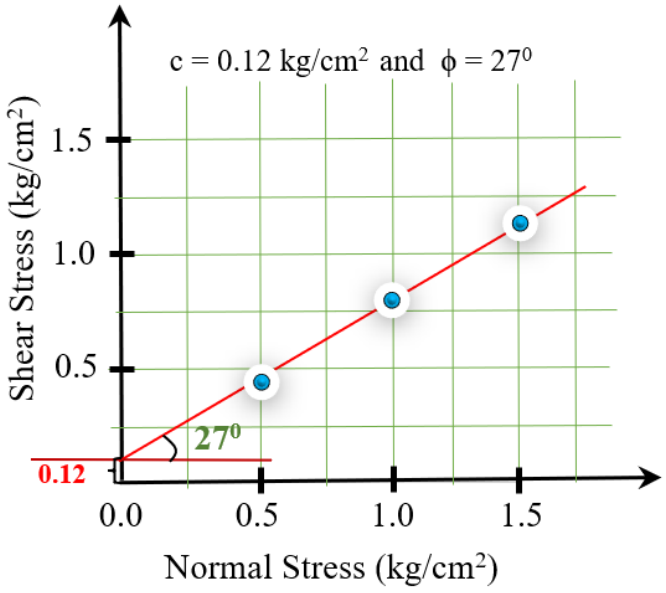

Figure 3.3: Direct shear test results for cohesion (c) and friction angle (ϕ)

The load frame held the shear box containing the specimen, with a plain grid plate placed over the bottom base plate and another plain grid plate on top. During the tests, the strain rate (mm/min) remained constant while the applied pressure (kg/cm^2) varied

across three different tests. Vertical and horizontal deformations were recorded using the data acquisition system. A shear normal-stress displacement curve was plotted, which allowed for the determination of the cohesive intercept and the angle of shearing resistance according to IS 2720-1986 (Part 13). Based on the plotted graph of recorded normal stress (kg/cm²) and shear stress (kg/cm²) shown in Figure 3.3, the cohesion (c) was determined to be 0.12 kg/cm², and the angle of internal friction (ϕ) was found to be 27°.

3.4 Materials Used and Their Properties

In this study, various materials are used in analysis and experimental study including soil, nails, asbestos plain sheet for wall and cement for grout, each characterized by specific physical and mechanical properties essential for slope stabilization analysis. Details are as follows:

3.4.1 Soil Properties

The soil used in the study was obtained from the South Delhi region, G. B. Pant Institute of Technology, Okhla Phase-III (near Govindpuri Metro Station) and was classified as poorly graded sand (SP) by sieve analysis (Figure 4.13). The key properties are: saturated unit weight (γ_{sat}) of soil is 19.50 kN/m³, angle of internal friction (φ) is 27°, Poisson's ratio (ν) is 0.35, maximum dry unit weight of the soil ($\gamma_{d,max}$) is 17.52 kN/m^3, minimum dry unit weight of the soil ($\gamma_{d,min}$) is 14.2 kN/m^3, the relative density of the soil is 62.75%, in situ moisture content of soil sample is 14.32 %, deformation modulus (E_{def}) is 25 N/mm², dilation angle (ψ): 0.00°. During the analysis, Geo 5 software was used and at the base of the foundation, 250 kN/m^2 soil's load-bearing capacity was considered.

3.4.2 Nails Properties

During the investigation by Geo5 (2018) software, High Yield Strength Deformed (HYSD) nails were used as reinforcement, their specifications are: length of the nail (L) is 9.00 m, spacing (S_h and S_v) is 1.00 m and 1.25 m, the diameter of nails (ϕ) is 20 mm, modulus of elasticity (E) is 2×10^5 N/mm², minimum yield stress (f_y) is 415

N/mm², Poisson's ratio (ν) is 0.3, and nail inclinations (α) are 0°, 5°, 10°, 15°, 20° and 25° with horizontal plane. The properties of the soil and nails used in the analysis are revealed in Table 3.2.

Table 3.2: Properties of soil and nails

Soil Properties	
Type of soil	Poorly graded sand (SP)
Model	Mohr-Coulomb
Surcharge Load (w)	18.00 kN/m^2
Unit weight of soil (γ_{sat})	19.50 kN/m^3
Cohesion of soil (c_{ef})	12 kPa
The angle of internal friction (φ_{ef})	27^0
Poisson's ratio (ν)	0.35
Dilation angle (ψ)	0.00
Nails Properties	
Nail Type	HYSD
Length (L)	9.00 m
Nails spacing (S_h and S_v)	1.00 m and 1.25 m
Diameter (ϕ)	20 mm
Modulus of Elasticity (E)	2 x 10^5 N/mm^2
Minimum yield stress (f_y)	415 N/mm^2
Poisson's ratio (ν)	0.3

3.4.3 Properties of Soil-Nailed Wall

(1) In the experimental study, a soil-nailed wall was placed to evaluate its stability and performance. For Setup -I the wall incorporated primary material is the asbestos plain sheet, 250 mm wide, 300 mm high and 15 mm thick, which was precisely fitted within the experimental model.

(2) Whereas, in the analytical study with Geo5 software, M25 Grade concrete with a wall thickness of 0.20 m and a wall height of 6.0 m including mesh type, Q335A reinforcement mesh with 8.0 mm diameter bars, arranged in a grid pattern of 150 x 150 mm spacing was used.

3.4.4 Properties for Cement Grouted Nails

Cement grout was utilized to bond the nails with the surrounding soil, featuring the following characteristics: Type of cement: Ordinary Portland Cement (OPC, 43 grade) and Portland Pozzolana Cement (PPC), Ultimate bond strength (q_u) is 0.12 N/mm² (refer Table 2.1), Elastic modulus of cement grout (E_G) is 2500 N/mm² for hardened cement paste (FHWA-2003) and Grout cover (G_C) is 20 mm. diameter of nail/bar 10 mm, modulus of elasticity (E) is 2×10^5 N/mm², minimum yield stress (f_y) is 415 N/mm², and Poisson's ratio (ν) is 0.3.

3.4.5 Bearing Plate

(1) In the experimental Setup-I: where the effects of various nail inclinations were investigated, 40 mm × 40 mm steel bearing plates were used. These plates were secured to the wall using 8 mm bolts and nuts.

(2) In the experimental Setup-II: Where utilized grouted nails to examine the failure patterns at the wall facing. For this model, the bearing plates, made of mild steel, were sized at 100 mm × 100 mm × 2 mm. Additionally, a washer with a diameter of 34 mm and a thickness of 3 mm was incorporated. The modulus of elasticity for steel used in this analysis is $2x10^5$ N/mm^2 and the Poisson ratio, p = 0.3 (as per IS:800-2007).

3.5 Numerical Modeling

In this investigation, 2D FEM analysis was conducted using Geo5 software, while 3D FEM simulations for the bearing plate were performed using Abaqus. The Mohr-Coulomb material model was applied during the 2D FEM analysis.

3.5.1 2D FEM Analysis of Soil Slope

Using the properties of the materials mentioned above (Section 3.4.1 to 3.4.3), a 2D finite element analysis was conducted with Geo5 (2018) software to investigate the settlement behaviour of an embankment, both with and without the inclusion of soil nails. The study aimed to evaluate the effectiveness of soil nailing as a reinforcement measure in reducing settlement and enhancing the stability of the embankment.

3.5.2 3D FEM Analysis of Bearing Plate

A 3D FEM analysis was conducted on a bearing plate with dimensions of 150 x 150 x 20 mm using Abaqus software. The material properties for steel were defined with a modulus of elasticity of $E = 2 \times 10^5$ N/mm² and a Poisson's ratio (ν) of 0.3, following the specification in IS 800:2007.

Elements and Mesh Details: The model was constructed using C3D8R elements, which are 8-node linear brick elements suitable for 3D stress analysis. In this analysis, 5,630 nodes and 4,212 elements were used to capture the interactions (refer to Section 5.5).

3.6 Experimental Setup

In this investigation, two distinct soil slope setups were developed to evaluate slope stability performance. Setup-I was prepared to examine the influence of different nail inclinations on slope behaviour, including cases with and without nails. Meanwhile, Setup-II focused on assessing the effect of grouted versus non-grouted nails on slope stability. Both Setups were designed to simulate slope conditions, enabling a comprehensive analysis of the factors influencing soil slope performance.

3.6.1 Experimental Setup – I: For identification of the effect of different nail inclinations

In this investigation, a physical model box with dimensions 800 mm (length) × 250 mm (breadth) × 500 mm (height) was used for experimental analysis. The soil slope, as depicted in Figure 4.1, was scaled down to a 1:20 ratio, and the soil sample was carefully filled within the model, as per schematic Figure 4.14(d). The experimental setup included a computerized Universal Testing Machine (UTM), which was used along with a display unit for recording and displaying observations. For reinforcement analysis, 10 steel bars, each 5 mm in diameter and 450 mm in length were utilized, along with 40 mm × 40 mm steel bearing plates secured with 8 mm bolts and nuts at the wall facing. The embedding material used was Poorly Graded Sand (SP), classified according to IS: 1498-1970. Two physical models were tested: one without reinforcement and the other with reinforcement. In this experimental setup (designated

as Setup-I), a 15 mm thick wall complete of an asbestos plain sheet was positioned at 600 mm from the back side of the model. For the 300 mm-high wall facing, the top and bottom edges were kept at a distance of 25 mm, and vertical spacing marks were made at 62.5 mm intervals for inserting nails. A steel plate measuring 500 mm × 240 mm × 3 mm was placed on top of the slope to ensure uniform load transfer across the entire span using the UTM. A total of five nails were positioned vertically along the wall facing (refer to Figure 4.16 c).

3.6.2 Experimental Setup – II: For Grouted Nails

For Setup-II, designed to study grouted nails and their effect on slope stability and observe soil nailed wall failure, the model dimensions were 750 mm × 450 mm × 650 mm, filled with 600 mm height of soil (SP). Reinforcement included grouted nails with 10 mm diameter steel bars, 700 mm length, and a gross diameter of 40 mm. The bearing plate dimensions were 100 mm × 100 mm × 2 mm, while washers had a 34 mm diameter and 3 mm thickness. Also, a 15 mm thick wall made of an asbestos plain sheet was used at the facing.

3.7 Preparation of Soil Slope Models for Testing in Laboratory

3.7.1 Experimental Setup – I: For Identification of Different Nail Inclinations

3.7.1.1 For the model without soil nails

A model with a slope angle of 90° to the horizontal was prepared without incorporating soil nails. During its preparation, an asbestos plain sheet was placed at the front, serving as a guide at a distance of 600 mm from the back of the model. The field soil sample, which had a moisture content of 14.32% and a relative density of 62.75%, was added layer by layer, with each layer measuring 50 mm. Each layer was properly compacted by hand to ensure consistent soil properties throughout the slope. This process continued until the final height of the slope was reached (Figure 4.14 d).

3.7.1.2 For the model with soil nails

The model slope was constructed at a predetermined angle of 90° to the horizontal, incorporating various nail inclinations for testing. The nails inclinations included 0°, 5°, 10°, 15°, 20°, and 25°. During preparation, points were first marked on the front wall of the model at 50 mm horizontal intervals and 63 mm vertical intervals, correlating with the designated nail positions (i.e. nail spacing). The nail inclinations were carefully measured by a protractor and marked on the inner side of the wall according to their respective positions then a given field soil sample has a moisture content of 14.32% and a relative density of 62.75% was filled in the model layer by layer. Each layer (i.e. 50 mm) was carefully filled and made inclined slope according to their reinforcement inclination and compressed properly by hand to ensure consistent soil properties throughout the slope then the 5mm diameter and 450 mm length steel bars or nails were placed on these inclined planes properly, along with 40 mm x 40 mm steel plates called bearing plates fixed at the facing of the wall with 8 mm diameter bolts/nuts. This process continued until the final height was reached (refer to Figure 4.14 d).

3.7.2 Experimental Setup – II: For grouted nails

In this investigation, the computerized universal testing machine (UTM) was used for experimental purposes. The physical model of size 750 x 450 x 650 mm is prepared which is filled 600 mm with an adopted soil sample (i.e. SP), the size of the bearing plate (MS) is 100 x 100 x 2 mm, washer (MS) 34 mm diameter and 3 mm thick, length of the grouted nail is 700 mm, the gross diameter of grouted soil nail is 40 mm, the diameter of the steel bar is 10 mm. The grouted soil nails were made by using Ordinary Portland cement (OPC-43 grade) and Pozzolana Portland cement (PPC). To ensure the cement slurry's optimal flowability within the PVC sleeve, the water-cement ratio was carefully balanced at 0.45. Subsequently, these grouted nails were placed for curing in potable water for 28 days. Before selecting the cement types and exploring their merits, a thorough split tensile strength test was conducted on these nails. Remarkably, the experimental results revealed a split tensile strength of 4.21 MPa (i.e. peak load is 185.3 kN) for OPC and a slightly lower strength of 4.13 MPa (i.e. peak load is 181.7

kN) for PPC. Given this marginal difference and considering the economic and eco-friendly advantages, the decision was made to position the PPC grouted nails within a model, orienting them at a 15^{o} nail inclination. This model was then mounted on a Computerized Universal Testing Machine (UTM) to enable a more comprehensive and discerning experimental analysis. This setup enabled the observation of maximum wall deflection and slope settlement under the applied load. Additionally, the test was conducted to evaluate the effect of varying moisture content on slope stability. For this purpose, the tests were carried out for moisture contents ranging from 15% to 20%. To prepare the soil samples with the desired moisture content, the soil was initially oven-dried at 110°C for 24 hours. After drying, a total of 50 kg of dry soil was divided equally into five pans, with 10 kg in each pan. Then, 1.5 liters of water was added to a 10 kg soil sample to achieve 15% moisture content, 1.6 liters for 16% moisture content, and so on. The water and soil were thoroughly mixed by hand properly. The prepared soil samples were then used to fill the slope model for experimental purposes.

Overall this chapter discussed the materials used in the investigation, highlighting their properties and testing methods. The study employed 2D numerical methods to analyze the settlement and stability of embankments and soil-nailed slopes. It outlines the procedures for model preparation, including software simulations and experimental setups. These methodologies are crucial for understanding the behaviour of soil-nailed slopes and embankments. In continuation of this chapter, the next chapters 5 and 6 provide a detailed examination explanation and discussion of the outputs and results obtained from these investigations, offering clear insights into the performance and effectiveness of the adopted approaches.

Chapter 4

NAIL INCLINATIONS EFFECT ON SLOPE STABILITY

4.1 Introduction

This chapter delves into the versatile construction technique of soil nailing, a widely used method for enhancing slope stability. Despite substantial research in this field, a notable gap exists in the application of Limit State Design (LSD) for determining the optimal nail inclination angle. To address this, the study investigates nail inclinations ranging from 0° to 25° with respect to the horizontal plane, aiming to identify the inclinations that maximize strength, stability, and the Factor of Safety (FOS) under LSD.

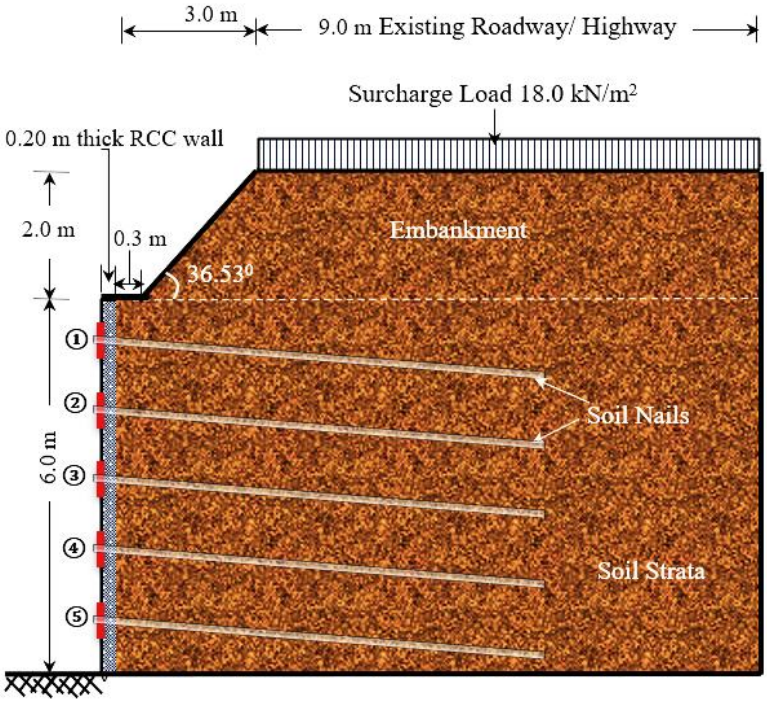

Figure 4.1: Profile diagram of soil nailed wall.

The soil slope profile shown in Figure 4.1, particularly applicable for roadway and highway development, forms the basis of this investigation. Such types of slopes were commonly useful in hilly areas as well as where one side face needs to be protected.

In this chapter, numerical analyses were conducted using Geo-5 (2018) software, with findings validated through Finite Element Method (FEM) simulations and laboratory experiments. Additionally, the chapter examines the effects of soil nails within the slope, considering key factors. The soil and nail properties used in this analysis are detailed in Chapter 3, Section 3.3.

4.2 The Influence of Nail Inclinations Within the Soil Slope

The impact of nail inclination within the soil slope was analyzed to evaluate slope stability and the performance of soil-nailing structures considering the soil slope shown in Figure 4.1. This analysis was conducted using Geo 5 software (Figure 4.2) incorporating the material properties outlined in Sections 3.3.1, 3.3.2, 3.3.3, and 3.3.5. This chapter analyzes pressure and nail force variations within the soil slope, focusing on shear forces (SF), bending moments (BM), the factor of safety (FOS), and slip surface resistance. It also presents the mathematical modelling used to predict displacements are discussed below.

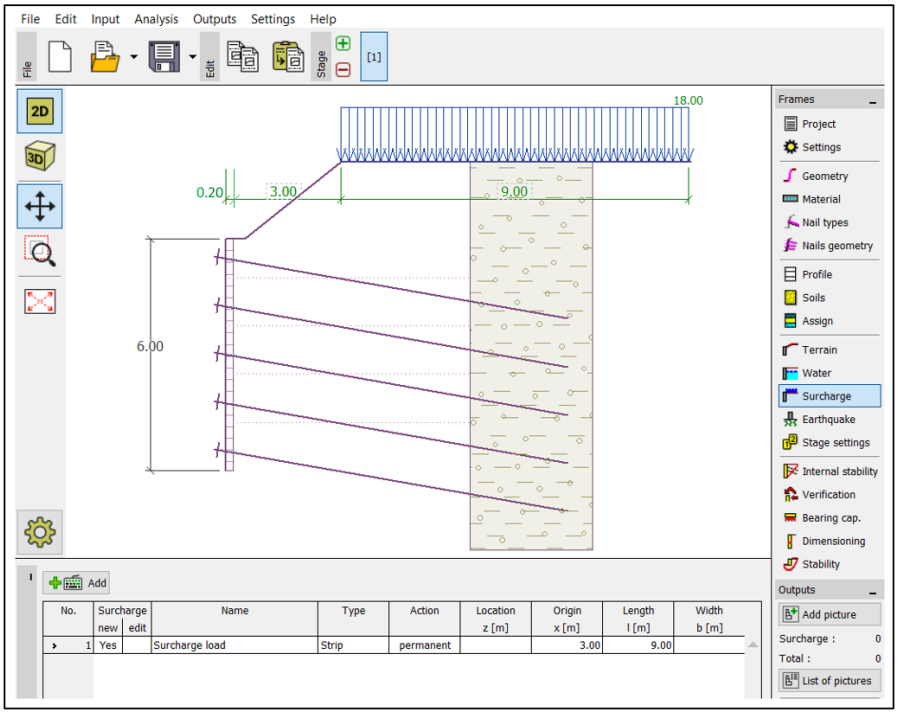

Figure 4.2: The geometrical figure for optimization of soil nailed slope by Geo5.

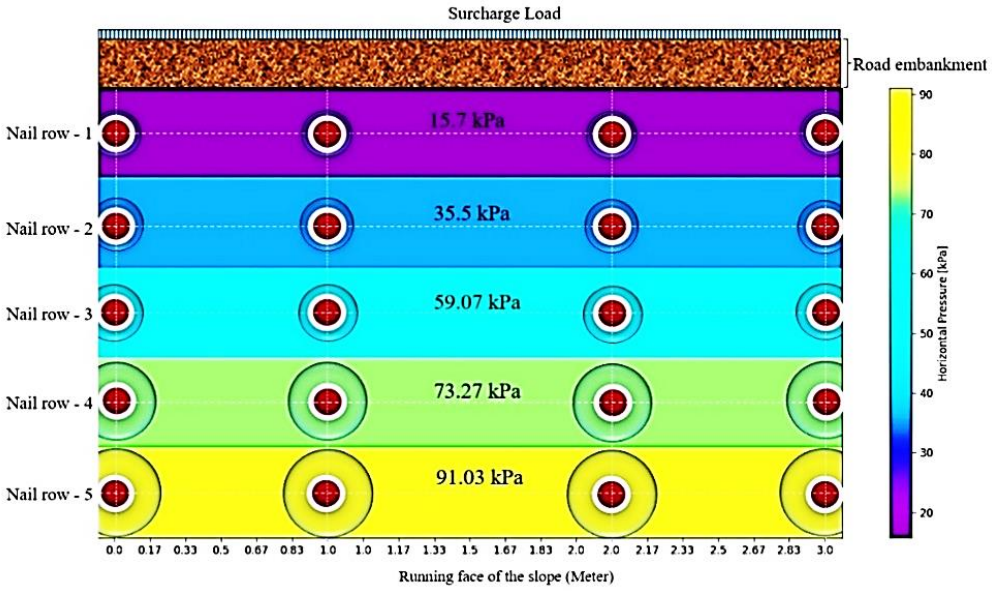

(a) Horizontal pressure distribution beneath soil nail (L-Section)

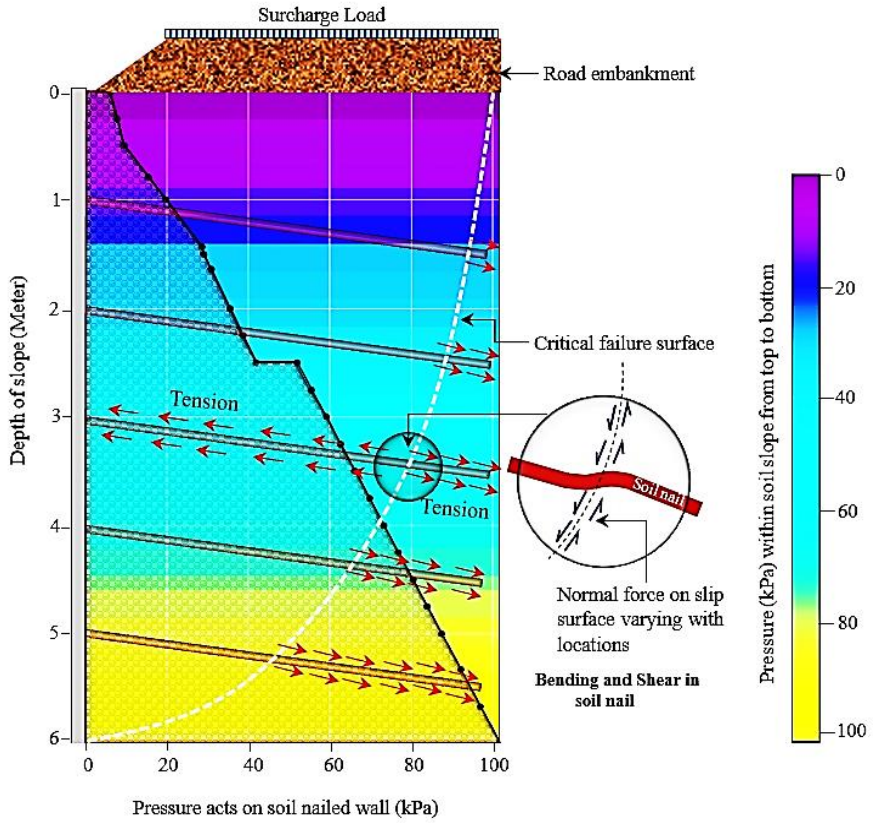

(b) Soil nailed slope behaviour under vertical loading (Cross-section)

Figure 4.3: Distribution of pressure in soil-nailed slopes (heatmap observation)

4.2.1 Observation of Nail Forces Under Different Nail Inclinations

Under a surcharge load of 18 kN/m² (Figure 4.2), the analysis was carried out to examine the effect of different nail inclinations within the soil slope. The results indicated that the pressure on the soil nail wall and the forces acting on the nails increased progressively from the uppermost nail (Nail 1) to the lowermost nail (Nail 5) (refer to Figure 4.3). Nail forces at various inclinations were observed and are presented in Figure 4.4. Minimal variation in nail forces was observed across inclinations of 0°, 5°, 10°, 15°, 20°, and 25° with the horizontal plane, indicating that the nail inclination had a relatively slight impact on force transmission. The consistent distribution of forces suggests symmetrical or well-distributed load-sharing characteristics within the soil-nailing system. This uniformity is influenced by factors such as the diameter and length of the soil nails, the geometry of the structure, load distribution, and material properties etc.

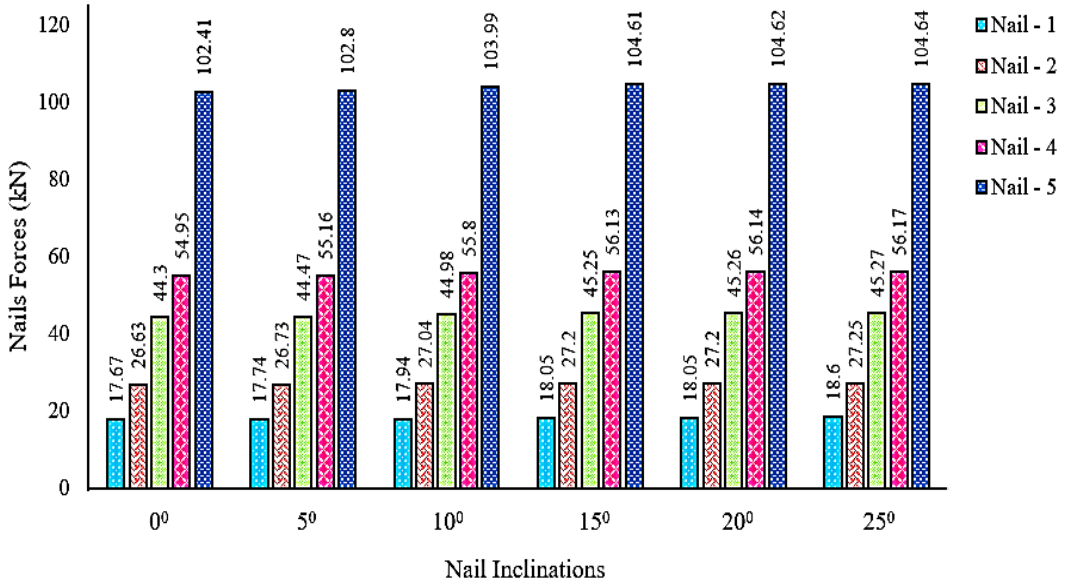

Figure 4.4: Nails forces at various nail inclinations under surcharge load (18 kN/m^2)

4.2.2 Forces on Slip Surface Resistance by Soil and Nails

The term "Forces on slip surface resistance by soil and nails" refers to the resistant forces acting on or near the critical slip surface within the soil mass at equilibrium conditions, as shown in Figure 4.5. These forces include contributions from the

internal shear strength and cohesion of the soil, as well as external factors such as the applied loads, slope geometry, and reinforcement provided by the nails. Together, these forces play a critical role in resisting slope failure and maintaining stability.

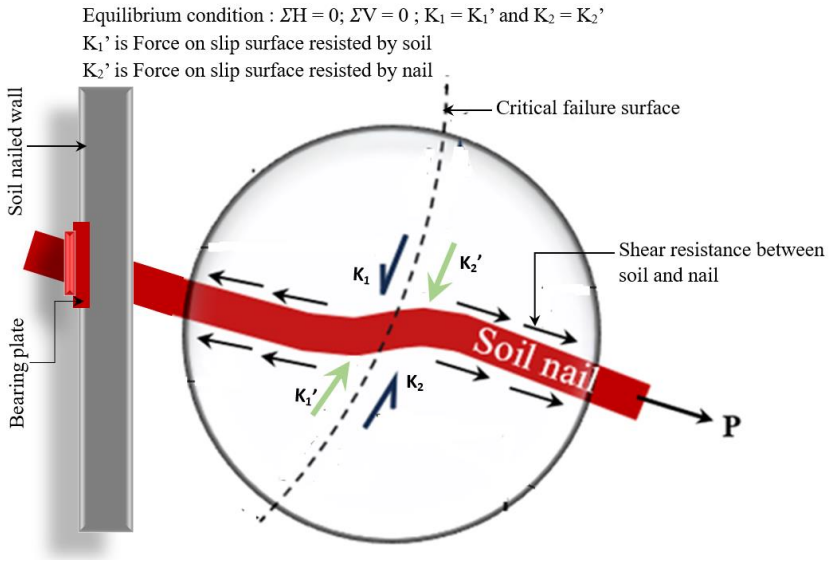

Figure 4.5: Emblematic figure for showing forces on slip surface resistance by soil and nails

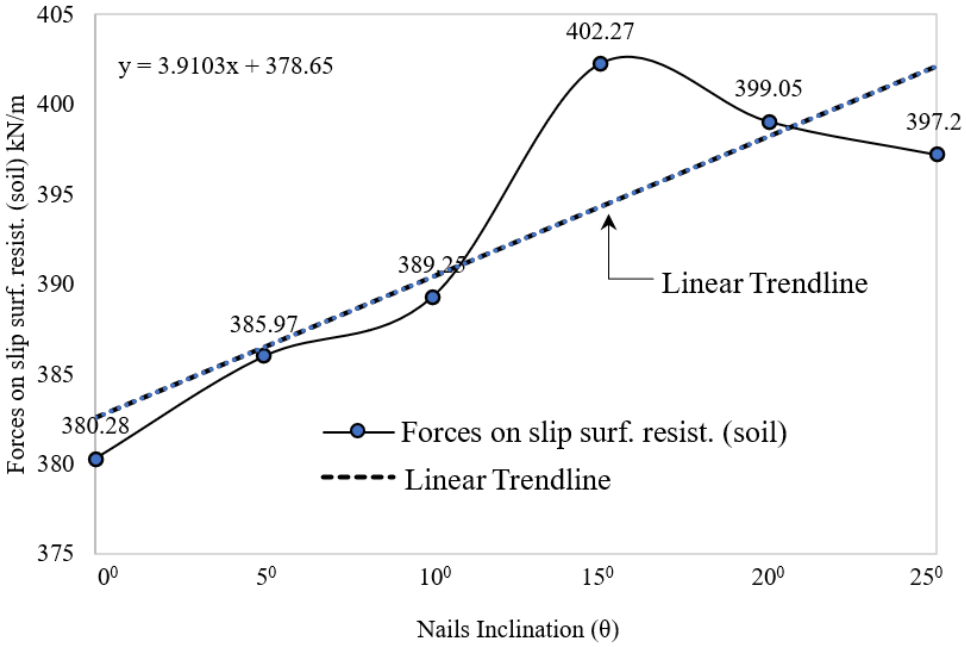

Figure 4.6: Force on slip surface resisted by soil mass

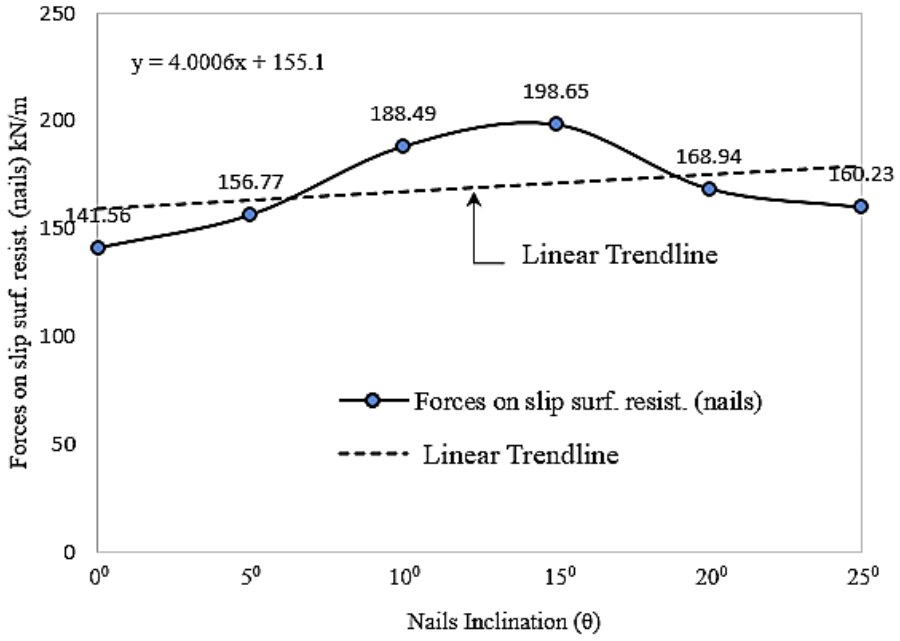

Figure 4.7: Force on slip surface resisted by nails

In the present study, it was observed that at a nail inclination of 15°, the soil on the slip surface resisted a maximum force of 402.27 kN/m, while the deformed nails provided additional resistance with a maximum force of 198.65 kN/m. This highlights the critical role of the combined resistance offered by the soil and the nails near the critical failure plane/surface. The relationship between various nail inclinations and the forces resisted by the soil and reinforcing nails is illustrated in Figure 4.6 and Figure 4.7. These figures provide valuable insights into how the orientation of nails influences the distribution of forces on and/or near the critical slip surface. Understanding this interplay is crucial for optimizing the design of slope stabilization systems, ensuring effective force redistribution, and enhancing overall stability.

4.2.3 Impact of Nail Inclinations on a Safety Factor

The analysis was performed by Geo5 software (Figure 4.2) for the soil slope model depicted in Figure 4.1, utilizing the material properties outlined in Chapter 3, specifically in Sections 3.3.1, 3.3.2, 3.3.3, and 3.3.5, to assess the effects of various nail inclinations on the FOS. Under a surcharge load of 18 kN/m², the FOS was determined to be 0.96 using Bishop's Method when no nails were provided. With the

inclusion of soil nails, the FOS increased consistently across nail inclinations ranging from 0° to 15°. However, beyond 15°, a noticeable decline in the FOS was observed, indicating a reduction in the reinforcing effectiveness of the nails as their inclination increased further. The maximum FOS of 1.630 was achieved at a nail inclination of 15°, while at 25°, the FOS dropped to 1.573, as illustrated in Figure 4.8. This analysis highlights that steeper nail inclinations diminish the FOS, thereby adversely affecting the stability of the soil slope. Hence it has been observed that The relationship between FOS and nail inclinations underscores the critical role of optimal nail orientation in enhancing slope stability.

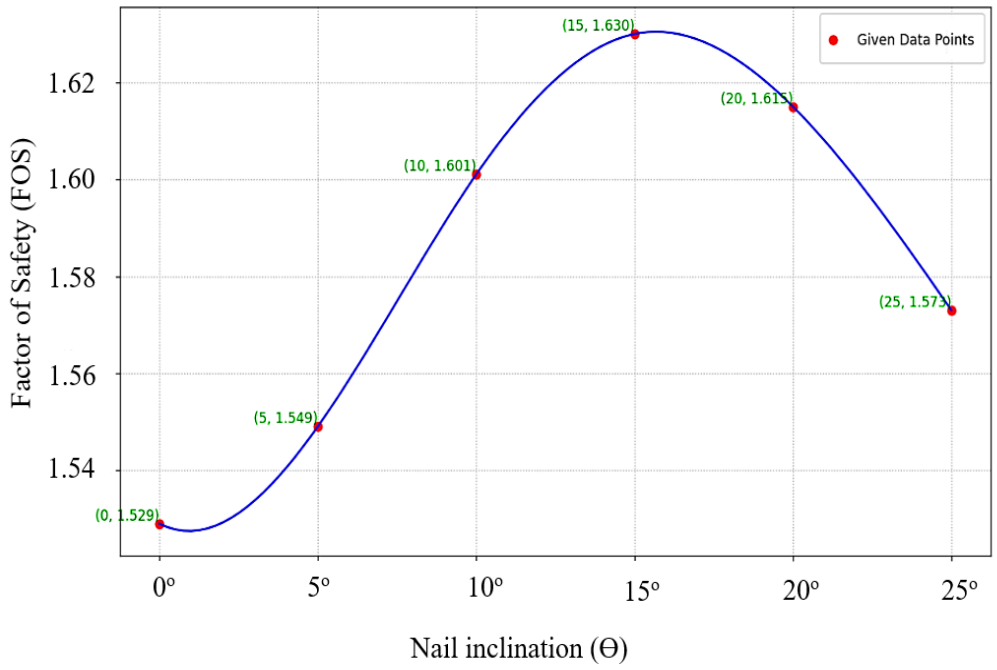

Figure 4.8: The factor of safety (FOS) for different angles of nails inclination

4.2.4 Maximum SF and BM in nail locations

During the above investigation, it was observed that the mobilized shear force (SF) and bending moment (BM) within the nails increased progressively from the top to the bottom of the slope. The roles of SF and BM varied significantly across different nail positions. Under a surcharge load of 18 kN/m², the distribution of SF along each nail was analyzed, revealing a maximum SF value of 45.52 kN at the lowermost nail, designated as nail number 5 (refer to Figure 4.9). While SF and axial tensile forces (P)

predominantly contribute to structural stability, BM, although smaller in magnitude, plays a crucial role in maintaining overall structural integrity. The analysis further indicated that, under surcharge loading, the lowermost nail experienced the highest BM of 7.59 kN-m.

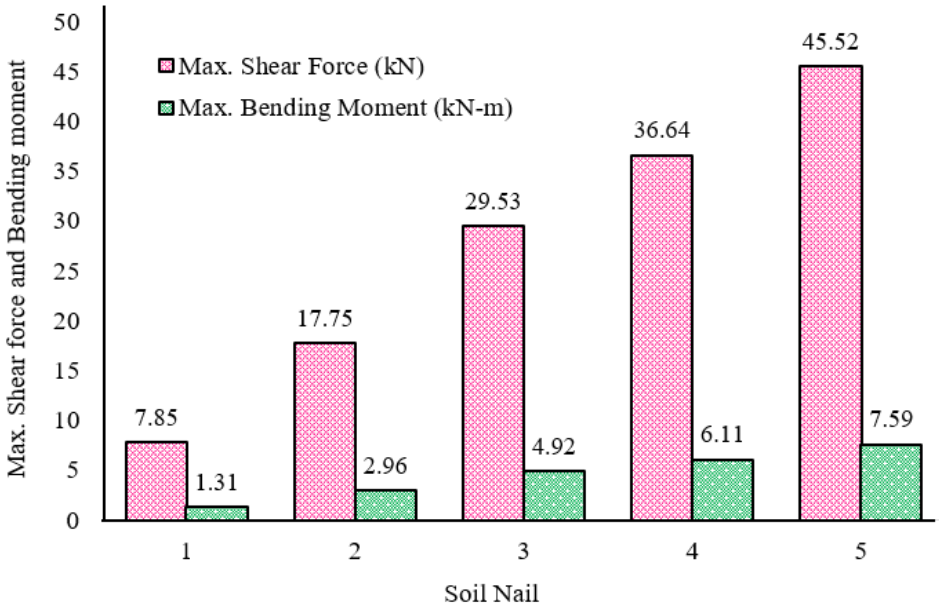

Figure 4.9: Maximum shear force (SF) and bending moment (BM) at the different nail locations (i.e. from nail number 1 to 5)

4.3 Mathematical Modelling For Predicting Nail Displacement in Soil Mass

In this study, some assumptions were made to develop the model shown in Figure 4.10. The soil was assumed to behave in an elastic-plastic manner within the range of applied loads. The interaction between the soil and nails was represented using linear spring constants considering the aspect of force resisted by soil and nails at the slip surface (i.e. K_1 and K_2), and the nail displacements were assumed to occur primarily along the slip surface and the nails provide their maximum reinforcing effect at the slip surface, where they resist soil movement by developing tension and shear forces etc.

The forces on the slip surface resisted by soil (K_1) and nails (K_2) are obtained by using Geo 5 (2018) software and results found from the analysis are shown in Figure 4.6 and Figure 4.7. During the analysis, it was observed that near the critical failure surface, the forces in the soil mass lead to the displacement of nails in the active and

passive zones (i.e. plastic zone and elastic Zone). This affects the overall structure's stability as the reinforcement does not get distributed evenly in the entire soil mass. To understand the displacement of nails in the soil mass, a predictable linear spring system model has been developed which consists of two spring systems connected in series with stiffness k_1 and k_2 (Figure 4.10 (a), (b) and (c)). A force P acts in the x-direction (i.e. +ve) on the right-hand side, while the left-hand side is rigidly fixed. By considering this mathematical model, the displacement of the reinforcement in the soil mass at different nail inclinations is observed.

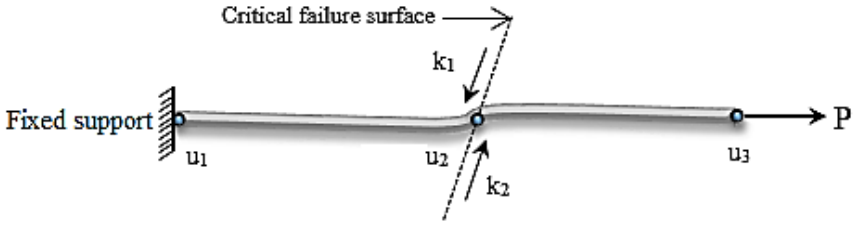

(a) Actual model

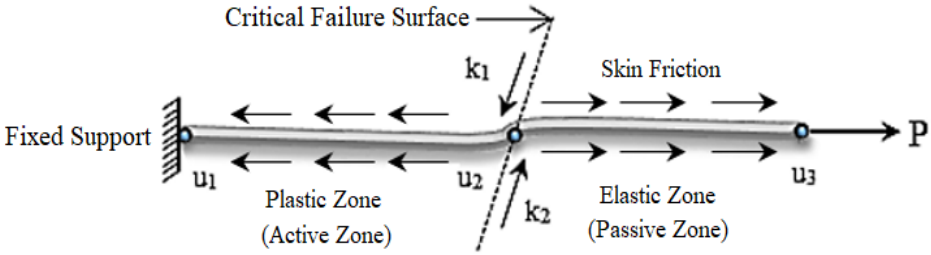

(b) Activity of internal forces in soil nail

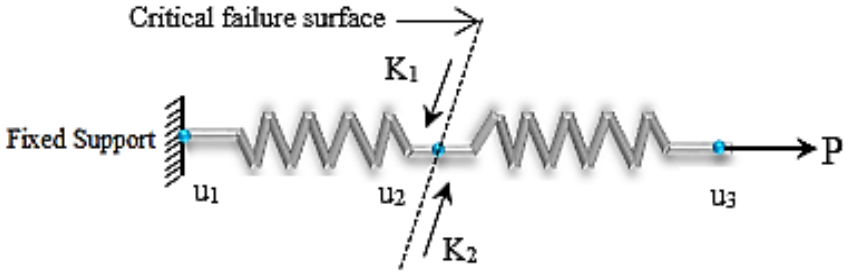

(c) Spring models develop from the actual model

Figure 4.10: Mathematical model of single-degree freedom system.

4.3.1 Global Stiffness Matrix

4.3.1.1 Establishment of element stiffness matrix for finding displacement of nail in soil mass

Figure 4.10 (c) shows a standard single-degree freedom system with two nodes, u_2 and u_3, each of these has a potential displacement. The spring component of this system has a stiffness of 'k' and only one direction of displacement is possible, i.e., x-direction. Using the theory of force equilibrium and taking into account the force on the slip surface resisted by soil (k_1) and the slip surface resisted by nails (k_2), a mathematical model has been developed. The model presented in this study allows for the formulation of the element stiffness matrix of elements. Particularly, the element stiffness matrix can be expressed as follows:

$$[k_1] = \begin{bmatrix} k_1 & -k_1 \\ -k_1 & k_1 \end{bmatrix}, \text{ and } [k_2] = \begin{bmatrix} k_2 & -k_2 \\ -k_2 & k_2 \end{bmatrix} \tag{4.1}$$

In a global format, the element stiffness matrix for (k_1) and (k_2) is placed as.

$$[k_1] = \begin{bmatrix} k_1 & -k_1 & 0 \\ -k_1 & k_1 & 0 \\ 0 & 0 & 0 \end{bmatrix}, \text{ and } [k_2] = \begin{bmatrix} 0 & 0 & 0 \\ 0 & k_2 & -k_2 \\ 0 & -k_2 & k_2 \end{bmatrix} \tag{4.2}$$

A global stiffness matrix [K] is formed by combining matrix [K_1] and matrix [K_2].

$$[K] = [K_1 + K_2]$$

$$= \begin{bmatrix} k_1 & -k_1 & 0 \\ -k_1 & k_1 & 0 \\ 0 & 0 & 0 \end{bmatrix} + \begin{bmatrix} 0 & 0 & 0 \\ 0 & k_2 & -k_2 \\ 0 & -k_2 & k_2 \end{bmatrix}$$

$$= \begin{bmatrix} k_1 & -k_1 & 0 \\ -k_1 & k_{1+}k_2 & -k_2 \\ 0 & -k_2 & k_2 \end{bmatrix} \tag{4.3}$$

In matrix form, the force-displacement equation is

$$\begin{bmatrix} k_1 & -k_1 & 0 \\ -k_1 & k_{1+}k_2 & -k_2 \\ 0 & -k_2 & k_2 \end{bmatrix} \begin{Bmatrix} u_1 \\ u_2 \\ u_3 \end{Bmatrix} = \begin{Bmatrix} R \\ 0 \\ P \end{Bmatrix} \tag{4.4}$$

Where, k_1 is a force on the slip surface resisted by soil, k_2 is a force on the slip surface resisted by nail, u_1 is the displacement at the fixed support (considered as 'Zero'), u_2 is the displacement at the slip surface, and u_3 is the displacement at the end of the soil nail in soil mass and P is the force acting in the nail (x-direction '+'ve).

4.3.2 Boundary Condition for Stiffness Matrix

The stiffness matrix becomes singular if appropriate boundary conditions are not defined for the structural equation model. In such cases, the determinant of the matrix is zero, rendering the matrix non-invertible. Without adequate support conditions, the structure behaves as a rigid body, resulting in unrestricted movement and an inability to resist any applied loads effectively. When finite non-zero displacement values are provided, non-homogeneous boundary conditions can occur. There are two types of boundary conditions: (i) homogeneous boundary conditions and (ii) non-homogeneous boundary conditions. Homogeneous boundary conditions occur when movement is completely prohibited. While Non-homogeneous boundary conditions occur when finite non-zero displacement values are specified. By directly eliminating the rows and columns corresponding to zero displacement and degrees of freedom, the homogeneous boundary conditions are enforced in the elimination method. The displacement at node 1 = 0, for fixed. When the first row and column are removed, the equation becomes:

$$\begin{bmatrix} k_1 + k_2 & -k_2 \\ -k_2 & k_2 \end{bmatrix} \begin{Bmatrix} u_2 \\ u_3 \end{Bmatrix} = \begin{Bmatrix} 0 \\ P \end{Bmatrix} \quad \text{OR} \quad \begin{Bmatrix} u_2 \\ u_3 \end{Bmatrix} = \begin{bmatrix} k_1 + k_2 & -k_2 \\ -k_2 & k_2 \end{bmatrix}^{-1} \begin{Bmatrix} 0 \\ P \end{Bmatrix} \tag{4.5}$$

The model here is a global stiffness matrix for determining the displacement of the nail at u_2 and u_3, by using equation (4.5). Where P is the force acting in the nail. Using the above stiffness matrix, at the various nail inclinations, the nodal displacement is observed separately for each nail. The displacements of nails in soil mass concerning their inclination are computed and stated in Table 4.1. Node u_2 reports standard deviation values of 0.079, 0.077, 0.077, 0.075, 0.076, and 0.076 m for 0^0, 5^0, 10^0, 15^0, 20^0, and 25^0, respectively. Similarly, node u_3 reports values of 0.288, 0.267, 0.237, 0.226, 0.225, and 0.265 m for the same respective nail inclinations shown in Figure 4.14. From these observations, it appears that soil slopes at 15^0 nail inclinations

indicate smaller displacements with an average displacement of 0.1252 m and a standard deviation of 0.075 m at node u_2. At u_3, the average displacement is 0.3782 m with a 0.226 m standard deviation. The minimum displacements at nodes u_2 and u_3 are observed at 15^0 nail inclinations. After 15^0 nail inclinations, displacements and standard deviation values increase at nodes u_2 and u_3, indicating a reduction in slope stability (refer to Figure 4.11).

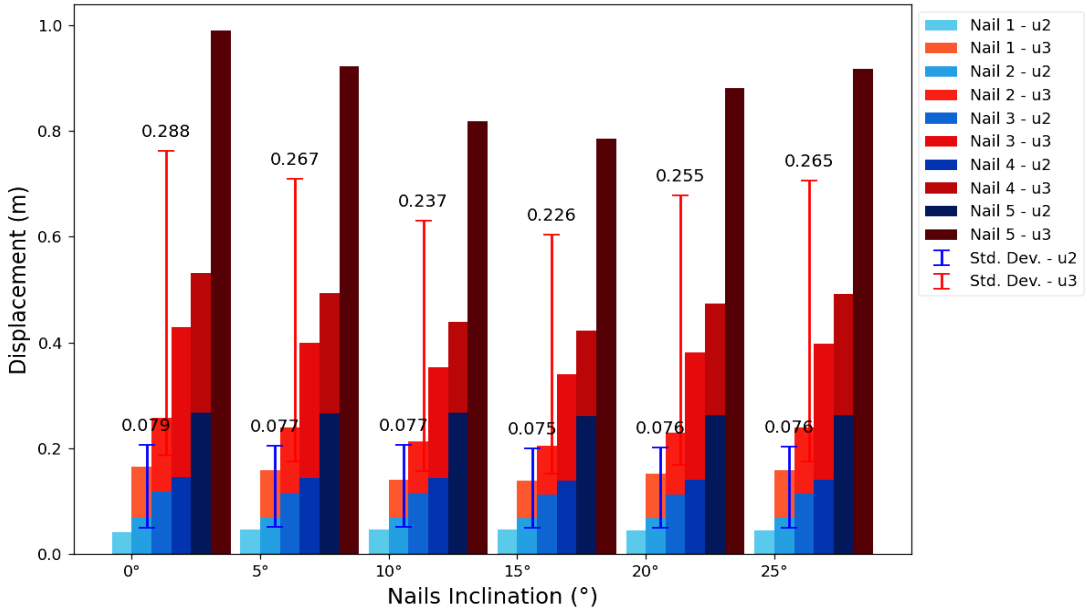

Figure 4.11: Standard deviation observation and correlation between displacement at node u_2 and u_3 by matrix method considering different nail inclinations.

Table 4.1: Displacement of nails observed near the slip surface in the soil mass at various nail inclinations

Nails inclination	Forces on Slip Surface Resist for Soil (k_1)	Forces on Slip Surface Resist for Nails (k_2)	**Nail 1**		**Nail 2**		**Nail 3**		**Nail 4**		**Nail 5**	
	kN/m	kN/m	u_2 (m)	u_3 (m)	u_2 (m)	u_3 (m)	u_2 (m)	u_3 (m)	u_2 (m)	u_3 (m)	u_2 (m)	u_3 (m)
0^0	380.28	141.56	0.041	0.165	0.070	0.258	0.117	0.429	0.145	0.532	0.268	0.990
5^0	385.97	156.77	0.046	0.159	0.069	0.239	0.115	0.399	0.143	0.494	0.266	0.922
10^0	389.25	188.49	0.046	0.141	0.069	0.213	0.116	0.354	0.143	0.439	0.267	0.819
15^0	402.27	198.65	0.046	0.139	0.068.	0.205	0.113	0.340	0.139	0.422	0.260	0.785
20^0	399.05	168.94	0.045	0.152	0.068	0.229	0.113	0.381	0.141	0.473	0.262	0.881
25^0	397.20	160.23	0.045	0.158	0.069	0.239	0.114	0.397	0.141	0.492	0.263	0.917

4.4 Identification of Settlement Embankment within the Soil Slope by 2D FEM

As discussed in the above sections especially 4.4 and 4.5, it was found that a 15^0 nail inclination increased the FOS and overall stability of the structure. In this section, numerical simulations have been conducted to investigate the effects of 15^0 nail inclination using 2D-FEM by using Geo5 fine software. Using the material properties outlined in Chapter 3, specifically in Sections 3.3.1, 3.3.2, 3.3.3, and 3.3.5, and focused on the soil slope profile shown in Figure 4.1. In this analysis, a 2D FEM model is developed using x and y coordinates, with boundary conditions applied after defining the geometry. The bottom and rear of the model are fully constrained in both the x and y directions, while vertical displacement is left unrestricted at the front and top of the slope (see Figure 4.12). These constraints are applied using standard fixities. Finally, a surcharge load UDL of 18 kN/m² was applied on the top of the slope (refer to Figure 4.1). Then the finite element mesh was successfully generated by employing multi-node elements. A total 1938 nodes and 1081 elements were created, consisting of 765 region elements, 79 beam elements, and 237 interface elements. A mesh smoothing option was also applied to optimize the element arrangement.

Both the unreinforced soil slope and the soil slope reinforced with nails, as illustrated in Figure 4.12, were simulated under a surcharge loading of 18 kN/m². After simulation, the unreinforced slope exhibited settlement rates ranging from <-59.7 mm to >998.6 mm (Figure 4.12a). Previous analyses (in sections 4.2 and 4.3) indicated that a nail inclination of 15° resulted in the highest FOS and the least displacement. Considering this observation, the reinforced soil slope with 15° nail inclination was simulated in this section. The results showed settlement rates ranging from <-95.2 mm to >259.3 mm (Figure 4.12b). Notably, the unreinforced slope (Figure 4.12a) experienced significantly higher displacement/settlement near the embankment face compared to the reinforced slope (Figure 4.12b), which exhibited minimal settlement due to the stabilizing effect of the nails within the soil slope. Considering this aspect, further experimental analysis was conducted, and the findings are discussed in the forthcoming section.

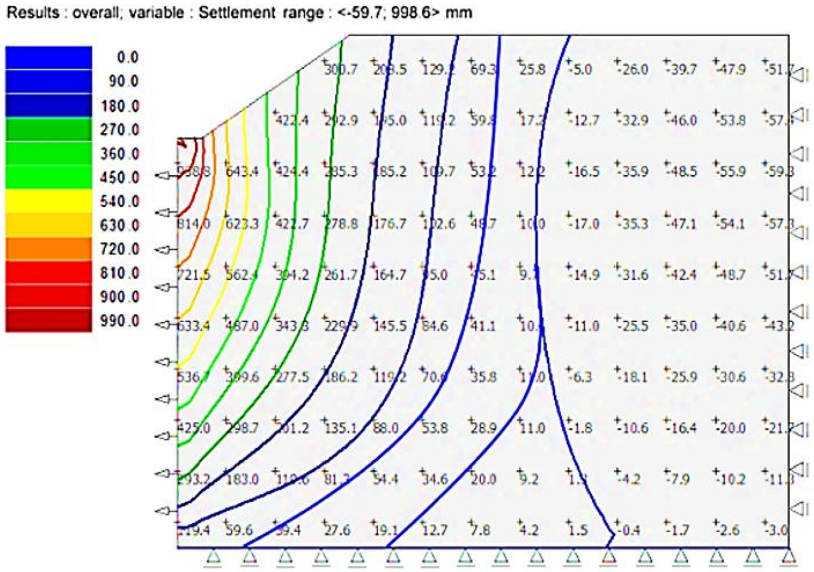

(a) Soil slope without soil nailing

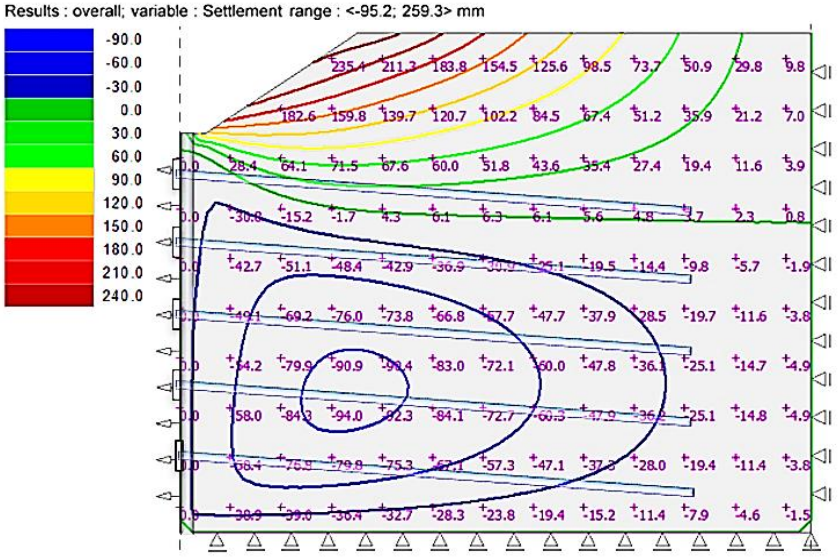

(b) Soil slope with soil nailing

Figure 4.12: Settlement of embankment under surcharge loading by 2D FEM

4.5 Experimental Investigation

The soil sample used in this study was collected from the South Delhi region, specifically Okhla Phase-III (near Govindpuri Metro Station). To classify the soil, a sieve analysis was performed in the laboratory. The results, illustrated in Figure 4.13,

indicated that the soil is poorly graded sand (SP) as per IS:1498-1970 classification. The materials and their properties used in this investigation are detailed in Chapter 3. Specifically, Section 3.3 outlines the materials used, including soil properties in Section 3.3.1, the soil-nailed wall in Section 3.3.3, and the bearing plate in Section 3.3.5. The experimental setup is comprehensively described in Section 3.6, with additional details provided in Section 3.6.1. The preparation of the soil bed slope is discussed in Section 3.7.1, covering two scenarios: (a) slopes without soil nails and (b) slopes with soil nails.

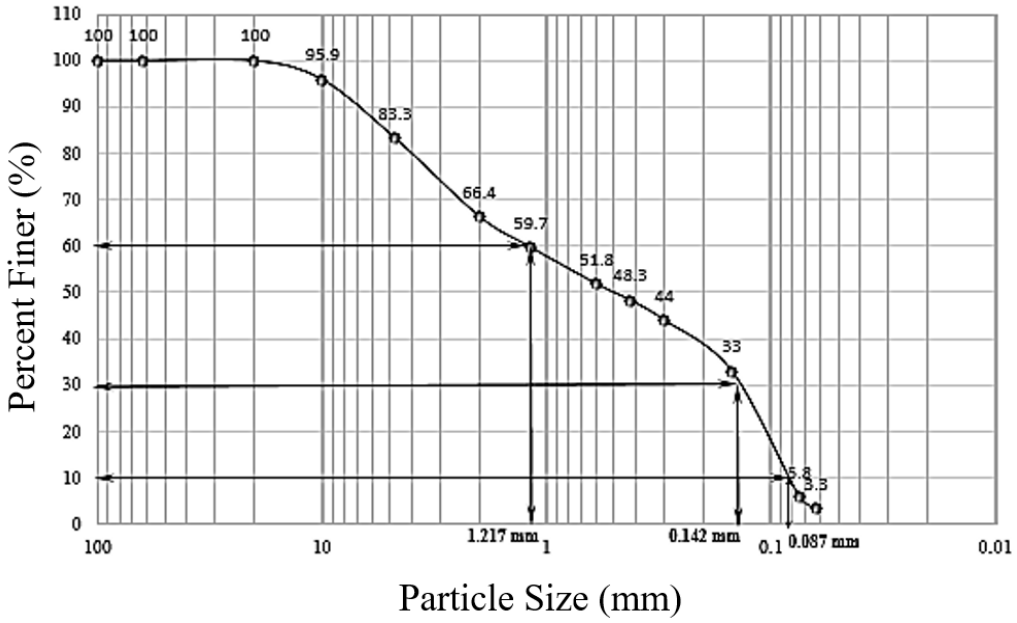

Figure 4.13: Grain size distribution curve for used soil sample.

For the study, the physical model was scaled down to a 1:20 ratio, as shown in Figure 4.14(c), based on the soil slope profile diagram presented in Figure 4.1. Figures 4.14 and 4.16 illustrate the experimental setup and model preparation, with further details provided in Section 3.7.1. Using the material properties and experimental setup described in Chapter 3, the experimental investigation was conducted, and the results are discussed in the following sections:

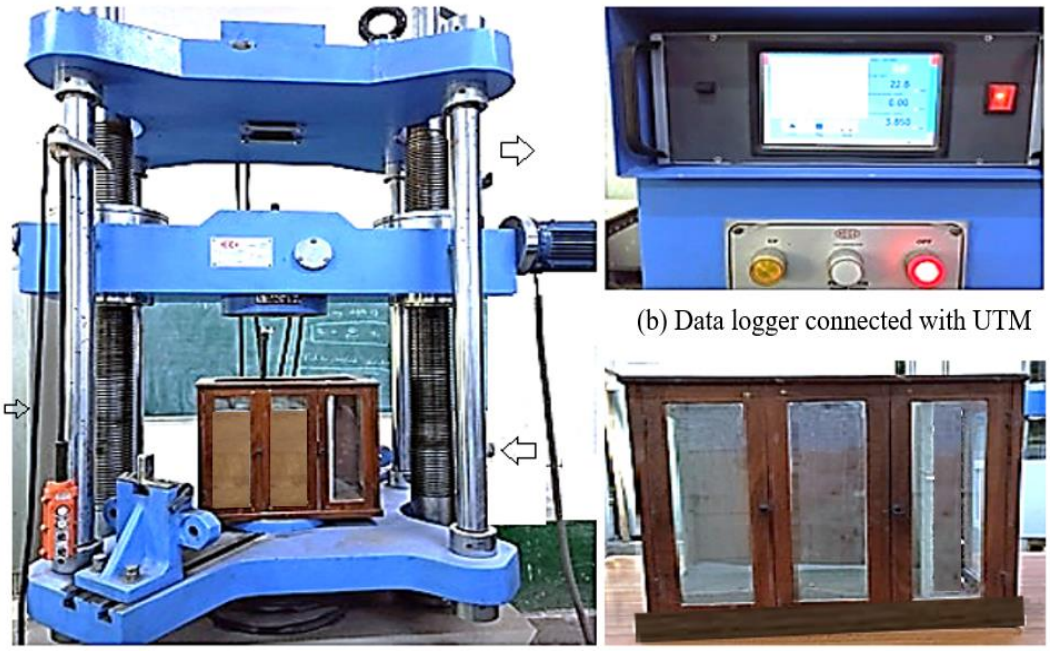

(b) Data logger connected with UTM

(a) Computerized universal testing machine (UTM) **(c)** Physical model

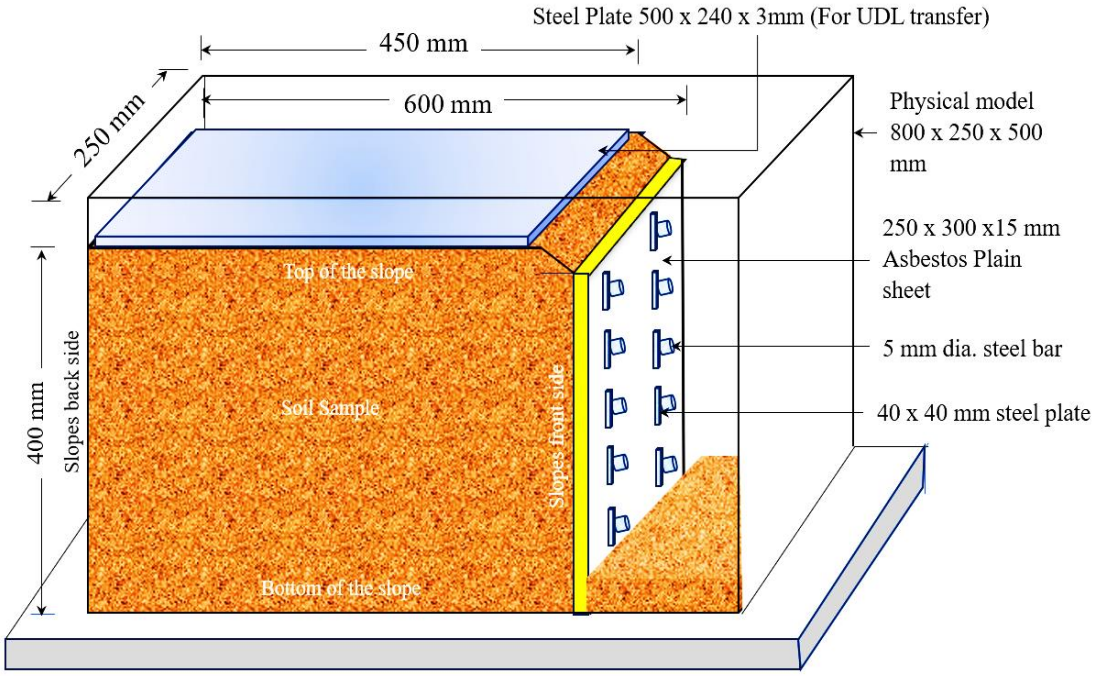

(d) Schematic diagram of a physical model

Figure 4.14: Experimental setup: soil slope model mounted on computerized UTM

(a) **(b)** **(c)**

Figure 4.15: Observation of soil slope model-I without reinforcement: (a) Model mounted on UTM, (b) Displacement measurement, (c) Displacement within the slope

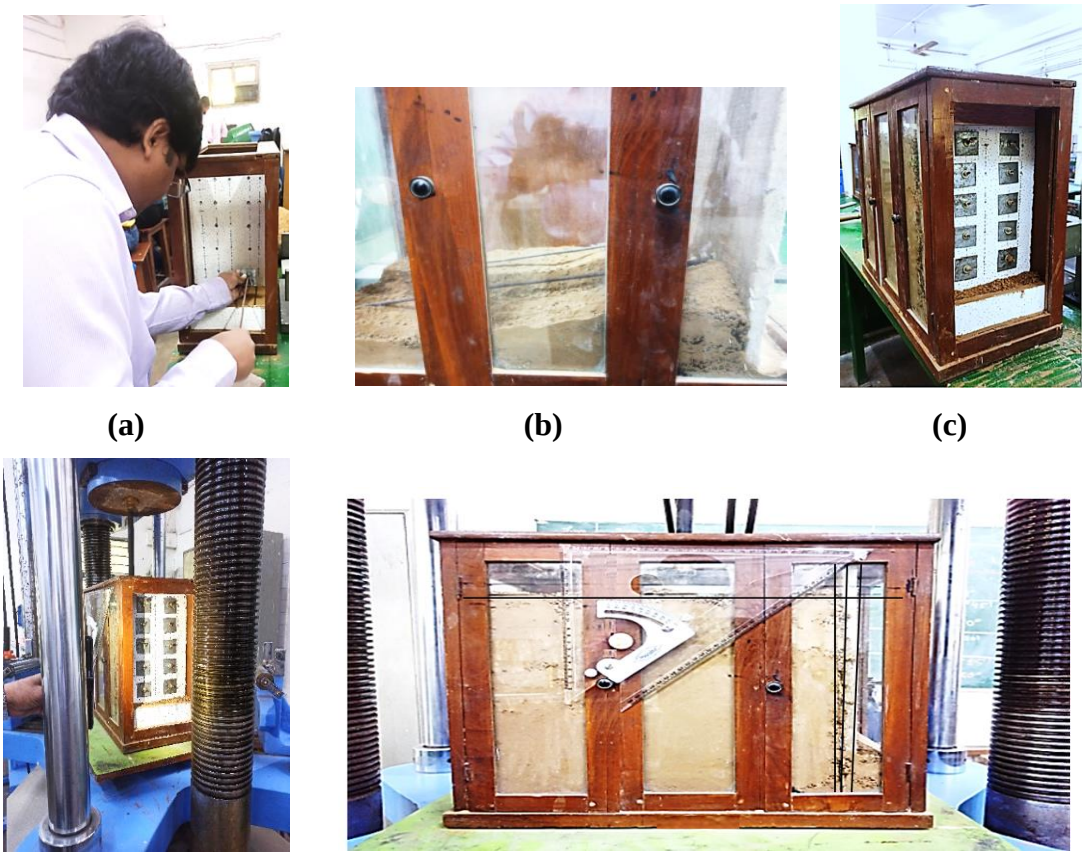

(a) **(b)** **(c)**

(d) **(e)**

Figure 4.16: Complete preparation of reinforced soil nailed slope models-II from installation to performance evaluation: (a) Installation of soil nails/bars in soil slope (b) Preparation of nail inclinations (c) Complete soil nailed wall model (d) Soil nailed model mounted on UTM (e) Measurement of displacement in soil nailed wall and slope.

During the experimental study, five trials were conducted for each nail inclination to analyze the performance of the soil-nailed slope/wall. It was observed that the displacement of the soil-nailed wall was minimized at a nail inclination of 15° with respect to the horizontal plane. Wall displacement measurements were recorded in both horizontal and vertical directions (refer to Figures 4.15 and 4.16). Under a surcharge load of 18 kN/m², the average maximum wall deflections (δΔ) corresponding to nail inclinations of 0°, 5°, 10°, 15°, 20°, and 25° were 28 mm, 25 mm, 21 mm, 16 mm, 18 mm, and 20 mm, respectively. In contrast, the maximum deflection of the wall without soil nails was observed to be 32 mm (average) at the top of the wall (refer to Figure 4.17). The investigation revealed that at a 15° nail inclination, soil reinforcement effectively reduced settlement by 61.90%. These findings demonstrate that soil nailing is a versatile and effective technique for slope stabilization, providing significant global stability to the structure when the nails are inclined at 15° to the horizontal plane.

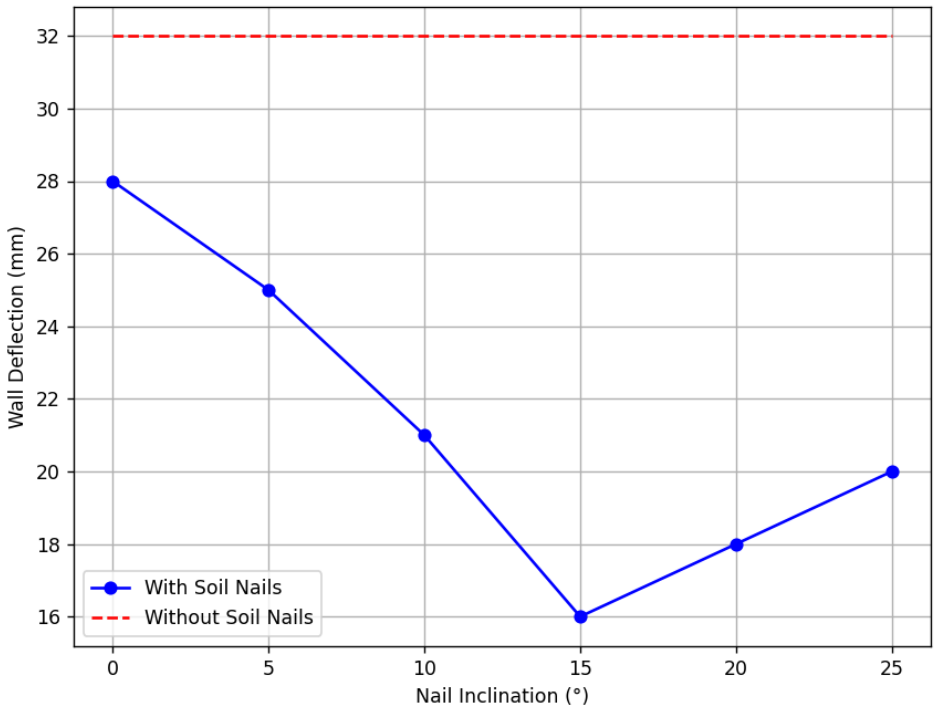

Figure 4.17: Effect of nail inclination on wall deflection

4.6 Comparative Analysis Between Various Methods Used in this Chapter

The findings from mathematical modelling, numerical analysis (FEM), and experimental investigations indicate that soil nail structures are most effective and stable when the nails are inclined at 15° to the horizontal plane. Under a surcharge load of 18 kN/m², soil displacement and settlement were analyzed, with unreinforced slopes exhibiting significantly greater settlement and displacement compared to reinforced slopes. The experimental results demonstrated that the maximum reduction in settlement occurred at a 15° nail inclination, attributed to the increased stiffness of the reinforced soil layer, which effectively minimized settlement and lateral displacement. At this inclination, soil reinforcement significantly enhanced the embankment's bearing capacity and reduced the risk of failure under surcharge loading. The experimental model showed a 61.72% reduction in settlement, while the analytical study observed a 58.90% reduction in slope failure. Furthermore, FEM analysis closely aligned with the experimental findings, reporting a 62.71% reduction in settlement. This consistency across experimental, analytical, and FEM approaches underscores the effectiveness of soil reinforcement at a 15° inclination, as illustrated in Figure 4.18.

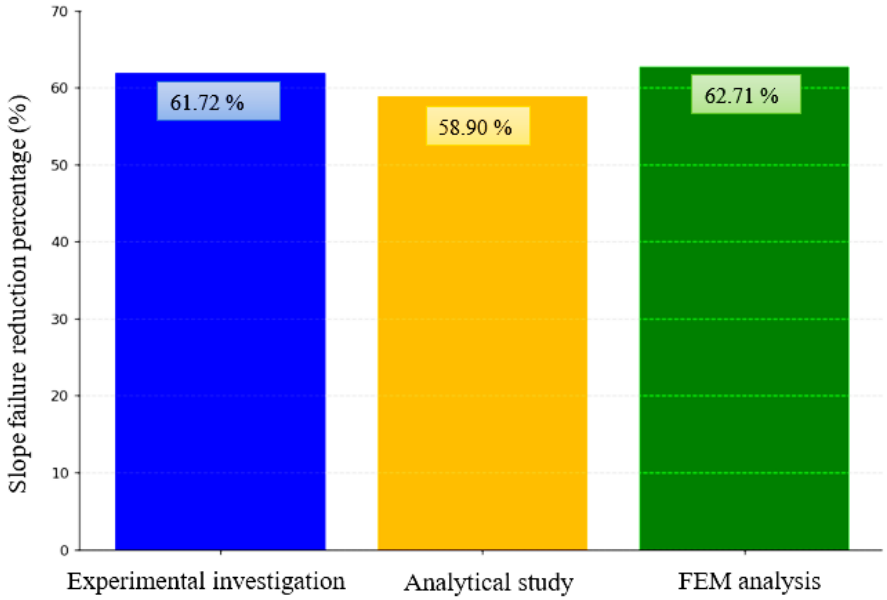

Figure 4.18: Comparing slope failure reduction at a 15° nail inclination for the experimental model, analytical method and FEM analysis.

The experimental results were corroborated by FEM analysis, demonstrating reliability and precision. Additionally, mathematical modelling confirmed that a 15° nail inclination resulted in the least displacement at nodes u_2 and u_3 compared to other inclinations (refer to Section 4.3). These findings collectively confirm that soil reinforcement at a 15° nail inclination is a highly effective solution for mitigating settlement and lateral displacement, significantly reducing the risk of slope failure for the present soil slope condition (i.e. Figure 4.1).

This chapter concludes that soil nailing at a 15° nail inclination is pivotal in enhancing slope stability and reducing settlement for the soil and material properties outlined in Chapter 3, specifically in Sections 3.3.1, 3.3.2, 3.3.3, and 3.3.5, with the soil slope profile depicted in Figure 4.1. The findings provide a strong foundation for understanding the crucial role of nail inclination in slope stabilization. Furthermore, grouted nails were identified as a key component of the soil nailing system, significantly contributing to slope integrity and stability. Building on these insights, the next chapter presents a comparative evaluation of the performance of grouted and non-grouted nails, examining their respective impacts on the stability of soil-nailed slopes/walls.

Chapter 5

SOIL NAILED SLOPES STABILITY AND PERFORMANCE

5.1 Introduction

This chapter presents the impact of soil nailing on soil slope structural stability, with a primary focus on understanding the interconnection and functionality of each component in slope stabilization. Special emphasis is placed on the critical role of grouted nails and bearing plates, which have demonstrated substantial contributions to enhancing slope integrity and stability. A comparative analysis of grouted and non-grouted nails is included to assess their respective performances in stabilizing soil-nailed slopes/walls. This evaluation provides deeper insights into the effectiveness of these techniques, emphasizing their potential applications and influence in advancing slope stabilization practices. The investigation aims to develop a comprehensive understanding of the interaction between nail types and structural stability, offering valuable guidance for optimizing soil-nailing slopes/structures.

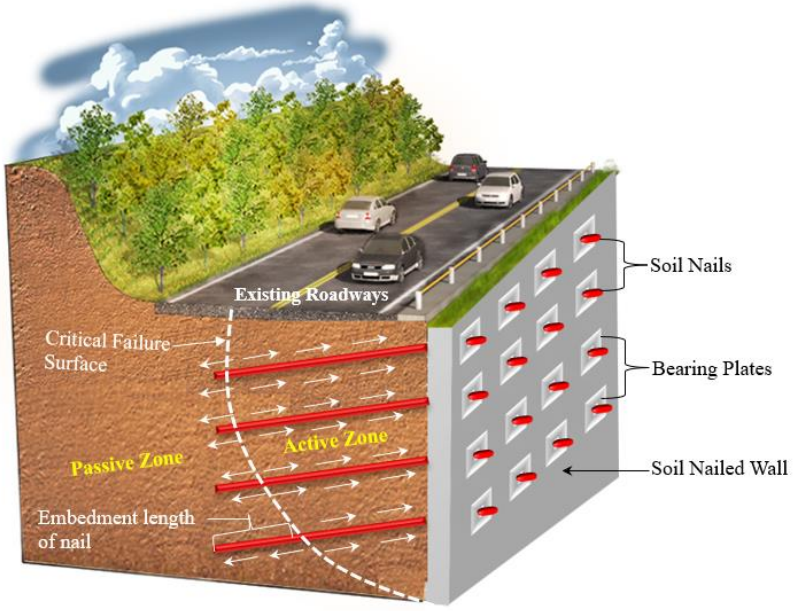

Figure 5.1 : Pictorial view of a soil-nailed slope with a soil-nailed wall (modified after ACE Geosynthetics)

5.2 Effects of Tensile Forces on the Soil Nails

Through each new excavation phase due to ground lateral dilation, tension is primarily induced in the soil nails. The maximum tension (T_{max}) is found in the nails at a certain distance from the facing. At the point where the maximum tension (T_{max}) characterises a surface, the reinforced soil mass is divided into two parts, the active and passive zone (refer to Figure 5.1). The embedment length of nails in the passive zone also plays an important role in slope stabilization (Gao et al. 2016).

In the soil nail design, the Modulus of Elasticity (E) plays an important role. Considering its importance the experimental investigation has been carried out to obtain the elongation within nails. The result obtained in the same is illustrated in Figure 5.2. It is observed that at the initial stage, it obeyed the proportional limit i.e. Hooks Law and thereafter increased displacement without an appreciable increase in load. In the next stage, there is an increase in displacement without an appreciable increase in load and the curve drops down (see Figure 5.2). Then again with a slight increase in load, the displacement increases slightly and remains particularly constant without an increase in load. This phenomenon of an increase in strain without any appreciable increase in load is called yielding. In this stage, the relationship between stress and strain also depends upon the rate of loading. During this phenomenon, the cross-sectional area decreases uniformly all over the length. At the last stage, the maximum load is reached and the cross-sectional area decreases considerably. Also, the load-carrying capacity of the specimen reduces and hence strain increases with a decrease in stress (refer to Figure 5.2).

For the experimental purpose, a computerised universal testing machine (UTM) is used in the laboratory to obtain the tensile properties of the 10 mm diameter steel bar, the same diameter of bars also used in the soil slope experimental model shown in Figure 5.14. During this investigation, Three specimens of 10 mm diameter mild steel bar were used and experimentally it is observed that the elongations are 22.46 %, 19.6 %, and 26.54 %. The properties obtained from the test result are enumerated in Table 5.1 and the Load-displacement curve for specimen 1 is plotted as shown in Figure 5.2.

Table 5.1: The tensile strength output of different specimens by using UTM

Description	Units	Specimen 1	Specimen 2	Specimen 3
Length of the bar	(mm)	600	600	600
Diameter of the bar	(mm)	10	10	10
Area of the specimen (a)	(mm^2)	78.539	78.539	78.539
Guage Length ($5.65\sqrt{a}$)	(mm)	50	50	50
Reduction in Area	(%)	100	100	100
Ultimate Load	(kN)	37.5	41.2	42.55
Displ. at Ultimate Load	(mm)	26.6	29.3	29.50
Breaking Load	(kN)	37.40	39.80	38.75
Maximum Displacement	(mm)	29.9	32.30	33.20
Tensile Stress	(N/mm^2)	477.47	482.45	488.60
Yield Load	(kN)	31.40	33.67	33.20
Yield Stress	(N/mm^2)	399.80	412.25	420.75
Breaking Stress	(N/mm^2)	476.20	480.56	485.67
Yield st./Tensile st.	---	0.837	0.854	0.861
Final gauge length	(mm)	61.23	59.80	63.27
Elongation	(%)	22.46	19.60	26.54

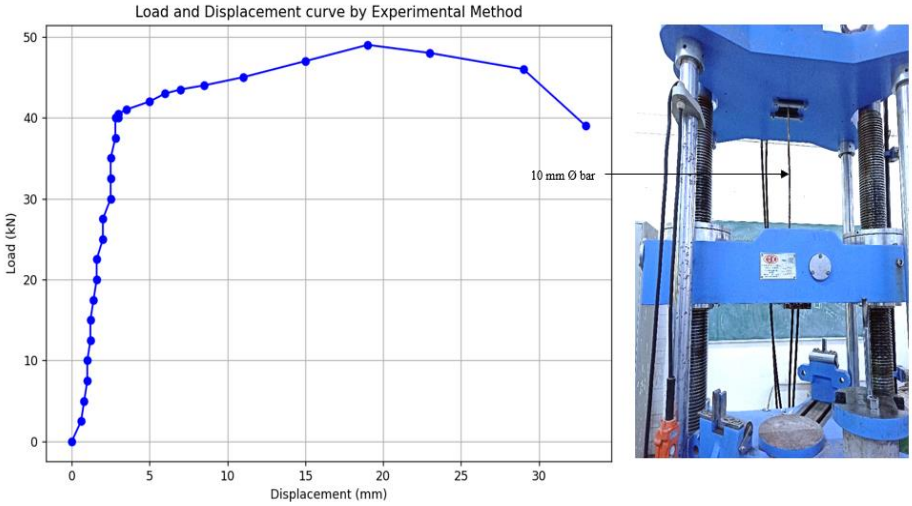

Figure 5.2: Load-displacement curve observed by the experimental method using a Computerized Universal Testing Machine (UTM) for Specimen 1.

5.3 The Pullout Function of Grouted Nail

Based on the multicriteria study conducted by Schlosser and Unterreiner (1991), as discussed in the literature review section 2.16.1, the effects of various parameters on soil nails have been analyzed in this section. Generally, the grouted nails play a very important role in slope stability. It holds the soil strata or soil mass in the entire structure. When the grouted nail diameter is very small, the maximum nail load can be assumed as the steel bar load. In soil nailing systems, grout nails refer to the hardened grout that surrounds the steel nail. This grout plays an important role in transferring loads between the nail and the surrounding soil, helping to distribute stresses more effectively. The steel bar inside the grout provides strength but cannot carry large loads on its own. The total force resistance in the nail system called the gross nail load, includes forces from soil pressure, external loads like surcharge, and other stresses acting on the slope. When the grout is strong and intact, it takes on a major part of the load, making the system more stable and reliable.

Generally, the length of the soil nails is defined by using the preliminary numerical simulation or design, in this situation the mobilization of soil-cement interface shear resistance can meet the stability requirements. In the region of grouted soil nails, Young's modulus was taken into account as

$$E_g = \left[\frac{(A_G \times E_G) + (A_S \times E_S)}{A_G + A_S}\right] \quad (5.1)$$

Where, "E_g is Young's modulus of Elasticity of the surrounding cement slurry and steel rebar; A_G is the areas of cement grout, A_S is the area of steel bars, E_G and E_s are the elastic moduli of cement grout and steel bar respectively."

The analysis has considered both the bond strength between the grout and the nails and the interaction between the soil and the grout. Design results are based on the FHWA manual (Lazarte et al. 2003), utilizing either the pullout capacity or bond strength per unit length. The pull-out capacity becomes fully effective when the ultimate bond strength is achieved.

Therefore,

$$P_o = T_{max} = P_u L_p \quad (5.2)$$

Where, "P_u is per unit length pullout capacity, L_p is the effective bond length or the pullout length (equation 5.4)."

$$P_o = \pi D_o L_p q_u \tag{5.3}$$

Where, "πD_o is the circumference of the drill hole, q_u is the ultimate bond strength." The effective length or pullout length can be calculated as

$$L_{eff} \text{ OR } L_p = L - \left\{(H - Z)\left[\frac{\text{Cos}(45+\frac{\emptyset}{2})}{\text{Sin}(45+\frac{\emptyset}{2}+\theta)}\right]\right\} \tag{5.4}$$

Where, "L is the total length of the nail, ϕ is the friction angle of the soil, θ is the nail inclination, H is the height of the wall, and Z is the nail-head depth."

Hence the allowable value of bond strength (q) is

$$q = \frac{q_u}{(FOS)_p} \tag{5.5}$$

and, allowable soil nail pullout resistance (P_o') is

$$P_o' = \frac{P_o}{(FOS)_p} \tag{5.6}$$

As per the FHWA manual (Lazarte et al. 2003) a minimum factor of safety $(FOS)_p$, recommended against pullout failure is 2.

When the soil has better shear strength capacity, in that case, it tries to resist the pullout of the soil nail from the soil mass and the minimum elongation takes place in the nail. The elongation can be obtained by

$$\delta l = \frac{P_o L}{A_s E_s} \quad \text{and} \quad \frac{P_o L}{A_s E_g} \tag{5.7}$$

Where, "L is the nail length, A_s is the area of the steel bar/nail, E_s is the elastic modulus of the steel and E_g is the averaged Young's modulus of a grouted soil nail (Equation 5.1)."

Table 5.2: Effect of different parameters in nails with and without grouting under surcharge loading

Dia. of bar	Grouted Nails						Non-Grouted Nails				
	Pu	**Po**	**q**	**Po'**	**E**	**δ*l***	**Pu**	**Po**	**Po'**	**E**	**δ*l***
(mm)	(N/mm)	(N)	(N/mm^2)	(N)	(N/mm^2)	(m)	(N/mm)	(N)	(N)	(N/mm^2)	(m)
10	18.85	128980	0.06	64490	31731	0.0186	3.77	25796	12898	200000	0.1478
12	19.6	134139	0.06	67069	33848	0.0168	4.52	30955	15478	200000	0.1232
16	21.11	144457	0.06	72229	38208	0.0138	6.03	41273	20637	200000	0.0924
18	21.87	149616	0.06	74808	40374	0.0126	6.79	46433	23216	200000	0.0821
20	22.62	154776	0.06	77388	42500	0.0116	7.54	51592	25796	200000	0.0739
22	23.37	159935	0.06	79967	44570	0.0107	8.29	56751	28376	200000	0.0672
25	24.5	167674	0.06	83837	47552	0.0096	9.42	64490	32245	200000	0.0591
28	25.64	175412	0.06	87706	50370	0.0086	10.56	72229	36114	200000	0.0528
30	26.39	180572	0.06	90286	52155	0.0081	11.31	77388	38694	200000	0.0493

In Chapter 4, the maximum Factor of Safety (FOS) for various nail inclinations (0°, 5°, 10°, 15°, 20°, and 25°) relative to the horizontal plane was investigated. The analysis revealed that the maximum FOS for poorly graded sand (SP) occurred at a nail inclination of 15°. Building on this observation, the present investigation examines the effects of various parameters in grouted nails, specifically analyzing different nail diameters (10, 12, 16, 18, 20, 22, 25, 28, and 30 mm) at the optimal 15° nail inclination. The basic properties of grouted cement are detailed in Chapter 3, Section 3.4.4.

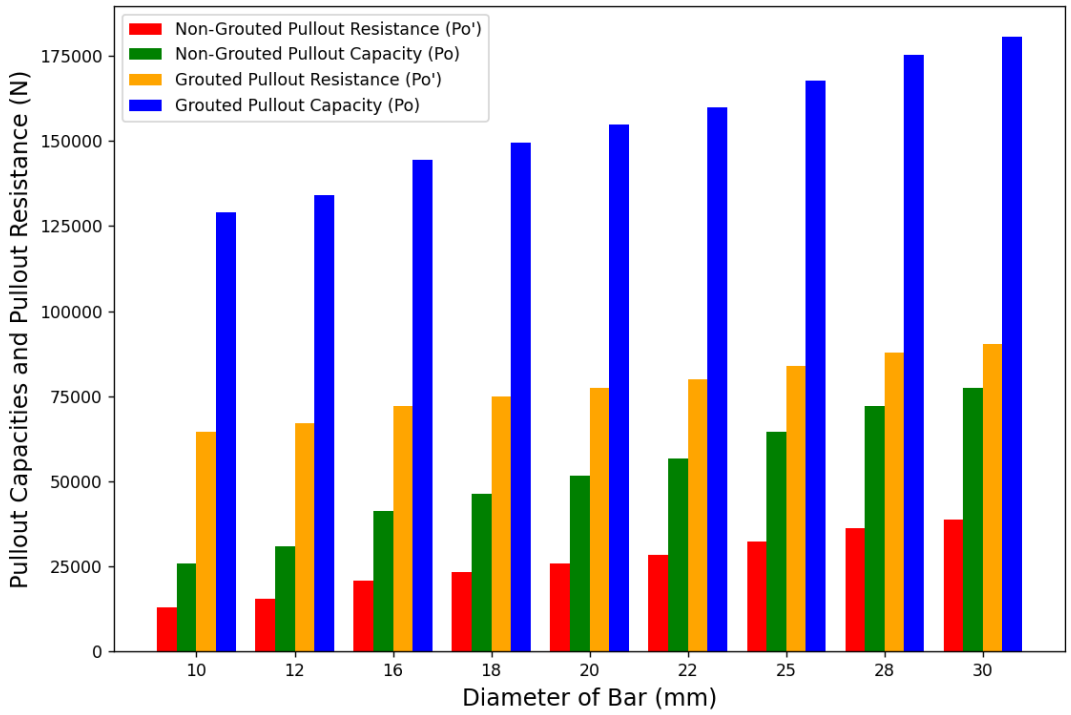

Figure 5.3 Comparison of grouted and non-grouted nails in response to pullout capacity and pullout resistance

Using Equations 5.1 to 5.7, the investigation revealed significant differences between grouted and non-grouted nails, as demonstrated in Table 5.2 and Figures 5.3 through 5.6. Grouted nails exhibited substantially higher pullout resistance and capacity compared to non-grouted nails, with consistent performance across increasing nail diameters from 10 mm to 30 mm (Figure 5.4 a). In contrast, non-grouted nails displayed notable variations in effective parameters with changing diameters (Figure 5.4 b), emphasizing the stabilizing influence of grouting nails in ensuring uniform and reliable performance.

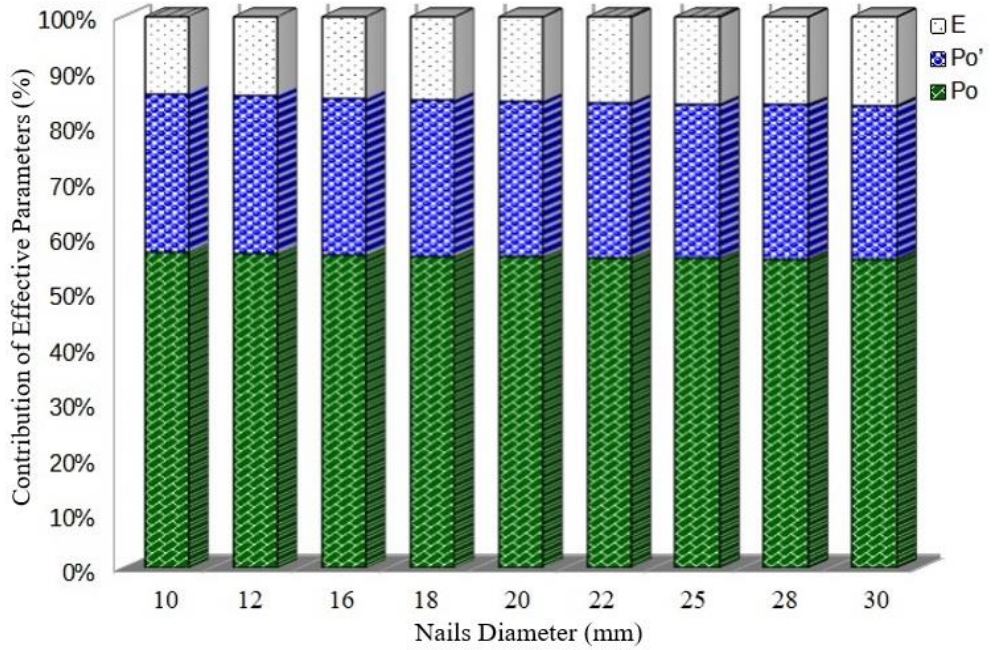

(a) grouted nails.

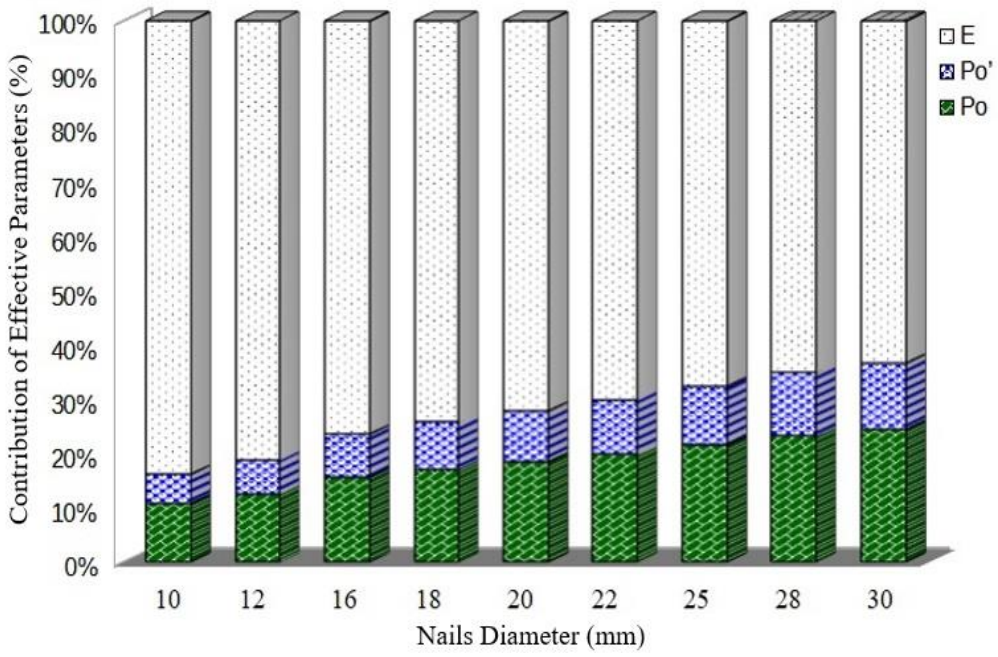

(b) non-grouted nails.

Figure 5.4: Contribution of effective parameters for: **(a)** grouted nails **(b)** non-grouted nails.

Figure 5.3 highlights the comparison of pullout resistance (P_o') and pullout capacity (P_o) across varying diameters, where non-grouted nails demonstrated significantly

lower values. For non-grouted nails, pullout resistance contributed less than 50% to their pullout capacity, whereas grouted nails exhibited pullout resistance contributing over 50%, reaching up to 58.6% of their pullout capacity (Figure 5.4 a). Furthermore, both pullout resistance (P_o') and pullout capacity (P_o) increased with bar diameter for both nail types, underlining the importance of larger bar diameters in achieving better constancy due to enhanced pullout strength (see Figure 5.3).

During this study, it was observed that the pullout capacity (P_o) contribution for grouted nails increased to an average of 58.6%, for non-grouted nails, this contribution averaged 18.35%. The effective parameter contributing to pullout resistance (P_o') averaged up to 31% for grouted nails and 22.83% for non-grouted nails (Figure 5.5). Compared to grouted nails, the contribution to pullout resistance was lower in non-grouted nails. Additionally, the modulus of elasticity (E) contributed less to grouted nails, whereas for non-grouted nails, the contribution was significantly higher (refer to Figure 5.4 and Figure 5.5), these results indicate that the modulus of elasticity (E) is more pronounced in non-grouted nails, resulting in greater elongation within the soil slope compared to grouted nails. The grouting process effectively controls the modulus of elasticity (E), minimizing nail elongation under applied force, thereby enhancing performance in resisting deformation.

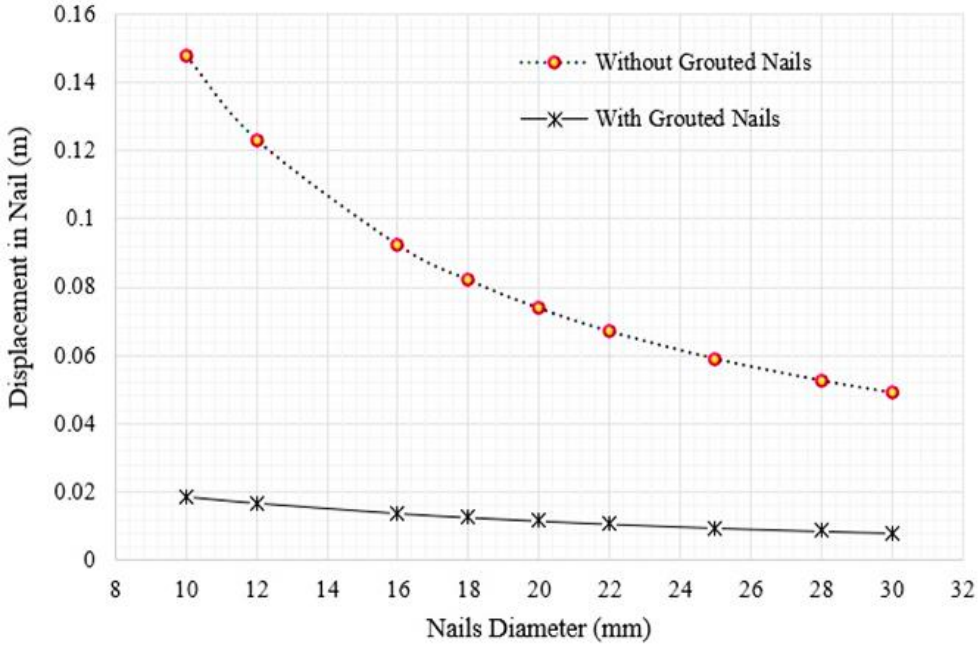

Figure 5.5: Displacement in grouted and without grouted soil nail

In this study, by comparing the results shown in Table 5.2, Figure 5.4 a, and Figure 5.4 b, it is evident that grouted nails are more stronger in response to pullout capacity and pullout resistance, resulting in less displacement compared to non-grouted nails (see Figure 5.5). Additionally, increasing nail diameter marginally increased the effect of the elastic modulus in grouted nails (refer to Table 5.2 and Figure 5.4). This can be attributed to the enhanced stiffness and reduced elongation under applied forces with larger nail diameters. Figure 5.6 provides a comprehensive comparison between grouted and non-grouted nails, revealing distinct performance differences across key parameters. Grouted nails exhibit significantly higher contributions in pullout capacity (P_o) and pullout resistance (P_o') compared to non-grouted nails. These findings highlight the superior anchoring strength and resistance capabilities of grouted nails, making them more effective in stabilizing slopes and resisting pullout forces compared to their non-grouted counterparts.

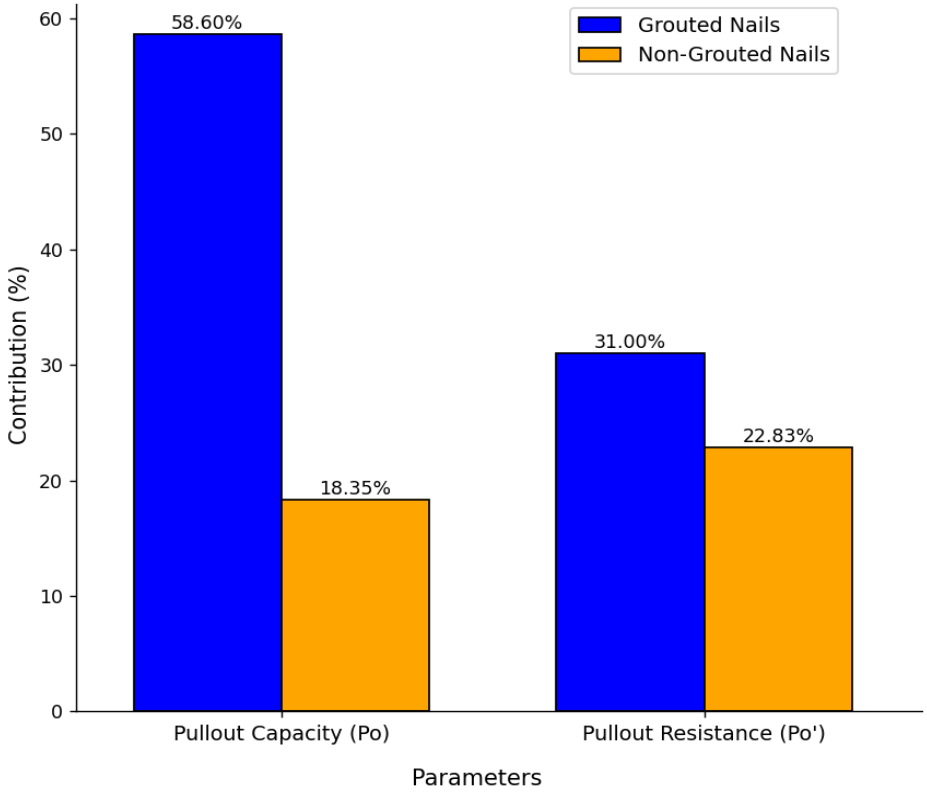

Figure 5.6 Comparison of contributions to nail performance in response to grouted and non-grouted nail

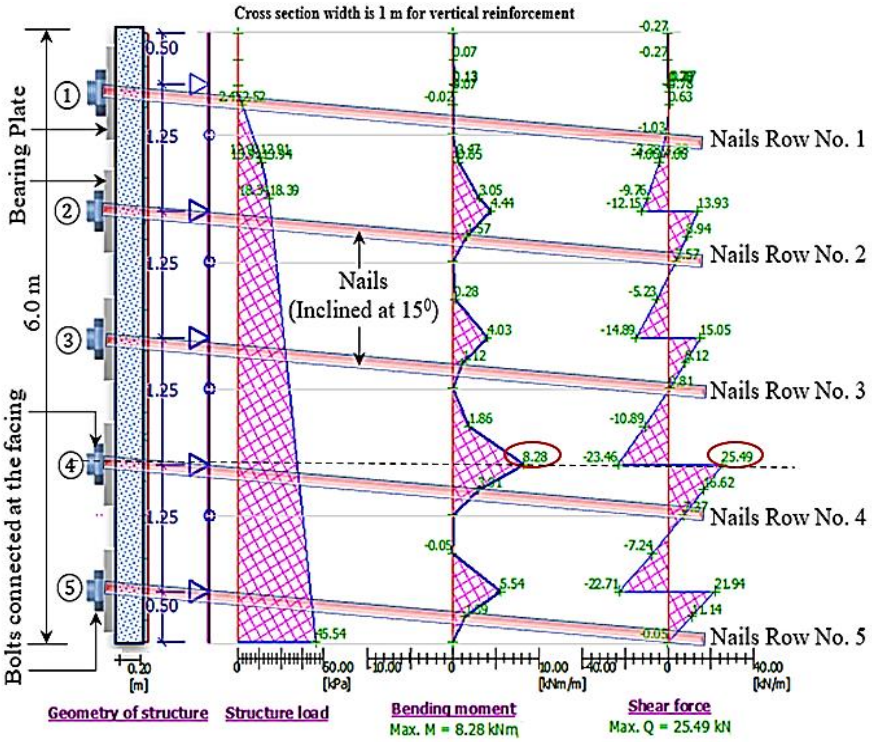

(a) SFD and BMD for vertical reinforcement (C/S)

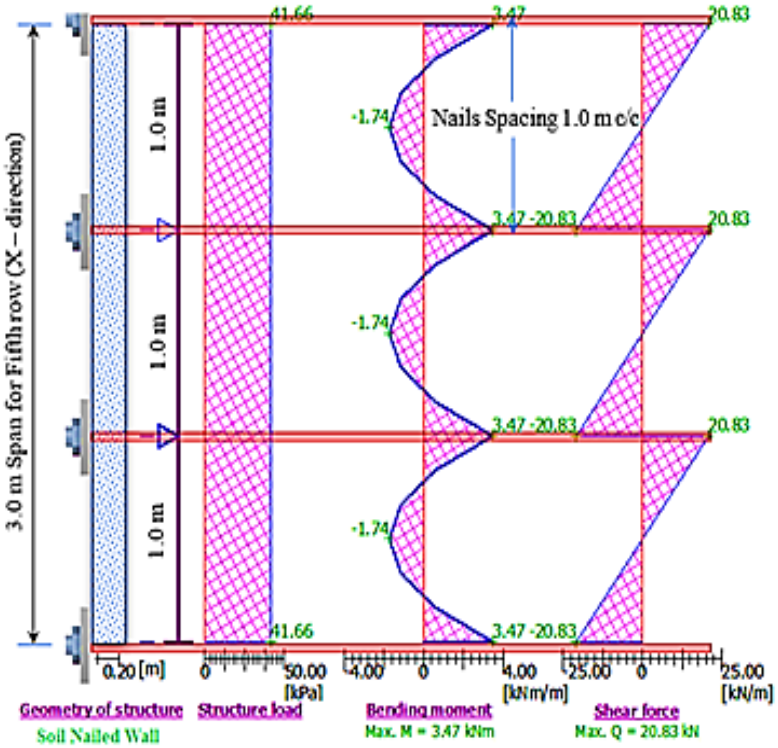

(b) SFD and BMD for Nails Row No. 5 (5th Nail) (Top view C/S)

Figure 5.7: Shear force and bending moment distribution in soil nailed wall

5.4 Design of Soil Nailed Wall at Slope Facing

5.4.1 Mobilization of SF and BM in soil-nailed wall

Shear Force (SF) and Bending Moment (BM) significantly affect the stability of soil-nailed walls, as improper soil nail design can lead to bending or shear failures at the facing. Ignoring nail stiffness can underestimate the wall's stability, making it essential to evaluate the facing design. This study analyzed SF and BM for a soil-nailed wall with 15° nail inclinations using material properties detailed in Chapter 3, Section 3.4. The analysis considered a vertical wall height of 6.0 meters (Figure 5.7 a) and a horizontal span of 3.0 meters (Figure 5.7 b) under a surcharge load of 18 kN/m². Geo5 (2018) software was used for the analysis. The maximum SF was 25.49 kN, and the maximum BM was 8.28 kN-m (vertical), while the bottom-most nail (5th nail) showed a maximum SF of 20.83 kN and BM of 3.47 kN-m (horizontal). Overall, BM values were significantly lower than SF values results shown in Figure 5.7.

5.4.2 Soil-Nailed Wall Verification (Flexural Failure at The Facing)

In the soil-nailed wall, the soil nails act as the supports and the lateral earth pressure acts as the loading behind it (see Figure 5.8 (a) and (b)). Due to the lateral earth pressure, the flexural moments are created in the entire face of the soil-nailed wall. If these moments are too excessive then the shotcrete could fail flexurally and progressive cracking occurs on both sides of the wall, ultimately leading to a flexural failure. It is experimentally proved and demonstrated in Figure 5.14 (b). Throughout this investigation, it became evident that the yielding and stability of slopes can be effectively controlled by various factors, including horizontal and vertical nail spacing, the type of steel used for the bearing plate, the size of the bearing plate at the facing, the grade of concrete used for the soil nail wall, soil types, lateral earth pressure behind the wall, facing thickness, maximum soil pressure, and the placement of reinforcement etc. Moreover, the study underscored the substantial role that reinforcing mesh, particularly reinforced steel mesh in R.C.C. walls, plays an important role in stabilizing slopes and enhancing the structural integrity of soil nail walls and slopes. With this insight in consideration, a numerical analysis was conducted using the versatile Geo 5

Fine software (refer to Figure 4.2), incorporating various mesh size outcomes, and their verifications are revealed in Table 5.3.

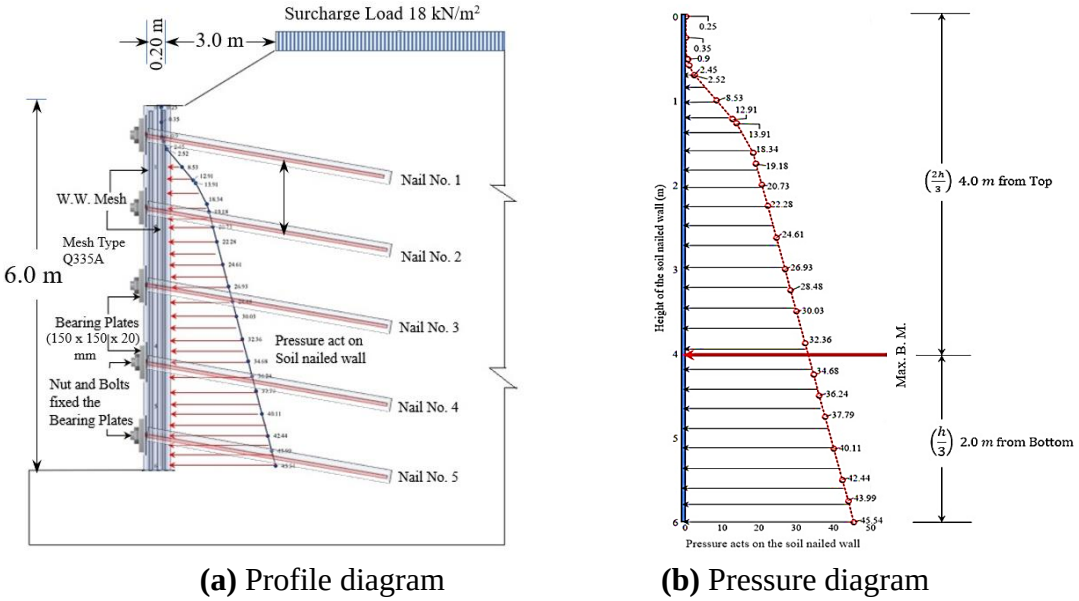

(a) Profile diagram **(b)** Pressure diagram

Figure 5.8: Pressure acts on the soil-nailed wall

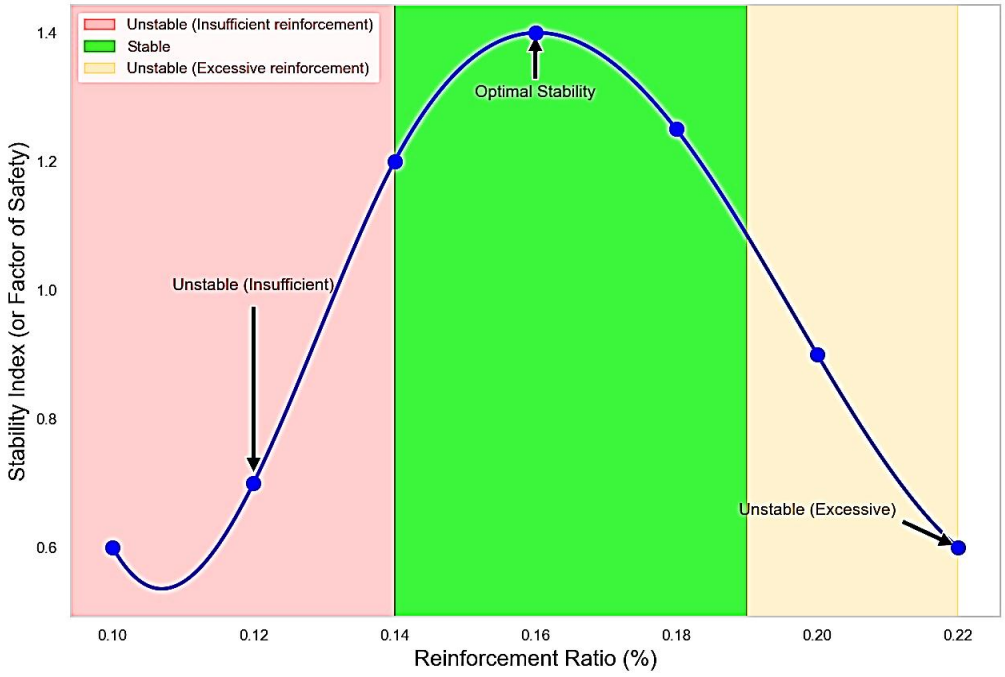

Figure 5.9: Effect of reinforcement ratio (in soil nailed wall) on slope stability.

Table 5.3: Verification of different mesh sizes for soil nailed wall

Sr. No.	Mash Type	Mesh Size (mm)	Dimensioning of concrete cover									Overall check
			Vertical direction - back		Horizontal direction - back		Vertical direction - front		Horizontal direction - front		Design principles	
			Position of N.A.	Ultimate Moment	Position of N.A.	Ultimate Moment	Position of N.A.	Ultimate Moment	Positi on of N.A.	Ultimate Moment	Reinforc ement ratio	
			(x) m	(M_{RD}) kN-m	(x) m	(M_{RD}) kN-m	(x) m	(M_{RD}) kN-m	(x) m	(M_{RD}) kN-m	(ρ) %	
1	A60	(6.0 x 5.0 /100 x 300)	0.00	5.09	0.01	21.67	0.00	-0.54	0.01	-2.01	0.04	N. S*.
2	A70	(7.0 x 5.5 /100 x 300)	0.00	6.16	0.01	29.28	0.00	-6.16	0.01	-29.28	0.04	N. S.*
3	A82	(8.2 x 6.5 /100 x 300)	0.00	8.59	0.02	39.75	0.00	-0.89	0.02	-39.75	0.06	N. S.*
4	AQ42	(4.2 x 4.5 /100 x 100)	0.00	10.73	0.00	10.73	0.00	-1.10	0.00	-1.10	0.08	N. S.*
5	AQ50	(5.0 x 5.0 /100 x 100)	0.01	15.14	0.01	15.14	0.01	-1.49	0.01	-1.49	0.11	N. S.*
6	AQ55	(5.5 x 5.5 /100 x 100)	0.01	18.27	0.01	18.27	0.01	-1.75	0.01	-0.75	0.13	N. S.*
7	AQ60	(6.0 x 6.0 /100 x 100)	0.01	21.67	0.01	21.67	0.01	-2.01	0.01	-2.01	0.16	SAFE
8	AQ 65	(6.5 x 6.5 /100 x 100)	0.01	25.34	0.01	25.34	0.01	-2.26	0.01	-2.26	0.18	SAFE
9	AQ70	(7.0 x 7.0 /100 x 100)	0.01	29.28	0.01	29.28	0.01	-2.28	0.01	-2.28	0.21	N. S.[@]
10	AQ 76	(7.6 x 7.6 /100 x 100)	0.01	34.33	0.01	34.33	0.01	-2.24	0.01	-2.24	0.25	N. S.[@]
11	AQ 80	(8.0 x 8.0 /100 x 100)	0.02	37.91	0.02	37.91	0.02	-1.75	0.02	-1.75	0.28	N. S.[@]
12	AQ 82	(8.2 x 8.2 /100 x 100)	0.02	39.75	0.02	39.75	0.02	-2.37	0.02	-2.37	0.29	N. S.[@]
13	AQ 90	(9.0 x 9.0 /100 x 100)	0.02	47.49	0.02	47.49	0.02	-1.30	0.02	-1.30	0.35	N. S.[@]
14	AQ100	(10 x 10 /100 x 100)	0.03	57.97	0.03	57.97	0.03	-1.34	0.03	-1.34	0.44	N. S.[@]
15	Q188A	(6.0 x 6.0 /150 x 150)	0.01	14.55	0.01	14.55	0.01	-1.44	0.01	-1.44	0.10	N. S. *
16	Q257A	(7.0 x 7.0/150 x 150)	0.01	19.71	0.01	19.71	0.01	-1.86	0.01	-1.86	0.14	SAFE
17	Q335A	(8.0 x 8.0 /150 x 150)	0.01	25.59	0.01	25.59	0.01	-2.28	0.01	-2.28	0.19	SAFE
18	KA16	(4.0 x 4.0 /100 x 100)	0.00	9.75	0.00	9.75	0.00	-1.00	0.00	-1.00	0.07	N.S. *
19	KA17	(4.0 x 4.0 /150 x 150)	0.00	0.52	0.00	6.52	0.00	-0.69	0.00	-0.69	0.05	N. S. *
20	KA18	(4.0 x 4.0 /200 x 200)	0.00	4.89	0.00	4.89	0.00	-4.89	0.00	-4.89	0.03	N. S. *
21	KD35	(5.0 x 5.0 /100 x 100)	0.01	15.14	0.01	15.14	0.01	-15.14	0.01	-15.14	0.11	N. S. *
22	KD36	(5.0 x 5.0 /200 x 200)	0.00	7.63	0.00	7.63	0.00	-7.63	0.00	-7.63	0.05	N. S. *
23	KD37	(5.0 x 5.0 /150 x 150)	0.00	10.15	0.00	10.15	0.00	-10.15	0.00	10.15	0.07	N. S. *
24	KH20	(6.0 x 6.0 /150 x 150)	0.01	14.55	0.01	14.55	0.01	-14.55	0.01	-14.55	0.10	N. S. *
25	KH30	(6.0 x 6.0 /100 x 100)	0.01	21.67	0.01	21.67	0.01	-21.67	0.01	-21.67	0.16	SAFE
26	KH31	(6.0 x 6.0 /200 x 200)	0.00	10.95	0.00	10.95	0.00	-10.95	0.00	-10.95	0.08	N. S. *
27	KY49	(8.0 x 8.0 /100 x 100)	0.02	37.91	0.02	37.91	0.02	-37.91	0.02	-37.91	0..28	N. S.[@]
28	KY50	(8.0 x 8.0 /150 x 150)	0.01	25.59	0.01	25.59	0.01	-25.59	0.01	-25.59	0.19	SAFE
29	KY51	(8.0 x 8.0 /200 x 200)	0.01	19.31	0.01	19.31	0.01	-19.31	0.01	-19.31	0.14	SAFE
30	KY86	(8.0 x 8.0 /150 x 150)	0.01	25.59	0.01	25.59	0.01	-25.59	0.01	-25.59	0.19	SAFE
31	KY81	(8.0 x 8.0 /100 x 100)	0.02	37.91	0.02	37.91	0.02	-37.91	0.02	-37.91	0.28	N. S. [@]
32	R188A	(6.0 x 6.0 /150 x 150)	0.00	8.78	0.01	14.55	0.00	-8.78	0.01	-14.55	0.06	N. S. *
33	R257A	(7.0 x 6.0 /150 x 250)	0.00	8.78	0.01	19.71	0.00	-8.78	0.01	-19.71	0.06	N. S. *
34	R335A	(8.0 x 6.0 /150 x 250)	0.00	8.78	0.01	25.59	0.00	-8.78	0.01	-25.59	0.06	N. S. *

Case-I: N.S. * - Not safe, required to increase reinforcement ratio.

Case-II: N.S. [@] - Not safe, due to too much reinforcement

***** The existing soil-nailed wall in the first case is deemed unsafe because there is not enough reinforcement to effectively withstand the applied loads. Either more reinforcement must be added or the existing one must be strengthened to ensure safety.

[@] The soil-nailed wall in the second instance is deemed unsafe because it has too much reinforcement. This excess can lead to construction difficulties, unpredictable behaviour and increased costs etc. It is advised to lower the reinforcement to a level that is more appropriate in order to address this problem.

Based on the results for different mesh types in soil-nailed walls (refer to Table 5.3), it was observed that for the soil slope analyzed in this study, reinforcement ratios below 0.14% lead to instability or insufficient safety. This is due to inadequate reinforcement to effectively resist the applied loads. To ensure safety, reinforcement must be increased or strengthened. Within the range of 0.14% to 0.19%, the slope was observed to be stable and safe. However, reinforcement ratios above 0.19% result in instability or inadequate safety due to excessive reinforcement in soil-nailed walls. Therefore, maintaining the stability and safety of a soil slope requires careful management of the reinforcement ratio within the soil-nailed wall. As per Figure 5.9 keeping reinforcement ratios within the optimal range of 0.14% to 0.19% is essential for ensuring slope stability and safety.

5.5 Behaviour of Bearing Plate Under Stressed Conditions

The bearing plates are made with steel plates, which are placed at the facing of soil nailed wall is suitable for the stability of the soil-nailed. Generally, it is square or rectangular in shape. Before a final facing is applied, bearing plates are installed to finish the soil nail wall. The choice of an appropriate bearing plate is crucial for supporting soil nails that stabilize masonry and MSE walls without causing any harm to the current facing. The bearing plate must be able to transfer loads completely at the soil-nailed wall facing (Byrne et al. 1993; Lazarte et al. 2003).

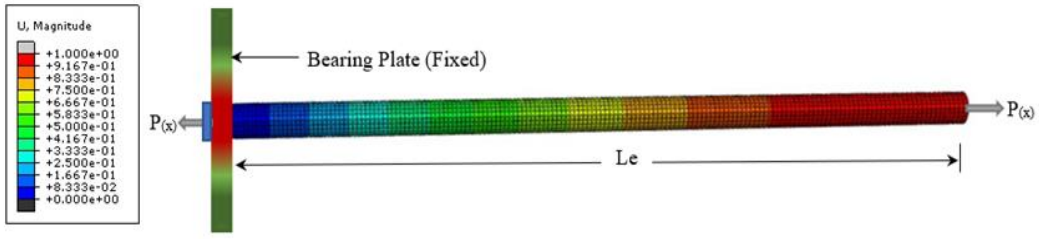

Figure 5.10: Distribution of the effective forces in the soil nail

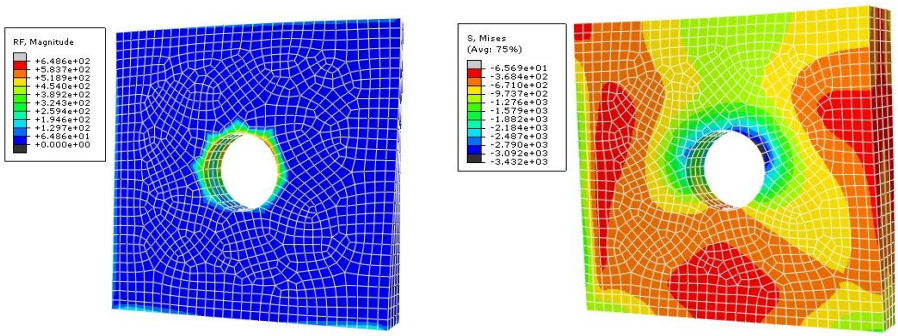

(a) Bearing plate under normal condition **(b)** Bearing plate under stressed condition

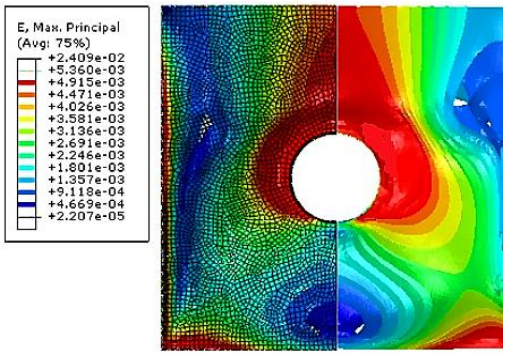

(c) Bearing plate under high-stressed conditions

Figure 5.11: Analysis of bearing plate by using 3D FEM

In this study, for numerical analysis, 150mm x 150mm x 20mm thick steel plates are considered using properties mentioned in Chapter 3, particularly in section 3.5.3. The main purpose of the analysis is to observe the behaviour of the bearing plate under surcharged loading. As depicted in Figure 5.10, the bearing plate is attached to the soil nail, where $P_{(x)}$ is the nail's force. Under the surcharge loading when soil nails undergo in tension, the bearing plates also experience tensile forces or high stresses due to pressure acting on it, as illustrated in Figure 5.11. Under typical loading circumstances, stress within the bearing plate remains controlled, as evidenced in Figure 5.11 (a) at 8.53 kN/m^2 pressure. However, in active loads, stresses act at the interface, subjecting the facing plate to tension, and stress propagation occurs across the entire bearing plate at 28.48 kN/m² pressure as exemplified in Figure 5.11 (b). When the pressure exceeds i.e. 42.44 kN/m², it also crosses the yielding as shown in Figure 5.11 (c). The results of the 3D-FEM analysis (Abaqus) for bearing plates at various stressed conditions are presented in Figure 5.11.

5.6 Overall slope stability performance of soil nailed slope

The slope is considered as globally stable, if the safety factor (FOS) determined along any potential sliding surface running from the top of the slope to its toe, is always greater than 1.0. The slope stability analysis (see Figure 5.12) has been carried out to find out the FOS considering the soil nail profile shown in Figure 4.1. The FOS has been calculated using Geo5 software, considering various numerical methods i.e. Bishops Method, Fellenius / Petterson method, Spencer method, Janbu method and Morgenstern-Price method. The FOS satisfies the requirements of the FHWA manual. The results are shown in Figure 5.12 and tabulated in Table 5.4.

Table 5.4: Slope stability verification under surcharge loading by different methods

S.N.	Methods of Slope Stabilisation	FOS with soil nails	Overall Stability
1	Bishops Method	1.98 > 1.5	Safe
2	Fellenius / Petterson method	1.72 > 1.5	Safe
3	Spencer method	1.95 > 1.5	Safe
4	Janbu method	1.97 > 1.5	Safe
5	Morgenstern-Price method	1.97 > 1.5	Safe

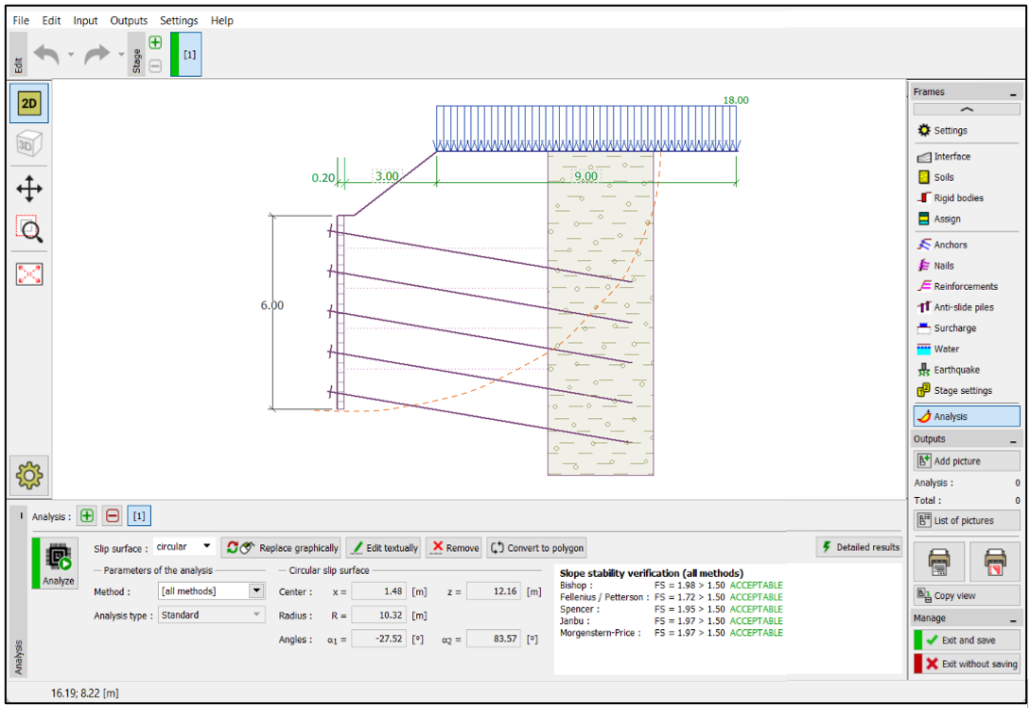

Figure 5.12: Output analysis of soil nailed slope by Geo5 software

5.7 Experimental investigation soil nailed wall

The experimental study was conducted to examine failure patterns at the wall facing and evaluate the effects of various components under surcharge loading. The properties of the soil, nails, bearing plate, cement grout, and wall facing used in this investigation are detailed in Chapter 3, specifically in Section 3.4. Using these properties, the model was prepared for laboratory testing following the detailed procedure outlined in Section 3.7.2, *Experimental Setup – II: For Grouted Nails*. The arrangement of grouted nails and the bearing plate at the wall facing is depicted in Figure 5.13. The prepared physical soil slope model was then mounted on a computerized Universal Testing Machine (UTM), as shown in Figure 5.14, enabling a comprehensive and precise experimental analysis. During the experimental investigation, it was observed that the use of soil nails significantly influences the stability of the wall under surcharge loading conditions (i.e. 18 kN/m^2). Without soil nails (Case-I), the wall exhibited substantial deflection (60 mm) and settlement (55.62 mm), indicating an unsafe condition with a FOS of 0.93. Introducing nails with bearing plates but without grout (Case-II) reduced deflection to 42 mm and settlement to 45.67 mm, resulting in a marginally safer FOS of 1.08. However, the most effective solution was observed in Case III, where grouted nails with bearing plates minimized deflection to 29.00 mm and settlement to 39.46 mm, achieving a significantly improved FOS of 1.36. The failure in the wall was observed at 65.7 kN/m^2 using grouted soil nails and 52.69 kN/m^2 without grouted nails. This demonstrates that grouted nails provide enhanced stability, reducing both deflection and settlement compared to configurations without grout, thereby ensuring safer structural performance under surcharge load. However, the variation of maximum settlement with change in moisture content is observed as: maximum settlement 42 mm at 15% moisture content, maximum settlement 46 mm at 16% moisture content, maximum settlement 48 mm at 17% moisture content, maximum settlement 52 mm at 18% moisture content, maximum settlement 56 mm at 19% moisture content and maximum settlement 58 mm at 20% moisture content (refer to Table 5.5). This observation clearly indicates that as the moisture content (MC) increases, the stability of the slope decreases. At the lowest moisture content, the given soil sample (i.e., poorly graded sand) demonstrates

maximum strength and stability, ensuring optimal slope performance at 15^0 nail inclination.

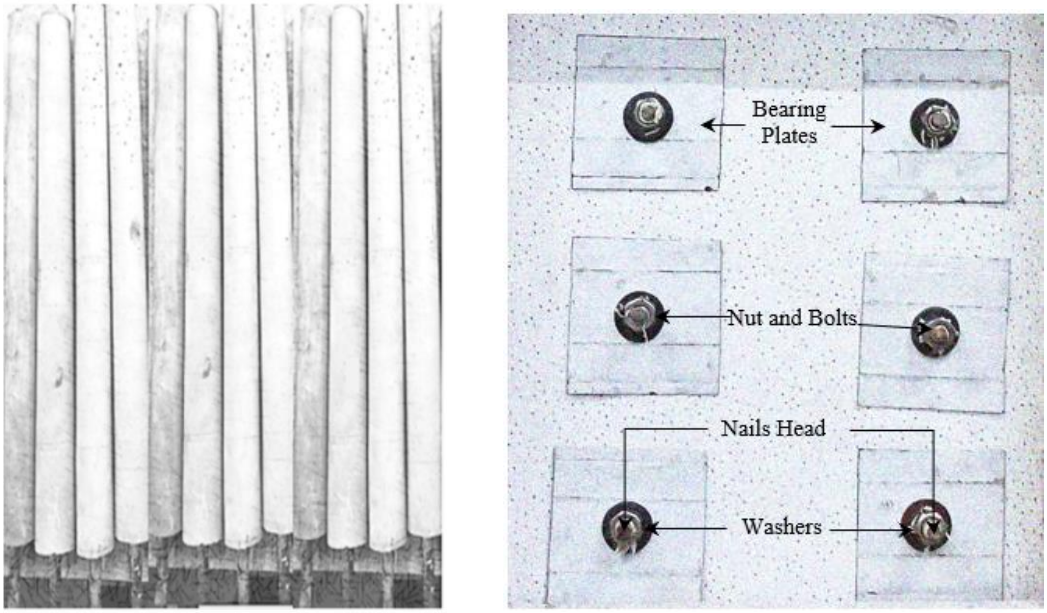

(a) Grouted Nails **(b)** Nailed wall-facing arrangement

Figure 5.13: Grouted nails and nailed wall (facing) used in the experimental study

Table 5.5: Variation of maximum settlement with different moisture content

Sr. No.	Moisture Content (%)	Maximum Settlement (mm)
1	15	42
2	16	46
3	17	48
4	18	52
5	19	56
6	20	58

Overall, from the above experimental investigation considering 15% moisture content, it was observed that the percentage of deflection and settlement varied significantly across the stabilization cases. For deflection, Case-I (Without Nails) exhibited the highest value at 45.8%, followed by Case-II (Nails without Grout) at 32.1%, and Case-III (Grouted Nails) at 22.1%, indicating a noticeable reduction with the use of grouted nails. Similarly, for settlement, Case-I accounted for 39.5% of the settlement, Case-II showed 32.4%, and Case-III recorded the lowest percentage at 28.0%. These findings demonstrate that grouted nails in Case-III were the most effective in minimizing

deflection and settlement, thereby enhancing the structural stability of the slope under surcharge loading conditions (refer to Figure 5.15).

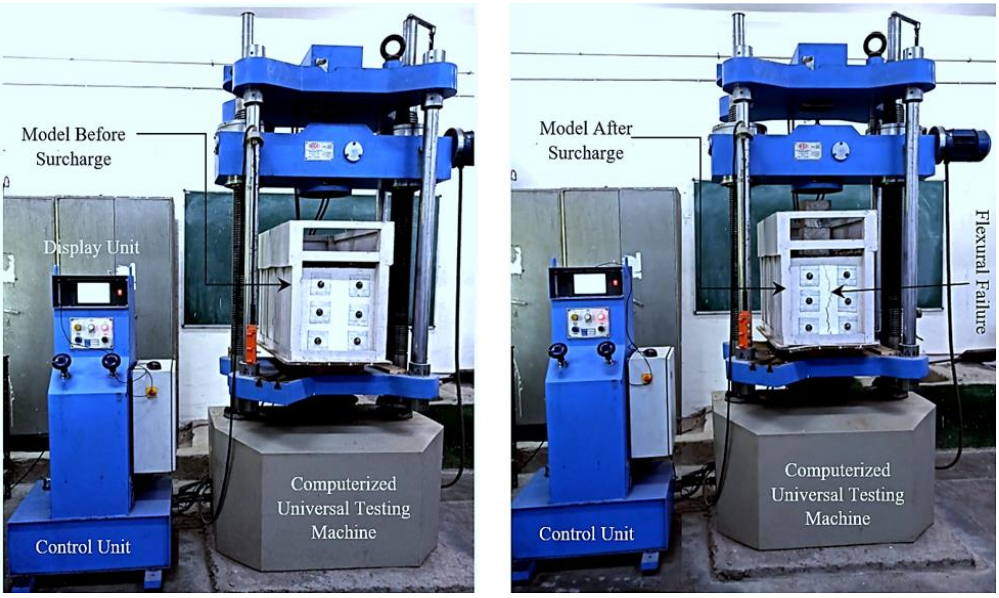

(a) **(b)**

Figure 5.14: Experimental setup mounted on universal testing machine (UTM): (a) Model before surcharge loading (b) Model after surcharge loading (Flexural Failure)

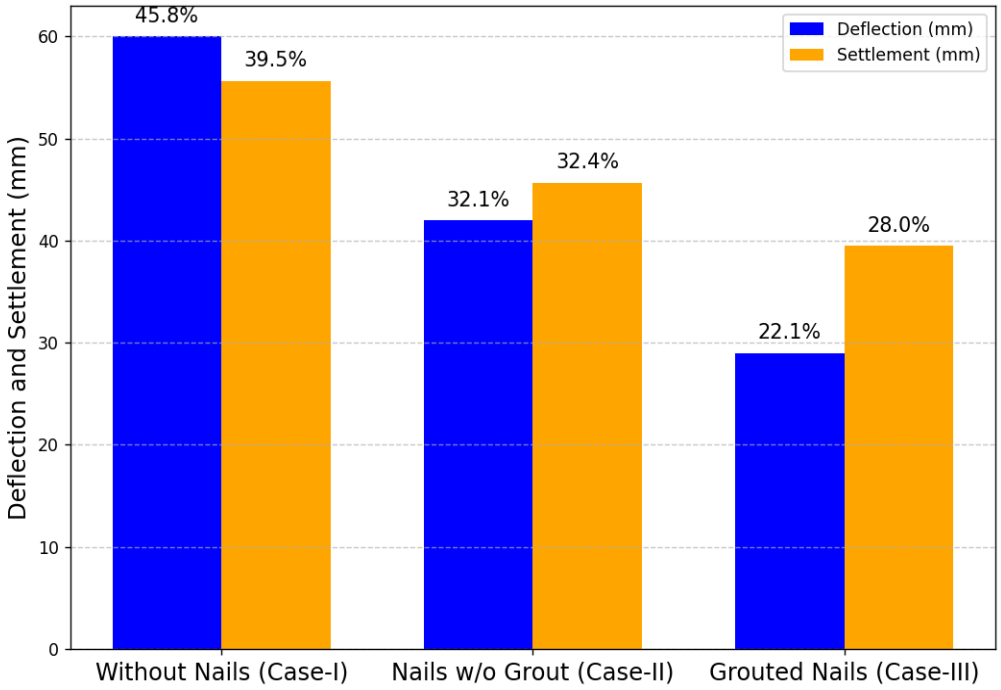

Figure 5.15: Comparison of deflection and settlement with percentages across different stabilization Cases

5.8 Comparative Study Between Various Methods Used in this Chapter

In this section, a comparative study is conducted considering various methods involved in this chapter. The role of reinforcement was examined, revealing that the maximum FOS of 1.4 is achieved at a reinforcement ratio of 0.16% (refer to Figure 5.9), underscoring the critical influence of reinforcement in enhancing structural stability under surcharge loading. From the experimental investigation, it was observed that the deflection and settlement behaviours varied significantly across stabilization cases. Case-I, without nails, exhibited the highest deflection (60 mm) and settlement (55.62 mm), contributing 45.8% and 39.5%, with a FOS of 0.93, indicating an unsafe condition. Case-II, with nails but without grout, reduced deflection to 42 mm (32.1%) and settlement to 45.67 mm (32.4%), achieving a marginally safer FOS of 1.09. The most effective solution was Case-III, utilizing grouted nails, which minimized deflection to 29 mm (22.1%) and settlement to 39.46 mm (28.0%), achieving the highest FOS of 1.36, demonstrating enhanced stability (Figure 5.16).

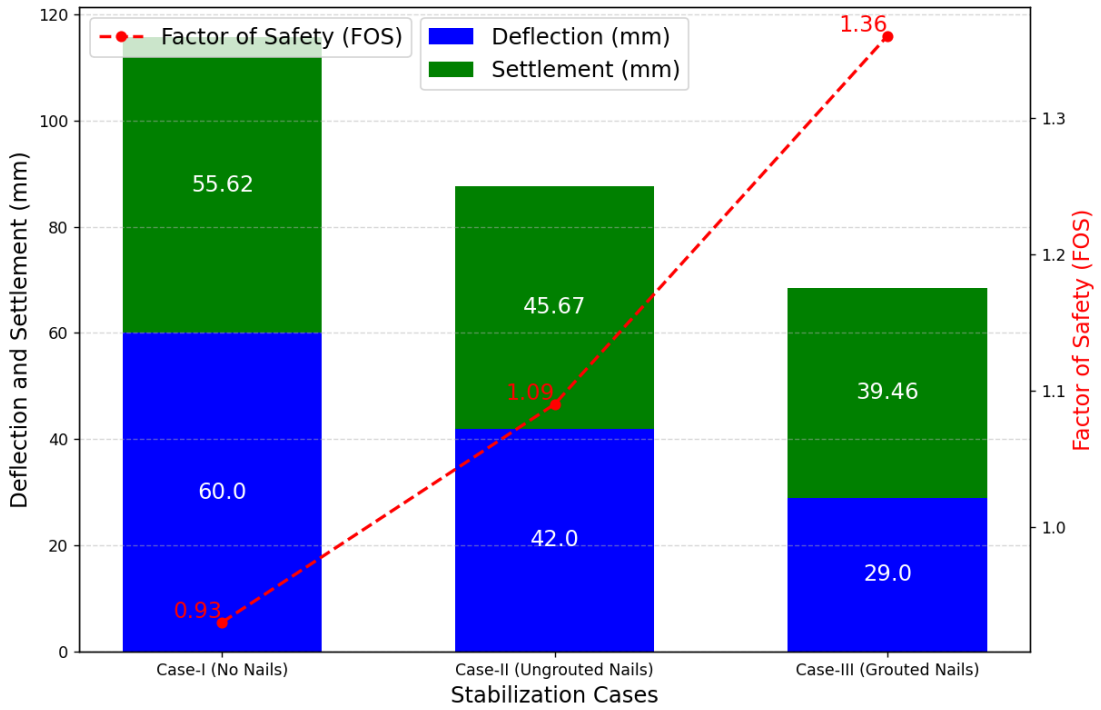

Figure 5.16: Stacked Comparison of deflection, settlement, and FOS across stabilization cases.

Moreover, a comparison of slope stability methods was conducted using Limit State Methods. Bishop's Method yielded the highest FOS at 1.98, followed by the Spencer Method at 1.95, the Janbu Method at 1.97, and the Morgenstern-Price Method also at 1.97, indicating their robust predictive capabilities in determining stability conditions. Conversely, the Fellenius / Petterson Method provided a slightly lower FOS of 1.72, reflecting its conservative approach. Experimental validation further reinforced these findings, confirming the reliability of grouted soil nails in ensuring stability. Collectively, these findings highlight the importance of integrating reinforcement considerations, experimental validation, and diverse analytical methods to optimize design decisions and ensure the robust performance of soil-nailed structures in geotechnical engineering applications.

Chapter 6

RESULTS AND DISCUSSION

6.1 Introduction

This chapter provides key findings from experimental investigations, numerical modelling, and analytical approaches, emphasizing their collective role in understanding and improving soil slope stability. This study examines the performance of soil nailing reinforced under surcharge loading conditions. The study highlights the important parameters influencing slope behaviour, including nail inclination, grouting, and reinforcement ratios, while assessing their impact on deflection, settlement, and the Factor of Safety (FOS) etc.

6.2 Effect of Soil Nail Inclination on Slope Stability and Load Distribution Under Surcharge Loading

The analysis under a surcharge load of 18 kN/m² (see Figure 4.1) examined the effects of varying soil nail inclinations on the stability and force distribution within the soil slope. The pressure on the soil nail wall and forces acting on the nails showed a progressive increase from the uppermost nail (Nail 1) to the lowermost nail (Nail 5), as depicted in Figure 4.3. Nail forces recorded at different inclinations (0°, 5°, 10°, 15°, 20°, and 25°) are presented in Figure 4.4, revealing minimal variation across inclinations. This indicates that nail inclination had a relatively slight impact on force transmission, suggesting that the soil-nailing system displayed symmetrical load-sharing characteristics. This uniform force distribution can be attributed to factors such as nail diameter, length, structure geometry, material properties etc. At a nail inclination of 15°, the soil on the slip surface resisted a maximum force of 402.27 kN/m, while the deformed nails provided additional resistance with a maximum force of 198.65 kN/m. Figures 4.6 and 4.7 illustrate the relationship between nail inclinations and the forces resisted by both the soil and reinforcing nails. These findings highlight

the crucial role of the combined resistance offered by soil and nails, emphasizing the importance of nail orientation in redistributing forces and enhancing slope stability. The analysis, performed using Geo5 software (see Figure 4.2), evaluated the Factor of Safety (FOS) for the soil slope model shown in Figure 4.1. Material properties specified in Chapter 3 (Sections 3.3.1–3.3.5) were utilized to assess the impact of varying nail inclinations on the FOS under a surcharge load of 18 kN/m². Without nails, the FOS was 0.96 using Bishop's Method. The inclusion of soil nails led to a consistent increase in the FOS as nail inclinations varied from 0° to 15°, achieving a maximum FOS of 1.630 at 15°. However, beyond 15°, a decline in the FOS was observed, dropping to 1.573 at 25°, as illustrated in Figure 4.8. This trend indicates that steeper nail inclinations diminish the reinforcing effectiveness, adversely affecting slope stability. The relationship between nail inclination and the FOS underscores the importance of optimizing nail orientation to enhance stability. The study confirms that a nail inclination of 15° provides the most effective reinforcement, balancing soil and nail resistance to maximize the FOS and maintain overall slope stability.

6.3 Optimization of Nail Inclinations Using a Global Stiffness Matrix Approach

The global stiffness matrix was employed to determine the nodal displacements of the nails at u_2 and u_3 under varying inclinations, with the nail force (P) acting on the nails (refer to Figures 4.10 and 4.11). Using Equation (4.5), the displacements were calculated for each nail inclination, and the results are summarized in Table 4.2. The observed displacements demonstrate how nail inclinations influence the stability of the soil slope. At node u_2, the standard deviation of displacements across nail inclinations (0°, 5°, 10°, 15°, 20°, and 25°) was found to be 0.079 m, 0.077 m, 0.077 m, 0.075 m, 0.076 m, and 0.076 m, respectively. At node u_3, the displacements varied more significantly, with standard deviation values of 0.288 m, 0.267 m, 0.237 m, 0.226 m, 0.225 m, and 0.265 m for the same inclinations, as shown in Figure 4.11. The results indicate that a nail inclination of 15° minimizes displacements, with an average displacement of 0.1252 m and a standard deviation of 0.075 m at u_2 Similarly, at u_3, the average displacement was observed to be 0.3782 m with a standard deviation of 0.226 m. These findings suggest that a nail inclination of 15° is optimal for reducing

displacements and enhancing slope stability. Beyond 15°, the displacements and standard deviations at both u_2 and u_3 increased, indicating a decline in the stabilizing effect of the nails. The observed trends underscore the importance of optimizing nail inclinations to achieve minimal displacements and improved slope stability. The results confirm that the 15° nail inclination offers the best performance in terms of reducing displacement and maintaining structural integrity (refer to Figure 4.11).

6.4 Comparison of Unreinforced and Reinforced Soil Slopes Using 2D FEM

The settlement behaviour of embankments under a surcharge loading of 18 kN/m² was analyzed for both unreinforced and reinforced soil slopes using 2D FEM by Geo5 (2018) software. The unreinforced soil slope exhibited settlement rates ranging from <-59.7 mm to >998.6 mm, as shown in Figure 4.12a. These high displacement values, particularly near the embankment face, highlight the vulnerability of unreinforced slopes under surcharge loading. In contrast, the reinforced soil slope, simulated with nails inclined at 15° (based on the previous analyses in sections 4.2 and 4.3, which identified this inclination as optimal), demonstrated significantly reduced settlement rates ranging from <-95.2 mm to >259.3 mm (Figure 4.12b). The presence of nails contributed to a considerable reduction in settlement near the embankment face, showcasing their stabilizing effect by improving the load-bearing capacity and redistributing stresses within the soil mass. The comparison between the unreinforced (Figure 4.12a) and reinforced (Figure 4.12b) slopes underscores the effectiveness of soil nails in mitigating settlement and enhancing slope stability under surcharge loading.

6.5 Experimental Investigation for Identification of Optimal Nail Inclination

In the experimental study, five trials were conducted for each nail inclination to assess the displacement of the soil-nailed wall under a surcharge load of 18 kN/m². The results indicated that the minimum displacement occurred at a nail inclination of 15° with the horizontal plane. Wall displacement measurements were taken in both horizontal and vertical directions, as illustrated in Figures 4.15 and 4.16. The maximum wall deflections ($\delta\Delta$) for nail inclinations of 0°, 5°, 10°, 15°, 20°, and 25°

were observed as 28 mm, 25 mm, 21 mm, 16 mm, 18 mm, and 20 mm, respectively (average values). In comparison, the maximum wall deflection for the unreinforced wall (without soil nails) was recorded as 32 mm (average) at the top of the wall. At a nail inclination of 15°, the use of soil nails reduced settlement by 61.90%, demonstrating the effectiveness of reinforcement in stabilizing the slope.

These findings highlight that soil nailing at an optimal inclination of 15° provides significant global stability to the structure, making it a highly effective slope stabilization technique. The observed reduction in wall displacement confirms the critical role of soil nails in improving structural integrity and mitigating settlement under surcharge loading conditions.

6.6 Comparative Analysis of Grouted and Non-Grouted Nails: Influence of Diameter and Pullout Resistance in Slope Stabilization

In this investigation, the effects of grouted and non-grouted nails of varying diameters (10 to 30 mm) at a 15° inclination with the horizontal plane were analyzed. The analysis aimed to compare the performance of grouted nails and non-grouted nails under surcharge loading conditions, as detailed in Chapter 3 (Section 3.4.4), which includes the basic properties of grouted cement.

The results revealed that grouted nails demonstrated significantly higher pullout strength compared to non-grouted nails, with the pullout capacity of grouted nails increasing with nail diameter. However, the effective parameters influencing the performance of grouted nails remained well-adjusted even with varying diameters, as shown in Figure 5.4(a). The pullout resistance (P_o) contribution of grouted nails averaged 58.6%, which was significantly higher than the 18.35% contribution observed for non-grouted nails. Additionally, the contribution of the effective parameters against pullout resistance (P_o') for grouted nails was up to 87% (average), whereas non-grouted nails contributed only 27.54% (average), highlighting the enhanced effectiveness of grouted nails in resisting pullout forces.

Remarkably, the analysis showed minimal variation in the effective parameters when grouted nails of different diameters were used (Figure 5.4a). This suggests that grouted nails exhibit a more consistent performance regardless of their diameter. On

the other hand, non-grouted nails showed notable variations in the effective parameters, especially in terms of pullout resistance and elastic modulus, as depicted in Figure 5.4 (b).

The stiffness of grouted nails was also higher than that of non-grouted nails, leading to reduced displacement under surcharge loading (i.e. 18 kN/m^2). As shown in Figure 5.5, grouted nails demonstrate significantly less displacement compared to non-grouted nails. For example, with a 10 mm nail diameter, the displacement was 0.1478 m for non-grouted nails and only 0.0186 m for grouted nails. Similarly, for a 30 mm diameter nail, the displacement was 0.0493 m for non-grouted nails and just 0.0081 m for grouted nails. This highlights the superior capacity of grouted nails to resist deformation and enhance slope stability. Additionally, as the nail diameter increases, the effect of the elastic modulus in grouted nails rallies marginally, contributing to better performance in slope stabilization.

Figure 5.6 provides a direct comparison between grouted and non-grouted nails, highlighting the distinct differences in their performance across key factors. Grouted nails exhibited significantly higher contributions to pullout capacity and effective parameters against pullout resistance, reinforcing their superiority in slope stabilization.

From these findings, it can be concluded that grouted nails provide significantly higher anchoring strength and resistance capabilities compared to non-grouted nails. The enhanced performance of grouted nails, particularly in terms of pullout resistance and stiffness, makes them more effective for stabilizing slopes and preventing failure under surcharge loading conditions. The analysis also suggests that increasing the nail diameter further enhances the performance of grouted nails, although the effects of diameter variations are less pronounced than the differences between grouted and non-grouted nails.

In short, grouted nails offer a more reliable and effective solution for slope stabilization, with increased pullout resistance, reduced displacement, and improved overall stability compared to non-grouted nails. These results underscore the importance of selecting grouted nails in applications where higher strength and stability are required, especially in situations involving surcharge loading.

6.7 Assessing the Effectiveness of Reinforcement Ratios in Soil-Nailed Walls for Slope Stabilization

In this investigation, the role of reinforced steel mesh in reinforced concrete (R.C.C.) walls, particularly in soil-nailed walls, was explored to assess its impact on slope stabilization and structural integrity. The analysis was conducted using Geo 5 (2018) Fine software, which enabled the simulation of various mesh sizes and obtained reinforcement ratios. The results of the numerical analysis, including the mesh size outcomes and verifications, are summarized in Table 5.3. The investigation revealed that the reinforcement ratio plays an important role in the stability of soil-nailed walls. For the soil slope analyzed, it was observed that reinforcement ratios below 0.14% led to instability or insufficient safety. This is because the reinforcement was insufficient to resist the applied loads effectively, causing the slope to fail or become unstable under stress.

On the other hand, reinforcement ratios within the range of 0.14% to 0.19% were found to provide stability and safety to the slope. The soil-nailed walls with reinforcement ratios within this range were able to resist the applied loads effectively, ensuring the stability of the slope. These findings suggest that maintaining an optimal reinforcement ratio is crucial for the structural integrity of soil-nailed walls.

However, when the reinforcement ratio exceeded 0.19%, the slope became unstable. In this case, excessive reinforcement led to unpredictable behaviour, which resulted in potential structural instability. This highlights the importance of balancing the reinforcement ratio to avoid both under-reinforcement and over-reinforcement, which could compromise the safety of the slope.

As shown in Figure 5.9, the optimal range for reinforcement ratios is between 0.14% and 0.19%. Keeping the reinforcement ratio within this range is essential for maintaining the safety and stability of soil-nailed slopes. Excessive reinforcement beyond 0.19% or insufficient reinforcement below 0.14% both resulted in failure to adequately stabilize the slope, demonstrating the delicate balance required in the design of soil-nailed walls.

In conclusion, the findings from this study underscore the importance of carefully managing the reinforcement ratio in soil-nailed walls. Properly selected reinforcement

within the optimal range ensures the structural integrity of the wall and the stability of the slope. These results provide valuable insights for designing more efficient and reliable soil-nailed systems for slope stabilization.

6.8 Impact of Grouted Soil Nails on Slope Performance and Stability under Varying Moisture Conditions

6.8.1 Impact of Grouted Soil Nails on Slope Performance

In this experimental study, the impact of grouted soil nails on the stability of slopes under surcharge loading conditions was investigated using Ordinary Portland Cement (OPC-43 grade) and Pozzolana Portland Cement (PPC), refer to Section 5.7. The split tensile strength test results showed a peak load of 185.3 kN for OPC nails (4.21 MPa) and a slightly lower peak load of 181.7 kN for PPC nails (4.13 MPa). Despite this marginal difference, the eco-friendly and cost-effective nature of PPC led to its selection for further investigation.

The soil nails were oriented at a 15° inclination for the model setup and subjected to experimental analysis using a computerized Universal Testing Machine (UTM). Three different configurations were analyzed: Case-I (without soil nails), Case-II (nails with bearing plates but no grout), and Case-III (grouted nails with bearing plates).

(1) Case-I: Without Soil Nails

In the absence of soil nails (Case-I), the wall experienced significant deflection and settlement. The deflection was observed to be 60 mm, with a settlement of 55.62 mm. This configuration resulted in a FOS of 0.93, indicating an unstable slope and highlighting the need for stabilization.

(2) Case-II: Nails with Bearing Plates, No Grout

In Case-II, the introduction of nails with bearing plates but without grout led to a reduction in deflection and settlement. The deflection decreased to 42 mm, and the settlement reduced to 45.67 mm, resulting in an improved FOS of 1.08. Although this

configuration provided a slight increase in stability, it was still insufficient for long-term safety.

(3) Case-III: Grouted Nails with Bearing Plates

The most effective configuration was observed in Case-III, where grouted nails with bearing plates were employed. The deflection was reduced to 29.00 mm, and the settlement decreased to 39.46 mm. The FOS significantly improved to 1.36, and the failure load (i.e. for wall flexure failure refer to Figure 5.17) increased to 65.7 kN with grouted nails compared to 52.69 kN with non-grouted nails. These results demonstrate that grouted nails provide superior stabilization by significantly reducing both deflection and settlement, ensuring a safer slope under surcharge loading.

6.8.2 Moisture Content Influence

Further analysis of the impact of moisture content (MC) on the slope's performance revealed a clear trend: as the MC increased, the slope's stability decreased. At 15% MC, the maximum settlement was 42 mm, which gradually increased with higher moisture content. At 20% MC, the maximum settlement reached 58 mm, highlighting the adverse effect of increased moisture on the slope's stability. This indicates that lower moisture content contributes to higher strength and stability, while higher moisture content exacerbates settlement, leading to reduced stability.

The results of the study underline the crucial role that grouted soil nails play in stabilizing slopes under surcharge loading conditions. The use of PPC for grouting proved to be a cost-effective and sustainable solution, offering stability similar to that of OPC while providing eco-friendly benefits.

Overall, the grouted soil nails, especially those made with PPC, exhibited significantly better performance than non-grouted nails, enhancing the stability and safety of the slope. The findings suggest that careful management of moisture content and reinforcement is essential for ensuring long-term slope stability, particularly under surcharge loading conditions. The results confirm that grouted nails provide a more effective and reliable solution for soil slope stabilization compared to configurations

without grout, making them an essential component in geotechnical engineering applications for slope safety.

6.9 Summary

Overall this research highlights the effectiveness of soil reinforcement techniques in improving slope stability. Across experimental investigations, numerical analyses, and analytical methods, consistent findings demonstrated significant reductions in settlement, deflection, and failure risks under surcharge loading. Grouted soil nails, particularly at optimal inclinations, emerged as the most effective solution, achieving enhanced stability and higher Factors of Safety (FOS). Comparative analysis of stabilization methods further validated the reliability of reinforcement techniques in mitigating slope failures. These findings emphasize the importance of integrating experimental, numerical, and analytical approaches to develop safer and more efficient geotechnical designs.

Chapter 7

CONCLUSIONS, FUTURE SCOPE AND SOCIAL IMPACT

7.1 Introduction

In geotechnical engineering, slope stability is crucial for infrastructure integrity, environmental preservation, and public safety. Various techniques address slope stability, with soil nailing standing out for its effectiveness and versatility. This thesis explores soil nailing for slope stabilization using experimental, numerical, and analytical methods. Research confirms that soil nails enhance slope stability and its performance, by experimental investigations, numerical analyses, and analytical methods. The findings highlight soil nailing as a reliable, cost-effective, and environmentally friendly technique, reducing settlement, displacement, and failure risk while ensuring infrastructure integrity and public safety.

7.2 Conclusions

Several key conclusions are drawn based on the comprehensive analysis of various aspects explored in this research. The findings highlight the effectiveness of soil nailing techniques in mitigating slope instability and enhancing overall stability. Through experimental investigations, numerical simulations, and analytical studies, significant insights have been gained into the behaviour of soil-nailed slopes under surcharge loading conditions. The investigation reveals the following important conclusions:

(1) The literature reviewed provides a comprehensive understanding of soil nailing, encompassing historical developments, fundamental principles, design methodologies, case studies, and sustainability considerations. Continued research and innovation in this field are essential for addressing emerging challenges, improving design practices, and promoting the sustainable

implementation of soil-nailing technology in geotechnical engineering projects.

(2) The preliminary design emphasizes the critical role of face inclination (α) and back slope (β) in soil nail design, highlighting the importance of slope geometry in stabilization. Higher friction angles (ϕ) improve load transfer efficiency, reducing the need for larger nail diameters, while variations in nail diameter (D) across different slope conditions underscore the need for tailored stabilization strategies based on soil properties and geometry. Drill hole diameter (D_{DH}) significantly influences nail dimensions, as larger D_{DH} may require larger nails and affect length, and spacing. Additionally, the maximum allowable tensile force ($T_{max\text{-}s}$) is essential for ensuring slope stability against external forces, as changes in D_{DH} can impact the required tensile force. (conclusion drawn from section 2.19.3 and *Annexure B*).

(3) The Limit State Design (LSD) method reveals a consistent increase in FOS up to a 15^0 nail inclination, followed by a sudden decline thereafter, with the peak FOS observed at 15^0 (1.630) for the soil sample (SP) used in this study (Section 4.2.3)

(4) Numerical analysis using 2D-FEM demonstrates a substantial 62.71% reduction in settlement with poorly graded sand (SP) when employing a 15^0 nail inclination, showcasing its effectiveness in stabilizing slopes (Section 4.4).

(5) Experimental results corroborate the numerical findings, showing a significant 58.33% reduction in wall displacement and a noticeable 61.61.72% decrease in embankment settlement with a 15^0 inclination, particularly in poorly graded sand conditions (Section 4.5)

(6) In this study, soil nailing at a 15° inclination proved highly effective, reducing slope failure by 58.90% in the analytical model, 62.71% in the FEM analysis, and 61.90% in the experimental model. This technique demonstrated excellent performance in stabilizing slopes and improving the global Factor of Safety (FOS), especially in poorly graded sand conditions for the South Delhi region (Section 4.6)

(7) The contribution of modulus of elasticity is decreased for grout nails compared to non-grouted nails (Table 5.2 and Figure 5.4)

(8) The increase in nail diameter led to higher pullout capacity and resistance (Figure 5.4).

(9) Grouted nails exhibited significantly less displacement than non-grouted nails, with displacement decreasing as nail diameter increased (Figure 5.5)

(10) The pullout capacity significantly increased from 18.35% (average) for nails non-grouted to 58.60% (average) for grouted nails (Section 5.3, Figure 5.6)

(11) The pullout resistance also showed a substantial increase from 22.83% (average) for nails non-grouted to 31% (average) for grouted nails (Section 5.3, Figure 5.6)

(12) Optimal reinforcement ratios between 0.14% and 0.19% ensured stability and safety, while ratios below 0.14% and above 0.19% led to instability due to insufficient reinforcement and excessive reinforcement (Figure 5.9).

(13) Portland Pozzolana Cement (PPC) was found to be more eco-friendly and effective for grouting compared with Ordinary Portland Cement (OPC). (Section 3.7.2).

(14) The comparison of slope stability methods showed that Bishop's, Janbu, Spencer, and Morgenstern-Price Methods had high FOS, with Bishop's giving the highest FOS of 1.98. In contrast, the Fellenius/Petterson Method provided a cautious FOS of 1.72 (Table 5.4).

(15) The experimental investigation revealed significant variations in deflection and settlement across different stabilization cases. Case-I (Without Nails) showed the highest deflection at 45.8%, followed by Case-II (Nails without Grout) at 32.1%, and Case-III (Grouted Nails) at 22.1%, highlighting the effectiveness of grouted nails in reducing deflection. Similarly, settlement values were highest in Case-I at 39.5%, decreased to 32.4% in Case-II, and reached the lowest in Case-III at 28.0%. These results confirm that grouted nails in Case-III provide the most effective solution for minimizing deflection and settlement, thereby significantly improving the structural stability of slopes under surcharge loading conditions (Figure 5.15)

(16) Comparing with without soil nails (Case I), significant deflection (60 mm) and settlement (55.62 mm) were observed, indicating an unsafe condition with an FOS of 0.93. Introducing nails with bearing plates but without grout (Case II)

reduced deflection to 42 mm and settlement to 45.67 mm, resulting in a marginally safer FOS of 1.08. However, the most effective solution was seen in Case III, where grouted nails with bearing plates minimized deflection to 29 mm and settlement to 39.46 mm, achieving a significantly improved FOS of 1.36. This highlights that grouted nails provide superior stability, markedly reducing deflection and settlement compared to configurations without grout, thereby ensuring enhanced structural performance under surcharge load (Figure 5.16).

Based on the concluding remarks, the use of soil nails at a 15^{o} inclination, combined with the soil slope and properties discussed in this research, significantly delays slope failure and enhances overall structural integrity.

7.3 Recommendations For Future Work

As the study of slope stabilization and soil nailing techniques continues to evolve, several avenues for future research and development emerge, aimed at enhancing effectiveness, sustainability, and resilience in slope engineering practices. Drawing upon the insights gleaned from this research effort, the following areas permit further exploration and innovation:

1. Investigate innovative materials and techniques for soil nailing, including alternative reinforcements and advanced fabrication methods.
2. Develop integrated risk assessment frameworks using geological, hydrological, and climatological data to predict and mitigate slope-related hazards.
3. Address the impact of climate change on slope stability by developing adaptive strategies and resilient infrastructure designs.
4. Explore green infrastructure solutions such as vegetative stabilization and bioengineering to complement soil nailing techniques.
5. Establish long-term monitoring programs to assess the performance of soil-nailed slopes and implement proactive maintenance strategies.
6. Advocate for robust policy and regulatory frameworks to promote the adoption of soil-nailing techniques.

7. Foster international collaboration and knowledge exchange to share best practices and technological innovations in slope stabilization.

By embracing these future endeavours and leveraging interdisciplinary collaboration, technological innovation, and community engagement, the field of slope stabilization and soil nailing techniques can continue to advance, providing sustainable solutions to mitigate slope hazards, protect infrastructure and communities, and promote resilience in the face of evolving environmental challenges.

7.4 Social Impact

Soil nailing enhances slope stability and safeguards both natural and manmade slopes. This practice helps preserve the environment and protects nearby structures. The study highlights the social impacts, underlining its role in improving community safety and resilience.

1. By reinforcing slopes and reducing the risk of landslides, soil nailing ensures the safety and security of communities living in hilly regions.
2. Soil nailing safeguards critical infrastructure such as roads, highways, railways, and tunnels, ensuring uninterrupted connectivity and safer transportation for residents.
3. By mitigating accidents and fatalities associated with slope instability, soil nailing directly contributes to saving lives and preventing injuries, enhancing the overall well-being of communities.
4. Reducing costs related to infrastructure damage and emergency repairs, soil nailing provides significant economic benefits, helping to preserve public funds for other community needs.
5. By increasing the lifespan and stability of manmade structures like highway and railway embankments, soil nailing ensures long-term reliability and reduces the frequency of costly maintenance.
6. Implementing soil nailing techniques can save considerable construction time, leading to economic benefits for the country by accelerating project completion and reducing labour costs.

7. Soil nailing is suitable for rapid construction, making it a preferred method in urgent projects where quick stabilization is required to ensure public safety and infrastructure integrity.
8. This technique is effective in earthquake-prone areas, mitigating hazards and protecting lives by making structures more resistant to shocks and vibrations, thus enhancing community resilience to seismic events.
9. By supporting sustainable land use practices and protecting natural and cultural heritage sites, soil nailing contributes to the well-being and prosperity of communities, ensuring that these valuable assets are preserved for future generations.

The study on soil slope stabilization using soil nailing enhances community safety and infrastructure stability in hilly regions. It prevents landslides, protects vital infrastructure, saves lives, and reduces economic losses. By promoting sustainable practices, it supports community well-being and also preserves natural and cultural heritage for future generations.

REFERENCES

Ahmad, F., Tang, X., Hu, J., Ahmad, M., and Gordan, B. (2023). Improved Prediction of Slope Stability under Static and Dynamic Conditions Using Tree-Based Models. *Computer Modeling in Engineering & Sciences*, 33(1), 455–487. https://doi.org/10.32604/cmes.2023.025993

Ahmed, S. M., Lakhdar, M., Abderrachid, A., Mohammed, K., and Aymen, S. (2024). Stability analysis of soil-nailed slopes using the Spencer method. Studies in *Engineering and Exact Sciences*, 5(2), e9279. https://doi.org/10.54021/seesv5n2-346

Ahmadi, M. M., and Borghei, A. (2018). Numerical investigation into the static behavior of stepped soil nail walls. *Scientia Iranica*, 25(1). https://doi.org/10.24200/sci.2017.4532

Ann, T., Cheang, W., Hai, O. P., and Tan, D. (2004). Finite element analysis of soil nailed slope-some recent experience; Proceedings of the third Asian Regional Conference on Geosynthetics, Seoul, Korea, 183-192.

Anthoine, A. (1987). Stabilite d'une fouille renforcee par clouage. Proc., 4th Franco-Polish Conference on Applications of Soil Mechanics, Grenoble, France. pp.129-154.

Azzam, W., and Sobhey, M. A. (2019). Utilization of Soil Nailing Technique to Improve Sand Slopes under Seismic Loading. International Conference Advance Structures Geotech Engineering, Hurghada, Egypt. April 2019, 1– 10.

Azzam, W., and Basha, A. (2017). Utilization of soil nailing technique to increase shear strength of cohesive soil and reduce settlement. *Journal of Rock Mechanics and Geotechnical Engineering*, 9(6), 1104–1111. https://doi.org/10.1016/j.jrmge.2017.05.009

Basta, M. M., Rabie, M. H., Mansour, M. A., and Elbanaa, W. (2024). A comparative study between soil nailing and berms for slope stabilization: Performance and

analysis. *Engineering Research Journal*, 1–24. https://doi.org/10.21608/erj.2024.303147.1072

Berg, R. R., Lazarte A. L., Helen Robinson, and Jesús E. Gómez, Andrew Baxter, and Allen Cadden. (2015). Soil Nail Walls-Reference Manual, Geotechnical Engineering Circular No. 7, Report No. FHWA-NHI-14-007, National Highway Institute, Washington, DC; February 2015.

Bhuiyan, M. Z. I., Wang, S., and Carter, J. (2022). New test facility for studying the behaviour of pressure-grouted soil nails. *Transportation Geotechnics*, 34. https://doi.org/10.1016/j.trgeo.2022.100752

Birendra, M. (2002). Isothermal Response of Geosynthetics To Different Loading Regimes. Bangladesh University of Engineering and Technology Dhaka, Bangladesh.

Bridle R. J., and Davies M. C. R. (1997). Analysis of soil nailing using tension and shear: experimental observations and assessment. Geotechnical Engineering, Proceedings of the Institution of Civil Engineers; July 1997: 155-167.

Bureau of Indian Standards. (2007). IS: 1498 -1970, Classification and identification of soils for general engineering purposes. New Delhi.

Burland, J. B. (2023). Strength and deformation behaviour of soils (pp. 195–214). Emerald (MCB UP). https://doi.org/10.1680/icemge.66816.0195

Byrne, R. J., Chassie, R. G., Keeley, J. W., Bruce, D. A., Nicholson, P., Walkinshaw, J. L., Ludwig, C. (1993). FHWA International Scanning Tour for Geotechnology-SoiI Nailing. Washington, D.C.

Byrne, R. J., Cotton, D., Porterfield J., Wolschlag C., and Ueblacker, G. (1998) Manual for design and construction monitoring of soil nail walls. Report FHWA-SA-96-69R, Federal Highway Administration, Washington, D.C.

Calladine, C.R. (2000). Plasticity for Engineers: Theory and Applications. Horwood Publishing Limited, 318p

Lazarte, A., Victor Elias., David Espinoza., and Paul J. Sabatini. (2003). FHWA-Soil Nail Walls, Geotechnical Engineering Circular No. 7. Report FHWA0-IF-03-

017, Office of Engineering/Bridge Division Federal Highway Administration U.S. Department of Transportation Washington, D.C. Retrieved from https://rosap.ntl.bts.gov/view/dot/50250.

Charles, W.W., Ng, C., Petrus, A. C., Min Zhang., and Muhammad Shakeel. (2022) Static liquefaction mechanisms in loose sand fill slopes. *Computers and Geotechnics*; 141 (2022) 104525.

Cheang, W. L., Luo, S. Q., Tan, S. A., and Ong, K. Y. (2018). Lateral bending of soil-nails in an excavation. In ISRM International Symposium 2000.

Cheuk C. Y., Ng C. W. and Sun H. W. (2005). Numerical Experiments of Soil Nails in Loose Fill Slopes Subjected to Rainfall Infiltration Effects. *Computers and Geotechnics*; 32(4): 290-303.

Das, B. M. (2007). Advanced Soil Mechanics. 3rd edition. Taylor & Francis. Milton Park.

Davies, M. C. R., and Le Masurier J. W. (1997). Soil/Nail Interaction Mechanism from Large Direct Shear Tests. Proceedings of the Third International Conference on Ground Improvement Geo-Systems, London: 493-499.

Derghoum, R., and Meksaouine, M. (2021). Numerical study for optimal design of soil nailed embankment slopes. *International Journal of Geo-Engineering*, 12(1). https://doi.org/10.1186/s40703-021-00144-5.

Duncan, J.M., and Wright, S.G. (2005). Soil Strength and Slope Stabilty. John Wiley & Sons, Inc., pp. 199.

Dywidag. (2022). DYWIDAG Soil Nails Geotechnical Product Range. https://dywidag.com/downloads/geotechnical-product-range-excl-us/es

Elahi, T.E., Islam, M.A., and Islam M. S. (2022). Parametric Assessment of Soil Nailing on the Stability of Slopes Using Numerical Approach. *Geotechnics*, (2):615–663 https://doi.org/10.3390/geotechnics2030030

Ersoy, H., Kaya, A., Angın, Z., and DaĞ, S. (2020). 2D and 3D numerical simulations of a reinforced landslide: A case study in NE Turkey. *Journal of Earth System Science*, 129(1). https://doi.org/10.1007/s12040-020-1343-y

Fan, Chia-Cheng, and Luo, Jiun-Hung. (2007). Numerical Study on the Optimum Layout of Soil nailed Slopes. *Computers and Geotechnics* 35(4): 585-599.

Federal Highway Administration (FHWA). (2015). Soil Nail Walls Reference Manual (AASHTO LRFD Bridge Design Specifications, 7 th Edition). Washington, DC.

FHWA (1993a) International Scanning Tour for Geo-technology, Soil Nailing Summary Report, Report No. FHWA-PL-93-020, Washington, DC; September-October 1992.

FHWA (1993b) French National Research Project Clouterre, 1991-Recommandations Clouterre 1991, (English Translation) Soil Nailing Recommendations, Report No. FHWA-SA-93-026, Washington, D. C.

FHWA (1994) Soil Nailing Field Inspectors Manual-Soil Nail Walls. Federal Highway Publication No. FHWA-SA-93-068, U.S. Department of Transportation, Federal Highway Administration, Washington, D. C.

FHWA (1998) Manual for design and construction monitoring of soil nail walls. Federal Highway Publication No. FHWA-SA-96-069R, Federal Highway Administration, Washington, D. C.

FHWA (1999) Demonstration Project 103: Design & Construction Monitoring of Soil Nail Walls, Project Summary Report. Federal Highway Publication No. FHWA-IF-99-026, Office of Infrastructure/Office of Bridge Technology, Federal Highway Administration, Washington, D. C.

FHWA (2009) Design and Construction of Mechanically Stabilized Earth Walls and Reinforced Soil Slopes-Volume I. Federal Highway Administration, Washington, D. C.

FHWA (2017) Ground Modification Methods Reference Manual – Volume I. Federal Highway Administration, Washington, D. C.

Fraccica, A., Romero, E., and Fourcaud, T. (2024). Exploring stress-paths and vegetation reinforcement mechanisms in a compacted soil. https://doi.org/10.5194/egusphere-egu24-19887

Gao, Y., Yang, S., Zhang, F., and Leshchinsky, B. (2016). Three-dimensional reinforced slopes: Evaluation of required reinforcement strength and embedment length using limit analysis. *Geotextiles and Geomembranes*, 44(2), 133–142. https://doi.org/10.1016/j.geotexmem.2015.07.007

Gassler, G., and Gudehus, G. (1981). Soil Nailing - Some Aspects of a New Technique. International Society of Soil Mechanics and Geotech Engineering. 12(20):665–670.

Geo5, (2018). Fine Ltd. User's Guide Edition - 2018. Retrieved from www.finesoftwar.eu

Guang-Hui, C., Jin-Feng, Z., Yu-Ming, S., and Jing-Yu, C. (2022). Stability assessment of soil-nailed slopes using the homogenisation approach. *European Journal of Environmental and Civil Engineering*. https://doi.org/10.1080/19648189.2022.2052969

Gurpersaud, N., Vanapalli, S. K. and Sivathayalan, S. (2011). Pull-out capacity of soil nails in unsaturated soils. Pan-Am CGS Geotechnical Conference, 2011: 1-8. Retrieved from www.geo-foundations.com

Hayashi, S., Ochiai, H., Yoshimoto, A., Sato, K., and Kitamura, T. (1988). Functions and Effects of Reinforcing Materials in Earth Reinforcement. Proceedings of International Geotechnical Symposium on Theory and Practice of Earth Reinforcement, Fukuoka; 5 -7 October 1988, 99-104.

Ilan, Juran. (1987). Nailed-Soil Retaining Structures: Design and Practice. *Transportation Research Record*. 1119: 139-150.

Ilan, Juran., Baudrand, G., Member, S., Farrag, K., and Elias, V. (1990). Kinematical Limit Analysis for Design of Soil-Nailed Structures. *Journal of Geotechnical Engineering*, 116, 54–72.

Jewell, R. A. (1980). Some effects of reinforcement on the mechanical behaviour of soils. PhD thesis, University of Cambridge.

Jewell, R. A. and Pedley, M. J. (1992). Analysis for Soil Reinforcement with Bending Stiffness. *Journal of Geotechnical Engineering*, ASCE, October 1992; Vol. 118(10):1505-1528.

Jewell, R. A. and Wroth, C. P. (1987). Direct shear tests on reinforced sand. Géotechnique, 37(1):53-68.

Jewell, R. A., and Pedley, M. J. (1990). Soil nailing design: the role of bending stiffness. *Ground Engineering*; March 1990: 30-36.

Johari, A., Hajivand, A. K., and Binesh, S. M. (2020). System reliability analysis of soil nail wall using random finite element method. *Bulletin of Engineering Geology and the Environment*, 79(6), 2777–2798. https://doi.org/10.1007/s10064-020-01740-y

Kempfert, H. G., and Raithel, M. (2015). Soil improvement and foundation systems with encased columns and reinforced bearing layers. In Ground Improvement Case Histories: Compaction, Grouting and Geosynthetics (pp. 609–633). Elsevier Inc. https://doi.org/10.1016/B978-0-08-100698-6.00021-0.

Lambe, T.W. and Whitman, R.V. (1969). Soil Mechanics. John Wiley & Sons.

Lazarte, C. A., Robinson, H., Gomez, J. E., Baxter, A., Cadden, A., and Berg, R. (2015). Geotechnical engineering circular No. 7 soil nail walls—Reference manual. Rep No FHWA-NHI-14- 007,.

Lazorenko, G., Kasprzhitskii, A., Kukharskii, A., Kochur, A., and Yavna, V. (2020). Failure analysis of widened railway embankment with different reinforcing measures under heavy axle loads: A comparative FEM study. *Transportation Engineering*, 2. https://doi.org/10.1016/j.treng.2020.100028

Li, Z., and Xiao, S. (2023). Seismic Overall Stability of Embankment Slopes Retained by Multi-step Cantilever Retaining Walls Using Pseudo-Static Method. *Geotechnical and Geological Engineering*. https://doi.org/10.1007/s10706-023-02378-9

Lin, H., Xiong, W., and Cao, P. (2013). Stability of soil nailed slope using strength reduction method. *European Journal of Environmental and Civil Engineering*, (17): 872–885. https://doi.org/10.1080/19648189.2013.828658

Lin, P., Bathurst, R. J., and Liu, J. (2016). Statistical Evaluation of the FHWA Simplified Method and Modifications for Predicting Soil Nail Loads. *Journal of Geotechnical and Geoenvironmental Engineering*, (04016107), 1–11. https://doi.org/10.1061/(ASCE)GT.1943-5606.0001614

Lin, P., Ni, P., Guo, C., and Mei, G. (2020). Mapping soil nail loads using Federal Highway Administration (FHWA) simplified models and artificial neural network technique. *Canadian Geotechnical Journal*, 57(10), 1453–1471. https://doi.org/10.1139/cgj-2019-0440

Liu, H., Ma, H., Chang, D., and Lin, P. (2021). Statistical calibration of federal highway administration simplified models for facing tensile forces of soil nail walls. *Acta Geotechnica*, 16(5), 1509–1526. https://doi.org/10.1007/s11440-020-01106-4

Liu, H., Tang, L., and Lin, P. (2017). Maximum Likelihood Estimation of Model Uncertainty in Predicting Soil Nail Loads Using Default and Modified FHWA Simplified Methods. *Mathematical Problems in Engineering*, 2017. https://doi.org/10.1155/2017/7901918

Liu, J. Y., Liu, Y., and Song, X. H. (2017). Research on the reasonable pile spacing of micro pile composite soil nailing. In IOP Conference Series: Earth and Environmental Science (Vol. 81). Institute of Physics Publishing. https://doi.org/10.1088/1755-1315/81/1/012157

Liu, J., Shang, K., and Wu, X. (2014). Stability Analysis of Soil Nailing Supporting Structure Based on System Failure Probability Method.

Liu, J., Shang, K., and Wu, X. (2016). Stability Analysis and Performance of Soil-Nailing Retaining System of Excavation during Construction Period. Journal of Performance of Constructed Facilities, 30(1). https://doi.org/10.1061/(asce)cf.1943-5509.0000640

Liu, S., Su, Z., Li, M., and Shao, L. (2020). Slope stability analysis using elastic finite element stress fields. *Engineering Geology*, 273. https://doi.org/10.1016/j.enggeo.2020.105673

Marchal, J. (1986). Soil Nail-Experimental Laboratory Study of Soil Nail Interaction. Transport and Road Research Laboratory, Department of Transport No. 239.

Masi, E. B., Segoni, S., and Tofani, V. (2021). Root reinforcement in slope stability models: A review. *Geosciences*. 11(212): 1-24. https://doi.org/10.3390/geosciences11050212.

Mazindrani, Z. H. and Ganjali, M. H. (1997). Lateral Earth Pressure Problem of Cohesive Backfill with Inclined Surface. *Journal of Geotechnical and Geoenvironmental Engineering*, 123(2), 110–112. doi:10.1061/(ASCE)1090-0241(1997)123:2(110)

Mitchell, J. K. (1981). Soil Improvement: State-of-the-Art, 10 International Conference on Soil Mechanics and Foundation Engineering, Stockholm, Sweden; June 1981, Vol. (4): 509-565.

Miyata, Y., and Bathurst, R. J. (2012). Measured and predicted loads in steel strip reinforced c - φ soil walls in Japan. *Soils and Foundations*, 52(1), 1–17. https://doi.org/10.1016/j.sandf.2012.01.009

Morrison, K., Harrison, F., and Anderson, S. (2006). Evolution of Mechanically Stabilized Earth Wall Design to Incorporate Permanent Shoring, GEO-Volution, Denver, CO:149-157.

Muthukumar, S., Kolathayar, S., Valli, A., and Sathyan, D. (2022). Pseudostatic analysis of soil nailed vertical wall for composite failure. *Geomechanics and Geoengineering*, 17(2). https://doi.org/10.1080/17486025.2020.1827163

Nasvi, M. C. M., and Krishnya, S. (2019). Stability Analysis of Colombo–Katunayake Expressway (CKE) Using Finite Element and Limit Equilibrium Methods. *Indian Geotechnical Journal*, 49(6). https://doi.org/10.1007/s40098-019-00357-7

Naylor, D.J. (1982). Finite Elements and Slope Stability. In: Martins, J.B. (eds) Numerical Methods in Geomechanics. NATO Advanced Study Institutes Series, vol 92. Springer, Dordrecht. https://doi.org/10.1007/978-94-009-7895-9_10.

Ng, C. W. W., Crous, P. A., Zhang, M., and Shakeel, M. (2022). Static liquefaction mechanisms in loose sand fill slopes. *Computers and Geotechnics*, 141. https://doi.org/10.1016/j.compgeo.2021.104525

Ng, C., and Lee, G. (2002) A Three-Dimensional Parametric Study of the Use of Soil Nails for Stabilising Tunnel Faces. *Computers and Geotechnics*. 29(8): 673-697.

Nguyen, H. B. K., Rahman, M. M., and Karim, M. R. (2023). Effect of soil anisotropy and variability on the stability of undrained soil slope. *Frontiers in Built Environment*, 9. https://doi.org/10.3389/fbuil.2023.1117858

Olia, A., and Liu, J. (2011). Numerical investigation of soil nail wall during construction. Pan-Am CGS, 2011 Geotechnical Conference, GEO 11, 820.

Ortigao, J.A.R., Palmeira, E.M. (2004). Soil nailing. In: Handbook of Slope Stabilisation. Springer, Verlag Berlin Heidelberg, pp 355–56. https://doi.org/10.1007/978-3-662-07680-4_13

Palmeira, M., and Milligan G. W. E. (1989). Large Scale Direct Shear Tests on Reinforced Soil. *Soils and Foundations*; March 1989, Vol. 29(1):18-30.

Pedley, M. J. (1990). The performance of soil reinforcement in bending and shear, Doctoral dissertation, University of Oxford.

Pei, H. F., Li, C., Zhu, H. H., and Wang, Y. J. (2013). Slope stability analysis based on measured strains along soil nails using FBG sensing technology. *Mathematical Problems in Engineering*, 2013. https://doi.org/10.1155/2013/561360

Pinuji, I., Dewi, P., Puspitasari, A., and Widiastuti, S. (2024). Soil Nailing Application for Railways Track Safety on Slope Area. *Journal of Physics*, 2916(1), 012015. https://doi.org/10.1088/1742-6596/2916/1/012015

Pinyol, N. M., Di Carluccio, G., and Alonso, E. E. (2022). A slow and complex landslide under static and seismic action. *Engineering Geology*, 297. https://doi.org/10.1016/j.enggeo.2021.106478

Plumelle, C., and Schlosser, F. (1990). A French National Research Project on Soil Nailing: Clouterre. In: Proceedings of a conference on design and performance of earth retaining structures, Ithaca, USA; 18-21 June 1990, Geotechnical Special Publication No. (25): 660–675.

Porterfield, J. A., Cotton, D. M., and Byrne, R. J. (1994). "Soil Nailing Field Inspectors Manual, Project Demonstration 103," Publication No. FWHA-SA-93-068, Federal Highway Administration, Washington, D.C.

Potgieter, J., and Jacobsz, S. W. (2019). Comparing the factors of safety from finite element and limit equilibrium analyses in lateral support design. Technical Paper Journal, South African Institute Civil Engineering. 2019; 61(4): Paper (0602):29-41.

Qin, C., and Zhou, J. (2023). On the seismic stability of soil slopes containing dual weak layers: true failure load assessment by finite-element limit-analysis. *Acta Geotechnica*. https://doi.org/10.1007/s11440-022-01730-2.

Que, Y., Dai, Y., Hong, Q., Fang, L., and Zhang, C. (2024). Pull-out tests for GFRP/BFRP/steel bars used as nailing for coal-bearing soil slopes in humid regions. *Journal of Testing and Evaluation*, 52(1), 491–510. https://doi.org/10.1520/JTE20220593

Rajhans, P., Ekbote, A. G., and Bhatt, G. (2022). Stability analysis of mine overburden dump and improvement by soil nailing. Materials Today: Proceedings. https://doi.org/10.1016/j.matpr.2022.03.282

Rawat, S., and Gupta, A. K. (2016). An experimental and analytical study of slope stability by soil nailing. *Electronic Journal of Geotechnical Engineering*. 2016; 21 (17).

Rawat, S., and Gupta, A. K. (2016). Analysis of a Nailed Soil Slope Using Limit Equilibrium and Finite Element Methods. *International Journal of Geosynthetics and Ground Engineering*. December-2016; 2(34):1–23.

Rotte, V.M., and Viswanadham, B. V. S. (2013). Influence of nail inclination and facing material type on soil-nailed slopes. Proceedings of the Institution of Civil Engineers: *Ground Improvement*.166:(86–107). https://doi.org/10.1680/grim.11.00026.

Sabermahani, M., Moghayad, M., and Taghavi Zargar, M. (2025). Innovative approach to optimize soil nail arrangement for stabilizing deep excavations. *Arab Journal of Science and Engineering*. https://doi.org/10.1007/s13369-025-09969-z

Sangdeh, M. K., Negahdar, A., and Tabandeh, F. (2023). Soil improvement to enhance resistance parameters using bacterial precipitation and nanosilica. *SN Applied Sciences*, 5. https://doi.org/10.1007/s42452-023-05551-0

Sanvitale, N., Simonini, P., Bisson, A., and Cola, S. (2013). Role of the facing on the behaviour of soil-nailed slopes under surcharge loading. In Proceedings of the 18th International Conference on Soil Mechanics and Geotechnical Engineering, Paris (pp. 2091–2094). Retrieved from

Sari, M. (2022). Evaluating rockfalls at a historical settlement in the Ihlara Valley (Cappadocia, Turkey) using kinematic, numerical, 2D trajectory, and risk rating methods. *Journal of Mountain Science*, 19(12). https://doi.org/10.1007/s11629-022-7412-8

Sawicki, A., Lesniewska, D., and Kulczykowski, M. (1988). Measured and predicted stresses and bearing capacity of a full scale slope reinforced with nails. *Soils and Foundations* 28(4): 47–56. https://doi.org/10.3208/sandf1972.28.4_47.

Sazzad, M. K. M., Atful Hie, A. B., and Hossain, S. (2016). Stability analysis of reinforcement slope using FEM, *International Journal of Advanced Structures and Geotechnical Engineering*. July-2016; 5(3):2319-5347.

Schlosser, F. (1982). Behaviour and design of soil nailing. Proceedings of Symposium on Recent Developments in Ground Improvements, Bangkok, 29 November. - 3 December 1982: 399-413.

Schlosser, F., and Unterreiner, P. (1991). Soil Nailing in France: Research and Practice. Behavior of Jointed Rock Masses and Reinforced Soil Structures, Transportation Research Record No. 1330, 72–79. Retrieved from http://onlinepubs.trb.org/Onlinepubs/trr/1991/1330/1330-009.pdf

Schlosser, F., Jacobsen, H. M., and Juran, I. (1983). General report-soil reinforcement, speciality session 5. In: Proceedings of the 8th European conference on soil mechanics and Foundation Engineering, Espoo, Finland. Vol. (3):1159–1180.

Seo, H. J., Lee, I. M., and Lee, S. W. (2014). Optimization of soil nailing design considering three failure modes. *KSCE Journal of Civil Engineering*, 18(2), 488–496. https://doi.org/10.1007/s12205-014-0552-9.

Sharma, M., Samanta, M. and Sarkar, S. (2020). Soil nailing: An effective slope stabilization technique. In: Advances in Natural and Technological Hazards Research. Springer Netherlands, pp 173–199.

Shen, C. K., Bang, S., and Herrmann, L. R. (1981). Ground Movement Analysis of an Earth Support System. *Journal of the Geotechnical Engineering Division*, American Society of Civil Engineers, 1981, Vol.107 (12): 1609-1624.

Shiu, Y. K., and Chang, G. W. K. (2006). Effects of Inclination, Length Pattern and Bending Stiffness of Soil Nails on Behaviour of Nailed Structures, Government of The Hong Kong GEO Special Project Report No. SPR- 6, 2005. Report No. 197, Geotechnical Engineering Office, Hong Kong. http://www.cedd.gov.hk

Singh, V., and Babu, G. (2010). 2D Numerical Simulation of Soil Nail Walls. *Geotechnical and Geological Engineering*. Vol. 28(4): 299-309.

Sivakumar Babu, G. L., and Singh, V. P. (2011). Reliability-based load and resistance factors for soil-nail walls. *Canadian Geotechnical Journal*, 48(6), 915–930. https://doi.org/10.1139/t11-005

Smith I. M., and Su N. (1997). Three-dimensional FE Analysis of a Nailed Wall Curved in Plan. *International Journal for Numerical and Analytical Mehtods in Geomechanics.* Vol. (21): 583-597.

Stocker, M. F., Korber G. W., and Gassler, G. (1979). Soil nailing. C.R. Col. Int. Reinforced des. Sols. Paris: 469–474.

Su, L. J., Yin, J. H., and Zhou, W. H. (2010). Influences of overburden pressure and soil dilation on soil nail pull-out resistance. *Computers and Geotechnics*, 37(4), 555–564. https://doi.org/10.1016/j.compgeo.2010.03.004

Sumartini, W. O., Hazarika, H., Kokusho, T., and Ishibashi, S. (2021). Volcanic Cohesive Soil Behaviour under Static and Cyclic Loading. *Geotechnical Engineering*, 55(1).

Tavakoli, S., and Aminfar, M. H. (2021). Numerical and Experimental Studies of the Effect of Mechanical Parameters on Nail Pull-Out Resistance in Sandy Soil. *Iranian Journal of Science and Technology - Transactions of Civil Engineering*, 45(4). https://doi.org/10.1007/s40996-021-00689-6

Tavakoli, S., and Aminfar, M. H. (2022). Study of Nail Group Efficiency on Sandy Soil Using Large Scale Pull-Out Box. *Journal of Rehabilitation in Civil Engineering*, 10(1), 69–87. https://doi.org/10.22075/JRCE.2021.22026.1463

Terzaghi, K. (1943). Theoretical soil mechanics. John Wiley & Sons, Inc., New York. N.Y., 35-41.

Terzaghi, K., Peck, R. B., and Mesri, G. (1996). Soil Mechanics in Engineering Practice (Third Edition). New York: John Wiley & Sons, Inc.

Tokhi, H., Ren, G., and Li, J. (2016). Laboratory study of a new screw nail and its interaction in sand. *Computers and Geotechnics*, 78, 144–154. https://doi.org/10.1016/j.compgeo.2016.05.009

Vidal, H. (1969). The Principle of Reinforced Earth. Paris

Viswanadham, B. V. S., and Rotte, V. (2015). Effect of facing type on the behaviour of soil- nailed slopes: centrifuge and numerical study. Discov Publ. October 2015; (46):214-223.

Wang, Y., Cong, L., Yin, X., Yang, X., Zhang, B., and Xiong, W. (2021). Creep behaviour of saturated purple mudstone under triaxial compression. *Engineering Geology*, 288. https://doi.org/10.1016/j.enggeo.2021.106159

Westergaard, H. (1938). A problem of elasticity is suggested by a problem in soil mechanics: soft material reinforced by numerous strong horizontal sheets. Contributions to the mechanics of solids, Stephen Timoshenko 60th anniversary volume, Macmillan, New York, 260-277.

Wood, T., Jayawickrama, P., and Lawson, W. (2009). Instrumentation and Monitoring of an MSE/Soil Nail Hybrid Retaining Wall, Contemporary Topics in Ground Modification, Problem Soils and Geo-Support, GSP No. 187, Reston, VA,177-184.

Yi, Z., and Kang, J. (2025). Finite element-based spatial distribution model for slope stability during earthquakes. *Earthquakes and Structures*, 28(2), 149–159. https://doi.org/10.12989/eas.2025.28.2.149

Yuan, J., Lin, P., Huang, R., and Que, Y. (2019). Statistical evaluation and calibration of two methods for predicting nail loads of soil nail walls in China. *Computers and Geotechnics*, 108, 269–279. https://doi.org/10.1016/j.compgeo.2018.12.028

Zahedi, P., Rezaei-Farei, A., and Soltani-Jigheh, H. (2021). Performance Evaluation of the Screw Nailed Walls in Tabriz Marl. *International Journal of Geosynthetics and Ground Engineering*, 7(1). https://doi.org/10.1007/s40891-020-00247-6

Zhang, M., Erxiang, S. and Zhaoyuan, C. (1999). Ground movement analysis of soil nailing construction by three-dimensional (3-D) finite element modelling (FEM), *Computer and Geotechnics*, (25), 191-204.

Zhou, J., and Qin, C. (2023). Influence of soft band on seismic slope stability by finite-element limit-analysis modelling. *Computers and Geotechnics*, 158. https://doi.org/10.1016/j.compgeo.2023.105396.

LIST OF CODES USED DURING RESEARCH WORK

This section presents the various design codes recommended and employed throughout the research process. These codes serve as crucial guidelines in slope stability analysis by soil nailing, soil mechanics, and geotechnical engineering, ensuring compliance with industry standards and safety protocols. The following design codes are recommended and used during this research :

1) FHWA-NHI-14-007 (2015), Soil Nail Walls-Reference Manual, Geotechnical Engineering Circular No. 7.

2) IS 456 (2000): Plain and Reinforced Concrete - Code of Practice. Tenth Reprint April. *Bureau of Indian Standard*; 2005.

3) IS 800 (2007): General Construction In Steel - Code of. Practice, 3rd revision, [CED 7: Structural Engineering and structural sections], Bureau of Indian Standard; December 2007.

4) IS 1498 -1970, (2007) Classification and identification of soils for general engineering purposes. New Delhi.

5) IS 2720-8 (1983): Methods of test for soils, Part 8: Determination of water content-dry density relation using heavy compaction (CED 43: Soil and Foundation Engineering). *Bureau of Indian Standard.*

6) FHWA-SA-96-69R (1998) Report, Manual for design and construction monitoring of soil nail walls.

7) FHWA0-IF-03-017 (2003) Manual for design and construction monitoring of soil nail walls.

8) FHWA NHI-06-019 (Vol. 1) and FHWA NHI-06-020 (Vol. 2):1056, (2006), Ground Improvement Methods.

9) FHWA-PL-93-020 (1993a) FHWA International Scanning Tour for Geo-technology, Soil Nailing Summary Report.

10) FHWA (1993b) Report No. FHWA-SA-93-026 French National Research Project Clouterre.

11) FHWA (1994) Federal Highway Publication No. FHWA-SA-93-068, Soil Nailing Field Inspectors Manual-Soil Nail Walls.

12) FHWA (1998) Federal Highway Publication No. FHWA-SA-96-069R Manual for design and construction monitoring of soil nails walls.

13) FHWA (1999) Publication No. FHWA-IF-99-026 Demonstration Project 103: Design & Construction Monitoring of Soil Nail Walls, Project Summary Report.

APPENDICES

Appendix A

(Figures A1 to A7)

- Figure A1: Face inclination (α) is 0^0 and Back slope (β) is 0^0 (FHWA-2003)
- Figure A2: Face inclination (α) is 0^0 and Back slope (β) is 10^0 (FHWA-2003)
- Figure A3: Face inclination (α) is 10^0 and Back slope is 0^0 (FHWA-2003)
- Figure A4: Face inclination (α) is 10^0 and Back slope (β) is 10^0 (FHWA-2003)
- Figure A5: Face inclination (α) is 0^0 and Back slope (β) is 30^0 (FHWA-2003)
- Figure A6: Face inclination (α) is 10^0 and Back slope (β) is 30^0 (FHWA-2003)
- Figure A7: Correction for drill-hole diameter (Lazarte et al. 2003)

(Tables A1 to A3)

- Table A1: The minimum recommended safety factors for the design of soil nail walls, ASD Method (Lazarte et al. 2003)
- Table A2 : Threaded bar properties [ASTM A615] (FHWA-2003)
- Table A3: Reinforcing bar dimensions (FHWA-2003)

A1. Case (I): Face inclination (α) = 0^0 and Back slope (β) = 0^0

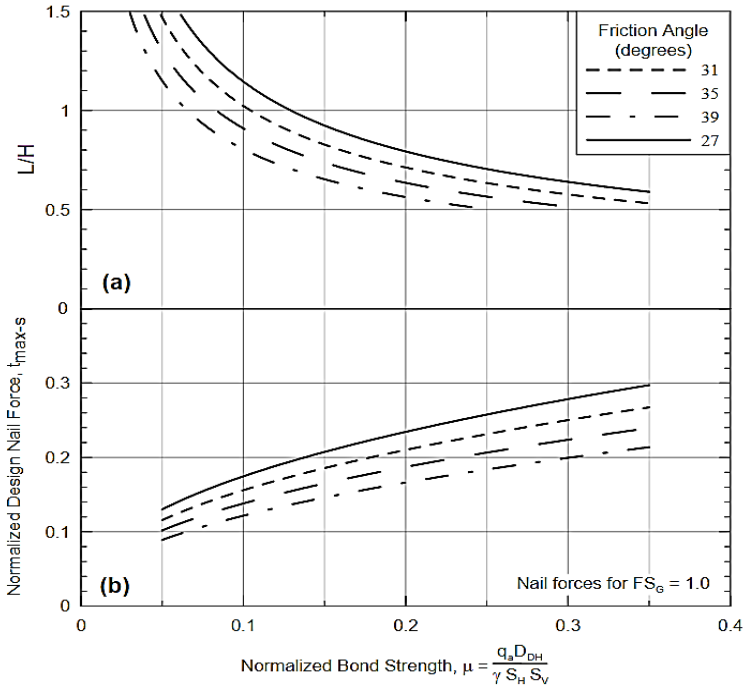

Figure A1: Face inclination (α) is 0^0 and Back slope (β) is 0^0 (FHWA-2003)

A2. Case (II) : Face inclination (α) = 0^0 and Back slope (β) =10^0

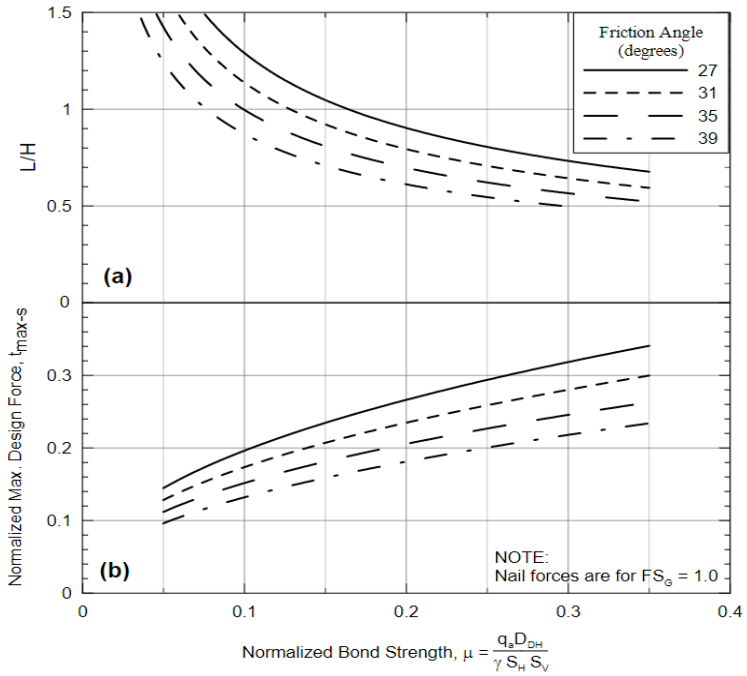

Figure A2: Face inclination (α) is 0^0 and Back slope (β) is 10^0 (FHWA-2003)

A3. Case (III): Face inclination (α) $= 10^0$ and Back slope (β) $= 0^0$

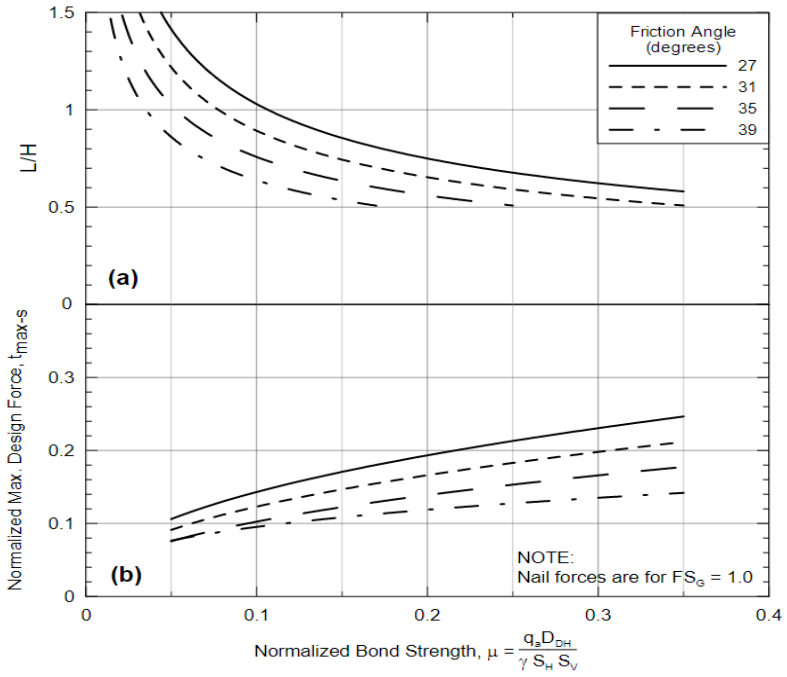

Figure A3: Face inclination (α) is 10^0 and Back slope is 0^0 (FHWA-2003)

A4. Case (IV): Face inclination (α) $= 10^0$ and Back slope (β) $=10^0$

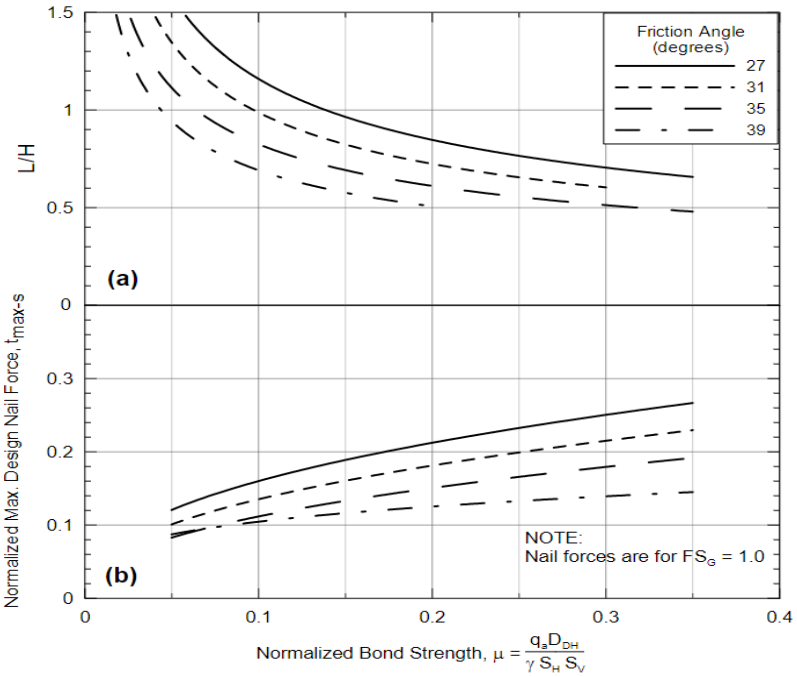

Figure A4: Face inclination (α) is 10^0 and Back slope (β) is 10^0 (FHWA-2003)

A5. Case (V): Face inclination (α) = 0^0 and Back slope (β) = 30^0

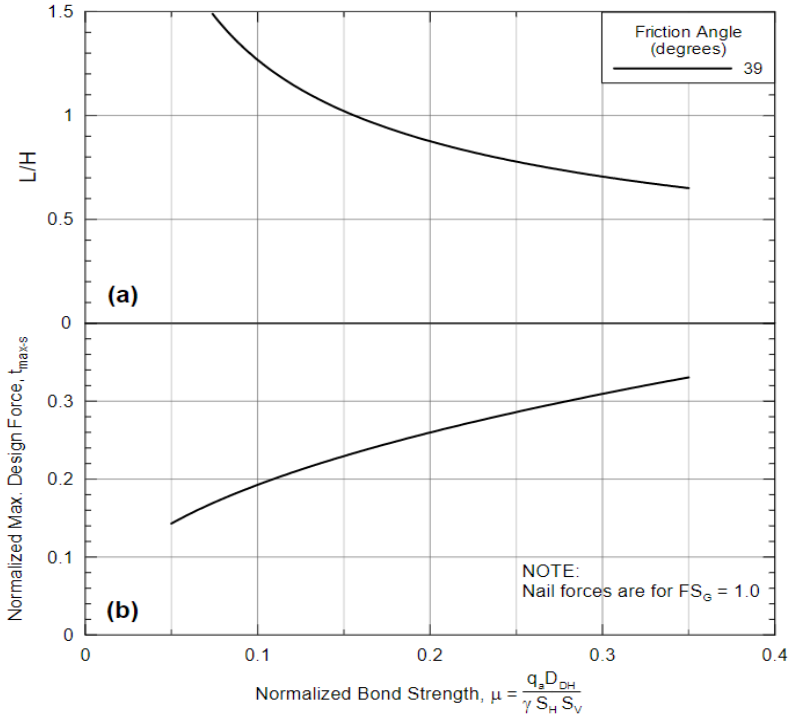

Figure A5: Face inclination (α) is 0^0 and Back slope (β) is 30^0 (FHWA-2003)

A6. Case (VI): Face inclination (α) = 10^0 and Back slope (β) = 30^0

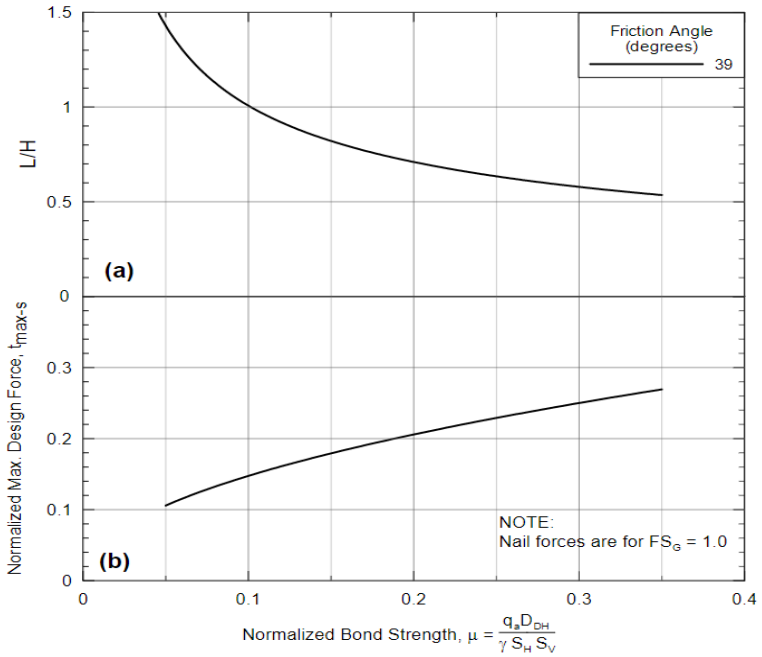

Figure A6: Face inclination (α) is 10^0 and Back slope (β) is 30^0 (FHWA-2003)

Table A1: The minimum recommended safety factors for the design of soil nail walls, ASD Method (Lazarte et al. 2003)

Failure Mode	Resisting Component	Symbol	Minimum Recommended Factors of Safety		
			Static Loads[1]		Seismic Loads[2] (Temporary and Permanent Structures)
			Temporary Structure	Permanent Structure	
External Stability	Global Stability (long-term)	FS_G	1.35	1.5[1]	1.1
	Global Stability (excavation)	FS_G	1.2-1.3 [2]		NA
	Sliding	FS_{SL}	1.3	1.5	1.1
	Bearing Capacity	FS_H	2.5 [3]	3.0 [3]	2.3 [5]
Internal Stability	Pullout Resistance	FS_P	2.0		1.5
	Nail Bar Tensile Strength	FS_T	1.8		1.35
Facing Strength	Facing Flexure	FS_{FF}	1.35	1.5	1.1
	Facing Punching Shear	FS_{FP}	1.35	1.5	1.1
	H.-Stud Tensile (A307 Bolt)	FS_{HT}	1.8	2.0	1.5
	H.-Stud Tensile (A325 Bolt)	FS_{HT}	1.5	1.7	1.3

Notes:

(1) In the case of permanent, non-critical structures, certain agencies might approve a design with FS_G = 1.35 for static loads and long-term conditions if there is less uncertainty because of the availability of adequate geotechnical data and successful local soil nailing experience.

(2) Temporary excavation lifts that are left unsupported for up to 48 hours prior to nail installation fall under the second set of safety factors for global stability. When there is greater uncertainty about the soil's conditions or when there are more critical structures, a larger value may be used.

(3) When using standard bearing capacity equations, the bearing capacity safety factors apply. The factors of safety for global stability are applicable when evaluating these failure modes using stability analysis programmes.

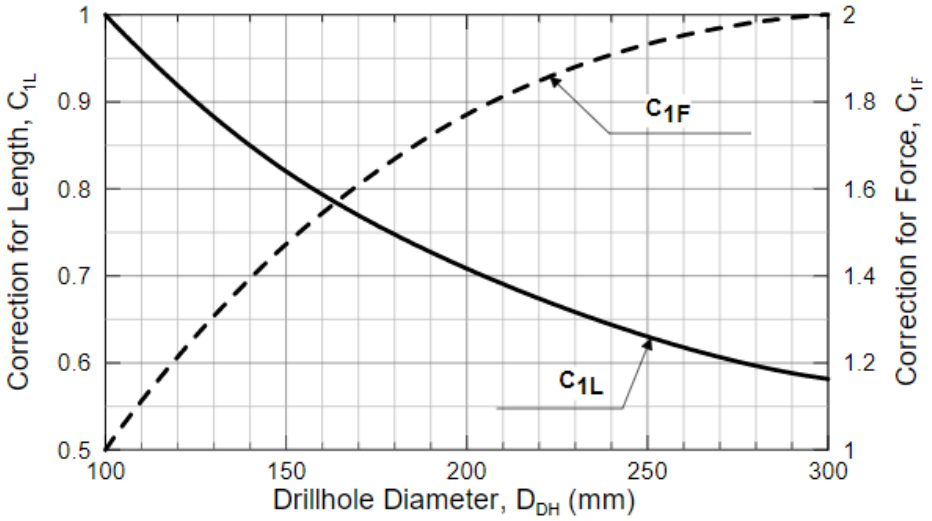

Figure A7: Correction for drill-hole diameter (Lazarte et al. 2003)

Table A2 : Threaded bar properties [ASTM A615] (FHWA-2003)

Nominal Bar Designation		Cross-Sectional Area		Nominal Unit Weight		Max. Diameter w/Threads		ASTM Grade	Yield Strength		Max. Axial Load	
English	mm	$in.^2$	mm^2	lbs/ft	kg/m	in.	mm	English	ksi	MPa	kips	kN
#6	19	0.44	284	1.50	2.24	0.86	21.8	60	60	414	26.4	118
								75	75	517	33.0	147
#7	22	0.60	387	2.04	3.04	0.99	25.1	60	60	414	36.0	160
								75	75	517	45.0	200
#8	25	0.79	510	2.67	3.98	1.12	28.4	60	60	414	47.4	211
								75	75	517	59.3	264
#9	29	1.00	645	3.40	5.06	1.26	32.0	60	60	414	60.0	267
								75	75	517	75.0	334
#10	32	1.27	819	4.30	6.41	1.43	36.3	60	60	414	76.2	339
								75	75	517	95.3	424
#11	36	1.56	1,006	5.31	7.91	1.61	40.9	60	60	414	93.6	417
								75	75	517	117.0	520
#14	43	2.25	1,452	7.65	11.39	1.86	47.2	60	60	414	135.0	601
								75	75	517	168.8	751

Source: Byrne et al. (1998).

Table A3 Reinforcing bar dimensions (FHWA-2003)

Bar Designation		Nominal Diameter		Nominal Area	
English	Metric	in.	mm	$in.^2$	mm^2
3	10	0.375	9.6	0.11	71
4	13	0.500	12.7	0.20	129
5	16	0.625	15.9	0.31	199
6	19	0.750	19.1	0.44	284
7	22	0.875	22.2	0.60	387
8	25	1.000	25.4	0.79	510
9	29	1.128	28.7	1.00	645
10	32	1.270	32.3	1.27	819
11	36	1.410	35.8	1.56	1,006
14	43	1.693	43.0	2.25	1,452
18	57	2.257	57.3	4.00	2,581

Source: Byrne et al. (1998).

Appendix B

(Table B1 and B2)

Preliminary Design Charts

Table B1: Preliminary design considering with different drill hole diameters (D_{DH}) from Table (A) to (C)

(A) Design chart for identification of size of soil nail considering various face inclination (α) and back slope (β) with different Friction Angle (ϕ) For D_{DH}=100 mm

(B) Design chart for identification of size of soil nail considering various face inclination (α) and back slope (β) with different Friction Angle (ϕ) For D_{DH}=150 mm.

(C) Design chart for identification of size of soil nail considering various face inclination (α) and back slope (β) with different Friction Angle (ϕ) For D_{DH}=200 mm

Table B2: Preliminary design considering with different ultimate bond strengths (q_u) from Table (A) to (C)

(A) Design chart for identification of size of soil nail considering various face inclination (α) and back slope (β) with different Friction Angle (ϕ) For q_u=70 kPa

(B) Design chart for identification of size of soil nail considering various face inclination (α) and back slope (β) with different Friction Angle (ϕ) For q_u=150 kPa

(C) Design chart for identification of size of soil nail considering various face inclination (α) and back slope (β) with different Friction Angle (ϕ) For q_u=200 kPa

Table B1: Preliminary design considering with different drill hole diameters (D_{DH}) from Table (A) to (C)

(A) Design chart for identification of size of soil nail considering various face inclination (α) and back slope (β) with different Friction Angle (ϕ) For **D_{DH}=100 mm**

(ϕ)	q_u (kPa)	D_{DH} (mm)	FSp	γ (kN/m^3)	S_H (m)	S_V (m)	μ	L/H	t_{max-s}	C_{1L}	H (m)	L (min)	$L_{(min)}$/H	Check	C_{1F}	T_{max-s} (kN)	A_t (mm^2)	Nails Dia. (D) mm
Case I : *Face inclination (α) = 0^0 and Back slope (β) = 0^0*																		
27	120	100	2.0	19.5	1.5	1.5	0.14	0.98	0.20	1.0	6.0	5.88	0.98	TRUE	1.0	52.65	158	16
31	120	100	2.0	19.5	1.5	1.5	0.14	0.86	0.18	1.0	6.0	5.16	0.86	TRUE	1.0	47.39	142	16
35	120	100	2.0	19.5	1.5	1.5	0.14	0.79	0.15	1.0	6.0	4.74	0.79	TRUE	1.0	39.49	118	13
39	120	100	2.0	19.5	1.5	1.5	0.14	0.70	0.14	1.0	6.0	4.20	0.70	TRUE	1.0	36.86	111	13
Case II : *Face inclination (α) = 0^0 and Back slope (β) = 10^0*																		
27	120	100	2.0	19.5	1.5	1.5	0.14	1.10	0.23	1.0	6.0	6.60	1.10	TRUE	1.0	60.55	182	16
31	120	100	2.0	19.5	1.5	1.5	0.14	0.95	0.20	1.0	6.0	5.70	0.95	TRUE	1.0	52.65	158	16
35	120	100	2.0	19.5	1.5	1.5	0.14	0.85	0.18	1.0	6.0	5.10	0.85	TRUE	1.0	47.39	142	16
39	120	100	2.0	19.5	1.5	1.5	0.14	0.75	0.15	1.0	6.0	4.50	0.75	TRUE	1.0	39.49	118	13
Case III : *Face inclination (α) = 10^0 and Back slope (β) = 0^0*																		
27	120	100	2.0	19.5	1.5	1.5	0.14	0.90	0.16	1.0	6.0	5.40	0.90	TRUE	1.0	42.12	126	13
31	120	100	2.0	19.5	1.5	1.5	0.14	0.80	0.14	1.0	6.0	4.80	0.80	TRUE	1.0	36.86	111	13
35	120	100	2.0	19.5	1.5	1.5	0.14	0.65	0.11	1.0	6.0	3.90	0.65	TRUE	1.0	28.96	87	13
39	120	100	2.0	19.5	1.5	1.5	0.14	0.58	0.10	1.0	6.0	3.48	0.58	TRUE	1.0	26.33	79	13
Case IV : *Face inclination (α) = 10^0 and Back slope (β) = 10^0*																		
27	120	100	2.0	19.5	1.5	1.5	0.14	1.00	0.19	1.0	6.0	6.00	1.00	TRUE	1.0	50.02	150	16
31	120	100	2.0	19.5	1.5	1.5	0.14	0.85	0.15	1.0	6.0	5.10	0.85	TRUE	1.0	39.49	118	13
35	120	100	2.0	19.5	1.5	1.5	0.14	0.70	0.12	1.0	6.0	4.20	0.70	TRUE	1.0	31.59	95	13
39	120	100	2.0	19.5	1.5	1.5	0.14	0.55	0.11	1.0	6.0	3.30	0.55	TRUE	1.0	28.96	87	13
Case V : *Face inclination (α) = 0^0 and Back slope (β) = 30^0*																		
39	120	100	2.0	19.5	1.5	1.5	0.14	1.10	0.22	1.0	6.0	6.60	1.10	TRUE	1.0	57.92	174	16
Case VI : *Fase inclination (α) = 10^0 and Back slope (β) = 30^0*																		
39	120	100	2.0	19.5	1.5	1.5	0.14	0.85	0.16	1.0	6.0	5.10	0.85	TRUE	1.0	42.12	126	13

Continue……..…

(B) Design chart for identification of size of soil nail considering various face inclination (α) and back slope (β) with different Friction Angle (ϕ) For **D_{DH}=150 mm.**

(ϕ)	q_u (kPa)	D_{DH} (mm)	FSp	γ (kN/m^3)	S_H (m)	S_V (m)	μ	L/H	t_{max-s}	C_{1L}	H (m)	L (min)	$L_{(min)}$/H	Check	C_{1F}	T_{max-s} (kN)	A_t (mm^2)	Nails Dia. (D) mm
Case I : *Face inclination (α) = 0^0 and Back slope (β) = 0^0*																		
27	120	150	2.0	19.5	1.5	1.5	0.21	0.80	0.24	0.83	6.0	3.98	0.66	TRUE	1.48	93.51	281	19
31	120	150	2.0	19.5	1.5	1.5	0.21	0.70	0.21	0.83	6.0	3.49	0.58	TRUE	1.48	81.82	245	19
35	120	150	2.0	19.5	1.5	1.5	0.21	0.65	0.19	0.83	6.0	3.24	0.54	TRUE	1.48	72.08	216	19
39	120	150	2.0	19.5	1.5	1.5	0.21	0.55	0.16	0.83	6.0	2.74	0.46	FALSE*	1.48	62.34	187	16
Case II : *Face inclination (α) = 0^0 and Back slope (β) = 10^0*																		
27	120	150	2.0	19.5	1.5	1.5	0.21	0.90	0.27	0.83	6.0	4.48	0.75	TRUE	1.48	105.19	316	22
31	120	150	2.0	19.5	1.5	1.5	0.21	0.75	0.24	0.83	6.0	3.74	0.62	TRUE	1.48	93.51	281	19
35	120	150	2.0	19.5	1.5	1.5	0.21	0.65	0.21	0.83	6.0	3.24	0.54	TRUE	1.48	81.82	245	19
39	120	150	2.0	19.5	1.5	1.5	0.21	0.60	0.18	0.83	6.0	2.99	0.50	FALSE*	1.48	70.13	210	19
Case III : *Face inclination (α) = 10^0 and Back slope (β) = 0^0*																		
27	120	150	2.0	19.5	1.5	1.5	0.21	0.75	0.20	0.83	6.0	3.74	0.62	TRUE	1.48	77.92	234	19
31	120	150	2.0	19.5	1.5	1.5	0.21	0.65	0.17	0.83	6.0	3.24	0.54	TRUE	1.48	66.23	199	16
35	120	150	2.0	19.5	1.5	1.5	0.21	0.55	0.14	0.83	6.0	2.74	0.46	FALSE*	1.48	54.55	164	16
39	120	150	2.0	19.5	1.5	1.5	0.21	0.45	0.11	0.83	6.0	2.24	0.37	FALSE*	1.48	42.86	129	13
Case IV : *Face inclination (α) = 10^0 and Back slope (β) = 10^0*																		
27	120	150	2.0	19.5	1.5	1.5	0.21	0.85	0.22	0.83	6.0	4.23	0.71	TRUE	1.48	85.71	257	19
31	120	150	2.0	19.5	1.5	1.5	0.21	0.57	0.19	0.83	6.0	2.84	0.47	FALSE*	1.48	74.03	222	19
35	120	150	2.0	19.5	1.5	1.5	0.21	0.55	0.15	0.83	6.0	2.74	0.46	FALSE*	1.48	58.44	175	16
39	120	150	2.0	19.5	1.5	1.5	0.21	0.50	0.12	0.83	6.0	2.49	0.42	FALSE*	1.48	46.75	140	16
Case V : Face inclination (α) = 0^0 and Back slope (β) = 30^0																		
39	120	150	2.0	19.5	1.5	1.5	0.21	0.85	0.27	0.83	6.0	4.23	0.7055	TRUE	1.48	105.19	316	22
Case VI : *Fase inclination (α) = 10^0 and Back slope (β) = 30^0*																		
39	120	150	2.0	19.5	1.5	1.5	0.21	0.70	0.22	0.83	6.0	3.49	0.581	TRUE	1.48	85.71	257	19

*****According to the FHWA 2003 code recommendation, the (L_{min}/H) value indicates that it is on the lower end, specifically less than/equal to 0.5. Therefore, to mitigate wall deformation, it is advisable to augment the length of nails required.

Continue……..…

(C) Design chart for identification of size of soil nail considering various face inclination (α) and back slope (β) with different Friction Angle (ϕ) For **D_{DH}=200 mm**

(ϕ)	q_u (kPa)	D_{DH} (mm)	FSp	γ (kN/m^3)	S_H (m)	S_V (m)	μ	L/H	t_{max-s}	C_{1L}	H (m)	L (min)	$L_{(min)}$/H	Check	C_{1F}	T_{max-s} (kN)	A_t (mm^2)	Nails Dia. (D) mm
Case I : *Face inclination (α) = 0^0 and Back slope (β) = 0^0*																		
27	120	200	2.0	19.5	1.5	1.5	0.27	0.7	0.26	0.71	6.0	2.98	0.50	FALSE*	1.78	121.83	365	22
31	120	200	2.0	19.5	1.5	1.5	0.27	0.65	0.24	0.71	6.0	2.77	0.46	FALSE*	1.78	112.46	337	22
35	120	200	2.0	19.5	1.5	1.5	0.27	0.55	0.21	0.71	6.0	2.34	0.39	FALSE*	1.78	98.40	295	22
39	120	200	2.0	19.5	1.5	1.5	0.27	0.5	0.19	0.71	6.0	2.13	0.36	FALSE*	1.78	89.03	267	19
Case II : *Face inclination (α) = 0^0 and Back slope (β) = 10^0*																		
27	120	200	2.0	19.5	1.5	1.5	0.27	0.75	0.3	0.71	6.0	3.20	0.53	TRUE	1.78	140.58	422	25
31	120	200	2.0	19.5	1.5	1.5	0.27	0.68	0.27	0.71	6.0	2.90	0.48	FALSE*	1.78	126.52	380	22
35	120	200	2.0	19.5	1.5	1.5	0.27	0.65	0.24	0.71	6.0	2.77	0.46	FALSE*	1.78	112.46	337	22
39	120	200	2.0	19.5	1.5	1.5	0.27	0.58	0.2	0.71	6.0	2.47	0.41	FALSE*	1.78	93.72	281	19
Case III : *Face inclination (α) = 10^0 and Back slope (β) = 0^0*																		
27	120	200	2.0	19.5	1.5	1.5	0.27	0.7	0.22	0.71	6.0	2.98	0.50	FALSE*	1.78	103.09	309	22
31	120	200	2.0	19.5	1.5	1.5	0.27	0.58	0.18	0.71	6.0	2.47	0.41	FALSE*	1.78	84.35	253	19
35	120	200	2.0	19.5	1.5	1.5	0.27	0.5	0.15	0.71	6.0	2.13	0.36	FALSE*	1.78	70.29	211	13
39	120	200	2.0	19.5	1.5	1.5	0.27	0.4	0.11	0.71	6.0	1.70	0.28	FALSE*	1.78	51.54	155	16
Case IV : *Face inclination (α) = 10^0 and Back slope (β) = 10^0*																		
27	120	200	2.0	19.5	1.5	1.5	0.27	0.75	0.23	0.71	6.0	3.20	0.53	TRUE	1.78	107.77	323	22
31	120	200	2.0	19.5	1.5	1.5	0.27	0.65	0.2	0.71	6.0	2.77	0.46	FALSE*	1.78	93.72	281	19
35	120	200	2.0	19.5	1.5	1.5	0.27	0.55	0.15	0.71	6.0	2.34	0.39	FALSE*	1.78	70.29	211	19
39	120	200	2.0	19.5	1.5	1.5	0.27	0.45	0.12	0.71	6.0	1.92	0.32	FALSE*	1.78	56.23	169	19
Case V : Face inclination (α) = 0^0 and Back slope (β) = 30^0																		
39	120	200	2.0	19.5	1.5	1.5	0.27	0.75	0.3	0.71	6.0	3.195	0.53	TRUE	1.78	140.58	422	25
Case VI : *Fase inclination (α) = 10^0 and Back slope (β) = 30^0*																		
39	120	200	2.0	19.5	1.5	1.5	0.27	0.6	0.25	0.71	6.0	2.556	0.43	FALSE*	1.78	117.15	351	22

*****According to the FHWA 2003 code recommendation, the (L_{min}/H) value indicates that it is on the lower end, specifically less than/equal to 0.5. Therefore, to mitigate wall deformation, it is advisable to augment the length of nails required.

Table B2: Preliminary design considering with different ultimate bond strength (q_u) from Table (A) to (C)

(A) Design chart for identification of size of soil nail considering various face inclination (α) and back slope (β) with different Friction Angle (ϕ) For **q_u=70 kPa**

(ϕ)	q_u (kPa)	D_{DH} (mm)	FSp	γ (kN/m^3)	S_H (m)	S_V (m)	μ	L/H	t_{max-s}	C_{1L}	H (m)	L (min)	$L_{(min)}$/H	Check	C_{1F}	T_{max-s} (kN)	A_t (mm^2)	Nails Dia. (D) mm
Case I : *Face inclination (α) = 0^0 and Back slope (β) = 0^0*																		
27	70	150	2.0	19.5	1.5	1.5	0.12	1.10	0.19	0.83	6.0	5.48	0.91	TRUE	1.48	74.03	222	13
31	70	150	2.0	19.5	1.5	1.5	0.12	0.95	0.16	0.83	6.0	4.73	0.79	TRUE	1.48	62.34	187	16
35	70	150	2.0	19.5	1.5	1.5	0.12	0.85	0.14	0.83	6.0	4.23	0.71	TRUE	1.48	54.55	164	16
39	70	150	2.0	19.5	1.5	1.5	0.12	0.78	0.13	0.83	6.0	3.88	0.65	TRUE	1.48	50.65	152	16
Case II : *Face inclination (α) = 0^0 and Back slope (β) = 10^0*																		
27	70	150	2.0	19.5	1.5	1.5	0.12	1.20	0.21	0.83	6.0	5.98	1.00	TRUE	1.48	81.82	245	19
31	70	150	2.0	19.5	1.5	1.5	0.12	1.05	0.19	0.83	6.0	5.23	0.87	TRUE	1.48	74.03	222	19
35	70	150	2.0	19.5	1.5	1.5	0.12	0.92	0.16	0.83	6.0	4.58	0.76	TRUE	1.48	62.34	187	16
39	70	150	2.0	19.5	1.5	1.5	0.12	0.82	0.14	0.83	6.0	4.08	0.68	TRUE	1.48	54.55	164	16
Case III : *Face inclination (α) = 10^0 and Back slope (β) = 0^0*																		
27	70	150	2.0	19.5	1.5	1.5	0.12	0.95	0.15	0.83	6.0	4.73	0.79	TRUE	1.48	58.44	175	16
31	70	150	2.0	19.5	1.5	1.5	0.12	0.85	0.13	0.83	6.0	4.23	0.71	TRUE	1.48	50.65	152	16
35	70	150	2.0	19.5	1.5	1.5	0.12	0.70	0.11	0.83	6.0	3.49	0.58	TRUE	1.48	42.86	129	13
39	70	150	2.0	19.5	1.5	1.5	0.12	0.60	0.10	0.83	6.0	2.99	0.50	FALSE*	1.48	38.96	117	13
Case IV : *Face inclination (α) = 10^0 and Back slope (β) = 10^0*																		
27	70	150	2.0	19.5	1.5	1.5	0.12	1.05	0.17	0.83	6.0	5.23	0.87	TRUE	1.48	66.23	199	16
31	70	150	2.0	19.5	1.5	1.5	0.12	0.90	0.14	0.83	6.0	4.48	0.75	TRUE	1.48	54.55	164	16
35	70	150	2.0	19.5	1.5	1.5	0.12	0.75	0.12	0.83	6.0	3.74	0.62	TRUE	1.48	46.75	140	16
39	70	150	2.0	19.5	1.5	1.5	0.12	0.60	0.11	0.83	6.0	2.99	0.50	FALSE*	1.48	42.86	129	13
Case V : *Face inclination (α) = 0^0 and Back slope (β) = 30^0*																		
39	70	150	2.0	19.5	1.5	1.5	0.12	1.15	0.21	0.83	6.0	5.727	0.95	TRUE	1.48	81.82	245	19
Case VI : *Fase inclination (α) = 10^0 and Back slope (β) = 30^0*																		
39	70	150	2.0	19.5	1.5	1.5	0.12	0.9	0.17	0.83	6.0	4.482	0.75	TRUE	1.48	66.23	199	16

*****According to the FHWA 2003 code recommendation, the (L_{min}/H) value indicates that it is on the lower end, specifically less than/equal to 0.5. Therefore, to mitigate wall deformation, it is advisable to augment the length of nails required.

Continue……..…

(B) Design chart for identification of size of soil nail considering various face inclination (α) and back slope (β) with different Friction Angle (ϕ) For **q_u=150 kPa**

(ϕ)	q_u (kPa)	D_{DH} (mm)	FSp	γ (kN/m^3)	SH (m)	SV (m)	μ	L/H	t_{max-s}	C_{1L}	H (m)	L (min)	$L_{(min)}$/H	Check	C_{1F}	T_{max-s} (kN)	A_t (mm^2)	Nails Dia. (D) mm
Case I : *Face inclination (α) = 0^0 and Back slope (β) = 0^0*																		
27	150	150	2.0	19.5	1.5	1.5	0.26	0.7	0.26	0.83	6.0	3.49	0.58	TRUE	1.48	101.30	304	22
31	150	150	2.0	19.5	1.5	1.5	0.26	0.68	0.23	0.83	6.0	3.39	0.56	TRUE	1.48	89.61	269	19
35	150	150	2.0	19.5	1.5	1.5	0.26	0.56	0.21	0.83	6.0	2.79	0.46	FALSE*	1.48	81.82	245	19
39	150	150	2.0	19.5	1.5	1.5	0.26	0.5	0.18	0.83	6.0	2.49	0.42	FALSE*	1.48	70.13	210	19
Case II : *Face inclination (α) = 0^0 and Back slope (β) = 10^0*																		
27	150	150	2.0	19.5	1.5	1.5	0.26	0.85	0.3	0.83	6.0	4.23	0.71	TRUE	1.48	116.88	351	22
31	150	150	2.0	19.5	1.5	1.5	0.26	0.75	0.25	0.83	6.0	3.74	0.62	TRUE	1.48	97.40	292	22
35	150	150	2.0	19.5	1.5	1.5	0.26	0.64	0.22	0.83	6.0	3.19	0.53	TRUE	1.48	85.71	257	19
39	150	150	2.0	19.5	1.5	1.5	0.26	0.55	0.2	0.83	6.0	2.74	0.46	FALSE*	1.48	77.92	234	19
Case III : *Face inclination (α) = 10^0 and Back slope (β) = 0^0*																		
27	150	150	2.0	19.5	1.5	1.5	0.26	0.65	0.22	0.83	6.0	3.24	0.54	TRUE	1.48	85.71	257	19
31	150	150	2.0	19.5	1.5	1.5	0.26	0.6	0.18	0.83	6.0	2.99	0.50	FALSE*	1.48	70.13	210	19
35	150	150	2.0	19.5	1.5	1.5	0.26	0.5	0.13	0.83	6.0	2.49	0.42	FALSE*	1.48	50.65	152	16
39	150	150	2.0	19.5	1.5	1.5	0.26	0.4	0.11	0.83	6.0	1.99	0.33	FALSE*	1.48	42.86	129	13
Case IV : *Face inclination (α) = 10^0 and Back slope (β) = 10^0*																		
27	150	150	2.0	19.5	1.5	1.5	0.26	0.85	0.23	0.83	6.0	4.23	0.71	TRUE	1.48	89.61	269	19
31	150	150	2.0	19.5	1.5	1.5	0.26	0.65	0.2	0.83	6.0	3.24	0.54	TRUE	1.48	77.92	234	19
35	150	150	2.0	19.5	1.5	1.5	0.26	0.55	0.16	0.83	6.0	2.74	0.46	FALSE*	1.48	62.34	187	16
39	150	150	2.0	19.5	1.5	1.5	0.26	0.45	0.12	0.83	6.0	2.24	0.37	FALSE*	1.48	46.75	140	16
Case V : Face inclination (α) = 0^0 and Back slope (β) = 30^0																		
39	150	150	2.0	19.5	1.5	1.5	0.26	0.75	0.29	0.83	6.0	3.735	0.6225	TRUE	1.48	112.99	339	22
Case VI : *Fase inclination (α) = 10^0 and Back slope (β) = 30^0*																		
39	150	150	2.0	19.5	1.5	1.5	0.26	0.6	0.22	0.83	6.0	2.988	0.498	FALSE*	1.48	85.71	257	19

*****According to the FHWA 2003 code recommendation, the (L_{min}/H) value indicates that it is on the lower end, specifically less than/equal to 0.5. Therefore, to mitigate wall deformation, it is advisable to augment the length of nails required.

Continue……..…

(C) Design chart for identification of size of soil nail considering various face inclination (α) and back slope (β) with different Friction Angle (ϕ) For **q_u=200 kPa**

(ϕ)	q_u (kPa)	D_{DH} (mm)	FSp	γ (kN/m^3)	SH (m)	SV (m)	μ	L/H	t_{max-s}	C_{1L}	H (m)	L (min)	$L_{(min)}$/H	Check	C_{1F}	T_{max-s} (kN)	A_t (mm^2)	Nails Dia. (D) mm
Case I : *Face inclination (α) = 0^0 and Back slope (β) = 0^0*																		
27	200	150	2.0	19.5	1.5	1.5	0.34	0.6	0.29	0.83	6.0	2.99	0.50	FALSE*	1.48	112.99	339	22
31	200	150	2.0	19.5	1.5	1.5	0.34	0.55	0.27	0.83	6.0	2.74	0.46	FALSE*	1.48	105.19	316	22
35	200	150	2.0	19.5	1.5	1.5	0.34	0.5	0.24	0.83	6.0	2.49	0.42	FALSE*	1.48	93.51	281	19
39	200	150	2.0	19.5	1.5	1.5	0.34	0.5	0.21	0.83	6.0	2.49	0.42	FALSE*	1.48	81.82	245	19
Case II : *Face inclination (α) = 0^0 and Back slope (β) = 10^0*																		
27	200	150	2.0	19.5	1.5	1.5	0.34	0.7	0.34	0.83	6.0	3.49	0.58	TRUE	1.48	132.47	397	25
31	200	150	2.0	19.5	1.5	1.5	0.34	0.65	0.29	0.83	6.0	3.24	0.54	TRUE	1.48	112.99	339	22
35	200	150	2.0	19.5	1.5	1.5	0.34	0.55	0.24	0.83	6.0	2.74	0.46	FALSE*	1.48	93.51	281	19
39	200	150	2.0	19.5	1.5	1.5	0.34	0.55	0.21	0.83	6.0	2.74	0.46	FALSE*	1.48	81.82	245	19
Case III : *Face inclination (α) = 10^0 and Back slope (β) = 0^0*																		
27	200	150	2.0	19.5	1.5	1.5	0.34	0.6	0.25	0.83	6.0	2.99	0.50	FALSE*	1.48	97.40	292	22
31	200	150	2.0	19.5	1.5	1.5	0.34	0.52	0.22	0.83	6.0	2.59	0.43	FALSE*	1.48	85.71	257	19
35	200	150	2.0	19.5	1.5	1.5	0.34	0.5	0.18	0.83	6.0	2.49	0.42	FALSE*	1.48	70.13	210	19
39	200	150	2.0	19.5	1.5	1.5	0.34	0.5	0.14	0.83	6.0	2.49	0.42	FALSE*	1.48	54.55	164	16
Case IV : *Face inclination (α) = 10^0 and Back slope (β) = 10^0*																		
27	200	150	2.0	19.5	1.5	1.5	0.34	0.65	0.27	0.83	6.0	3.24	0.54	TRUE	1.48	105.19	316	13
31	200	150	2.0	19.5	1.5	1.5	0.34	0.6	0.22	0.83	6.0	2.99	0.50	FALSE*	1.48	85.71	257	19
35	200	150	2.0	19.5	1.5	1.5	0.34	0.5	0.18	0.83	6.0	2.49	0.42	FALSE*	1.48	70.13	210	19
39	200	150	2.0	19.5	1.5	1.5	0.34	0.5	0.14	0.83	6.0	2.49	0.42	FALSE*	1.48	54.55	164	16
Case V : *Face inclination (α) = 0^0 and Back slope (β) = 30^0*																		
39	200	150	2.0	19.5	1.5	1.5	0.34	0.65	0.33	0.83	6.0	3.24	0.5395	TRUE	1.48	128.57	386	22
Case VI : *Fase inclination (α) = 10^0 and Back slope (β) = 30^0*																		
39	200	150	2.0	19.5	1.5	1.5	0.34	0.55	0.26	0.83	6.0	2.74	0.4565	FALSE*	1.48	101.30	304	22

*****According to the FHWA 2003 code recommendation, the (L_{min}/H) value indicates that it is on the lower end, specifically less than/equal to 0.5. Therefore, to mitigate wall deformation, it is advisable to augment the length of nails required.

LIST OF PUBLICATIONS AND THEIR PROOF

(A) Papers Published in SCI/SCIE Journals

(1) Ramteke, P.C., and Sahu, A.K. (2024). Soil-slope stability investigation using different nail inclinations: a comprehensive LSD, FEM and experimental approach. Sādhanā, 49, (62). https://doi.org/10.1007/s12046-023-02418-3.

(2) Ramteke, P. C. and Sahu, A. K. (2024). Reliability Assessment of Soil Nailed Slope Under Surcharge Loading: A Numerical and Experimental Investigation with Theoretical Aspects. Zeitschrift Der Deutschen Gesellschaft Für Geowissenschaften (J. Appl. Reg. Geol.) 175(3):417 – 440. https://doi.org/10.1127/zdgg/2024/0422.

(3) Ramteke, P. C., and Sahu, A. K. (2023). Enhancing soil slope stability by soil nailing: A comprehensive review. Zeitschrift Der Deutschen Gesellschaft Für Geowissenschaften (J. Appl. Reg. Geol.),174(4):729-744. https://doi.org/10.1127/zdgg/2023/0403.

(B) Participation in the International Conferences/Paper Published

(3) Ramteke, P. C., and Sahu, A. K. (2023). Ground improvement technique by soil nailing: A theoretical analysis. International Conference on Smart Materials and Structures, ICSMS-2022, vol. 2810, AIP Publishing 050001–12. https://doi.org/10.1063/5.0146861.

(4) Ramteke, P. C., and Sahu, A. K. (2022). Slope Stability Analysis of Soil Nailed Structure by using ASD and LRFD Methods. IARJSET: International Advanced Research Journal in Science, Engineering and Technology, https://doi.org/10.17148/iarjset.2022.9258.

Sādhanā (2024)49:62
https://doi.org/10.1007/s12046-023-02418-3

© Indian Academy of Sciences

Soil-slope stability investigation using different nail inclinations: a comprehensive LSD, FEM and experimental approach

PRASHANT C RAMTEKE* and ANIL KUMAR SAHU

Civil Engineering Department, Delhi Technological University, New Delhi 110 042, India
e-mail: prashant_2k16phdce12@dtu.ac.in; anilsahu@dtu.ac.in

MS received 16 June 2023; revised 19 November 2023; accepted 22 November 2023

Abstract. Soil nailing is a versatile construction technique used for retaining structures, offshore structures, structures rehabilitation, and stabilizing natural as well as man-made earth slopes. This method was initially evolved in Europe and recognized in various provinces. This research investigates the relationship between uniform vertical and uniform horizontal loading on soil slopes to gain new insights into the effectiveness of soil nailing in stabilizing earth slopes. This study used a novel numerical investigation to determine the maximum factor of safety (FOS) at various nail inclinations of 0°, 5°, 10°, 15°, 20°, and 25° with the horizontal plane. To evaluate the effectiveness of the soil nail system for slope stabilization, the study considered significant limiting factors by using the limit state design (LSD) approach. In addition, the numerical method for identifying slope displacement, mathematical modelling for identifying nail displacement within soil slope, and experimental investigation in the laboratory were carried out in this study. The investigation's findings show that soil nailing is the more effective technique for slope stabilization. The 15° nail inclination with the horizontal plane produced the best results in terms of stability and FOS. Furthermore, considering the critical limiting factors, an inclination of 15° for soil nails exhibits optimal effectiveness in strengthening the stability of a vertical cut soil slope. This inclination angle allows for efficient load transfer and distribution and decreases the risk of slope failure. Overall, the 15° nail inclination with the horizontal plane provides valuable insights and an increased FOS.

Keywords. Factor of safety; limit states design; reinforced soil; soil nailing; slope settlement; slope stabilization.

1. Introduction

Soil nailing is a construction technique that makes existing slopes stronger and more stable [1]. It is commonly used for slope stabilization in highways and railways. The construction of the soil nailing process starts from the top to the bottom. In most cases, this technique is more cost-effective than some other slope stabilization techniques [2–4]. Due to the economic benefits and advantages associated with soil nailing, nowadays this technique is more popular and has produced rapid development of nailing technology. Soil nails reproduce their reinforcing action by soil deformation [5–8]. In the soil nails, tensile forces are developed due to deformations, and most of the resistance gives rise to tension [9–12]. There are various ground improvement and slope stabilization techniques available to increase soil quality and these methods can be categorized in several ways. The soil reinforcement, compaction, vertical drainage, electro-osmosis, thermal stabilization, ion exchange, and soil stabilization by grouting, methods were suggested by Mitchell [13]. Similarly, Munfakh and Wyllie [14] proposed eight main groups for slope stabilization such as reinforcement, consolidation, weight reduction, densification, thermal stabilization, biotechnical stabilization, electro-treatment, and chemical treatment etc. The experimental studies described by Jewell and Pedley [15] in their most prominent and broad research explored soil nail bending stiffness and the effect of displacement.

Various methods are available for designing the soil-nailed structures on the limit equilibrium method (LEM) concept. Due to the reduced number of required parameters and their simplicity, most of the methods are popular. However, they are not capable of anticipating soil movements. During soil nailing, to develop the maximum tensile force, the reinforcements are installed horizontally as well as slightly inclined parallel to the direction of tensile stresses. Soil nailed slope improves soil shearing resistance because of passive inclusions [16]. The soil nailing structures get split into the active zone and passive zone (refer to figure 1). The active zone is deformed first, and at the time of slope failure, the tensile forces are developed in the soil nails in the active and passive zones. This tensile force

*For correspondence
Published online: 10 February 2024

Z. Dt. Ges. Geowiss. (J. Appl. Reg. Geol.), 175 (3), p. 417–440, 30 figs., 8 tables
Published online August 2024

Article

Reliability assessment of soil nailed slopes under surcharge loading: a numerical and experimental investigation with theoretical aspects

Prashant C. Ramteke & Anil Kumar Sahu*

Ramteke, P. C. & Sahu, A. K. (2024): Reliability assessment of soil nailed slopes under surcharge loading: a numerical and experimental investigation with theoretical aspects. – Z. Dt. Ges. Geowiss., 175: 417–440, Stuttgart.

Abstract: Soil nailing is a slope stabilisation technique used for strengthening of natural as well as manmade earth/soil slopes. Nowadays, this technique is commonly used worldwide in civil engineering projects like highways, railways, tunnelling processes, etc. It plays a very effective role in slope stabilisation in hilly or landslide-prone areas. Because of the ease of construction and due to the economic benefits, this technique is more popular than other slope stabilisation techniques. In this paper, considering slope stabilisation issues, a Three-Dimensional Finite Element Method (3D-FEM) model has been developed for simulation to investigate the behaviour of the entire structure under the surcharge loading. Consequently, the slope failure surface is classified into different areas/zones based on the outcomes of the 3D-FEM analysis. The reliability of various elements like soil slope, soil nailed wall, soil nails, and bearing plate at the facing has been studied in detail. The contribution of effective parameters in grouted nails has been obtained. An experimental investigation was carried out to identify the effects of surcharge load on the soil-nailed slope and wall. Based on the analytical and experimental observations, it is found that grouted nails play an important role in slope stabilisation, reducing settlement and wall deflection. The overall stability is found satisfactory at 15° nail inclination.

Keywords: factor of safety, pullout resistance, soil nailing, slope stability, soil-nailed wall, soil reinforcement

1. Introduction

Soil nailing is a rapid construction, flexible, time-efficient, easy-to-construct and cost-effective technique. For improving the soil surroundings the soil nailing technique is most suitable (Ghareh 2015; Azzam & Basha 2017). Soil slopes or embankments have been constructed in railway tracks, tunnel portals, highways, etc. (Bruce & Jewell 1986; Ramteke & Sahu 2023a). Many departments, including disaster relief authorities and government bodies, frequently face the challenge of slope or embankment failures caused by landslides in hilly areas. In India, the loss of life per 100 km² per year is greater than one, as well as more loss of investments happens due to landslides and slope failures (Jain et al. 2023). Approximately 12.6% of the land area, excluding snow-covered regions, is prone to landslides. This includes 0.18 million km² in the North East Himalayas, 0.14 million km² in the North West Himalayas, 0.09 million km² in the Western Ghats and Konkan hills, and 0.01 million km² in the Eastern Ghats of Andhra Pradesh (Jain et al. 2023). In these areas, failure affects or disturbs socioeconomic enrichment. To mitigate casualties and economic losses, the soil nailing technique has been embraced in numerous developed regions and countries. Western countries have harnessed the distinctive advantages of this technique since the late 1960s (Ortigao & Palmeira 2004). Due to the benefits and cost-effectiveness of this technique, engineers and construction experts have preferred it worldwide (Lazarte et al. 2003; Ramteke & Sahu 2023b). While designing and implementing this technique, geotechnical experts and engineers face challenges related to excessive settlement and low shear strength of soil. To address these concerns, various new and traditional methods have been recommended.

Jessica et al. (2019) presented a case study from Hong Kong, demonstrating the effectiveness of soil nailing in stabilising slopes. Sharma & Ramkrishnan (2020) conducted parametric optimisation and multi-regression analysis using numerical approaches, emphasising the importance of soil-nail interaction and pull-out strength. Also, Pham et al. (2020) explored the effects of soil nail parameters on vertical slope stability, highlighting potential improvements. Mugahed Sakr et al. (2020) studied the use of microsilica fume for expansive soil stabilisation, providing insights into environmentally friendly additives. Despite this fact, Mugahed Sakr et al. (2020) and Ramteke & Sahu (2024) analysed the impact of surcharge loading and nail characteristics on slope stability through experimental studies. Lehn et al. (2021) investigated the load-bearing behaviour of soil nailing with flexible facing using 3D-FEM. Correspondingly, Jared & Noorasyikin (2021) examined the role of vetiver grassroots

*Address of the authors:
Department of Civil Engineering, Delhi Technological University, Delhi, India – 110 042 (prashant_2k16phdce12@dtu.ac.in)

© 2024 E. Schweizerbart'sche Verlagsbuchhandlung, Stuttgart, Germany
DOI: 10.1127/zdgg/2024/0422
www.schweizerbart.de
1860-1804/0422 $ 10.80

Z. Dt. Ges. Geowiss. (J. Appl. Reg. Geol.), 174 (4), p. 729–744, 12 figs.
Published online September 2023

Article

Enhancing soil slope stability by soil nailing: A comprehensive review

Prashant C. Ramteke & Anil Kumar Sahu*

Ramteke, P. C. & Sahu, A. K. (2023): Enhancing soil slope stability by soil nailing: A comprehensive review. – Z. Dt. Ges. Geowiss., 174: 729–744, Stuttgart.

Abstract: This paper provides a comprehensive review of soil nailing as a technique for strengthening slopes and retaining walls. It deliberates various methods and materials associated with soil nailing, while also examining the advantages and disadvantages of this approach. The review incorporates previous studies to demonstrate the extensive practical application of soil nailing. To study the influence of soil nail stiffness, both physical modelling and numerical techniques, such as Finite Element Method (FEM) and Finite Difference Method (FDM), are studied. The conclusions confirm that soil nailing is a reliable and very effective method for improving soil strength and minimising settlement. Also, the review highlights the significance of considering the bending stiffness of soil nails to optimise the effectiveness of this technique in ground improvement projects. As a result, this review paper serves as a valuable resource for engineers seeking guidance in soil nailing techniques. The primary objective of this paper is to explore fundamental concepts and state-of-the-art approaches in soil slope stability, with a particular focus on soil-nailed slopes and walls.

Keywords: slope stability, soil nailing, ground improvement, embankment, nail inclination, reinforced soil

1. Introduction

Soil nailing is a ground improvement technique that enhances soil strength and provides stability to embankments. The process involves inserting steel nails into the soil and connecting them to a steel mesh in a soil nail wall (Byrne et al. 1998; FHWA 1998; Lazarte et al. 2015). These nails are typically made of steel. First, a rotary drilling machine is used to insert the nails into the soil, which are then grouted with cement. The grout secures the nails and ensures tight compaction of the surrounding soil. Once the grout has dried and the soil has been compacted, the steel mesh is connected to the nails, completing the soil nail wall (Byrne et al. 1998; Lazarte et al. 2015). This wall serves as a support system, effectively preventing soil movement and collapse. Soil nailing can be applied in various ways, depending on factors such as soil type, embankment slope, and structural weight. Its uses include enhancing embankment stability, reducing landslide risks, and providing additional support to structures.

For embankments, soil nailing is used to construct roads, railroads, dams, and other civil engineering structures. When embankments are built on stable ground with good geotechnical properties, there won't be any problems with the soil's ability to compress and break. If they are built on unstable ground, this may not make stability. Due to the difficulty of finding good land for building, many projects have to be built on soft land. Over the past few decades, there has been more construction on unstable ground. This is because there is more demand for construction and not enough good land. However, the world's population is growing quickly and more infrastructure needs to be built. Most of the time, geotechnical engineers have a hard time building or designing slopes or embankments on unstable or unreliable ground. Because soft soils have a low bearing capacity, settle too much, and don't have enough shear strength. Accordingly, the embankments will change a portion and move side to side, which is likely to cause the embankment and structure to fail. So, to avoid these problems, the soft ground needs to be fixed up before it can be used for project work. Mitchell (1981) and Magnan (1994) extensively explained various methods of ground improvement in their study.

The ground improvement technique is used to make the soil stronger so it can hold more weight, make the soil less likely to break apart, make the soil layers denser, give stability on the side, reduce loads, increase resistance to liquefaction, stop deformations, stop settlement, speed up consolidation, and fill voids (Mumfakh 1997a, b; Terashi & Juran 2000; Ochiai et al. 2005; Elias et al. 2006; Schaefer et al. 2012).

This paper examines several essential aspects of soil nailing, such as the orientation of soil nails, proper nail placement, the impact of soil nailing on the surrounding environment, and the performance of soil nailing systems etc. Ad-

*Address of the authors:
Civil Engineering Department, Delhi Technological University Delhi, India – 110 042 (prashant_2k16phdce12@dtu.ac.in)

© 2023 E. Schweizerbart'sche Verlagsbuchhandlung, Stuttgart, Germany
www.schweizerbart.de
DOI: 10.1127/zdgg/2023/0403
1860-1804/0403 $ 7.20

Ground Improvement Technique by Soil Nailing: A Theoretical Analysis

Prashant C. Ramteke [1, 2, a)] and Anil Kumar Sahu [1]

[1] *Civil Engineering Department, Delhi Technological University Delhi, New Delhi – 110042, India*
[2] *Civil Engineering, G. B. Pant, DSEU Okhla-III campus, New Delhi-110020, India*

[a)] Corresponding author: prashant_2k16phdce12@dtu.ac.in

Abstract: Soil nailing is a versatile construction technique used in stabilizing natural as well as man-made earth slopes. In Europe, this technique was initially developed and probable in various provinces. Now, this technique is widely used worldwide and used in India also. The process of soil nailing is simply embracing reinforcement for passively strengthening soil slopes. The soil nailing is mostly incumbent on the method of construction as well as the type and nature of soil or rock. The nail bending, dilation, soil moisture, overburden pressure, grout pressure, and nail roughness also affect the soil nail resistance. This paper aims to explore some important ideas or state of the art on ground improvement techniques, such as nailed soil slope and systematic techniques prolonged by a broad investigation of the method of slope stability.

INTRODUCTION

Soil nailing is used in the construction of highways, railways, dams, etc. for the embankment. When embankments are constructed on stable ground with good geotechnical characteristics, there will not be difficulties due to the compressibility and shear strength of the soil. If they are built on unreliable ground, this may be contradictory. Due to the unapproachability of appropriate land for construction, many projects are forced to be accepted on soft lands. Over the past few decades, construction on the lenient ground has amplified due to more demand for construction and the non-availability of suitable land because of the fast growth of the world population and the need for infrastructure development. Generally, geotechnical engineers are facing many difficulties while constructing and designing embankments or slopes over unreliable/unstable ground. Because soft soils have (a) low bearing capacity (b) excessive settlements, (c) high compressibility, and (d) insufficient shear strength, etc. These embankments will undergo large deformations and lateral movements, which are likely to cause the failure of the embankment and structure. Hence, the soft ground has to be improved before using it for project work to prevent these incidents. Various techniques have been used for ground improvement like vertical drains, preloading, stepped construction, excavating the existing soft soil and replacing it with suitable materials, grout injection, reinforcing the embankment with geo-grids, or providing additional supports by adding column supports [22]. Ground improvement technique has role play in (i) increase in bearing capacity of soil, (ii) increase in shear strength of soil, (iii) increase in density of soil strata (iv) provide lateral stability (v) decrease imposed loads, (vi) increase in liquefaction resistance, (vii) control deformations, (viii) control settlement, (x) accelerated consolidation, and (x) fill voids [42, 43].

CONVENTIONAL GROUND IMPROVEMENT TECHNIQUES

Mitchell [22]; Terashi and Juran [29] has explained various ground improvement techniques as under:

Reinforcement. The main function of reinforcement is to provide lateral stability and improve engineering characteristics. The methods of reinforcement are: (a) Mechanically stabilized earth (b) Fiber reinforcement (c) Soil nailing/anchoring (d) Column supported embankments (e) Micro piles (f) Geosynthetic reinforced embankments (g) Columns: (i) Stone and lime columns (ii) Jet grouting (iii) Aggregate piers (iv) Geotextile encased columns (v)

International Conference on Smart Materials and Structures, ICSMS-2022
AIP Conf. Proc. 2810, 050001-1–050001-12; https://doi.org/10.1063/5.0146861
Published by AIP Publishing. 978-0-7354-4562-8/$30.00

IARJSET ISSN (O) 2393-8021, ISSN (P) 2394-1588

International Advanced Research Journal in Science, Engineering and Technology

Impact Factor 7.105 ⁜ Vol. 9, Issue 2, February 2022

DOI: 10.17148/IARJSET.2022.9258

Slope Stability Analysis of Soil Nailed Structure by using ASD and LRFD Methods

Prashant C. Ramteke[1, 2]*, Anil Kumar Sahu[1]

[1] Civil Engineering Department, Delhi Technological University Delhi, India.

[2] Civil Engineering Department, G. B. Pant, DSEU, Okhla-III campus, New Delhi, India.

Abstract: Many departments where embankments are constructed for highways and railway tracks face the problem of failure of embankments. Safety of the human beings and infrastructure is endangered because of slope failures resulting in loss of life and loss of investment which is a matter of concern in the Government bodies, and disaster relief authorities. These failures impede the socio-economic development of the country. This comprehensive study includes slope stabilization by using soil nails known as reinforcement in soil slopes. In this paper, analysis is carried out for slope stability by ASD (Allowable Stress Design) methods and LRFD (Load and Resistance Factor Design) for various nails inclinations to find out the better nails inclination for better slope stability. By using ASD and LRFD analytical methods the maximum FOS is observed in the range of 15° to 25° nails inclination.

Keywords: soil nailing, slope stability, ground improvement, reinforced soil, embankment, nail inclination.

1. INTRODUCTION

Engineers and construction experts in different countries like America, Europe, and Japan have been utilizing the unique benefits of soil nailing since the late 1960s. The insitu reinforcement of soils is a geotechnical engineering process that has various types of applications for stabilizing slopes and excavations. Reinforced soil is an advanced composite material made up of soil and reinforcement. This material is similar to reinforced cement concrete in terms of compressive and tensile strength. The fundamental principles of soil reinforcement can be found in nature. Vidal was the first to use an advanced technique of soil reinforcement in 1969. As per Vidal's theory, the gravitational pull friction is caused by the reciprocal interaction of the reinforcing horizontal members and soil. Using this concept in 1986, in France, the retaining walls were built. Nowadays in developing countries, slope reinforcement techniques are widely used. In the field of reinforced soil, there has been a lot of theoretical development. In France, near Versailles, for the first time, an 18 m high sand cut slope was stabilized in a railroad widening project (Rabejac and Toudic, 1974). Due to the less time required for construction and less expensive than other methods, soil nailing is more suitable. In France and other parts of Europe, soil nailing is more popular. In Germany, a soil nail wall was used first time in 1975. (Stocker et al., 1979).

2. LITERATURE REVIEW

In the analysis/design of a soil nailing structure, the stability or strength of the soil nailing is important. The stability of soil nailing is affected by several factors, including nail properties such as length, spacing, and inclination. The stability of a soil-nailed structure is also affected by soil properties, pull-out strength, grout bond strength, and wall inclination. Many researchers have a look into these parameters. Because of the limited number of parameters and its simplicity, the Limit Equilibrium Method (LEM) is generally used for soil nailed wall stability analysis. Internal stability, external stability, and facing stability are the three major requirements that must be seen in this method. FHWA manual, Davis Method, French method, and German Method, are represented by Byrne et al. (1996), Shen et al. (1981), Schlosser (1981), and Stocker et al. (1979) respectively. By using the Finite Element Method (FEM) Chang (2008) examined the various effective factors in the slope stability analysis. Sivakumar B and Singh V. P. (2011) analyzed the soil nailing retaining wall for vertical cut/support by using 2D FEM, also they designed a soil nail wall based on the LRFD approach. Byene et al. (1998), worked on the use of uniform or variable nail lengths, and he suggested that continuous nails length are suitable in areas where ground moments or extreme displacement does not occur. In 1980, Jewell used a shear box test and identify the effect of soil nails orientation on the shear strength of the soil. It was observed that w.r.t. the nails orientation the shear strength of soil is changed.

3. APPLICATIONS OF SOIL NAIL WALLS:

In excavation applications for vertical or nearly vertical cuts, the soil nail walls are particularly used. End slope removal during retaining structure repair, highway cut stabilization, under existing bridge abutments, underpass widening &

© IARJSET This work is licensed under a Creative Commons Attribution 4.0 International License

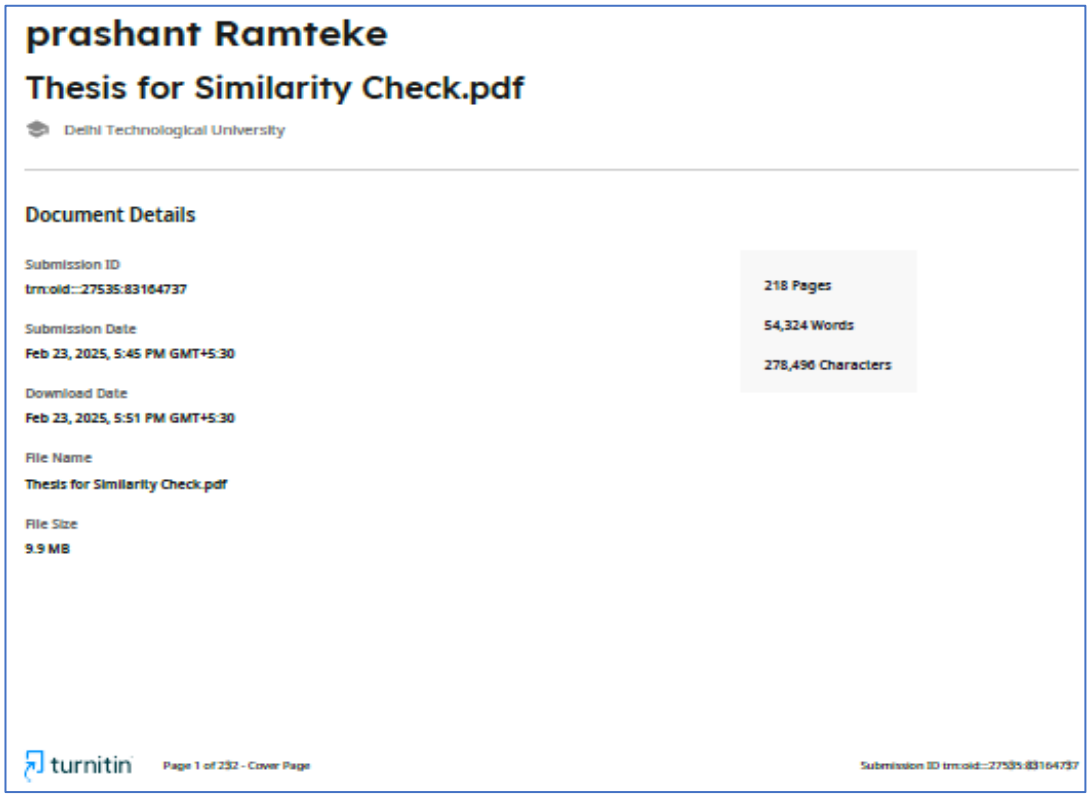

prashant Ramteke

Thesis for Similarity Check.pdf

Delhi Technological University

Document Details

Submission ID
trn:oid:::27535:83164737

Submission Date
Feb 23, 2025, 5:45 PM GMT+5:30

Download Date
Feb 23, 2025, 5:51 PM GMT+5:30

File Name
Thesis for Similarity Check.pdf

File Size
9.9 MB

218 Pages

54,324 Words

278,496 Characters

turnitin Page 1 of 232 - Cover Page Submission ID trn:oid:::27535:83164737

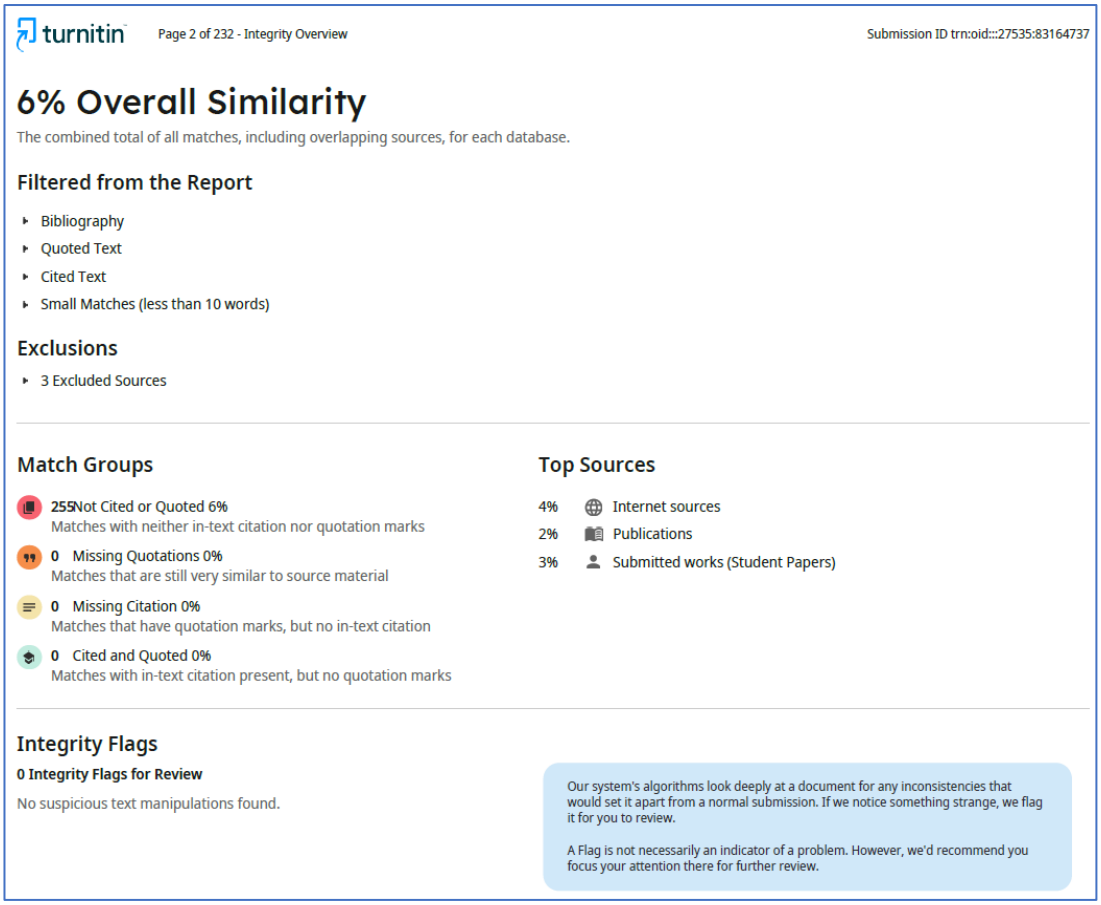

turnitin Page 2 of 232 - Integrity Overview Submission ID trn:oid:::27535:83164737

6% Overall Similarity

The combined total of all matches, including overlapping sources, for each database.

Filtered from the Report

- Bibliography
- Quoted Text
- Cited Text
- Small Matches (less than 10 words)

Exclusions

- 3 Excluded Sources

Match Groups

255 Not Cited or Quoted 6%
Matches with neither in-text citation nor quotation marks

0 Missing Quotations 0%
Matches that are still very similar to source material

0 Missing Citation 0%
Matches that have quotation marks, but no in-text citation

0 Cited and Quoted 0%
Matches with in-text citation present, but no quotation marks

Top Sources

4% Internet sources
2% Publications
3% Submitted works (Student Papers)

Integrity Flags

0 Integrity Flags for Review

No suspicious text manipulations found.

Our system's algorithms look deeply at a document for any inconsistencies that would set it apart from a normal submission. If we notice something strange, we flag it for you to review.

A Flag is not necessarily an indicator of a problem. However, we'd recommend you focus your attention there for further review.

DELHI TECHNOLOGICAL UNIVERSITY

(Formerly Delhi College of Engineering)

Shahbad Daulatpur, Main Bawana Road, Delhi-110042

PLAGIARISM VERIFICATION

Title of the Thesis: **Behaviour of Soil Nailed Slope Under Surcharge Loading**

Total Pages: **218** Name of the Scholar: **Prashant Chudaman Ramteke**

Supervisor (s): **Prof. Anil Kumar Sahu.**

Department: **Civil Engineering**

This is to report that the above thesis was scanned for similarity detection. Process and outcome is gven below:

Software used:**Turnitin** Similarity Index: **6 %** Total Word Count: **54324**

Date: 23/02/2025

Candidate's Signature **Signature of Supervisor**

CURRICULUM VITAE/BRIEF PROFILE

Mr. Prashant C. Ramteke, is Assistant Professor in Civil Engineering Department, G. B. Pant DSEU Okhla-III Campus (formerly G. B. Pant Institute of Technology), New Delhi, India. He holds a Master's Degree (M.Tech.) in Engineering Structures from the National Institute of Technology, Warangal, India. Having approx. 3 years field experience in Construction, Planning, Estimating and Surveying etc. He has more than 14 years of teaching and 08 years (approx.) of research experience in Civil Engineering. His research interests are Slope Stabilisation, Ground Improvement Techniques, Repairs and Rehabilitation of Structures, Geotechnical Hazards, Stability of Natural and Manmade Slopes, utilization of soil nailing techniques, Earthquake Engineering and Engineering Structures etc. Mr. Ramteke is an active reviewer for several esteemed SCIE journals. He is also a Life Member of the Indian Geotechnical Society (IGS), Delhi Chapter, a Member of the Seismological Society of America since February 2023 and a Member of the Institution of Green Engineers (IGEN), Chennai, India. etc.